Infrared study of hydrogen bonding of methanol in the liquid phase

Farwaneh, Sahab Sadi

Infrared Study of Hydrogen Bonding of Methanol in the Liquid Phase

An M.Sc. Thesis Submitted

to

The University of Durham

Department of Chemistry

by

Sahab Sadi Farwaneh

(St Mary's College)

October 1991

To my

Mother and Father

Declaration

The work described in this thesis was carried out by me in the Chemistry Department of the University of Durham between May 1990 and October 1991. I declare that this work has not been accepted in substance for any degree and is not being concurrently submitted in candidature for any other degree. The work is my original work except where indicated by reference to other work.

Signe

Supervisor

Date:

Abstract

The ν_s(OH) band of methanol in binary system has been studied by using infrared spectroscopy, over the whole concentration range between 0.01 – 0.7 methanol mole fraction.

The aim of this study is to analyze this band which is very complicated, due to overlapping between its band components, and to correlate the results to the possible underlying equilibrium.

Also the change in the ν_s(OH) band shape across the concentration range, imposed the necessity of studying the ν_s(OH) of methanol in non-polar solvent at a very low concentrations (0.0049 to 0.0246 mol/dm^3) in order to identify the existing varieties of methanol hydrogen bonded species, as well as the monomer.

A study of the ν_s(OH) for methanol in the ternary system ($CH_3OH/CH_3CN/CCL_4$) was undertaken, in order to defferentiate the band components of the hydrogen bonded complexes formed from methanol and acetonitrile molecules, from the hydrogen bonded methanol aggregates. This study was carried out in a concentration range of 0.0044 to 0.0177 mol/dm^3.

For the binary system, because of the complexes of the bands, a band fitting programs were used as a means of estimating the number of bands present, their positions and band shapes of each component. As a result, this study has shown that the I.R. data for methanol in acetonitrile band fitting model contained: monomer, dimer, 1:1 and 2:1 complexes, trimer, tetramer and pentamer species.

Acknowledgements

I am indebted to many people for help and advice during the period of research leading to this thesis.

Above all, I must express my many thanks to my supervisor, Dr J. Yarwood, for his interest in this project, his kindness and understanding of what I went through during this period, from the Gulf Crisis to over two months of illness including hospitalization and two operations.

I would further like to acknowledge Dr J.V. Armitage who kindly helped me to get the financial assistance necessary for continuing this project.

Thanks are due to many people in the Chemistry Department of the University of Durham for technical advice and useful discussions.

Finally, I would like to record my thanks to Ms S. Stewart and Mr C. Greenhalgh for typing this thesis.

CONTENTS

Chapter One

Introduction

1.1 The Hydrogen–bond Interactions

When two closed shell molecules, A and B, come close together (as in the liquid phase), several types of interaction potential may contribute to the overall potential energy curve (Figure 1):–

a) Long ranged coulombic and dipole/dipole interactions due to electrostatic interaction between the permanent charge distribution of the two polar molecules, giving a strong dipole interaction. Their interaction potential energy may be calculated from[1]

$$u(\mu_A,\mu_B) = -\mu_A\mu_B(2\cos\theta_A\cos\theta_B - \sin\theta_A\sin\theta_B\cos(\phi))/r^3 \qquad (1)$$

where,

u is the potential energy of the two molecules A and B

μ_A and μ_B are the two molecular dipoles

θ, ϕ are the orientation dependent parameters shown in Figure 2.

b) Long ranged dispersive interactions which are caused by an attraction between the instantaneous charge distribution of the two molecules. These are due to small-scale correlated motions of the electrons giving rise to a dispersion term. The leading term is the instantaneous dipole–induced dipole interaction, which is r^{-6} dependent. The accurate expression for the dispersive interaction may be approximated to allow calculation from experimentally measurable quantities.

c) Short ranged repulsive forces due to the violation of the Pauli exclusion principle. It is a valence repulsion interaction between the two molecules caused by overlap of the electronic distributions resulting in a large distortion, with a consequent decrease in charge density between the two nuclei involved.

d) Short ranged attractive forces (charge transfer process) lead to bonding, as in molecular complexes. These kinds of Donor/Acceptor forces have a mutual potential energy[1] of u_o (i.e. no bond potential energy).

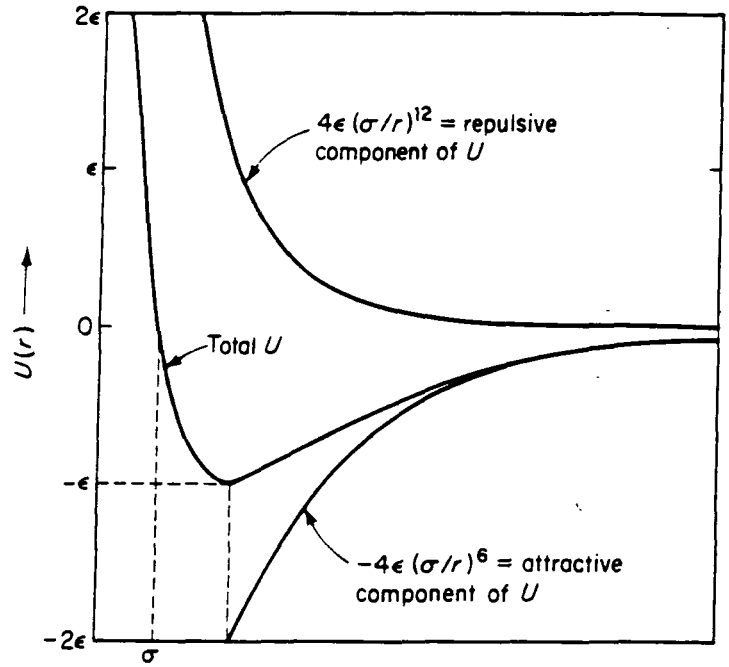

Figure 1. The Lennard-Jones 6-12 potential[9]

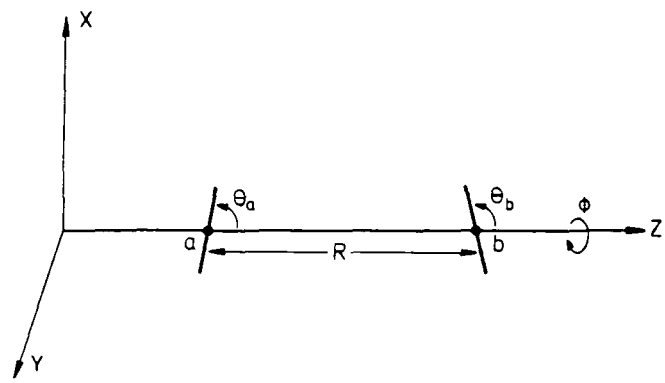

Figure 2. The relative orientation of two molecules a and b which are a distance R apart along the Z axis in a Cartesian coordinate system X,Y,Z. The angles θ_a and θ_b refer to the Y,Z plane, the angle ϕ is relative to the X,Y plane.[1]

$$\Delta E = E_1 - E_0 = I_D^V - E_A^V + u_0(r_0) - u_1(r_0) \qquad (2)$$

Here, E_1 is the dative bond state energy

E_0 is the no-bond state energy

$I_D^V - E_A^V$ is the consumed energy needed to produce the ions D^+ (donor) and A^- (acceptor) at the excited state

r_0 is as shown in figure 3

and u_1 is the mutual potential energy of the ions D^+ and A^- (see Table 1 for well recognized hydrogen bonding acids and bases)

Table 1 Well Recognized Hydrogen Bonding Compounds[2]

Hydrogen Bonding Acids		Hydrogen Bonding Bases	
A	Examples	B	Examples
F	HF	F	HF
O	Carboxylic acids Water Alcohols Phenols Oximes	O	Carboxylic acids Water Alcohols Phenols Amides Ketones Aldehydes Ethers Esters
N	Amides Pyrrole Amines Ammonia	N	Amines Pyridines Ammonia Pyrrole

Lippincott[14] and Schroeder[17,18] developed a model for the overall potential function of the hydrogen bond which describes the complete potential curve for the proton within the hydrogen-bond, from which the barrier height for the proton transfer can be obtained. This potential function for the hydrogen-bonding in X–H···Y is made up of four terms[24] (based on the four interactions described above).

$$u = u_1 + u_2 + u_3 + u_4 \qquad (3)$$

u_1 is the potential function for the X-H bond

$$= D\left\{1 - \exp[-n(r - r_0)^2 / 2r]\right\} \qquad (4)$$

u_2 the potential function for the H···Y bond

$$= -D^{*}\exp[-n^{*}(R-r^{*}-r_0^{*})^2/2(R-r^{*})] \quad (5)$$

u_3 the Donor/Acceptor repulsion between the two atoms

$$= Ae^{-bR} \quad (6)$$

and u_4 the electrostatic attraction between the atoms

$$= BR^{-m} \quad (7)$$

A,B,b,m are constants, D and D^{*} are the strengths of the A-H and H···B bonds n and n^{*} are related to the ionisation potentials of the atoms, r_0 and r_0^{*} are the internuclear distances in the absence of the hydrogen bond, r and r^{*} are the distances on formation of the hydrogen bond, R is the A···B distance, and R_0 is the A···B distance at the minimum in the potential function. A schematic diagram of the hydrogen bond between atoms A and B is shown in Figure 3.

If the electrostatic contribution alone were the major controlling factor in determining hydrogen bond energy, there should be a correlation between the strength of the hydrogen bond and the dipole moment of the electron donor. Infra-red spectroscopic studies[20] show an increase in intensity of the O-H stretching band on hydrogen bond formation; sometimes greater than the increase expected on purely electrostatic grounds. Coulson[21,22] has interpreted this behaviour as due to a charge movement (charge-transfer) to and from the donor during the hydrogen vibration, implying electron delocalization. The polarization and charge-transfer contributions are small but not negligible at long range and although larger at the equilibrium distance, is still smaller[23] than either E_E (exchange repulsion energy) or E_C (coulomb energy) individually (see Figure 1). The E_C contribution alone would lead to a stable complex and explains the relative success of early electrostatic models of the hydrogen bond[23]

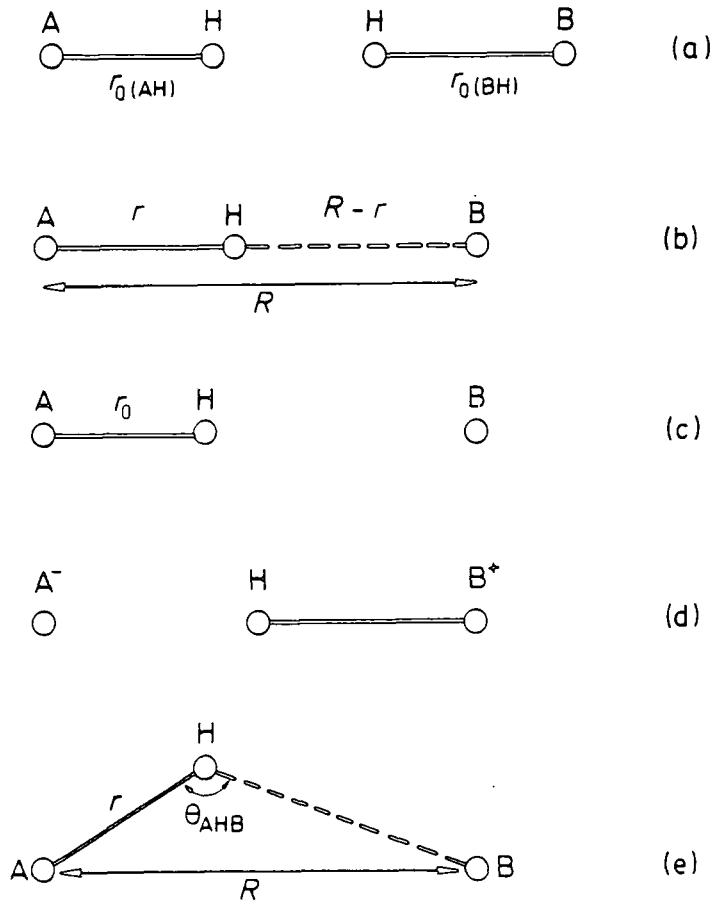

Figure 3. Schematics of the hydrogen bond.

(a) Bond distances of hydrogen atoms bonded to A atoms, r_0(AH), and to B atoms, r_0(BH), in isolated groups.

(b) The equilibrium position of the hydrogen bond, the A-H distance stretched to r, the B-H distance much longer than either r or r_0(BH).

(c) The unbonded contribution to the hydrogen bond structure.

(d) The charge transfer contribution to the hydrogen bond structure.

(e) The bent hydrogen bond, a state of higher energy than (b).[1]

Among the various types of intermolecular interactions, the hydrogen-bond plays the most significant role in determining the structure and the properties of molecular systems of importance in chemistry and biology. The unique function of hydrogen arises because it has no inner shell electrons and, as a result, the repulsive exchange energy is low. In weak or medium strength hydrogen bonds the largest attractive term is the coulombic energy.[23] This is only weakly directional so that the hydrogen bond can be easily bent. The exchange repulsion is also low and if the molecules joined by the bond do not have symmetry about the bond, as is usually the case, the bond may bend to reduce the repulsive interactions between the molecules. Charge-transfer and polarization contributions only appear to become important in short, *i.e.* strong bonds. However, although of smaller magnitude than the coulombic and exchange energies, they may be sufficient to significantly influence the equilibrium geometry and the spectral properties.

The enthalpy of association ΔH is written in terms of electronic, vibrational, translational and rotational components,[10] as follows:–

$$\Delta H(T) = \Delta E_{el}+\Delta E_{vib}+\Delta E_{tr}+\Delta E_{rot}+\Delta(PV) \qquad (8)$$
$$(\text{at } 300K,\ \Delta PV = -RT)$$

The experimental ΔH cannot be compared directly with the calculated results which gives only the electronic contribution (ΔE_{el}) to this enthalpy. The two are related by equation 8.

In going from 2-monomer molecules to one dimer, 3-degrees of translational and 3-degrees of rotational freedom are lost, each of which contribute ($\frac{1}{2}RT$) to the enthalpy. Thus $\Delta E_{tr}+\Delta E_{rot} = -3RT$. Each vibration contributes $h\nu[\frac{1}{2} + (e^{h\nu/RT} - 1)^{-1}]$ to the external energy. Assuming each rotational and translational degree of freedom contributed RT/2 to ΔE, equation 8 becomes,

$$\Delta H(T) = \Delta E_{el}+\Delta E_{vib}+4(1-n)RT \qquad (9)$$

where, n is the number of atoms.

The vibrational energy is related to the vibrational frequency ν_i as follows

$$E_{vib}(T) = E_{vib}(0)+\Sigma h\nu_i/(e^{h\nu_i/RT}-1) \quad (10)$$

where, $$E_{vib}((0) = \tfrac{1}{2}h\Sigma\nu_i \quad (11)$$

(units of ΔH and ΔE are per mole of complex). The $\Delta E_{vib}(T)$ is composed of intermolecular and intramolecular contributions (see Figure 4 for the difference between these two).

$$\Delta E_{vib}(T) = \Delta E_{intra}(T)+\Delta E_{inter}(T) \quad (12)$$

The last equation is evaluated from the vibrational frequencies of the high aggregate and monomer (as described below).

The study of hydrogen bonding in liquid alcohols is not easy. As a result there is no general agreement regarding the size or geometry of alcohol aggregates in either vapour or condensed phases.[4] The detailed studies of self-association by hydrogen bonding are of quite general interest since alcohols (and other associating species) are widely used as reagents, extractants and solvents. This association may have considerable influence on the chemical and physical properties of the mixtures and solvents.

A study of methyl alcohol, as an example of hydrogen bonding interactions is very important, in order to determine the configurations of its aggregates and eventually the methanol structure in the liquid phase. A number of experimental studies[3,15,16] of self–association in methanol, have been carried out in the vapour phase. These studies have shown that the intermolecular hydrogen bond may produce chains, rings or a three dimensional network.

The assumed gas phase geometry of the methanol molecule is shown in Fig 5. Wetner and Pitz[5] suggested the presence of monomers, dimers and tetramers in the vapour phase, based upon available PVT data and a few measurements of the heat capacity of gaseous methanol. However, as they stated, their results did not absolutely distinguish between tetramer formation and the presence of a

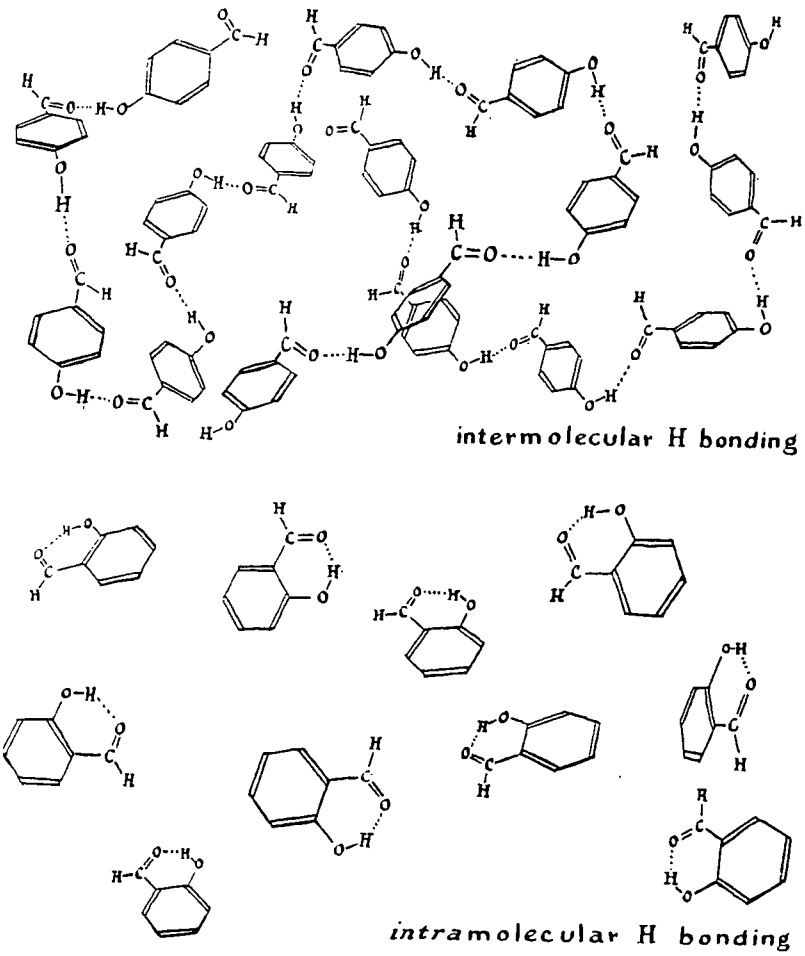

Figure 4. Comparison of the structure of associated chains and chelated molecules.[2]

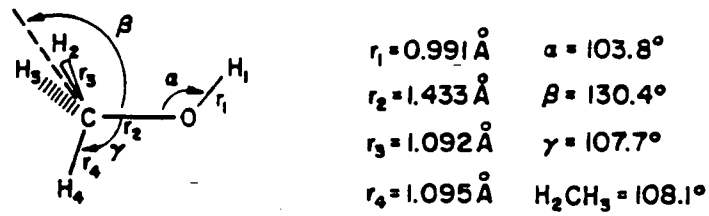

Figure 5. Geometry of the optimized structure for the methanol monomer.[7]

mixture of aggregated species larger than the dimer. Infra-red studies[66] of methanol supported the same monomer-dimer-tetramer model.

The chemical reactions occurring in the methanol vapour mixture of aggregates is assumed to be represented by

$$n(CH_3OH) \rightleftharpoons (CH_3OH)_n \qquad (13)$$

where n = number of molecules = 2,3,4 ... etc. . The corresponding equilibrium constants of these reactions will be explained later.

The geometry of the methanol dimer has been optimized by Del Bene[8] while the geometries of the higher polymers of methanol were set up based on the water polymer structure.

In the open structure of the methanol aggregates, the methanol molecule added to form the next higher polymer, is positioned in such a way that the newly added molecule and the molecule to which it is hydrogen bonded have the same relative positions with respect to each other as the two equilibrium forms of the dimer (Figure 6).

Binding energies[4] indicate that the open trimers are more stable than three isolated molecules. Three non-equivalent forms of the open trimers are shown in Table 2. Curtiss[4] found that structure III is the most stable of the methanol trimers. The same results from the water trimer structure were obtained by Del Bene and Pople.[9]

The addition of another methanol molecule to the trimer structures gives four tetramer structures listed in Table 2. In the case of the chain pentamer four possible structures were considered. The lowest energy structure (species XI) is nearly a closed cyclic structure. Because of that, the chain hexamer could not be formed as it is in the case of water aggregates[9].

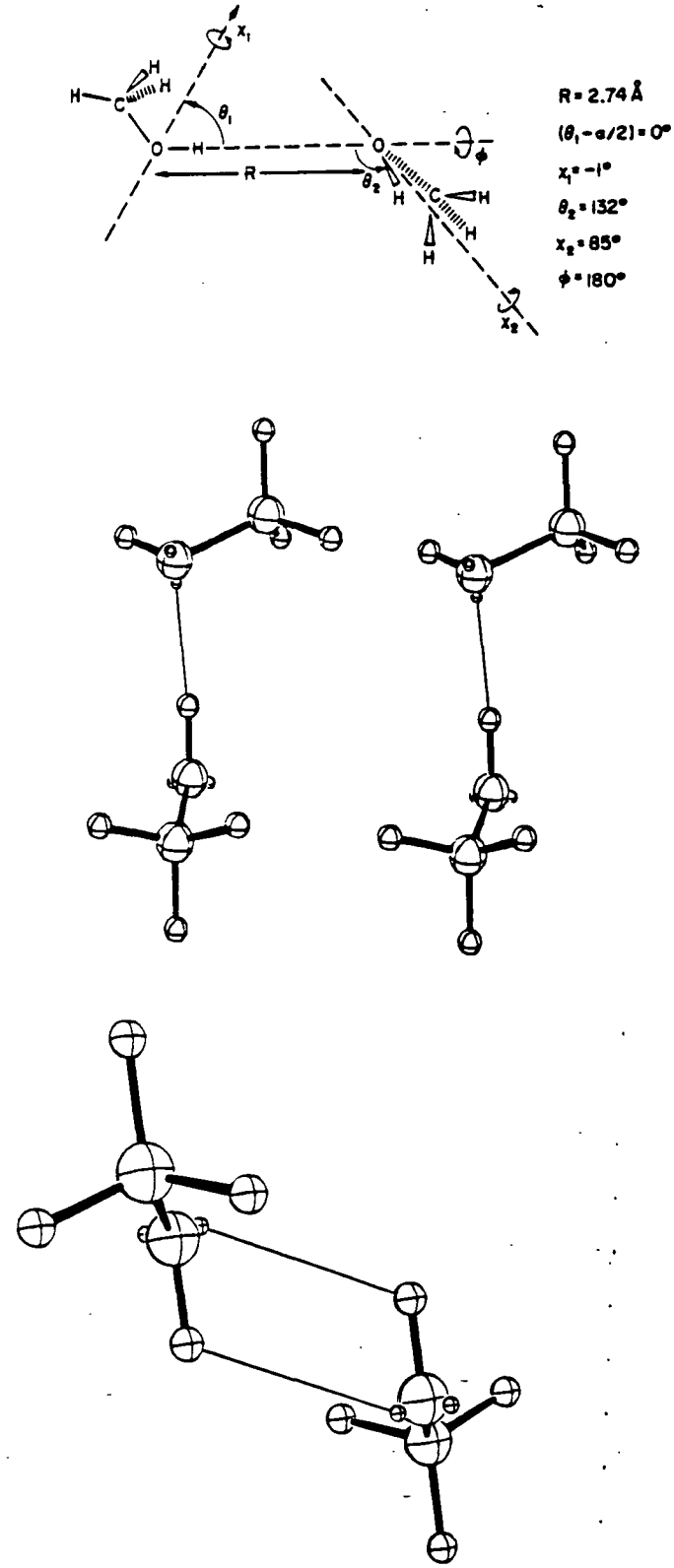

Figure 6 (a) Geometry of the optimized structures for the methanol dimer.[8]

(b) Lowest-energy methanol dimer, the trans near-linear dimer, shown as a stereo–isometric pair. The hydrogen bond is represented as a thin line.[4]

(c) Trans cyclic methanol dimer, local energy minimum configuration.[4]

Table 2 Energies of open methanol aggregates[4]

	Structure	Energy (a.u.)	Binding energy (kcal/mole)
Trimer			
I	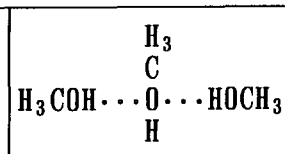	−340.66190	−8.67
II	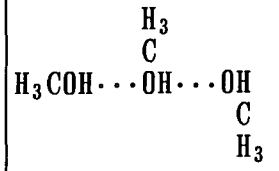	−340.66873	−13.26
III	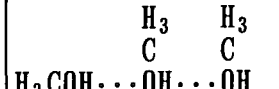	−340.66875	−13.27
Tetramer			
IV	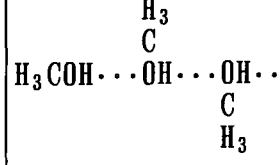	−454.23046	−21.12
V	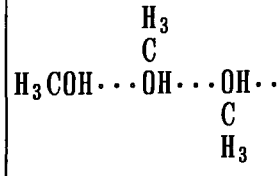	−454.23047	−21.13
VI	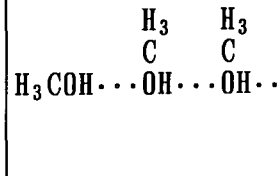	−454.23171	−21.91
VII	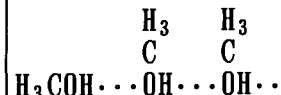	−454.23178	−21.95
Pentamer			
VIII	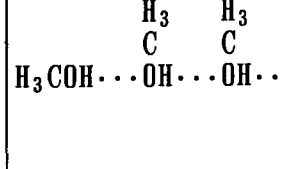	−567.68556	+37.93
IX	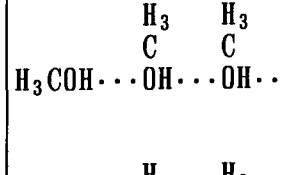	−567.79310	−29.55
X	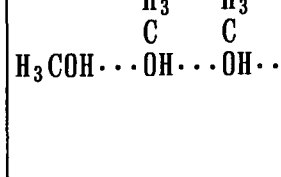	−567.23046	−29.58
XI	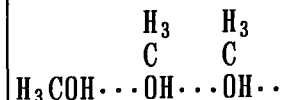	−567.80134	−34.73

1.2 υ_s(OH) Interpretation

Infra-red (IR) spectroscopy was historically one of the first techniques used to investigate hydrogen bonding and a very large number of systems have been studied by this method. IR spectroscopy is still the most amenable and rapid method for demonstrating the existence of hydrogen-bonding and crudely characterizing the interaction.

This study is limited only to those aspects of IR spectroscopy which are important for the understanding of the nature of the hydrogen-bond. Thus we shall consider the effects of hydrogen bonding on the stretching mode of A–H··B systems after a general discussion of other vibrational modes.

Vibrational modes which result from hydrogen bond formation are shown in Figure 7. The arrows show the principle displacements involved in the oscillatory movements of the atoms. Note that Roman letters are assigned to identify vibrational modes existing prior to formation of the hydrogen bond and the Greek letters are used to identify vibrational modes created by the formation of the complex. Also shown is an indication of the usual spectral region (in cm^{-1} and μm) for the absorption.

The most prominent effect of hydrogen bonding on the vibrational spectrum is the shift of the absorption of the A-H stretching mode (ν_s) and its harmonics ($2\nu_s$, $3\nu_s$ ...) to lower frequencies. In addition it has been found[25] that the intensity and frequency of ν_s of an alcohol are dependent on concentration and temperature. This behaviour has been attributed to molecular association.

The effect of the hydrogen bonding on vibrational spectra (ν_s mode) can be discussed under the following headings.

1.2.1 Frequency Shift

The ν(A-H) stretching band (and its harmonics) is shifted to lower frequencies by hydrogen bond formation. In many systems these shifts, $\Delta\nu_s$, are of the order of 10% of ν_s.[2] For example, it is found[26] that the frequency shift of

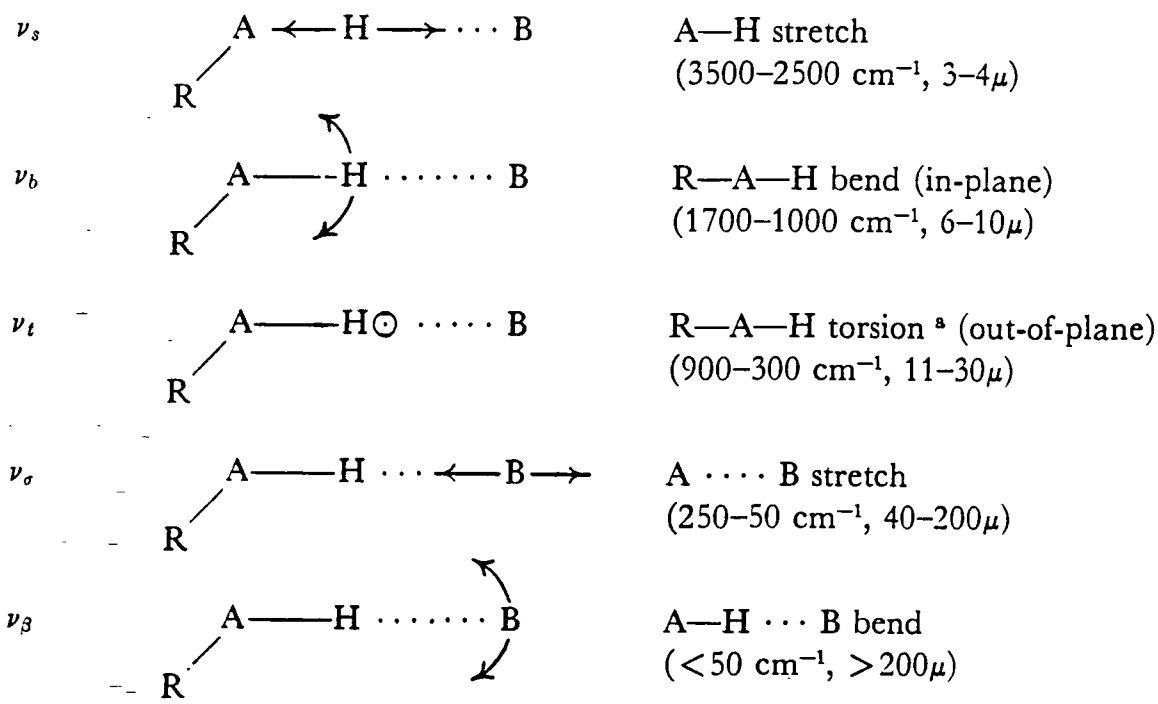

[a] The symbol ⊙ indicates a vibrational movement of the hydrogen atom perpendicular to the RAB Plane

Figure 7. Some vibrational modes of a hydrogen bonded complex.[2]

the C_1 complex band (OH···N) of methanol in acetonitrile solution, increases as the acetonitrile concentration increases. This can be determined through a plot of the OH-bond shift versus the concentration of the acetonitrile.

According to the Badger-Bauer rule[27] for hydrogen bonded systems, the frequency shift, $\Delta\nu$, is proportional to the hydrogen bond energy, ΔH_H

$$\Delta\nu \propto \Delta H_H$$

whereas it is inversely related to the A···B distance. There is uncertainty in the identity of the multiple species present, inspite of the precise determination of the hydrogen bond enthalpies (see Table 2). Thus the determination of the hydrogen bond enthalpy per mole in pure alcohol, as given by Mecke,[28] is of restricted value because of the variety of species present.

The low frequency region in vibrational spectroscopy provides a direct measurement of the strength of the intermolecular bond. This strength of the hydrogen bond determines the amount of anharmonicity. Such anharmonicity decreases when a weak hydrogen bond is formed and increases when a medium or a strong hydrogen bond is formed.

1.2.2. Half–width

The ν_s band is broadened when a hydrogen bond is formed.

The free ν(OH) band in pure alcohols is usually found as a sharp peak near 3620cm^{-1} which is replaced by a broad absorption at about 3330cm^{-1} due to the hydrogen bonded species. This behaviour can be explained in terms of a potential curve where, if the first excited state of the ν(OH) vibration occurs above the level of the second minimum of the double well potential curve, Figure 8, the probability of proton transfer from one potential well to the other will be very much increased. This leads to shortening of the lifetime in excited states, and so to a broadening of the absorption band. Table 3 provides examples of changes in the band widths of different methanol species in solid nitrogen.

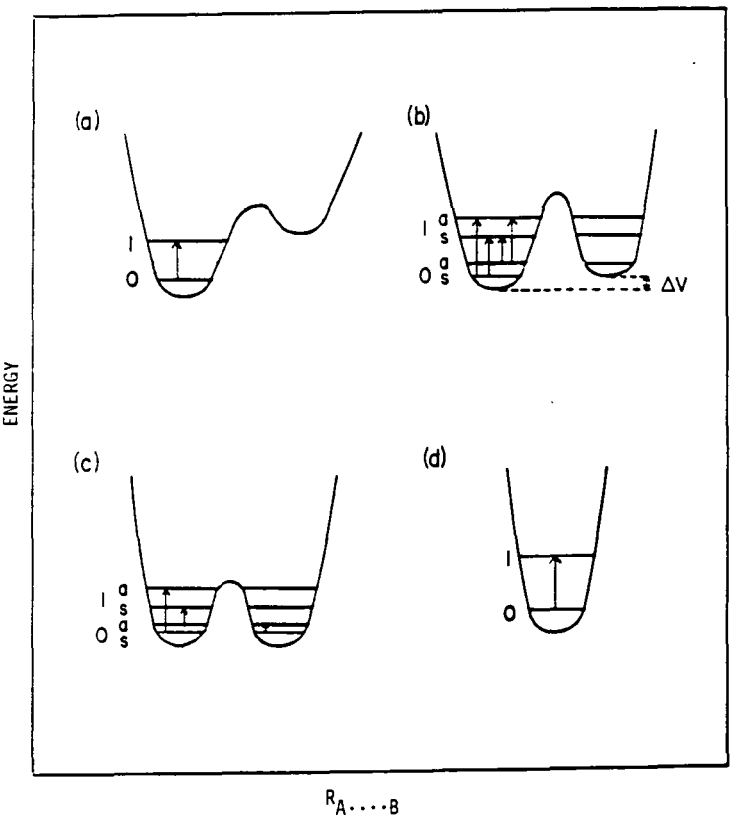

Figure 8 (a) Asymmetric double-minimum potential function;
(b) slightly asymmetric double-minimum potential function;
(c) symmetric double-minimum potential function;
(d) single-minimum potential function.[10]

Table 3 Frequency Shifts and Band widths of Methanol Polymers in Solid Nitrogen at 20°K[2]

Polymer	$\Delta\nu_s$ (cm^{-1})	$\Delta\nu_{\frac{1}{2}}$ (cm^{-1})
Monomer	(0)	20
Dimer	170	28
Trimer	215	~40
Tetramer	370, 410	—
High polymer	410	~100
Annealed solid	440	190

An analysis of the shape and structure of ν_s in hydrogen bonded species explains why the behaviour is common to gas, liquid and solid states of a variety of systems. Three proposals have been offered:

a. The wide ν_s band is caused by the superposition of many sharper bands of a variety of species.
b. The ν_s band is broadened by interaction between ν_s and the very low frequency deformation of the hydrogen bond, such as ν_σ and ν_β (see Figure 7) (coupling $\nu_s \pm \nu_\sigma$).
c. The structure of the ν_s band is caused by combinations of other fundamentals than ν_s intensified by Fermi resonance with ν_s.

The first proposal (a)–(by, for example, Fuson and Josien[29]) has recieved some support while the second suggestion (see for example, Badger and Bauer[27], Davies and Sutherland[30] etc.)is the most popular theory. Proposal (c) requires an assumption to explain why Fermi resonance extends over such a wide spectral range. This suggests that there is a correlation between the half-width of the fundamental band ν_s in different solvents as function of ν_s.

1.2.3 Intensity Change

The integrated absorption coefficient of the fundamental, ν_s, increases many-fold when a hydrogen bond is formed[2], whereas the corresponding intensities of the overtone bands decrease slightly. This change in absorption seems to be every bit as characteristic of hydrogen bond formation as is the frequency shift, $\Delta\nu_s$.

It was found[26] that the "free" ν(OH) band intensity decreases on addition of acetonitrile to phenol which indicates that a complex is formed, *i.e.* the OH-concentration is proportional to the intensity of the absorption at a particular frequency

$$C = \alpha/\epsilon L \qquad (14)$$

where C = OH-concentration, α = spectral absorption,

ϵ = molar extinction coefficient and L = cell length

This relative increase in integrated intensity is more reliable than frequency shift measurements for detecting weak hydrogen-bonds. However, the integrated intensity is dependent on the ν_s(A-H) spectral parameters which are sensitive to the changes in environment.

1.2.4 Temperature Variations

Both the frequency and intensity of ν_s may be altered by a temperature change of several degrees. Table 4 shows an example of the effect on the ν(OH) band by changing the temperature.

Table 4. ν_s(OH) Band Parameters of Hydrogen–complex of CH_3OH in Xe

	T(K)	T(°C)	$\nu(cm^{-1})$	$\Delta\nu_{\frac{1}{2}}$	$\Delta\nu/\Delta T$	$\Delta\nu_{\frac{1}{2}}/\Delta T$
Monomer	220	–53	3663	45	0.11	0.33
	205	–68	3661	40		
CH_3OH/CH_3CN	240	–33	3592	25	0.18	0.11
	195	–78	3584	20		

The extreme sensitivity of ν_s to temperature changes reflects the following characteristics:

a) Hydrogen bonding systems involve monomeric and usually several higher species in rapid equilibrium.

b) Each species has a characteristic $\bar{\nu}_s$ and the higher the degree of aggregation, the lower is $\bar{\nu}_s$.

c) Each type of aggregate has a characteristic absorption coefficient at $\bar{\nu}_s$ and the larger the aggregate, the higher is that coefficient[44] (Table 5).

d) Since the absorption coefficient may increase by as much as an order of magnitude on hydrogen bond formation, a small shift of equilibrium produces magnified spectral changes.

Table 5. Frequency Shifts, Band Widths and Absorption Coefficients[44]

Species	Alcohol	ν_s	$\nu_m-\nu$ (cm^{-1})	$\Delta\nu_{\frac{1}{2}}$ (cm^{-1})	$B^0 \times 10^{-3}$ (1./mole cm^2)†
Monomer	Methanol	3630	0	22	4.7
	Ethanol	—	0	24	4.6
	t–Butanol	—	0	15	3.3
Dimer	Methanol	3515	115 ± 3	80±30	—
	Ethanol	3505	125 ± 5	90±20	15 ± 5
	t–Butanol	3506	124 ± 4	76±15	11 ± 2
Polymer	Methanol	3319	311 ± 6	205±15	54
	Ethanol	3332	298 ± 6	195±15	55
	t–Butanol	3366	264 ± 6	160±15	53

†B^0 is the integrated molar absorption coefficient per OH bond; $B^0 \equiv (2.3/NC_i d) \int \log_{10}(I_0/I) d\nu$ where C_i is the concentration of the species in question in mol dm^{-3}, d is the cell thickness in cm, and N is the number of OH oscillators per molecule contributing to the band. For a monomer a Lorentzian shape was assumed, giving

$$B_m^0 = 2.3/C_m d \,.\, (\log I_0/I)_{max}\ \Delta\nu_{\frac{1}{2}} K,$$

where $K(\sim\pi/2)$. For the hydrogen bonded species B^0 was determined by graphical integration.

Liddel and Becker[31] examined the peak intensity and frequency of the ν_s band for monomeric methanol in carbon tetrachloride. They discovered that the intensity decreases by almost 36% if a dilute solution in carbon tetrachloride (0.005M) is warmed from 263K (–10°C) to 323K (50°C) and the frequency increases by about 6 cm^{-1} (0.2%). Since little dimeric or polymeric material is present, the change of absorption coefficient implies that the OH group interacts with carbon tetrachloride in a fashion that influences the intensity of the stretching mode and which is very temperature sensitive.

Figures 9 and 10 give the temperature-dependence of the fundamental OH-stretching band of liquid methanol[32] and ethanol to demonstrate how the intensity function of the fundamental band behaves. Luck and Zheng[33] showed the influence of temperature on the OH-stretching mode, ν_{01}, of *t*-butyl alcohol in carbon tetrachloride. They found that for $\Delta T = -40°C$ the influence on OH is much higher [$\Delta\nu(OH/CCl_4) = -2cm^{-1}$] than at room temperature. This observation, which agrees with the remarks of other authors, favours the assignment of $\Delta\nu$ to intermolecular interactions. They reported the OH-frequency shift $\Delta\nu_{01}$ (defined by $\nu_{vapour} - \nu_{solvent}$) which decreases linearly with increasing temperature (over the measured range of 10 – 60°C) by the following equation

$$\Delta\nu_{01} = \Delta\nu_0 - aT \qquad (15)$$

This linearity was also deduced in previous papers[34,35] Equation 15 can be understood in terms of excitation of higher vibration energies within the intermolecular potential curve. Thus, the half-width of the OH-bands should be expected to increase linearly with temperature[33]

$$\Delta\nu_{\frac{1}{2}} = (\Delta\nu_{\frac{1}{2}})_0 + bT \qquad (16)$$

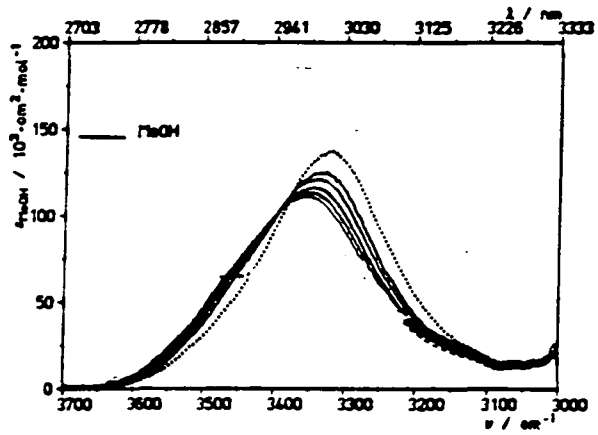

Figure 9 Fundamental ν(OH) band of CH_3OH. Temperature dependence of liquid methanol ν(OH) stretching band from the lowest to the highest band : 10°, 20°, 30°, 40°, 50°C.[32]

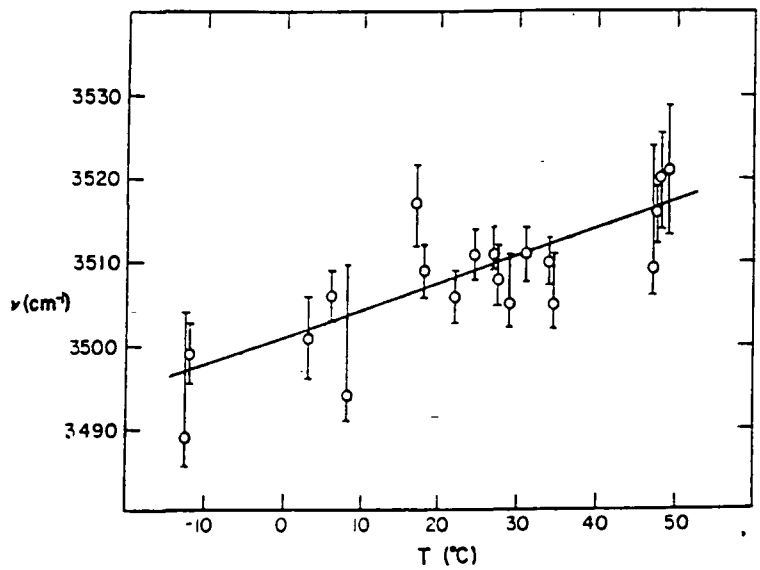

Figure 10 Frequency of the band near 3510cm^{-1} in ethanol as a function of temperature[44]

1.2.5. Concentration Variations

The frequency and intensity of the ν_s band are concentration dependent. It is found that the variation of ν_s band structure with concentration (in the case of self-association) or with composition (in the case of mixtures) is a good indication of more than a single form of complex and it is not related to the strength of the hydrogen bond.

Allerhand and Schleyer[36] examined the effect of base concentration on IR spectra of hydrogen bonded systems. The peaks of the free proton donor are essentially constant but the bonded peaks vary with concentration in several solvents. Therefore, they concluded that frequency shifts will often be dependent upon the concentration of base used, even if values are measured in the same solvent, so they recommended that frequency shift measurement should be studied in an inert solvent with as low a concentration of base as possible.

Nitriles are examples of bases which show a large concentration dependence. Figure 11 illustrates the effect of nitrile concentration on phenol frequency shifts in carbon tetrachloride solution, while Figure 12 shows the effect of concentration changes on the band intensities of methanol in *n*-hexane.

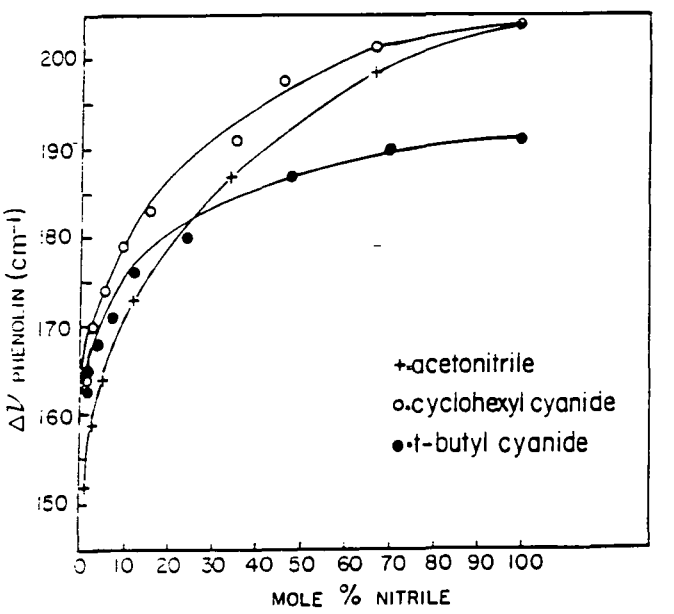

Figure 11 Effect of nitrile concentration on $\Delta\nu$ of phenol in CCl_4[10]

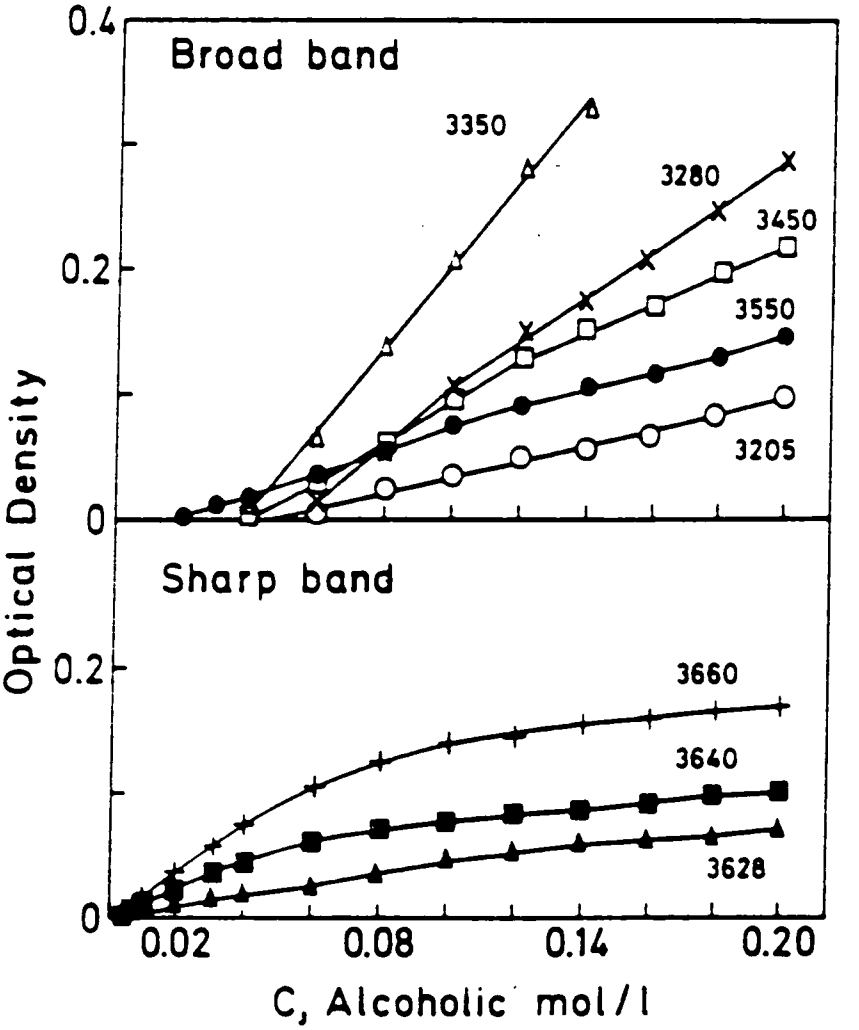

Figure 12 Optical densities of the $\bar{\nu}_{ij}$ band assigned for different species versus molar concentration in the methanol / n-hexane system.

(+) 3660cm^{-1} assigned to monomers.
(▪) 3640cm^{-1} assigned to linear dimers.
(▵) 3628cm^{-1} assigned to linear trimers.
(•) 3550cm^{-1} assigned to cyclic dimers.
(□) 3450cm^{-1} assigned to cyclic trimers.
(▵) 3350cm^{-1} assigned to cyclic tetramers.
(x) 3280cm^{-1} assigned to cyclic pentamers.
(o) 3205cm^{-1} assigned to cyclic hexamers[55]

1.2.6 Solvent Variations

The absorption of the ν_s band may be altered either by acidic or basic solvent.

In the case of weak hydrogen bond acceptor solvents one must take into account that the band profile consists of two components: the bonded and non-hydrogen bonded ν(OH) band. The ν(OH) bands show very strong interaction with other molecules having proton-attracting power. Naturally, there is a strong influence exerted by these compounds when they are used as solvents on the OH-group, which can be detected spectroscopically. Changing from "inert" solvents (e.g. carbon tetrachloride) to solvents which are supposed to possess a stronger interaction (Figure 13), always results in a broadening of the band, combined with decreasing intensity, in addition to a change to lower frequency. This shows that the equilibrium internuclear distance increases on account of inter-molecular interaction and a decrease in the OH dipole moment, and weaker absorption follows. So the absorption spectra of alcohols are of special value in the study of the association of substances. In dilute solutions in inert solvents a narrow band at 3638cm^{-1} arises which is attributed to the ν(OH) mode of the isolated molecule. As the concentration of the solution increases, a broad OH-band at 3520cm^{-1} arises, attributed to the OH-vibration of the dimer. Its intensity increases rapidly and finally masks completely the band of the monomer.

Early solvent theories were based on dielectric effects. The Kirkwood-Bauer-Magat[37] relationship (KBM) is generally written as

$$\frac{\nu_0 - \nu_s}{\nu_0} = C(\epsilon-1) / (2\epsilon+1) \qquad (17)$$

Where ϵ is the macroscopic dielectric constant and

C is a constant that depends on the dimensions and electrical properties

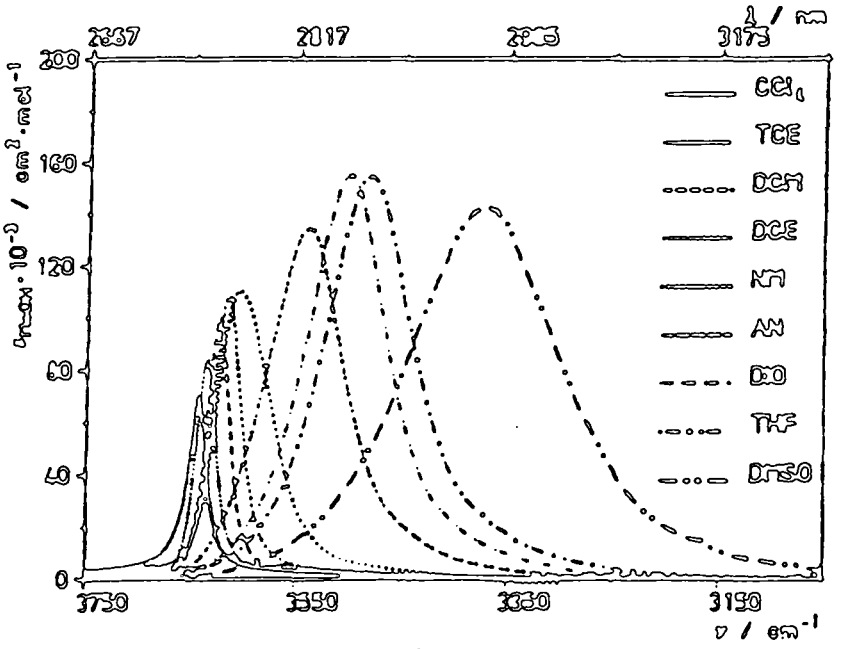

Figure 13(a) Fundamental ν(OH) bands of CH_3OH solutions at 20°C. Series of solvents are from higher to lower frequency.[32]

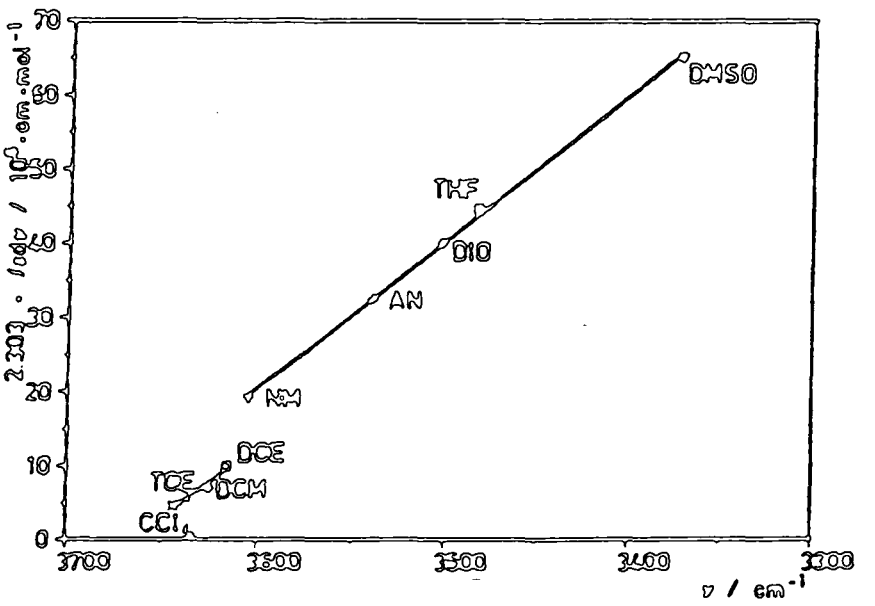

Figure 13(b) Integrated ν(OH) fundamental intensities increase with increasing interactions in different solvents.[32]

CCL_4=Tetrachloromethane ;TCE=1,1,1–Trichloroethane.;
DCM=Dichloromethane.;DCE=1,2–Dichloroethane.;
NM=Nitromethane.;AN=acetonitrile.;
DIO=Dioxane.;THF=Tetrahydrofuran.;DMSO=Dimethylesulfoxide.

This equation has been modified to

$$\frac{\nu_0 - \nu_s}{\nu_0} = C(n_0^2 - 1) / (2n_0^2 + 1), \qquad (18)$$

where n_0 is the refractive index.

This equation is not satisfactory[10] for predicting the magnitude of solvent shifts. So Pullin[38] derived the following equation

$$\frac{\nu_0 - \nu_s}{\nu_0} = C_0 + A\left\{[(n^2 - 1)/(2n^2 + 1)R] + B[(\epsilon - 1)/(2\epsilon + 1)R]\right\} \qquad (19)$$

then Buckingham[39] gives better agreement,

for polar solvent

$$\frac{\nu_0 - \nu_s}{\nu_0} = C + C_\epsilon(\epsilon - 1)/(2\epsilon + 1) + C_n(n^2 - 1)/(2n^2 + 1) \qquad (20)$$

or

$$\frac{\nu_0 - \nu_s}{\nu_0} = C + \tfrac{1}{2}(C_\epsilon + C_n)\left(\frac{\epsilon - 1}{2\epsilon + 1}\right) \qquad (21)$$

for non-polar solvents.

However these are still not satisfactory for explaining ν_{AH} frequency shifts since they do not consider specific association or hydrogen bonding.

1.2.7. Correlation of $\Delta\nu_s$ with physical properties

The quantity $\Delta\nu_s$ is related to important chemical and physical properties of hydrogen bonding systems: hydrogen bond enthalpy, interatomic distances, chemical reactivity, ΔH of solution, base strength, ...etc.

For example there is a different influence of hydrogen bonds and of Van der Waals interactions on the fundamental intensities, corresponding to the bigger frequency shift $\Delta\nu$ by hydrogen bond energies ΔH compared with Van der Waals ones. In the case of a strong increase in absorption ($\int \epsilon d\nu$) of the ν_s(OH) band, the intensity-frequency distribution is not directly related to the distribution of different hydrogen bond energies.

Purcell and Drago[40] found that the enthalpy shift correlates in terms of ΔE_{OH}, the change in OH bond energy when OH···B forms, and E_{HB} the energy of the hydrogen bond H···B. The enthalpy change, ΔH, is represented as

$$\Delta H = \Delta E_{OH} + E_{HB} \tag{22}$$

The equations

$$\Delta H = -(hcN/4x_e)\,\Delta\omega_{OH} + E_{HB} \tag{23}$$

and

$$\Delta E_{OH} = -(hcN/4x_e)\,\Delta\omega_{OH} \tag{24}$$

were derived, where h is Planck's constant, c is the speed of light, N is Avogadro's number, x_e is the anharmonicity constant, and $\Delta\omega_{OH}$ is the anharmonicity energy in cm^{-1}. Values for both ν_{OH} and $\nu_{H\cdot\cdot B}$ are needed to calculate $\Delta\omega_{OH}$.

Equation 22 was expanded[10] to include V_{OB}, the Van der Waals repulsion between O and B

$$\Delta H = E_{HB} + (\Delta E_{OH} + V_{OB}) \tag{25}$$

The equation

$$\Delta\nu = \Delta\nu_{OH} + \nu_{HB} \tag{26}$$

was used to represent the frequency shift, where $\Delta\nu_{OH}$ is the decrease in OH frequency as a result of weakening of the OH bond and ν_{HB} is the increase in the OH frequency caused by forming the HB bond and mixing of OH and HB motions. Figure 14 is used as an explanation for the change in sensitivity of ΔH and $\Delta\nu$ for weak hydrogen bonds and the non-zero intercepts for $\Delta\nu - \Delta H$ correlations.

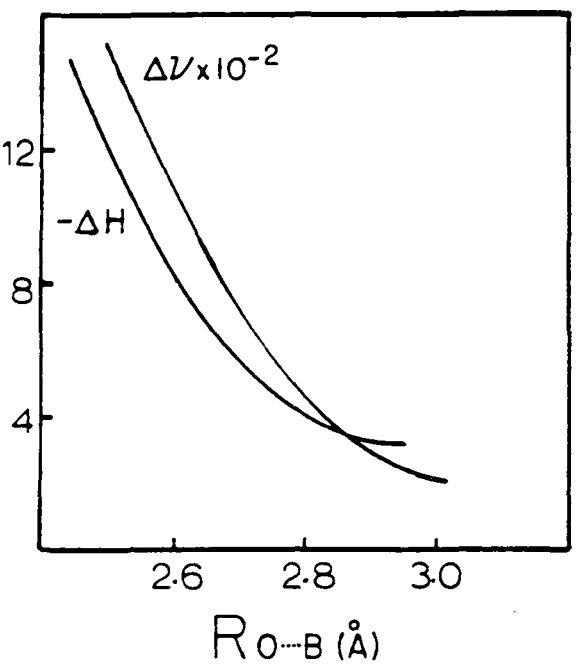

Figure 14 Lippincott-Schroeder relations of $-\Delta H$ and $\Delta\nu$ versus oxygen donor distance. $\Delta\nu$ in hundreds of cm^{-1}, ΔH in kcal/mole.[10]

1.3 Multiple Equilibrium

Data obtained by infrared absorption measurements are used to study the equilibrium of alcoholic materials between the free (or unassociated) state and the hydrogen bonded (or associated) state.

Kempter and Mecke[41] considered equilibria of the type

$$(ROH)_n + (ROH) \rightleftharpoons (ROH)_{n+1} \qquad (27)$$

where the subscripts n and n+1 refer to complexes of the n^{th} and $n+1^{th}$ order.

They assumed that the dissociation constants were equal for all sizes of complexes and hence derived the equation

$$K_C = \frac{\alpha C}{(1-\sqrt{\alpha})} \qquad (28)$$

where K_C is the general dissociation constant applicable to each series complex.

α is the fraction of alcohol molecules which are unassociated and C is the initial molar concentration. When they plotted αC *versus* $\sqrt{\alpha}$ for phenol, they obtained a straight line plot from which they concluded that agreement between their theory and experiments was satisfactory.

Coggeshall and Saier[42] rejected the assumption of equality of all dissociation constants. They used instead, a distinct constant K_1 for dissociation of the dimer complex (n = 1) and a general constant K_C for all others (*i.e.* $K_2 = K_3 = K_4 \cdots = K_C$). This procedure is based on evidence from three different considerations:-

a) The shape and wavelength maxima of the complex bands at low concentration

b) the disagreement with data encountered using the simpler scheme (described above) and,

c) the evidence that the potential energy in the formation of a dimer complex is considerably less than the potential energy change when an n-fold complex adds a member to become an n+1-fold complex.

To simplify the theory, Franks[43] considers the formation of dimers

$$2\ \text{mono} \rightleftharpoons \text{dimer} \tag{29}$$

$$K_{12} = (\text{di})/(\text{mono})^2 \tag{30}$$

where (mono) is the concentration of monomers *i.e.* molecules not forming hydrogen bonds (IR assignment for CH_3OH/CCl_4 at $3643cm^{-1}$) and K_{12} is the equilibrium constant for equation 29.

In pure liquid substances which have a strong tendency to form hydrogen bonds, the proportion of potential bonds not actually formed will be very small. In many systems there will be only a few per cent of the "free" X-H groups present. On the assumption that sharp X-H bands are caused only by free X-H groups but not by those bound by hydrogen bonds, it can be stated that

$$\alpha = \epsilon_c/\epsilon_0 = \text{mono}/C \tag{31}$$

where C is the analytical concentration and α is a fraction representing the ratio of the extinction coefficient ϵ_c at concentration C to ϵ_0 at infinite dilution ($C \rightarrow 0$). In the case of dimer formation, equation 31 becomes

$$(\text{di}) = \tfrac{1}{2}[C-(\text{mono})] = \tfrac{1}{2}C[1-(\tfrac{\epsilon_c}{\epsilon_0})] \tag{32}$$

substituting from equation 32 and 31 for equation 30 becomes

$$K_{12} = [2C^2(\epsilon_c^2/\epsilon_0^2)]/[C\{1-(\epsilon_c/\epsilon_0)\}] \tag{33}$$

i.e.
$$1-(\epsilon_c/\epsilon_0) = (2/K_{12})(\epsilon_c^2/\epsilon_0^2)C \tag{34}$$

$\therefore$
$$\epsilon_c = \epsilon_0(2/K_{12})(\epsilon_c^2/\epsilon_0)C \tag{35}$$

Plotting ϵ_c against $\epsilon_c{}^2C$, should result in a straight line (if the assumption of exclusive dimerization is correct) with an intercept of ϵ_o.

From equation 33 it then follows that

$$(\text{mono})^2/[C-(\text{mono})] = \tfrac{1}{2}K_{12} \qquad (36)$$

At a given temperature the variation of the dimer concentration with total alcohol concentration can be found from the relation

$$(\text{di}) = K(\text{mono})^2 = KC^2(\epsilon_m/\epsilon_m^0)^2 \qquad (37)$$

Where ϵ_m^0 is the extrapolated extinction coefficient at zero concentration of the monomer species. Table 6 shows the effect of temperature on K_c.

From the integrated intensity, B_d, of the 3500cm^{-1} band and the calculated dimer concentration the true integrated molar absorption coefficient, B_d^0 can be determined at each concentration and checked for constancy. In both ethanol and *t*-butanol an approximately constant value was found,[43] but in methanol the calculated dimer absorption coefficient increased with concentration at each temperature. Such behaviour indicates either that the 3500cm^{-1} band is increasing with concentration more rapidly than expected for a dimer absorption or that the concentration of monomer has been underestimated at the higher concentrations of alcohol. The latter is highly improbable since absorption by other species (non-bonded OH-groups of open dimers or multispecies) at the monomer frequency would cause the calculated monomer concentration to be too high, rather than too low. The 3500cm^{-1} band does not increase rapidly enough with concentration to be due only to trimer, but it is possible that two species, dimer plus presumably, trimer, absorb at this frequency. No separate band was found for any of the alcohols studied in others work which could be correlated with the band found in the matrix isolated studies at 3445cm^{-1} and attributed to trimer. It is conceivable that dimer and trimer bands overlap so as to be

Table 6 Equilibrium Constants for (monomer–trimer–octamer) Fits of Liddel and Becker's IR Data[a,16]

T, °C	MeOH	EtOH	*t*–BuOH
	0.0048	0.0080	0.0048
–10	$K_3=(3.15\pm0.39)\times10^2$	$K_3=(3.16\pm0.65)\times10^2$	$K_3=(5.88\pm0.14)\times10^2$
	$K_8=(1.63\pm0.28)\times10^9$	$K_8=(2.21\pm0.60)\times10^9$	$K_8=(1.59\pm0.08)\times10^9$
	0.0047	0.0066	0.0035
0	$K_3=(1.71\pm0.24)\times10^2$	$K_3(1.31\pm0.26)\times10^2$	$K_3=(2.22\pm0.05)\times10^2$
	$K_8=(9.4\pm1.6)\times10^7$	$K_8(1.03\pm0.23)\times10^8$	$K_8=(5.08\pm0.22)\times10^7$
		0.0056	0.0022
5		$K_3=84.7\pm15.4$	$K_3=(1.34\pm0.02)\times10^2$
		$K_8=(2.55\pm0.46)\times10^7$	$K_8=(9.70\pm0.30)\times10^6$
	0.0042		
10	$K_3=70.8\pm9.8$		
	$K_8=(4.71\pm0.50)\times10^6$		
	0.0052	0.0046	0.0016
15	$K_3=51.2\pm12.8$	$K_3=33.3\pm5.9$	$K_3=57.2\pm0.8$
	$K_8=(9.7\pm2.3)\times10^5$	$K_8=(1.61\pm0.18)\times10^6$	$K_8=(5.97\pm0.15)\times10^5$
	0.0010	0.0041	0.0024
25	$K_3=6.21\pm0.53$	$K_3=15.5\pm2.9$	$K_3=25.7\pm0.7$
	$K_8=(1.24\pm0.02)\times10^5$	$K_8=(1.36\pm0.16)\times10^5$	$K_8=(4.20\pm0.19)\times10^4$
	0.0017	0.0037	0.0027
35	$K_3=5.38\pm0.54$	$K_3=6.7\pm1.5$	$K_3=14.0\pm0.6$
	$K_8=(7.6\pm1.6)\times10^3$	$K_8=(1.51\pm0.50)\times10^4$	$K_8=(4.50\pm0.28)\times10^3$
	0.0005	0.0033	0.0033
45	$K_3=1.23\pm0.10$	$K_3=2.8\pm1.0$	$K_3=8.9\pm0.7$
	$K_8=(2.49\pm0.14)\times10^3$	$K_8=(3.5\pm1.9)\times10^3$	$K_8=(6.1\pm0.5)\times10^2$

[a] All quantities are in molar units

unresolvable in the temperature range of -15° to $+60^{\circ}$C in Liddel and Becker's work.[44]

Theoretically the next simplest case is the aggregation to form trimers. For a superimposition of dimer and trimer formation we have

$$3\ \text{mono} \rightleftharpoons \text{tri} \tag{38}$$

$$K_{13} = (\text{tri})/(\text{mono})^3 \tag{39}$$

$$C = (\text{mono}) + 2(\text{di}) + 3(\text{tri}) \tag{40}$$

$$[C-(\text{mono})] / (\text{mono})^2 = \left[\frac{2}{K_{12}}\right] + \frac{3}{K_{13}}(\text{mono}) \tag{41}$$

If instead of equation 36 we use equation 41 and plot $[C-(\text{mono})] / (\text{mono})^2$ against (mono) we should expect a straight line, the slope of which allows the calculation of K_{13} and the intercept that of K_{12}, while the equation for the extinction coefficient becomes

$$\epsilon_m = \epsilon_m^0 [(C - 2K_{12}C^2 - 3K_{13}C^3) / C] \tag{42}$$

The aggregation tendency can be expressed by the mean number of monomers, f, forming the multiple species (found in CH_3OH/CCl_4 at $3332cm^{-1}$ band), thus describing the average aggregation number by defining f.

$$f = (\sum_n nC_n) / \sum_n C_n = C/\sum_n C_n \tag{43}$$

Where

C_n designates the concentration of the n-mer in mole/dm^3, then f may be calculated from the formula

$$f = C / \int_0^{\epsilon_c} (\frac{1}{\epsilon_c}) d(\epsilon_c C) \tag{44}$$

According to equation 44 one obtains f by graphical integration of the plot of $1/\epsilon_c$ against $\epsilon_c C$.

Multiple species would cause a large deviation from the straight line. The theoretical calculation of such a high degree of association is possible only approximately. One of the best known methods is the one worked out by Mecke and Kempter.[45] They assumed superimposed equilibria from dimer formation up to aggregates of n-molecules:–

$$C = (\text{mono}) + 2(\text{di}) + 3(\text{tri}) + 4(\text{tetra}) + \cdots n(\text{n–mer}) \tag{45}$$

$$C = (\text{mono}) + \frac{2}{K_{12}}(\text{mono})^2 + \frac{3}{K_{13}}(\text{mono})^3 + \frac{4}{K_{14}}(\text{mono})^4 \cdots \frac{n}{K_{1n}}(\text{mono})^n \tag{46}$$

$$C = (\text{mono}) \sum_{i=1}^{n} \frac{i}{K_{1i}} (\text{mono})^{i-1} \tag{47}$$

$$C = (\text{mono}) \sum_{i=1}^{n} \frac{i}{K_{1i}} (\alpha C)^{i-1} \tag{48}$$

with $K_{11} = 1$. The following simplifying assumption was introduced

$$K_{12} = K_{23} = \ldots + K_{(i-1)i} = K_{MK} \tag{49}$$

Thus

$$K_{1i} = K_{MK}^{(i-1)} \tag{50}$$

and

$$[\alpha(\text{mono})/K_{MK}] < 1 \tag{51}$$

Then for $n \longrightarrow \infty$

$$\alpha = (\text{mono})/C \sim [1-(\alpha C/K_{MK})]^2 \tag{52}$$

or

$$\epsilon_c^{\frac{1}{2}} = \epsilon_0^{\frac{1}{2}} - (\epsilon_c C / \epsilon_0^{\frac{1}{2}} K_{MK}) \tag{53}$$

By plotting $\epsilon_c^{\frac{1}{2}}$ against $\epsilon_c C$, a straight line should be obtained with an intercept of $\epsilon_0^{\frac{1}{2}}$. For equilibrium constant calculations

$$K_{1n} = (\text{mono})^n/N_0 = n(\text{mono})^n/[C-(\text{mono})]$$
$$= n\ \alpha_n^n\, C^{n-1} \,/\, 1-\alpha_n \qquad (54)$$

Where N_0 = concentration of aggregate of n–molecules

or with
$$\alpha = (\text{mono})/C \qquad (55)$$

where
$$\alpha_n = 1-(n-K)\alpha_n^n\, C^{n-1} \qquad (56)$$

For medium concentration of alcohols equation 53 is fairly well-satisfied. At low concentrations, however, clear deviations occur. A question which becomes important in this range is whether the broad band of hydrogen bonds overlap with the region of "free" vibrations. As a first consideration one should not expect this to be the case, because hydrogen bonding ought to induce a displacement to longer wavelengths. The large bandwidth has, however, not yet been satisfactorily explained. If it is due to a short lifetime of the hydrogen bonds, an overlap into the range of the vibrations may have to be considered. With this assumption one would have to consider a correction of the extinction coefficients in the range of high concentration, and this can be done approximately. The difficulties are greater in the fundamental range, where the intensity of the bands due to hydrogen bonding is much higher and thus the superimposition effects are quite a different order of magnitude. This is particularly true for spectra of pure liquids where free vibration and hydrogen bond vibration bands are much less well separated.

One may use a constant K_{MK} in equation 49 as a first approximation for concentrations above 0.02 - 0.1 mole/dm^3.[43] At low concentrations however, large deviations appear (as explained before). This being the case, one would

expect similar deviations for a large range of substances and they have in fact been observed for alcohols. Various corrections to this approximation have been suggested for small aggregates.. Hoffman[46] in the case of methanol makes use of the the assumption

$$K_{12} \neq K_{23} \neq K_{34} \quad \text{for} \quad i > 4K_{(i-1)_i} = K_{MK} \tag{57}$$

His experiments yielded $K_{12} \rightarrow \infty$ or $(di) \rightarrow 0$.

When determining the mean degree of association n (equation 54) it is clearly seen that $n \geq 3$. From his careful measurements of the second harmonic vibration, Hoffman[46] found the equilibrium constants shown in Table 7.

Table 7 Equilibrium Constants for Alcohols in CCl_4 at 21.5°C[43]

K^*	Methanol	*t*–Butanol	Phenol
K_{12}	∞	1.52	0.88
K_{13}	0.062	0.28	0.19
K_{14}	0.013	0.08	0.05
K_{23}	0.25	0.53	0.43
K_{34}	0.23	0.43	0.37
K_{MK}	0.24	0.99	0.42

*K values are in molar units

But when Coggeshall and Saier[42] suggested the approximation of $K_{12} = K_{23}$ for $i > 3K_{(i-1)_i} = K_{MK}$ the suggestion of separating only the dimer and trimer formation from the higher aggregations is in agreement with the estimate from dipole-dipole interactions. The suggestion receives experimental support from the hint that at low concentrations all the alcohols display a band in the fundamental frequency range due to hydrogen bonding which is different from those appearing at high concentrations ($3250cm^{-1}$ in Figure 15 and References 47, 48, 49). Franks[43] disagrees with that suggestion for the methanol case.

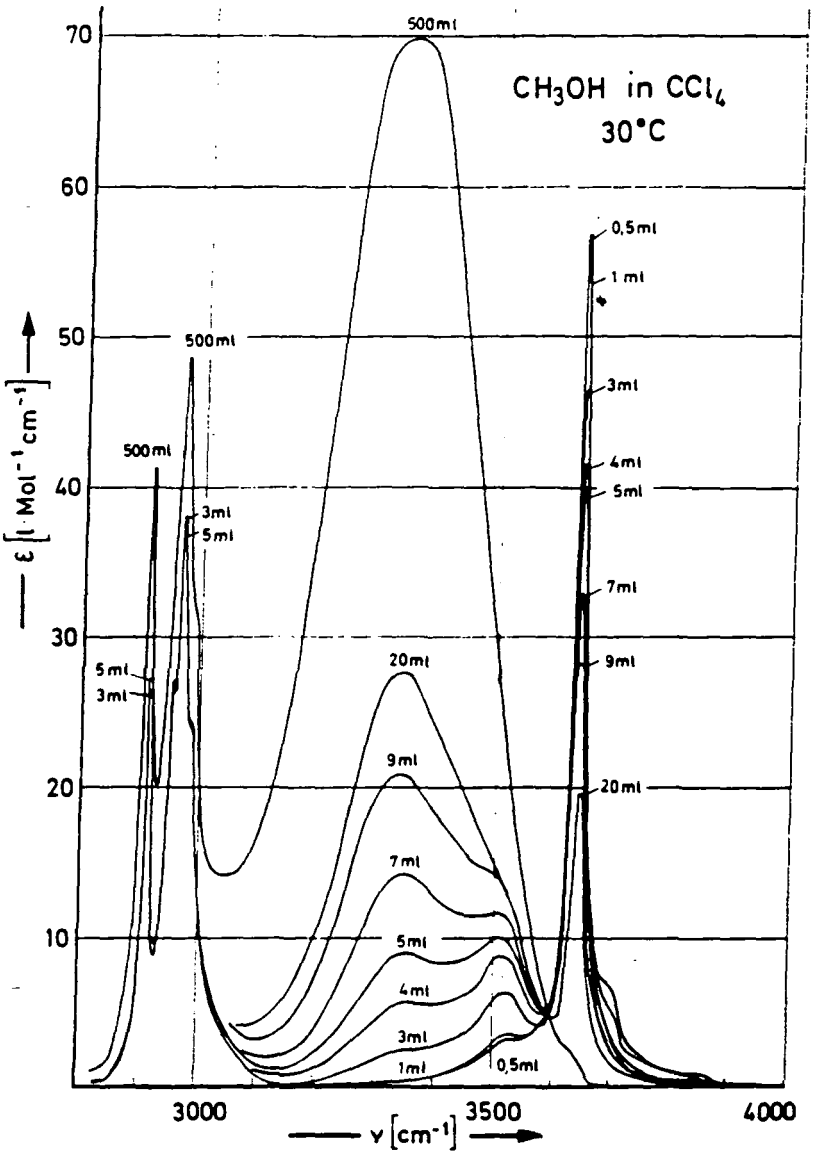

Figure 15 Extinction coefficients of CH_3OH at different concentrations in CCl_4 at 20°C (fundamental vibration). The intensity of the hydrogen bonded band is much higher than the unperturbed band.[43]

From his measurements of the fundamental vibration one obtains equilibrium constants at 20°C displaying a systematic difference with concentration. In the concentration range of 1.5 to 3.2 g/dm^3 (0.046 – 0.1 mol/dm^3) methanol in carbon tetrachloride it is, however, possible to fit the results of the fundamental vibration measurements into the assumption that cyclic tetramers are formed exclusively with $K_{14} = 0.007$. This is in agreement with the experience of other authors that only small amounts of dimers are formed in solutions of methanol. At high concentrations the mean degree of association rises steeply with increasing methanol concentration. In highly concentrated solutions the fraction of OH-groups not participating in hydrogen bonds falls far below 10% in the case of methanol (see Figure 16). From the theories of systems consisting of pure associated liquids it should follow from the above that the hydrogen bond share dominates.

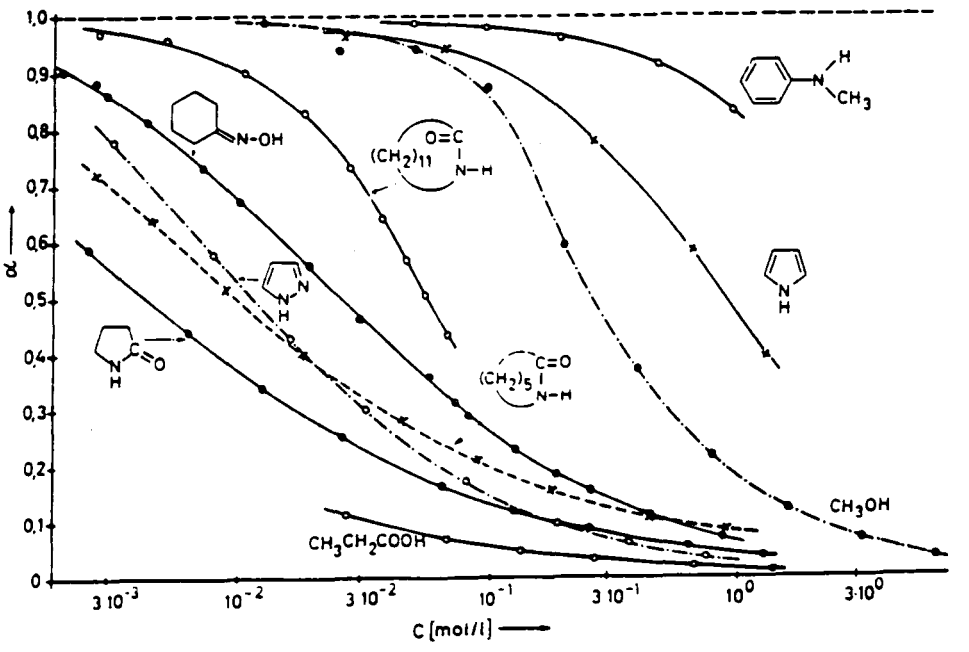

Figure 16 Amounts of spectroscopically determined non-hydrogen bonded X-H groups in CCl_4 solutions at 20°C[43]

Besnard, Cabaço, Strehle and Yarwood[50] have used a set of equilibria explaining the band shape of acetonitrile in methanol (binary mixture)

$$\underset{A-x_1}{CH_3CN} + \underset{B-x_1-x_2-2x_3-3x_4-4x_5}{CH_3OH} \rightleftharpoons \underset{x_1}{C_1\text{-complex}},$$

$$K_1 = \frac{x_1}{([A]-x_1)([B]-x_1-x_2-2x_3-3x_4-4x_5)} \tag{58}$$

$$\underset{X_1-X_2}{C_1\text{-complex}} + \underset{B-x_1-x_2-2x_3-3x_4-4x_5}{CH_3OH} \rightleftharpoons \underset{x_2}{C_2\text{-complex}},$$

$$K_2 = \frac{x_2}{(x_1-x_2)([B]-x_1-x_2-2x_3-3x_4-4x_5)} \tag{59}$$

$$\underset{B-x_1-x_2-2x_3}{2CH_3OH} \rightleftharpoons \underset{x_3}{(CH_3OH)_2},$$

$$K_3 = \frac{x_3}{([B]-x_1-x_2-2x_3)^2} \tag{60}$$

$$\underset{B-x_1-x_2-2x_3-3x_4}{3CH_3OH} \rightleftharpoons \underset{x_4}{(CH_3OH)_3},$$

$$K_4 = \frac{x_4}{([B]-x_1-x_2-2x_3-3x_4)^3} \tag{61}$$

$$\underset{B-x_1-x_2-2x_3-3x_4-4x_5}{4CH_3OH} \rightleftharpoons \underset{x_5}{(CH_3OH)_4},$$

$$K_5 = \frac{x_5}{([B]-x_1-x_2-2x_3-3x_4-4x_5)^4} \tag{62}$$

where [A] is the CH_3CN initial experimental concentration

and [B] is the CH_3OH initial experimental concentration

Since the values of the equilibrium constants required to simulate the concentrations in these equations are not easy to obtain due to difficulties in deciding the presence and number of aggregates, (as described above), they used previous data, Table 8, obtained from experiments in non-polar solvents[50-52], to predict the expected number of CH_3OH species existing in solution.

Table 8 Collected equilibrium constants and frequencies for various monomer *n*–mer theoretical curves[51]

	MeOH–CCl_4	EtOH–CCl_4	*t*–BuOH–CCl_4	phenol–CCl_4	Units
K_2	0.60	0.70	0.72	0.67	L/M
K_3	3.83	5.19	5.6	4.78	L^2/M^2
K_4	28.4	44.9	50.3	39.6	L^3/M^3

Chapter 2

Experimental

2.1 Materials

Aldrich spectrophotometric grade carbon tetrachloride, methanol and acetonitrile were used without further treatment other than drying over molecular sieves.

Binary mixtures of methanol in acetonitrile solutions were prepared in the concentration range of 0.01:0.99 mole fraction (0.197:20.39 mol dm^{-3}) to 0.9:0.1 mole fraction (21.94:2.28 mol dm^{-3}). For each collected sample spectra the corrected solvent (percentage mole fraction used) background spectra were subtracted. Four of these concentrations (0.04:0.96, 0.06:0.94, 0.55:0.45 and 0.9:0.1 mole fraction) were used for a temperature study in the range from –22.6°C (250K) to 82.2°C (355K).

For ternary mixtures, a stock solution of methanol in carbon tetrachloride in the concentration range 4.937 $x10^{-3}$ to 0.0246 mol dm^{-3} of methanol were prepared. Only two stock concentrations of 4.937$x10^{-3}$ and 0.0197 mol dm^{-3} of methanol were used. A concentration range of acetonitrile of 0.0411–6.168 mol dm^{-3} (4.927$x10^{-3}$ – 0.138 mol dm^{-3} CH_3OH) was obtained by mixing different amounts of the stock solutions. For each solution, the spectra of the same acetonitrile concentration in carbon tetrachloride were subtracted from the solution spectra.

2.2 Spectrometer

Spectra were taken with a Perkin-Elmer 580B Infrared Spectrophotometer in the frequency range 4000-3000cm^{-1} with a spectral resolution of 2.5cm^{-1}.

Solution spectra were measured in a cell with potassium bromide windows and with different suitable path lengths depending on the concentration. For methanol in acetonitrile binary mixtures, three different cell thicknesses were used. A path length of 17.5μm used in the concentration range of 0.01-0.08 methanol mole fraction (0.197-1.65 mol dm^{-3}) , 18.5μm in a concentration range of 0.1-0.5 methanol mole fraction (2.08–13.71 mol dm^{-3}) and 6μm for a concentration range of 0.55-0.9 methanol mole fraction (12.45-21.94 mol dm^{-3}).

In the case of ternary mixture solutions of methanol:acetonitrile:carbon tetrachloride, different cell thicknesses between 550μm-and 5mm were used; the exact thickness used will be written on each spectra. All thicknesses were measured either from their optical interference pattern or by micrometer. Care was taken to fill the cells without introducing the smallest traces of moisture. The temperature measurements were made directly in the thermostatted stoppered absorption cell.

Spectra obtained were controlled by computerized Perkin-Elmer Infrared Data Station.

The spectrophotometer was attached to a purge unit in order to reduce water moisture circulation inside the instrument during the experimental work.

2.3 Computer

Frequency and intensity data measured were reformatted by a personal basic program to be used in different band fitting computer programs.

The spectra of binary mixture of methanol in acetonitrile in the concentration range of 0.35-0.45 methanol mole fraction (7.59-9.98 mol dm^{-3}) were used extrapolated to a frequency lower than 3300cm^{-1}, and smoothed to eliminate the band interference of the residual of subtracted band observed at 3200cm^{-1} and to obtain the best possible band fitting.

Chapter 3

Results and Data Analysis

3.1 Introduction

Because of a lack of comprehensive quantitative interpretation, the study of hydrogen bonding in alcohols remains controversial and unsettled. In this work, the absorption of infra-red radiation in the hydroxyl stretching region (4000-3000cm^{-1}) was investigated.

This chapter describes the observed spectra of methanol in carbon tetrachloride which reduces the degree of hydrogen bond self association of methanol. Such information will help in analyzing the spectra of methanol in ternary and then binary systems (which is the aim of our study).

Due to complications observed in the spectra of ν_s(OH) of methanol in acetonitrile solution, a band fitting program was used to elucidate the possible number of band components for each concentration. Finally, a model fitting program was used to explore the multiple equilibria which exists in methanol-binary systems.

3.2 Methanol in Inert Solvent

With a few exceptions, the general agreement of studying hydrogen bonding in alcohols is only of a qualitative nature. Liquid phases of alcohols, either neat or dissolved in inert solvents, are constituted of labile clusters (often called multimers) of molecules linked by hydrogen bonds between their hydroxyl group and the oxygen electronic lone pair of a nearest neighbour acting as a proton acceptor. Non-bonded hydroxyl groups nevertheless exist in a proportion which increases with the dilution. Obviously these "free" OH groups can belong either to monomers or to one of the two ends (termini) of an open chain cluster or to end groups. The clusters are permanently breaking and reforming at mean time intervals. Infra-red spectroscopy, whose intrinsic time scale is shorter than this mean time interval, can distinguish between free and bound hydroxyl groups as described below.

Spectra of methanol in carbon tetrachloride, at a very low concentration of methanol (from 0.00493 to 0.0246 mol/dm^3), were collected and shown in

Figures 17 and 18. Figure 17 shows the spectra of methanol at different concentrations: 0.00987 – 0.0246 mol/dm^3. A sharp band was observed at 3645cm^{-1} which has been assigned (by most authors[57,62]) to the monomer band. This band increases almost linearly in intensity (with no change in frequency) with increasing methanol concentration, as shown in Figure 19. This is in agreement with Montague and Dore.[53] A small band appears at high frequency of the monomer band at 3710cm^{-1}, which also increases linearly in intensity with increasing methanol concentration (Figure 19). This band still exists even after 100% carbon tetrachloride spectra subtraction from the sample spectrum (Figure 20). To our knowledge no one has assigned this band before, although it did appear in some references[43] Palinkas and his workers[54] assigned the ν(OH) of methanol in the gas phase at 3693cm^{-1} at 22°C.

To the low frequency side of the monomer band, two bands could be identified. The first band is at 3527cm^{-1} while the second is at 3442cm^{-1}. Both were assigned by Martinez[55] to the cyclic dimer and cyclic trimer respectively.

Going to lower methanol concentration, (0.00493 mol/dm^3), and using higher pathlength the spectra are as shown in Figure 18, the 3710cm^{-1} band became relatively more intense, with a very small shoulder appearing at 3620cm^{-1} which was assigned[57] as the linear trimer.

In Figure 18 a band starts to appear at 3464cm^{-1} at 0.0098 mol/dm^3, and on increasing the concentration further this band disappeared and was replaced by another band at 3527cm^{-1}. This might be due to the cyclic dimer. This proves that although most of the studies[15,5,56] did not consider the dimer to be an important species (compared with the tetramer) in the vapour state, its concentration may be significant in dilute solutions of alcohols in non-polar solvents, as shown in this work. Table 9 shows the summary of the collected data from the major band in the spectra of methanol in carbon tetrachloride.

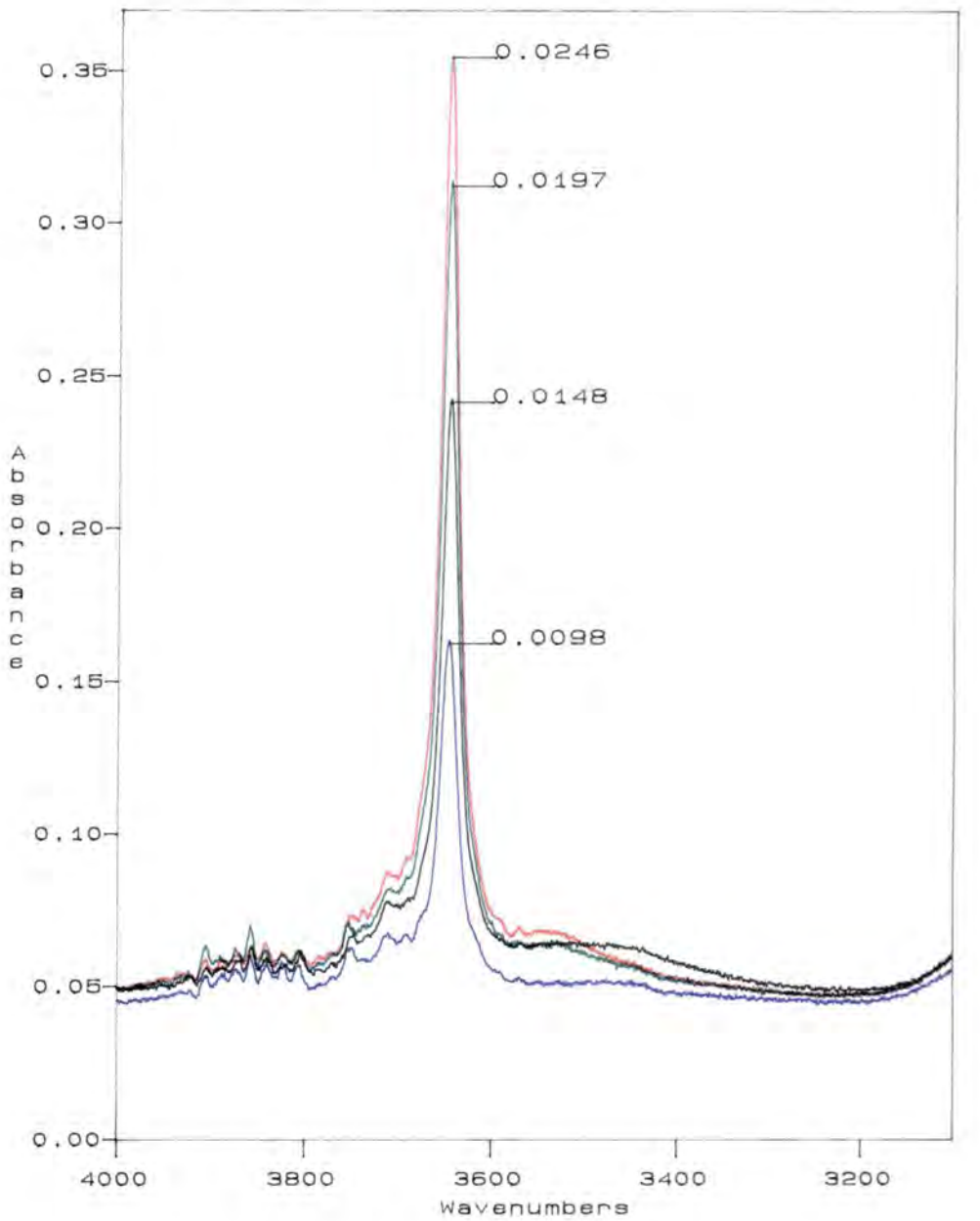

Figure 17 ν(OH) stretching mode of methanol in CCl_4 at different concentrations in mol/dm^3, using 2.5mm pathlength

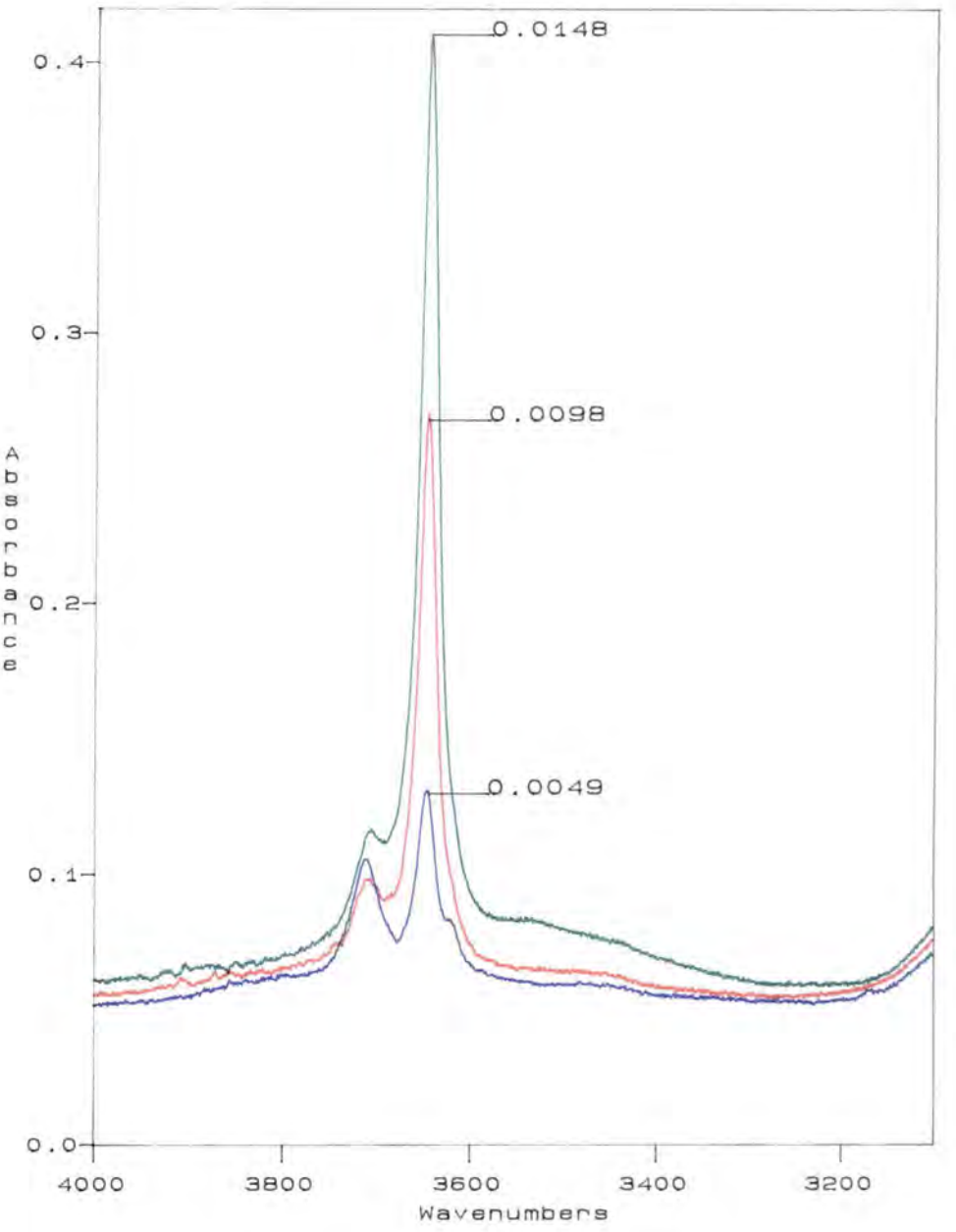

Figure 18 ν(OH) stretching mode of methanol in CCl_4 at different concentrations in mol/dm^3, using 5mm pathlength

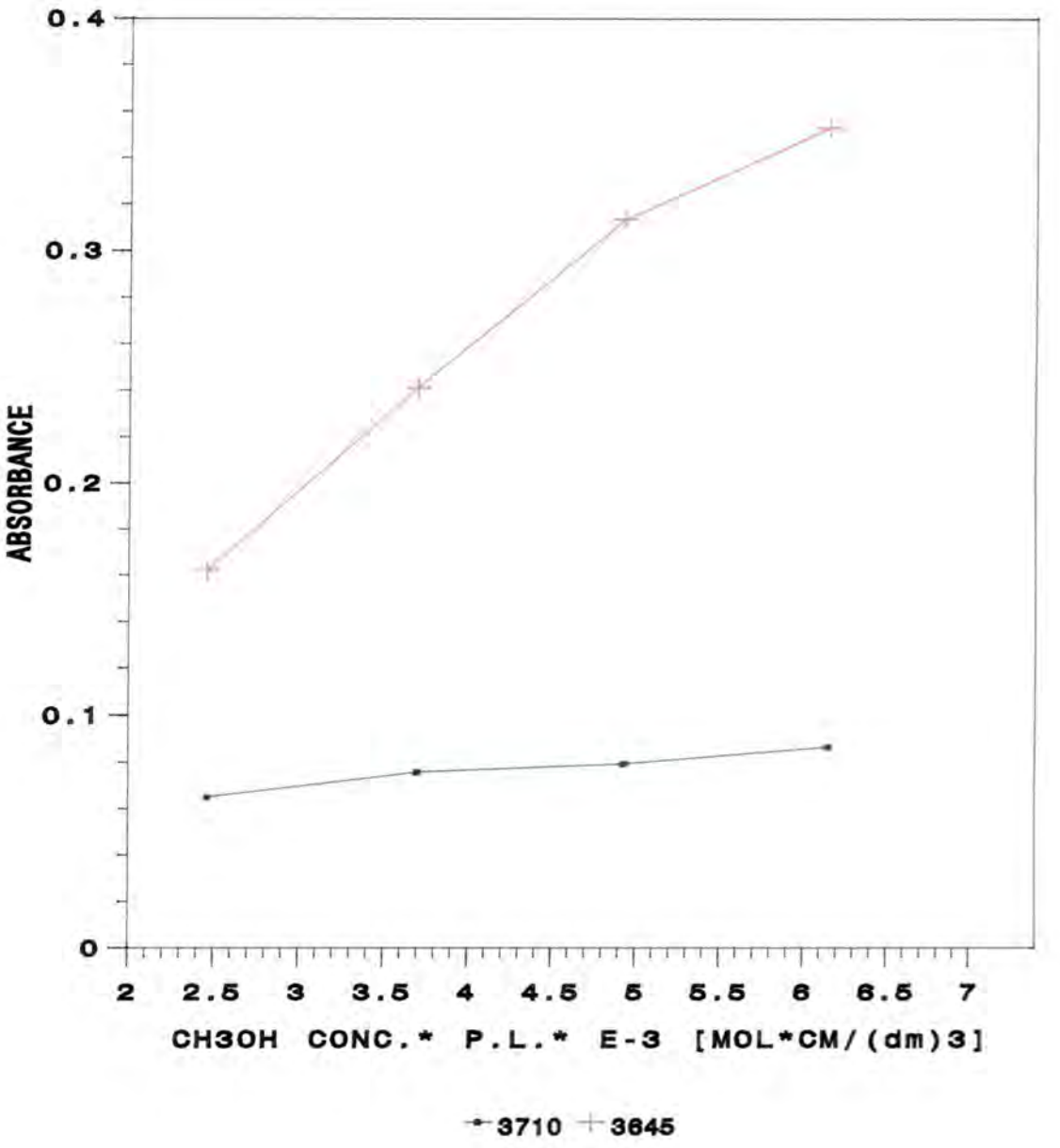

Figure 19 ν(OH) stretching absorbances of methanol in carbon tetrachloride at different frequencies.

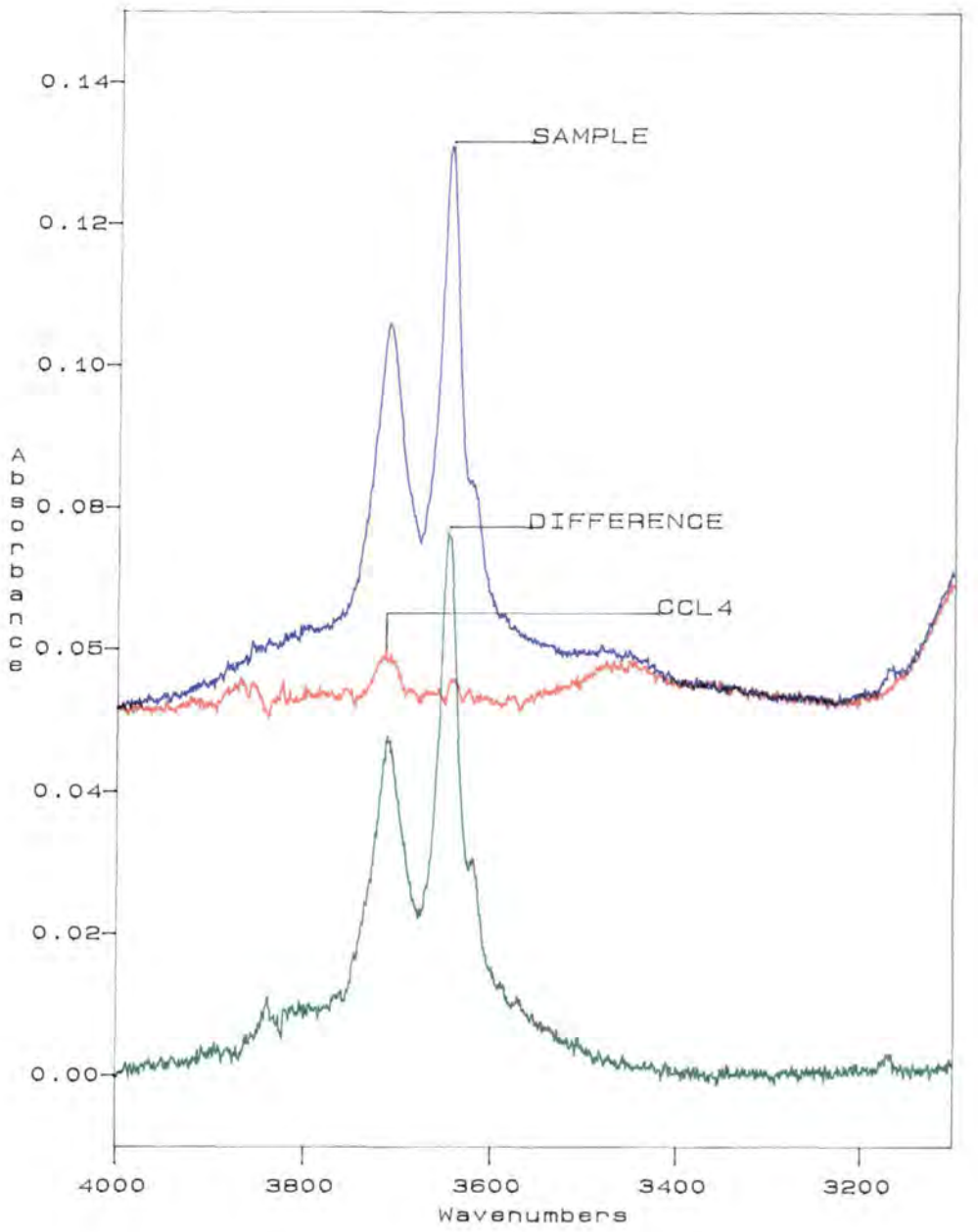

Figure 20 ν(OH) stretching mode of methanol in carbon tetrachloride at 0.0049 mol/dm^3.

Table 9 Band Absorbances of Methanol in Carbon tetrachloride

$CH_3OH/\ CCl_4$ concentration (mol/dm^3)	At 2.5 mm ± 0.1		At 5 mm ± 0.1	
	Absorbance $3710cm^{-1}$	Absorbance $3645cm^{-1}$	Absorbance $3710cm^{-1}$	Absorbance $3645cm^{-1}$
4.93×10^{-3}		-	0.104	0.1292
9.87×10^{-3}	0.0648	0.162	0.0968	0.266
0.0148	0.0756	0.2412	0.1148	0.4064
0.0197	0.0792	0.3132	—	—
0.0246	0.0864	0.3528	—	—

*All absorbance values are in ± 0.01 error

It is worth mentioning that assigning the frequency of observed bands with regard to previous published information was not easy due to the complication of understanding methanol equilibria. For example, Martinez[55] assigned the bands at $3660cm^{-1}$ and $3640cm^{-1}$ to the methanol monomer and linear dimer respectively, while Sandorfy and his co-workers[57] assigned the $3650cm^{-1}$ and $3485cm^{-1}$ as the monomer and linear dimer respectively. So it is not surprising to find differing assignments of observed methanol bands elsewhere. But both authors agree in that the relative intensity of the aggregate in the fundamental region is much more intense than the free band, which might be true if we kept increasing methanol concentration as presented in this work.

The possible geometry of each methanol species is described in Chapter 1, where it is generally accepted that each oxygen atom of an alcohol molecule can accept only one hydroxyl proton. Thus each molecule can be at most doubly bonded. This assumption has been deduced from measurements in the crystalline phases[67] but is yet unproven for the liquid phase. The question remains whether the chains (of multiple species) behave as "freely jointed" ideal chains or not. Dielectric studies[67] of neat alcohol show that the chains are predominantly open and stiffer than if freely jointed. However, at medium dilutions in an inert solvent a cyclic chain is presented as described before. Finally, very high dilution in some solvents suggests that open clusters, probably very short, predominate again. This proves that methanol represents a relatively simple "single acceptor/single donor" system. This is an important conclusion for understanding methanol aggregation.

3.3 Ternary System of [$CH_3OH/CH_3CN/CCl_4$]

Extensive studies, by infra-red and other methods, of the proton accepting power of the (C≡N) group have been reported in the literature. However, very little information seems to be available on the interaction between methanol and nitriles using methanol spectra. For example, Flett[58] reported the formation of hydrogen bonding between acetonitrile and phenol in a ternary solution with carbon tetrachloride, from measurements of the hydroxyl stretching fundamental of phenol. The aim of this section is to confirm and study the hydrogen bond formation between methanol as a proton donor and acetonitrile as a proton acceptor in a non-polar solvent.

Figure 21 shows the spectra of a ternary system at different cell thicknesses where seven bands are observed in the region of interest. The 2.5mm thickness proved to be the most suitable path length for applying such work, although a 5mm path length was used later as well. Figures 22 and 23 show the spectra of CH_3OH:CH_3CN in carbon tetrachloride in concentration ratios of 0.0177:2.056 and 0.0138:6.168 molar concentration respectively, along with the background of CH_3CN in carbon tetrachloride. The difference between the subtracted spectra is shown at a lower baseline, where the previous seven observed bands in the sample spectra are reduced to four bands (which will be used in our analysis from now on) in the subtracted spectrum.

It was noticed that the intensities of all observed bands increases with increasing acetonitrile concentration and at the same time the band at the higher frequency of the sharp band almost vanished. By increasing the acetonitrile concentration, it was expected to reduce the intensities (concentration) of the methanol aggregates and to maximise the intensity of the C_1 complex of the (O–H···N) band. The latest expectation was true, but with regard to methanol aggregates its representative bands were increased, *i.e.* even in such diluted methanol concentration, it is still likely to get methanol aggregation, although it is of a relatively small concentration with regard to the

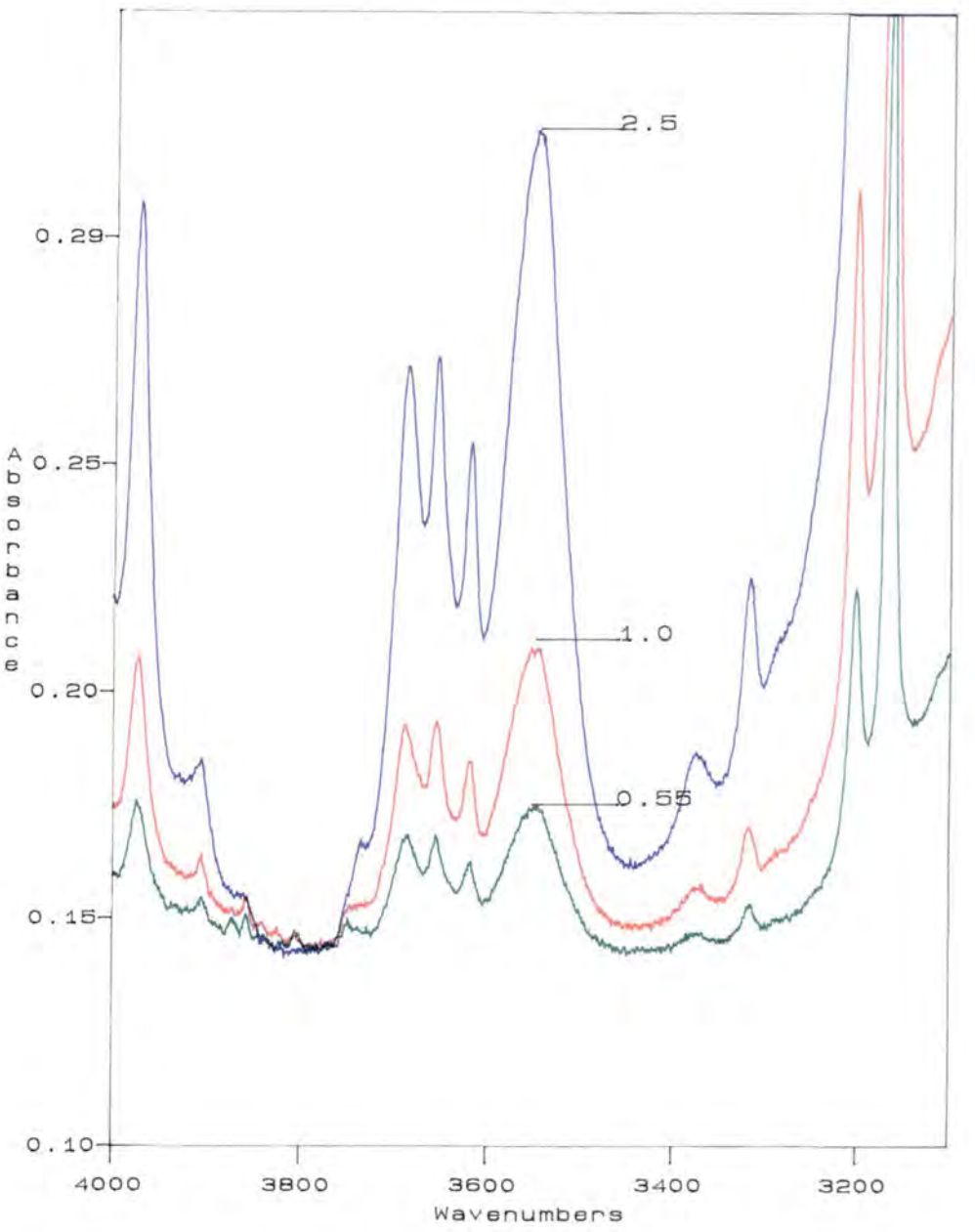

Figure 21 ν(OH) stretching mode of methanol in ternary systems at 0.0049 mol/dm^3 of methanol and 2.0 mol/dm^3 of acetonitrile in carbon tetrachloride, by using different path lengths.

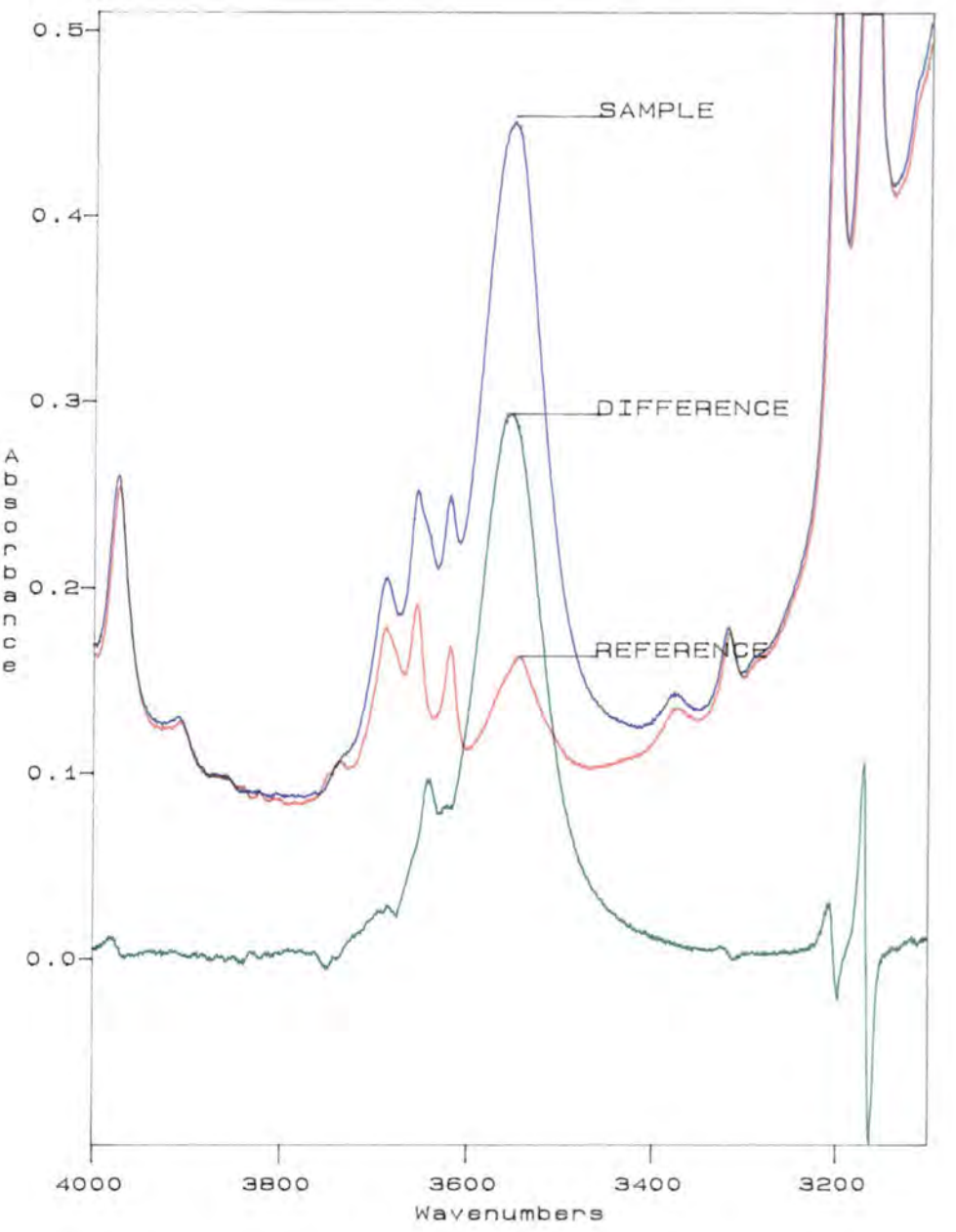

Figure 22 ν(OH) stretching mode of methanol in ternary systems at 0.0177 mol/dm^3 of methanol and 2.0 mol/dm^3 of acetonitrile in carbon tetrachloride.

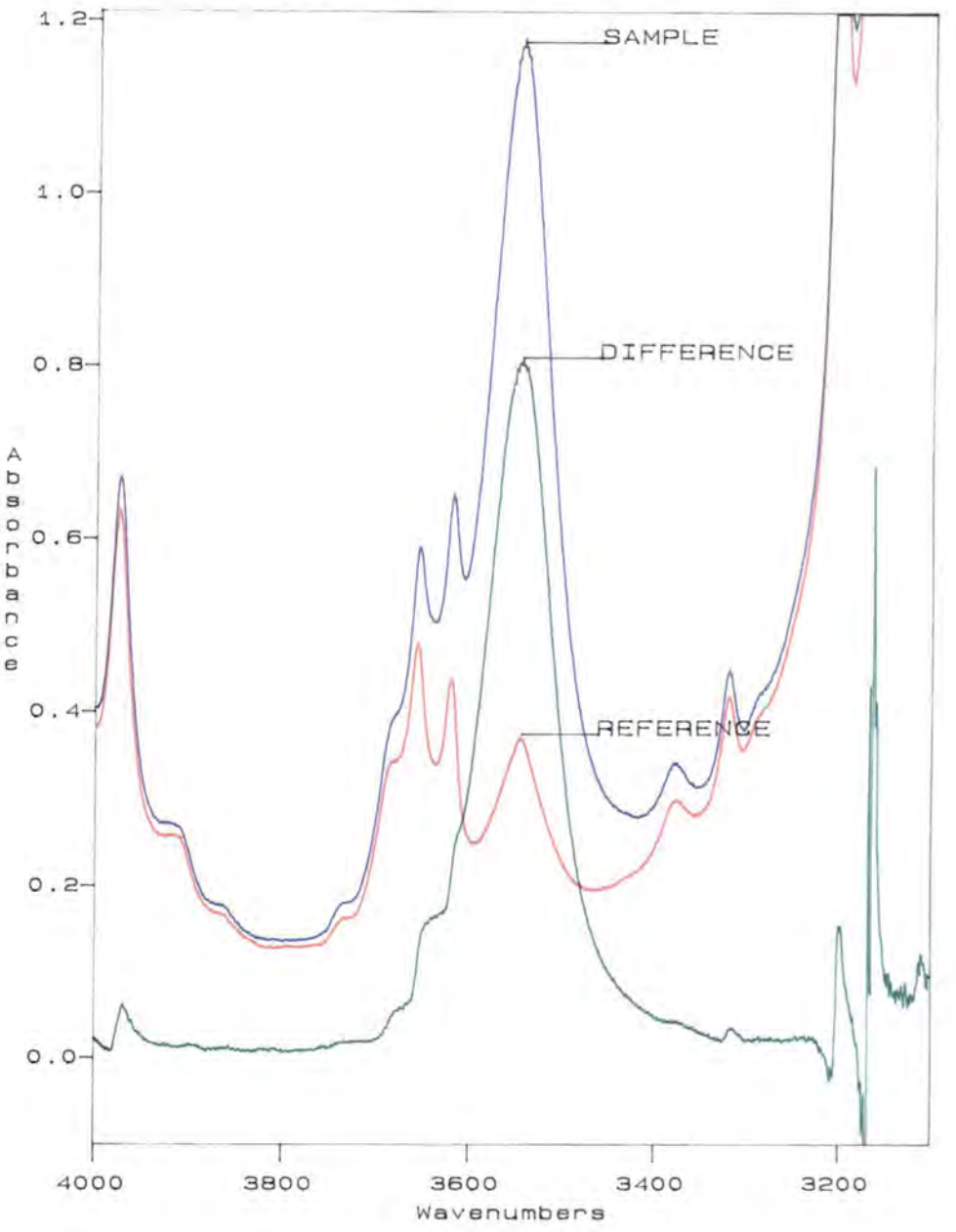

Figure 23 ν(OH) stretching mode of methanol in ternary systems at 0.0138 mol/dm^3 of methanol and 6.16 mol/dm^3 of acetonitrile in carbon tetrachloride.

C_1 complex band (6-10% as shown in Table 10). This should not be true at higher methanol concentration as will be described later.

Again assigning the bands to particular species is not easy. The band at 3645cm^{-1} of methanol in carbon tetrachloride was assigned (in the previous section) as the monomer (un-bonded molecules) as suggested by Sandorfy and his co-workers[57] But the presence of a band at 3680cm^{-1} in the ternary mixture was not assigned before except that it was assigned by Burneau and co-workers[60] as the stretching frequency of the free OH group (non-hydrogen bonded in the given environment) equals the most value observed for gaseous methanol 3682cm^{-1} and the 3640cm^{-1} band, as observed for solutions in inert solvents. This assignment is different from the assignment of the 3693cm^{-1} band as the free OH in the methanol gas phase as published by Palinkas and his co-workers[54], or it could be the monomer as assigned by Martinez[55] but at a higher frequency than the 3660cm^{-1}, while the linear dimer was assigned at 3645cm^{-1} and the 3620cm^{-1} will be the linear trimer.

The major band at 3551cm^{-1} is assigned by almost all authors as the ν(OH) band in the $CH_3OH\cdots NCCH_3$ complex. This band increases in intensity with increasing acceptor (acetonitrile) concentration, according to the well-known 1:1 equilibrium

$$CH_3OH + CH_3CN \longrightarrow H_3C\text{–}OH\cdots N{\equiv}C\text{–}CH_3 \qquad (63)$$

It was noticed also that, with the exception of the band at 3645 cm^{-1}, increasing the acceptor concentration shifts almost all observed bands (along with the self-association bands) to lower frequency as shown in Table 10.

On going to higher acetonitrile concentrations, Figure 24 shows that the band at 3620cm^{-1} disappeared or overlapped with the 3640cm^{-1} band. The frequency assignment along with the observed absorbances of such spectra are presented in Table 11 and plotted in Figure 25. Such data confirms the frequency shift to lower wave number and increase in the band absorbance (including the C_1 complex) band when the acetonitrile concentration is increased. In other words, the absorbance increases with the increase in the acceptor concentration.

Table 10 Frequencies and Absorbances of Methanol Fundamental Bands in Ternary Systems

CH_3OH mol/dm^3	CH_3CN mol/dm^3	MONOMER		LINEAR DIMER		TRIMER		C_1 complex	
		Frequency cm^{-1}	Absorbance	Frequency cm^{-1}	Absorbance	Frequency cm^{-1}	Absorbance	Frequency cm^{-1}	Absorbance
0.0177	2.056	3688	0.031	3641	0.096	3620	0.0802	3551	0.293
0.0138	6.168	3676	0.0515	3648	0.154	3613	0.2606	3545	0.801

Table 11 Frequencies and Absorbances of Methanol Fundamental Band by using 2.5 mm pathlength

CH_3OH mol/dm^3	CH_3CN mol/dm^3	Frequency cm^{-1}	Absorbance	Frequency cm^{-1}	Absorbance	Frequency cm^{-1}	Absorbance
4.8×10^{-3}	0.411	3692	0.0246	3644	0.036	3564	0.033
4.6×10^{-3}	1.23	3688	0.0234	3641	0.0288	3557	0.041
4.4×10^{-3}	2.056	3684	0.0946	3641	0.0959	3552	0.1635

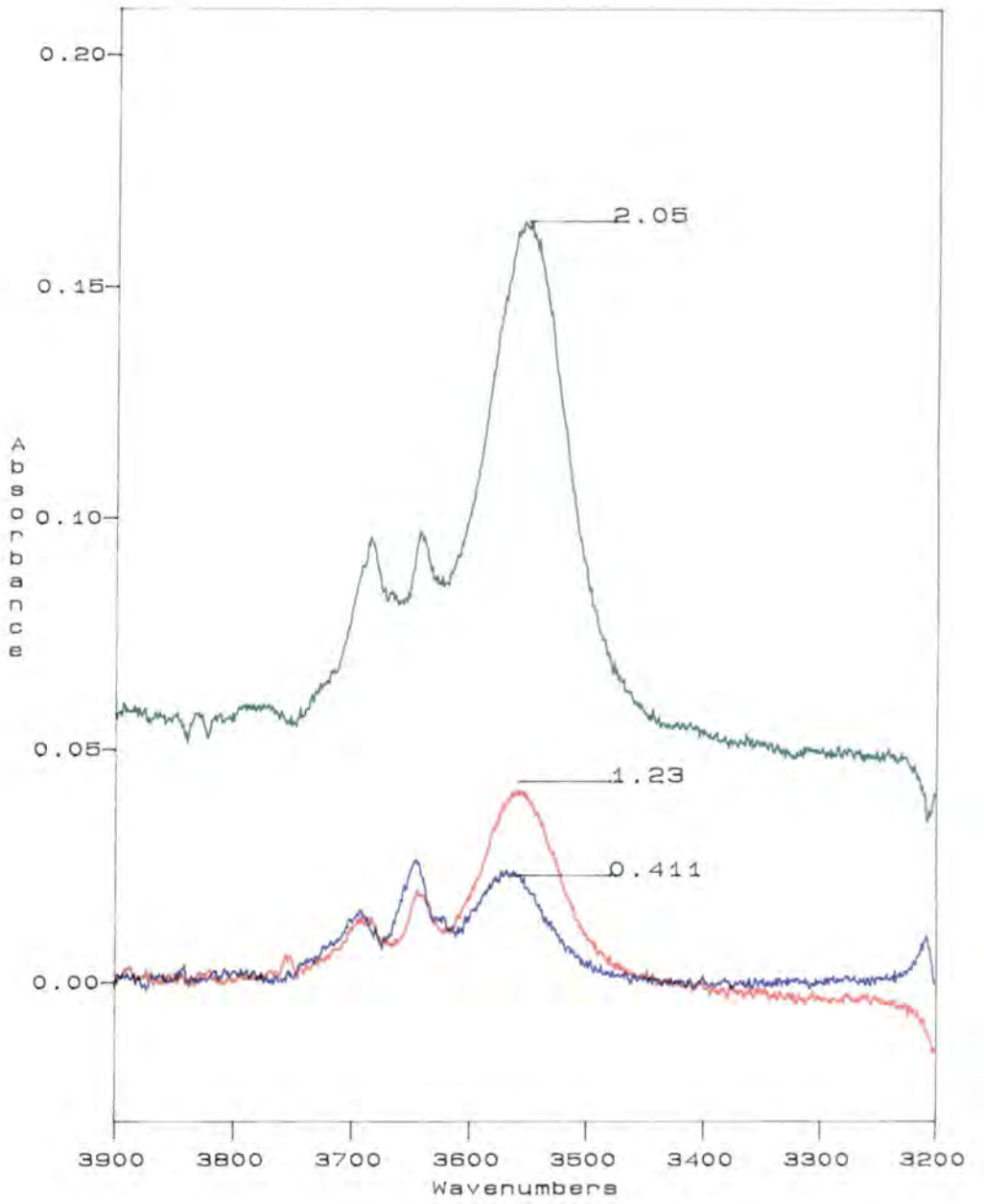

Figure 24 ν(OH) stretching mode of methanol in ternary systems at different acetonitrile concentrations in mol/dm^3

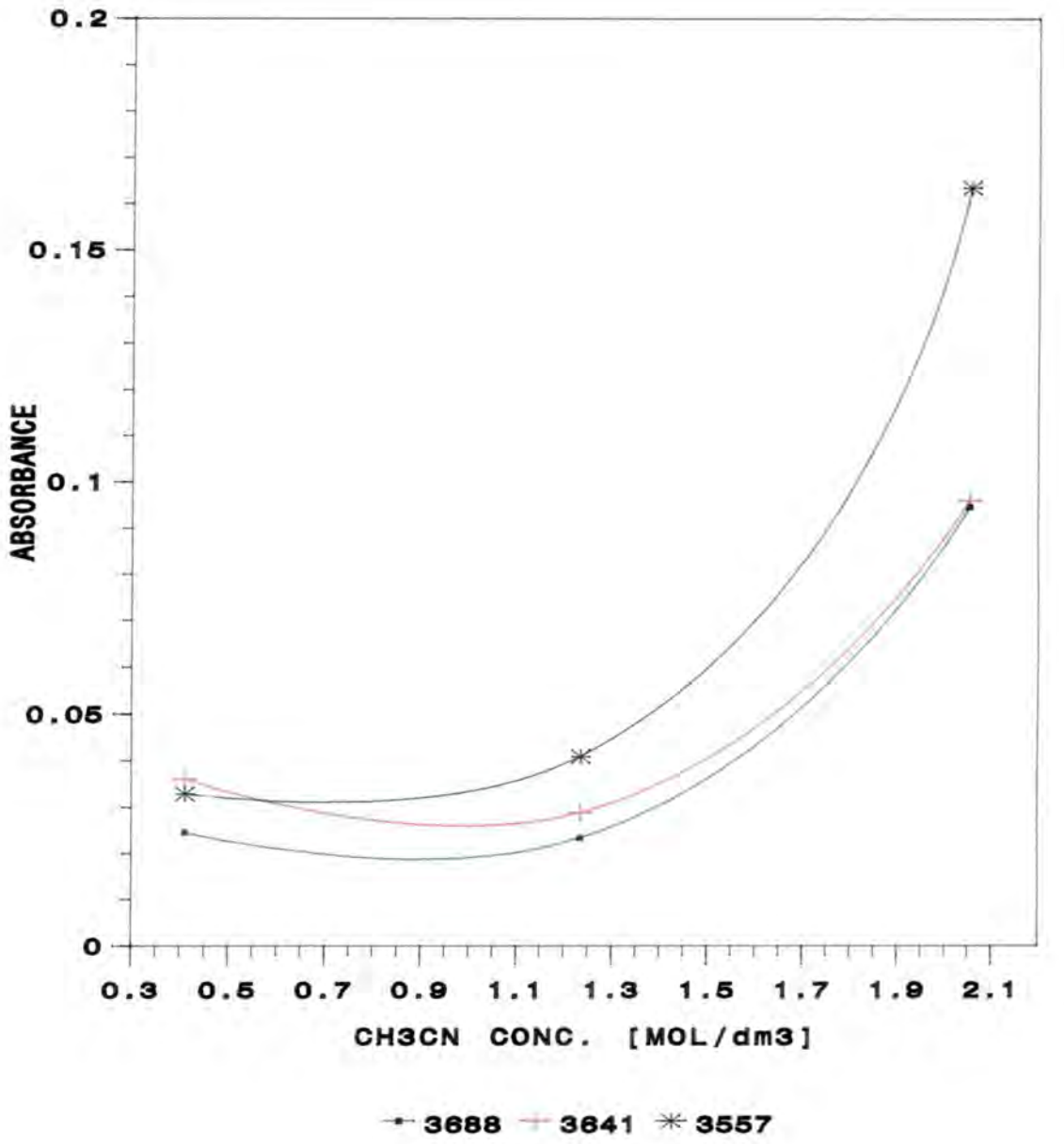

Figure 25 ν(OH) stretching absorbances of methanol in ternary systems at different acetonitrile concentrations in mol/dm^3 as presented in table 11.

The same experiments were applied by reducing the acetonitrile concentration and using higher path length. These data are presented in Figure 26 and summarized in Table 12. In such acetonitrile concentration, the band at 3705cm^{-1} became the most intense band as shown in Figure 27, and increased in absorption with increasing acetonitrile concentration. Other bands have the same trend (as explained before) due to formation of hydrogen bonds with (C≡N) group (at 3565cm^{-1}) along with having greater methanol aggregate with increasing the acceptor concentration.

Table 12 **Frequencies and Absorbances of Methanol Fundamental Band by using 5 mm pathlength**

CH_3OH mol/dm^3	CH_3CN mol/dm^3	Frequency cm^{-1}	Absorbance	Frequency cm^{-1}	Absorbance
$4.92x10^{-3}$	0.411	3705	0.0315	3642	0.020
$4.91x10^{-3}$	0.0822	3705	0.0460	3642	0.0228
$4.9\ x10^{-3}$	0.1233	3705	0.0415	3645	0.0215
$4.89x10^{-3}$	0.1644	3707	0.0502	3642	0.0248

CH_3OH mol/dm^3	CH_3CN mol/dm^3	Frequency cm^{-1}	Absorbance	Frequency cm^{-1}	Absorbance
$4.92x10^{-3}$	0.411	3619	0.0175	3564	0.014
$4.91x10^{-3}$	0.0822	3619	0.0207	3565	0.0175
$4.9\ x10^{-3}$	0.1233	3610	0.0207	3560	0.0165
$4.89x10^{-3}$	0.1644	3619	0.0215	3565	0.0236

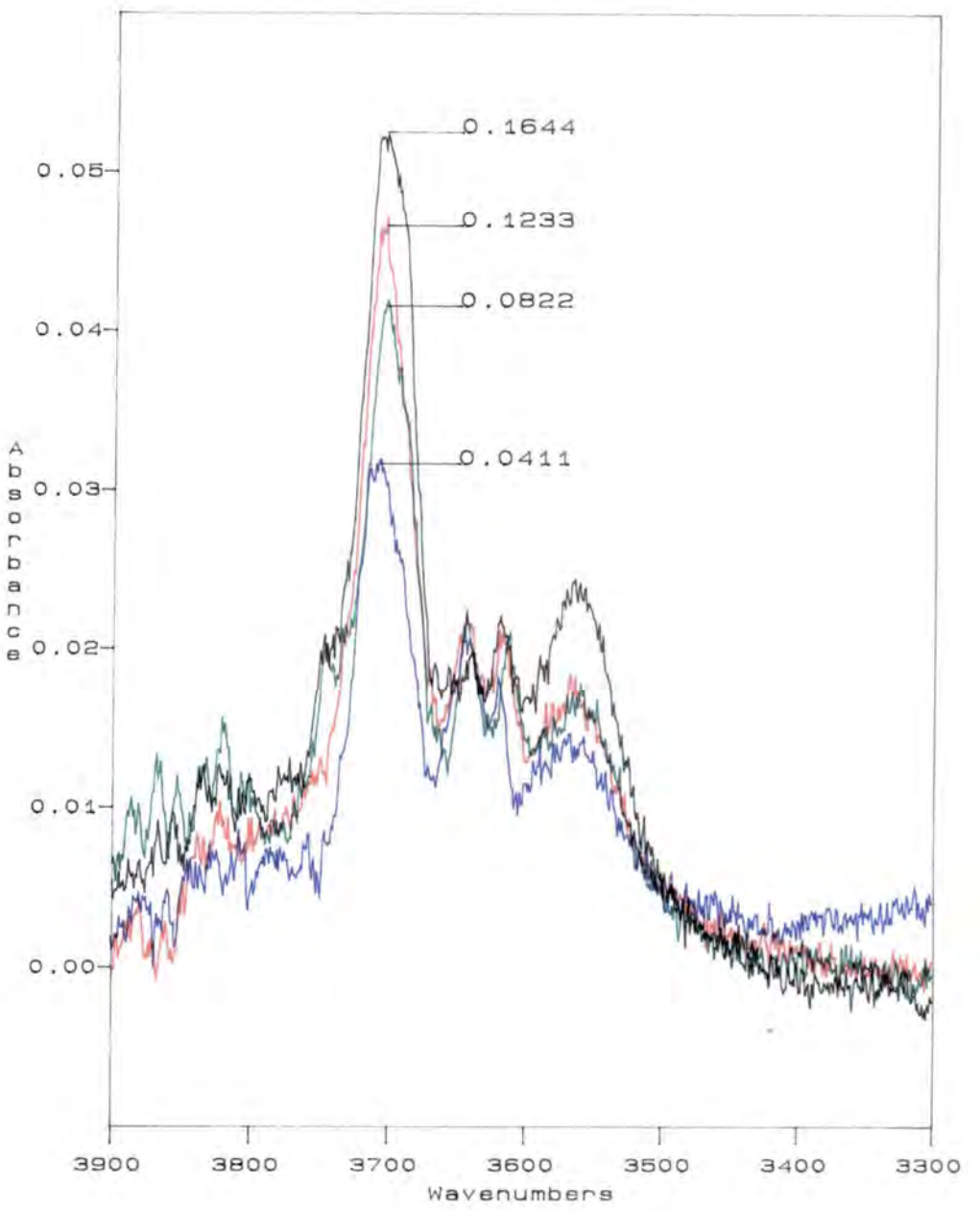

Figure 26 ν(OH) stretching mode of methanol in ternary systems at different acetonitrile concentrations in mol/dm^3

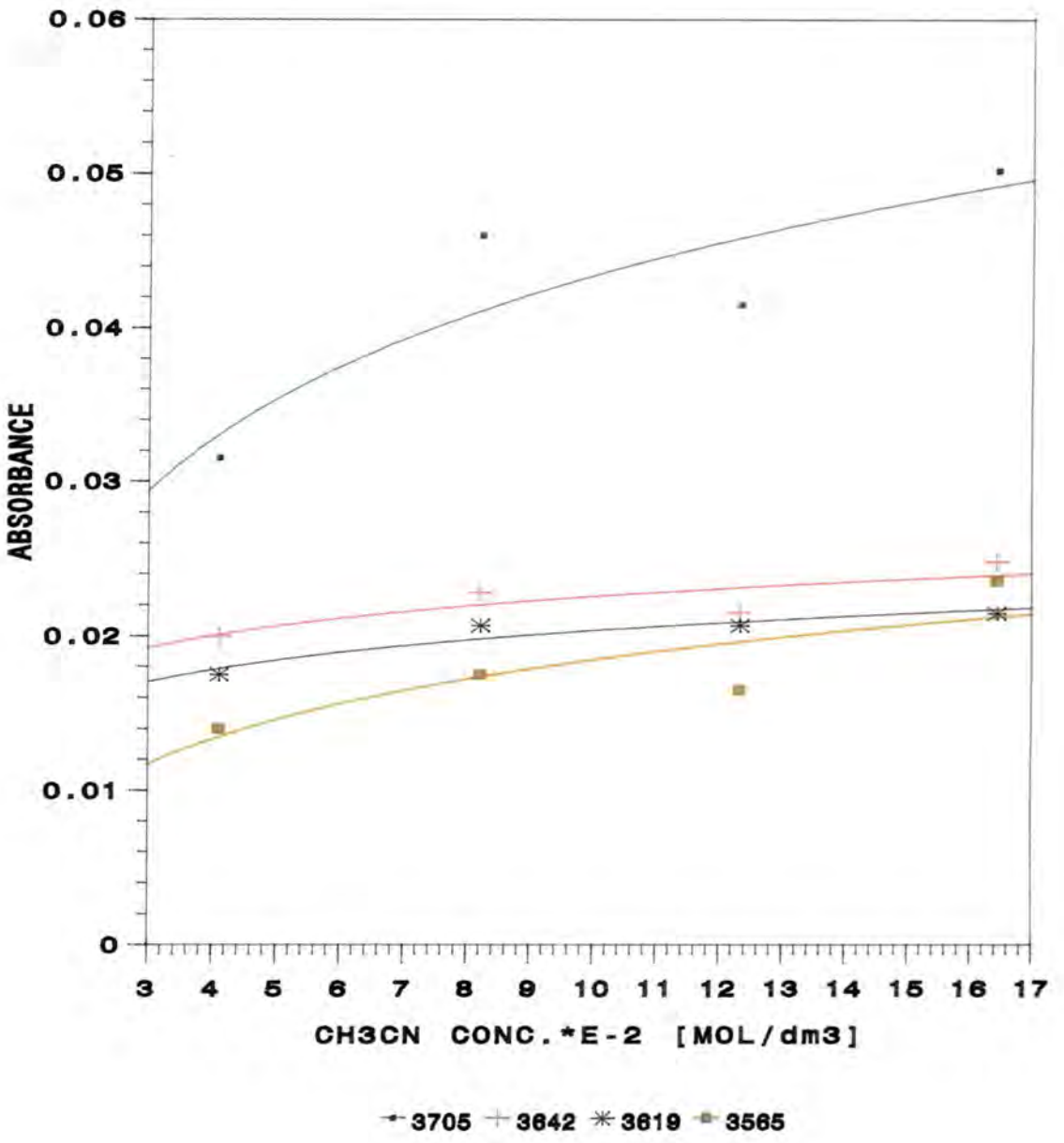

Figure 27 ν(OH) stretching absorbances of methanol in ternary systems at different acetonitrile concentrations in mol/dm^3 as presented in table 12.

3.4 Binary System of CH_3OH/CH_3CN

The case of binary systems is even more complicated than that of the ternary systems. The observed spectra of methanol in acetonitrile in the concentration range 0.01 – 0.9 mole fraction of methanol are shown in Figures 28–34 after subtracting acetonitrile spectra. Cell thickness are as described in Chapter 2.

It is clear that the spectra of the lowest methanol concentrations in a range of 0.01 - 0.03 mole fraction (0.197 - 0.596 mol/dm^3) consist of at least two overlapped bands (Figure 28). One is at 3620cm^{-1} which could be the linear dimer (as analyzed before), and the major band at 3538cm^{-1} due to the hydrogen bond association between oxygen and nitrogen. Increasing the methanol concentration reduces the intensity of the higher frequency band until it vanishes (~ 0.04 - 0.05 methanol mole fraction). This means that the hydrogen bonding in the (O···N) group becomes more preferable than that between (O···O) in the methanol dimer. At the same time another band starts to appear to the low frequency side of the major band, at about 3430cm^{-1} in a concentration range of 0.055 – 0.08 methanol mole fraction (Figure 30). This shoulder increases in intensity as the methanol concentration is increased and it becomes very clear at about 0.1 – 0.3 methanol mole fraction (Figure 31). An exciting spectrum is observed in Figure 32, where the band at 3430cm^{-1} grows very quickly and overlaps with the 3538cm^{-1} band to form a very broad band, which is always present at the higher methanol concentration (0.55 – 0.7 mole fraction), as shown in Figure 33. In Figure 33, the band at 3430cm^{-1} is shifted (or replaced) to lower frequency (3380cm^{-1}) and decreased in intensity with increasing methanol concentration,as shown in figure 34.

Due to overlapping between bands and the difficulty in identifying them, it was necessary to use a band fitting program to analyse the band components at each methanol concentration. This will be discussed in the band fitting section(3.4.2). A temperature study was carried out on the binary system in order to get more information about the ν_s(OH) band,this is discussed next.

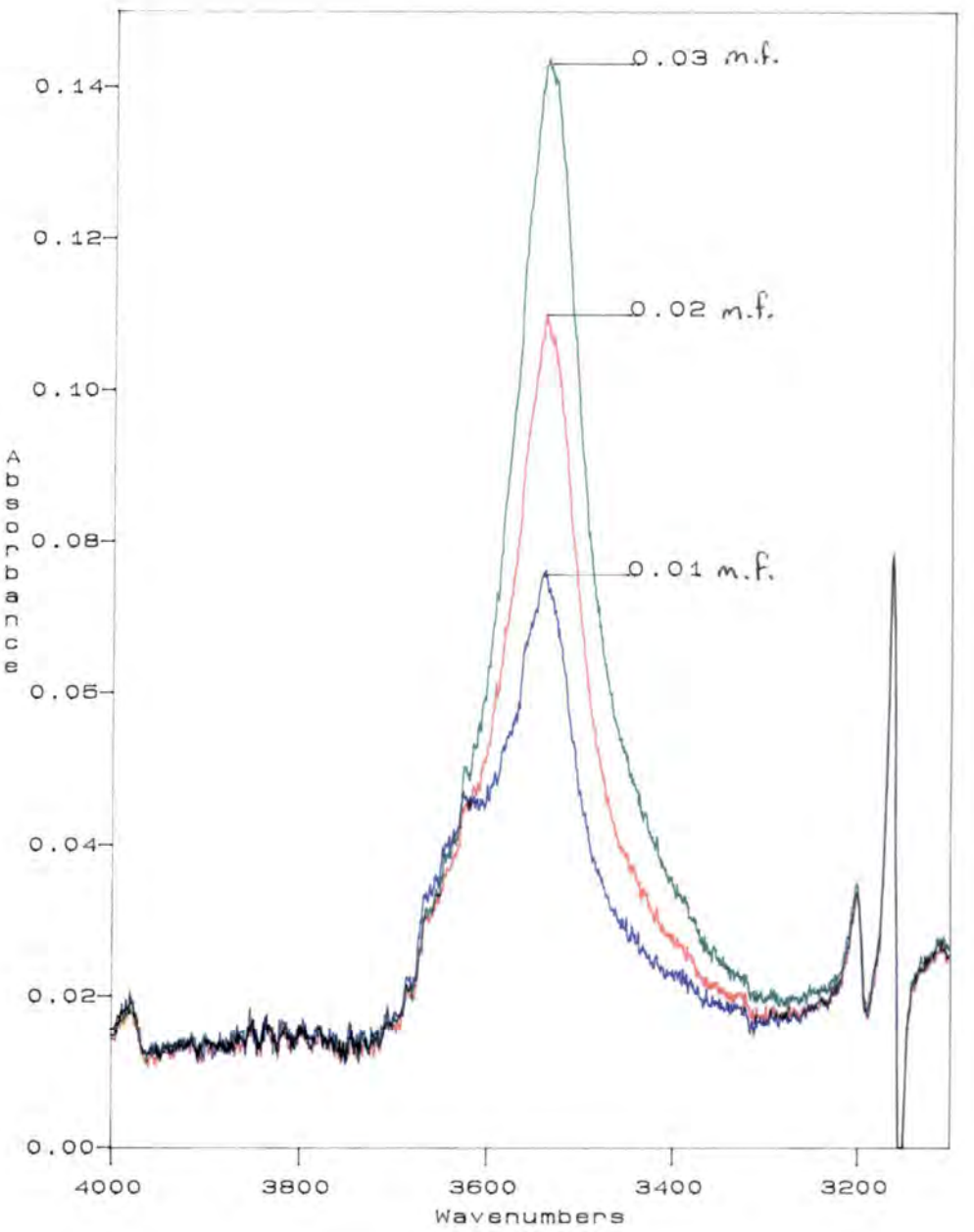

Figure 28 ν(OH) stretching mode of methanol in acetonitrile at different acetonitrile mole fraction concentrations, using a 17.5μm pathlength.

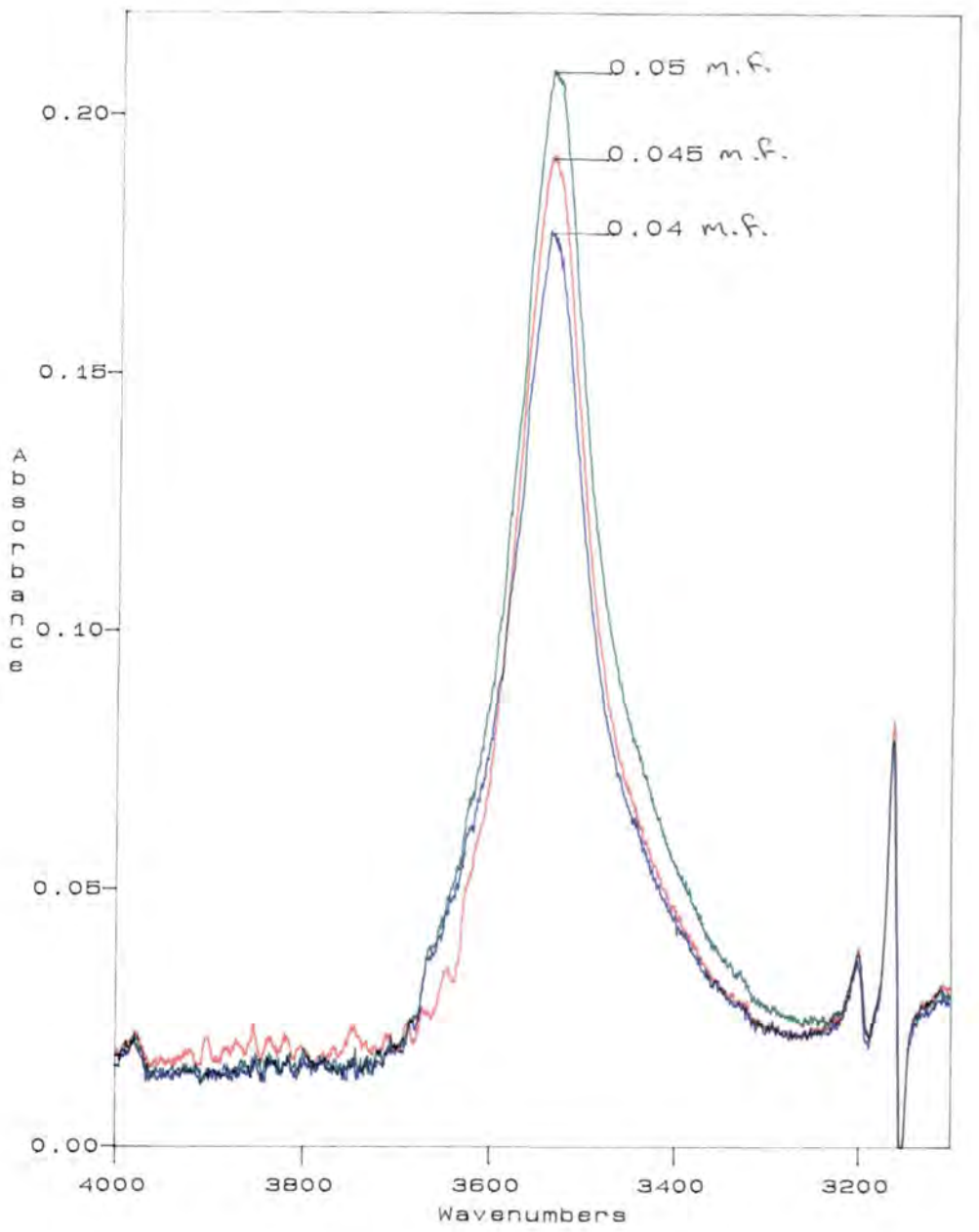

Figure 29 ν(OH) stretching mode of methanol in binary systems at different methanol mole fraction concentrations, using a 17.5μm path length.

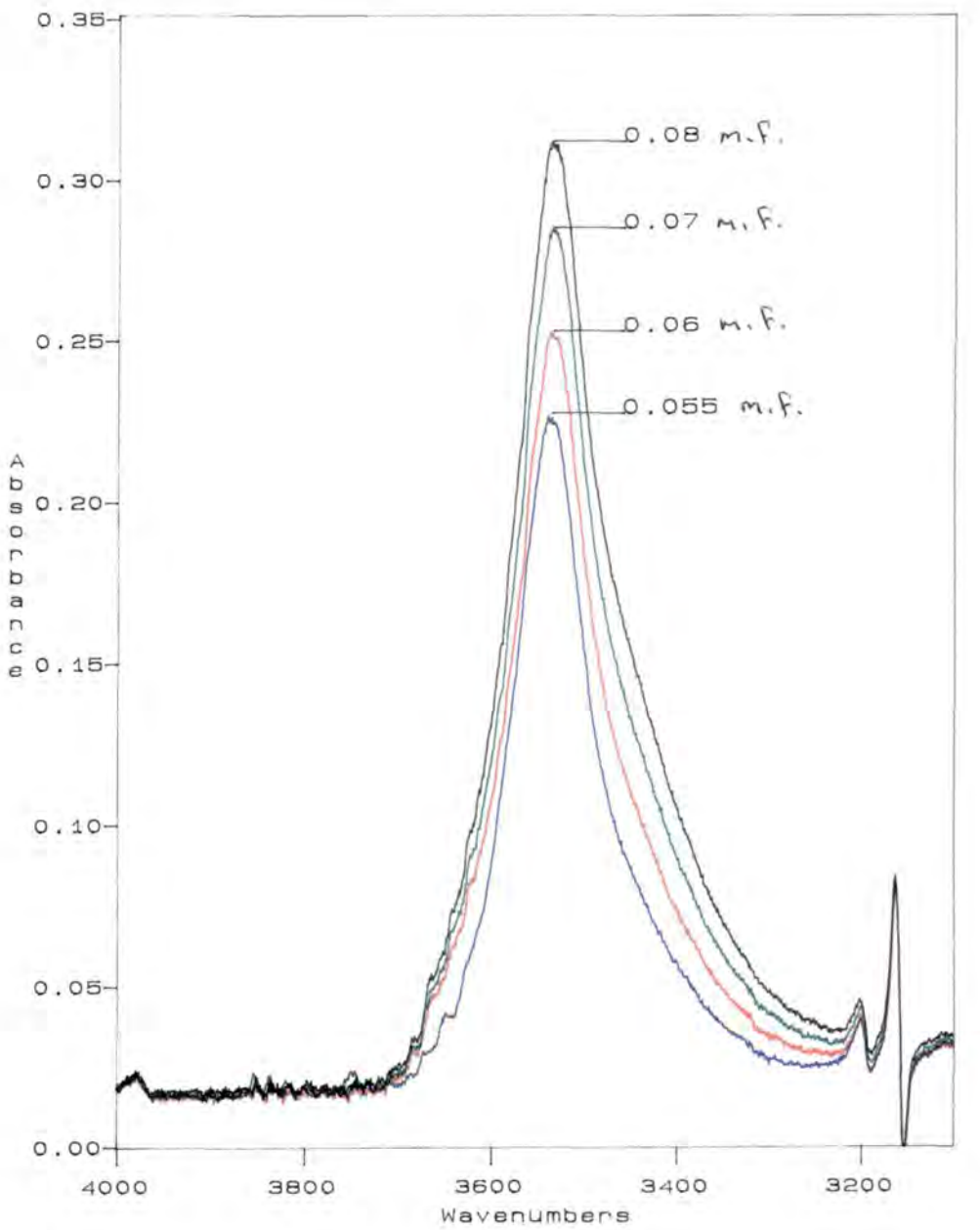

Figure 30 ν(OH) stretching mode of methanol in binary systems at different methanol mole fraction concentrations, using a 17.5μm path length.

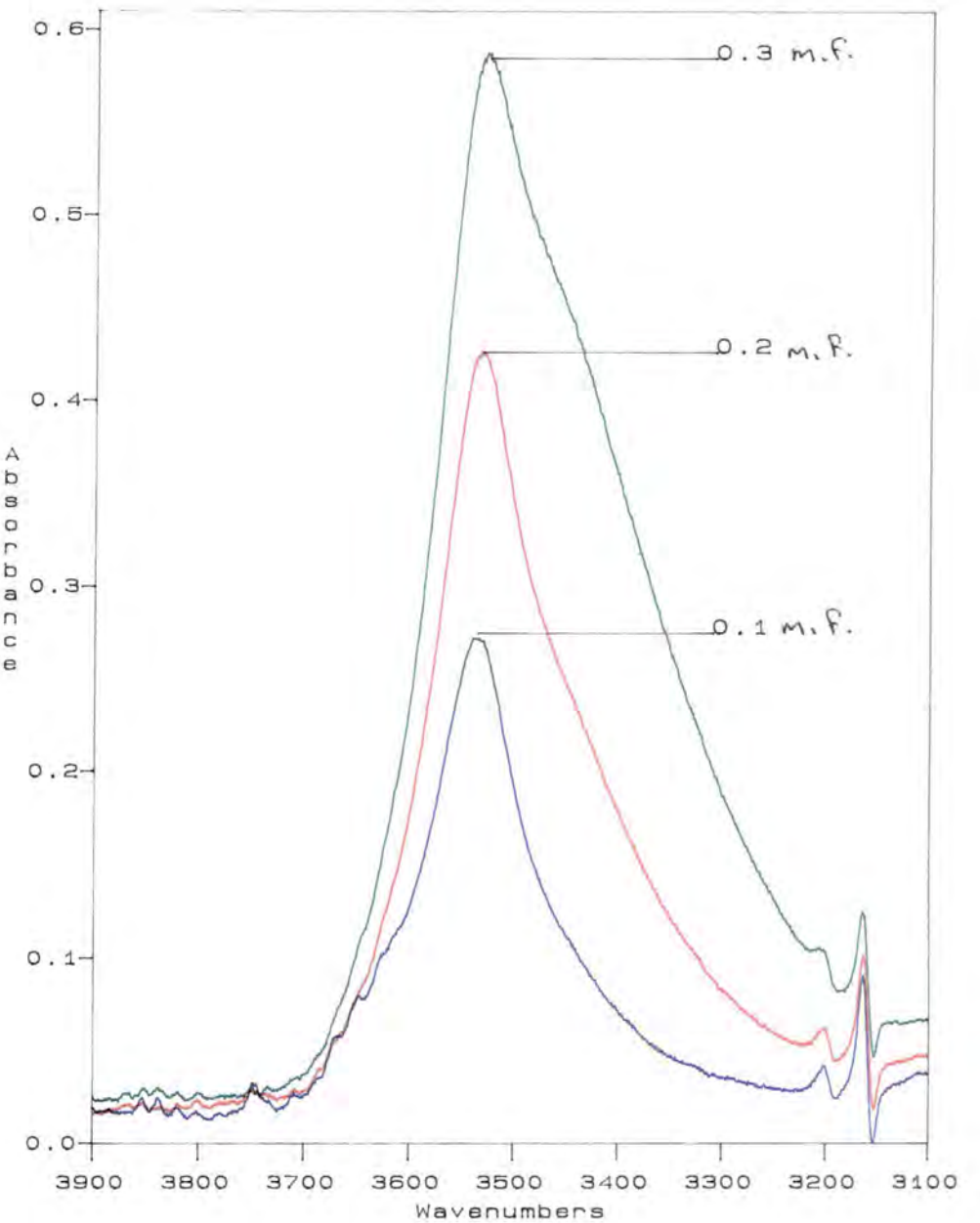

Figure 31 ν(OH) stretching mode of methanol in binary systems at different methanol mole fraction concentrations, using a 18.5/μm Path length.

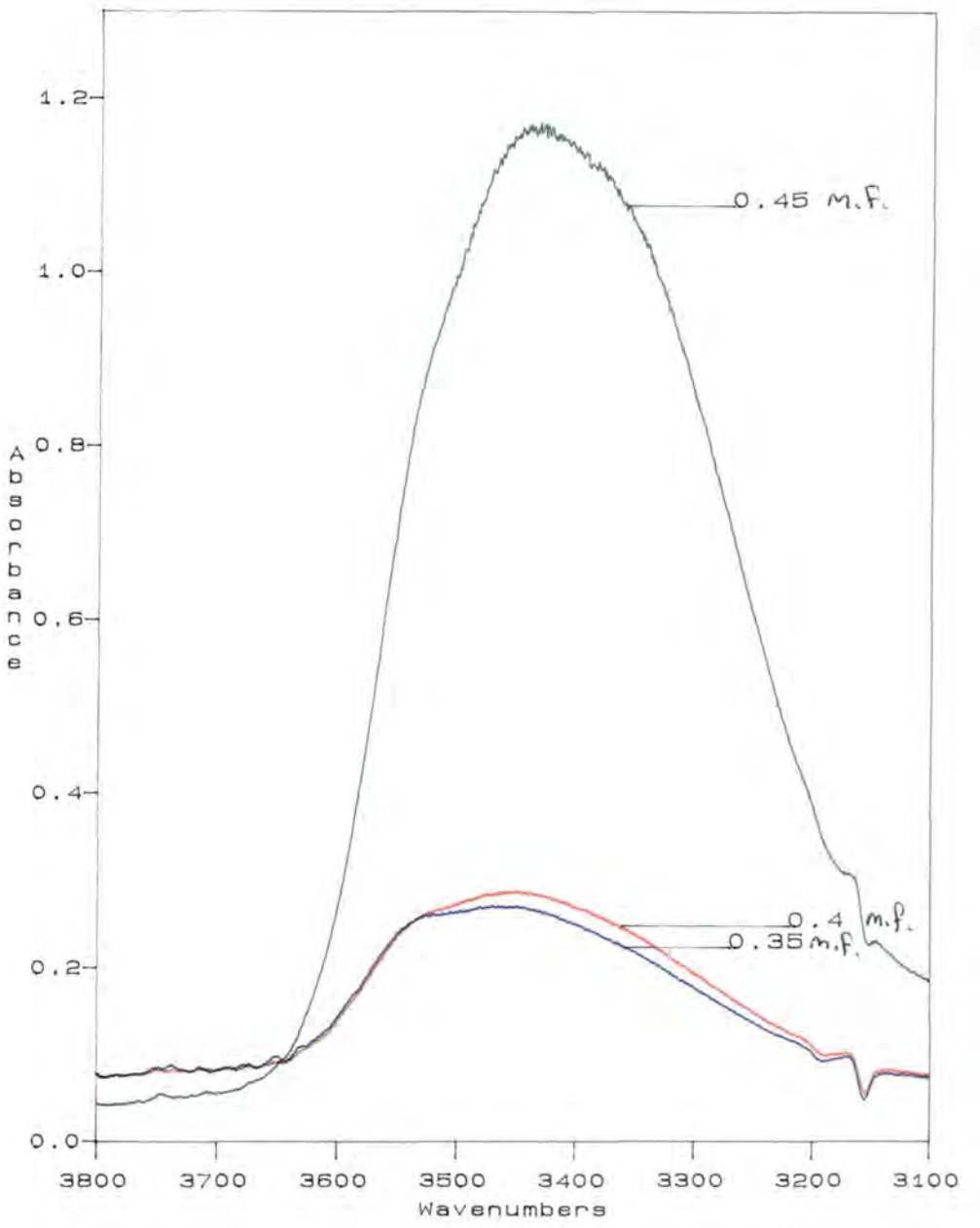

Figure 32 ν(OH) stretching mode of methanol in binary systems at different methanol mole fraction concentrations, using a 18.5μm path length.

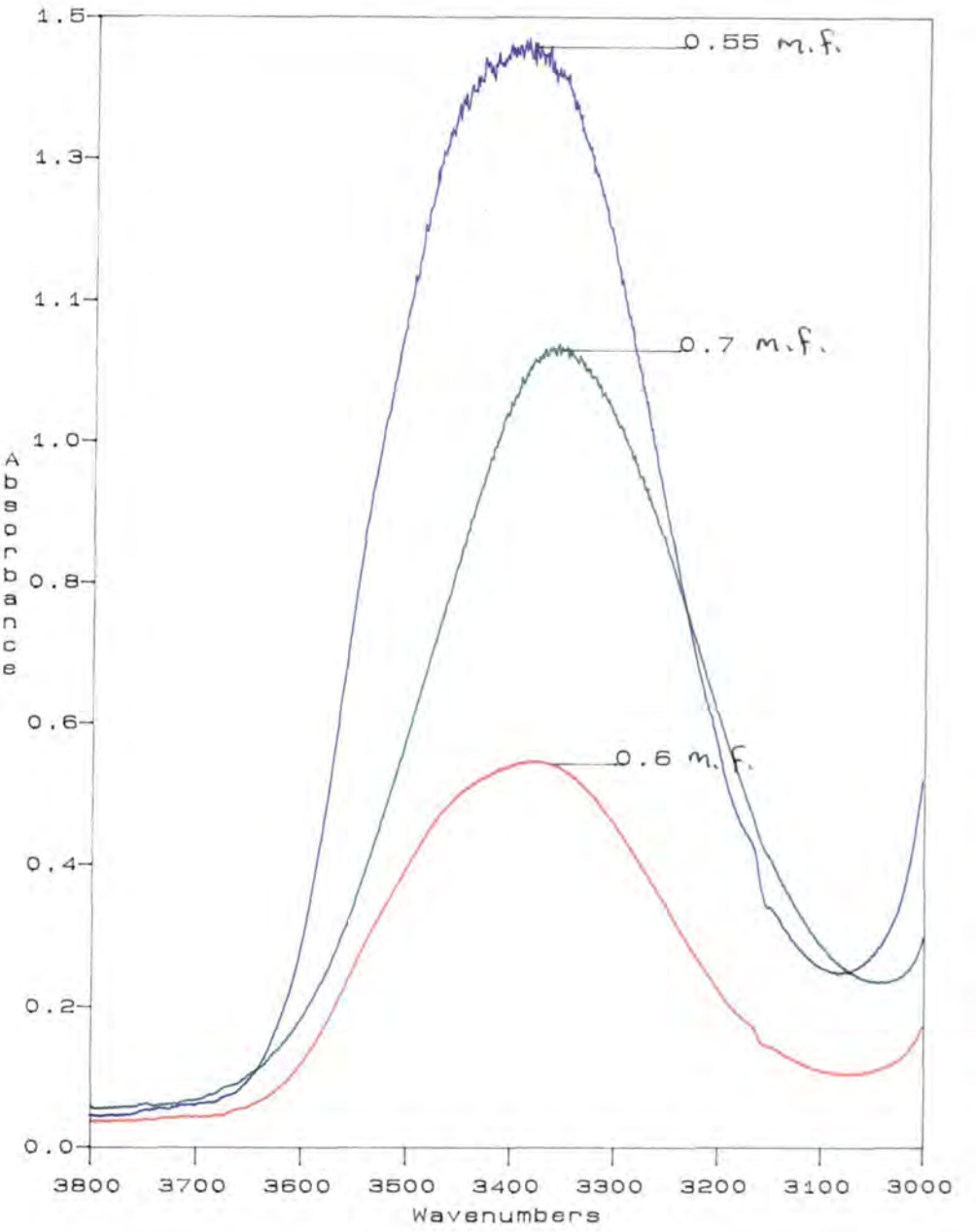

Figure 33 ν(OH) stretching mode of methanol in binary systems at different methanol mole fraction concentrations, using a 18.5μm path length for 0.55 m.f. and 6μm for others.

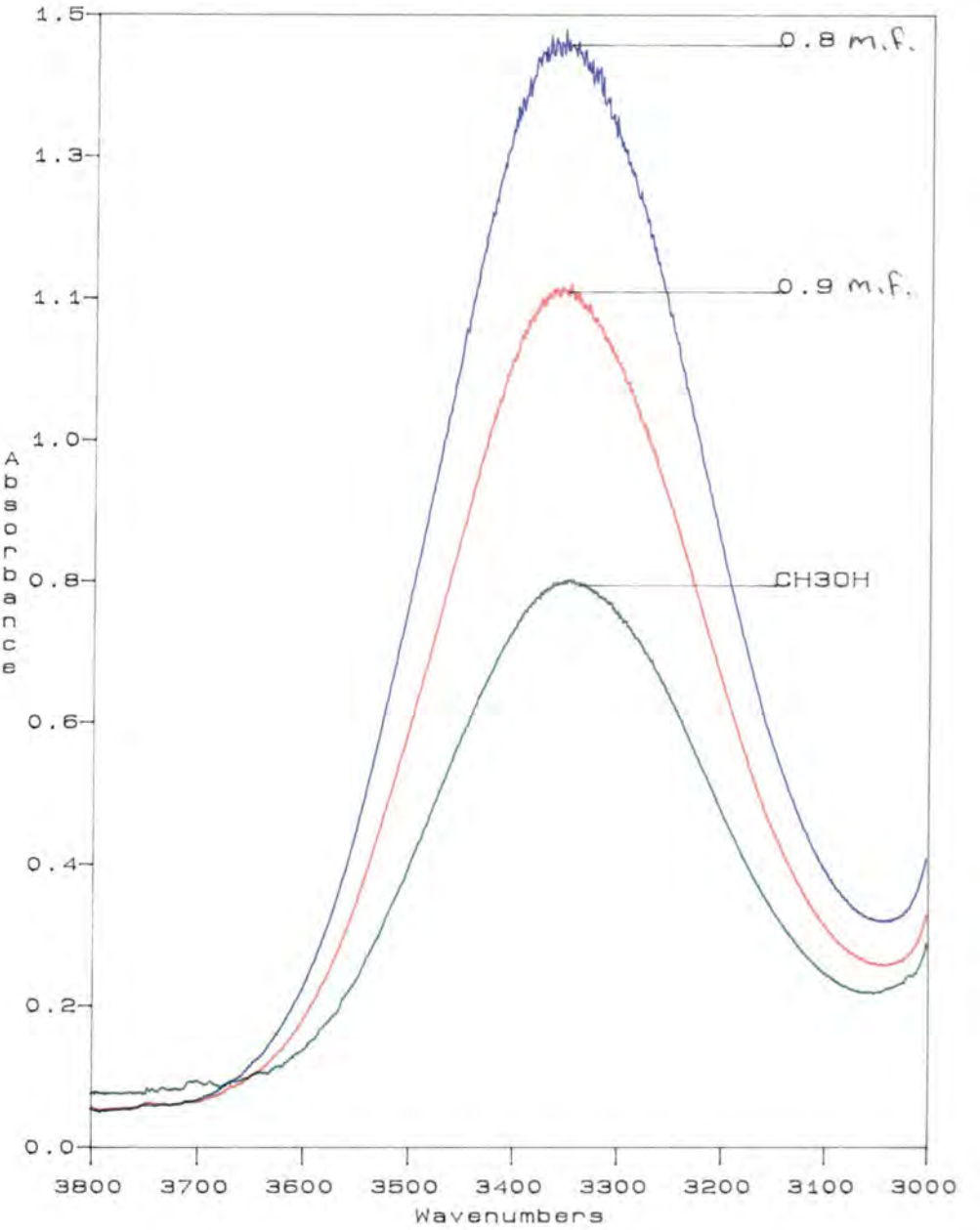

Figure 34 ν(OH) stretching mode of methanol in binary systems at different methanol mole fraction concentrations, using a 6/1m Pathlength.

3.4.1 Temperature Effect on Binary Systems

It is well known[33,52] that temperature has a large effect on the frequency and the absorbance of the ν(OH) band. Figures 35-38 show spectra of four different methanol concentrations (0.04, 0.06, 0.55 and 0.9 methanol mole fraction) in acetonitrile solutions, at different temperatures from 30°C to 80°C.

At 0.04 methanol mole fraction, one major band is observed at 3542cm^{-1} which is well known[68] as the ν(OH) of the C_1 complex band. This band shifts to higher frequency (3550cm^{-1}) with increasing temperature (82°C), as shown in Table 13 which summarises the data collected from figures 35 to 38. This indicates that increasing temperature weakens or breaks the hydrogen bonding between hydroxyl and nitrogen groups. It was expected to see the free ν(OH) band increasing with temperature, but due to the small cell thickness (18.4 μm) this was not possible. On the other hand, two small bands can be seen at 3650cm^{-1} and 3615cm^{-1} (the first band might be the methanol monomer). These bands became clearer when the band spectra of higher temperatures were subtracted from the lowest temperature (30°C) spectra as seen in Figure 39–a and the expanded spectra in Figure 39–b. These two bands could be the linear dimer and the linear trimer, (as described in the Martinez paper[55]), respectively. The intensity of all bands decreased with increasing temperatures (as expected) due to breaking the hydrogen bond in methanol aggregates.

The frequency shift (from the methanol monomer frequency) of the C_1 complex band was plotted against temperature as in Figure 40. It was clear that the frequency shift decreases with increasing temperature, in agreement with the Badger-Bauer rule for hydrogen bonded systems that the frequency shift, $\Delta\nu$, is proportional to the hydrogen bond energy (Chapter 1). From Figure 40 we predict that the 1:1 complex band decreases or disappears at about 0.55 mole fraction and what is left is due to methanol aggregate only.

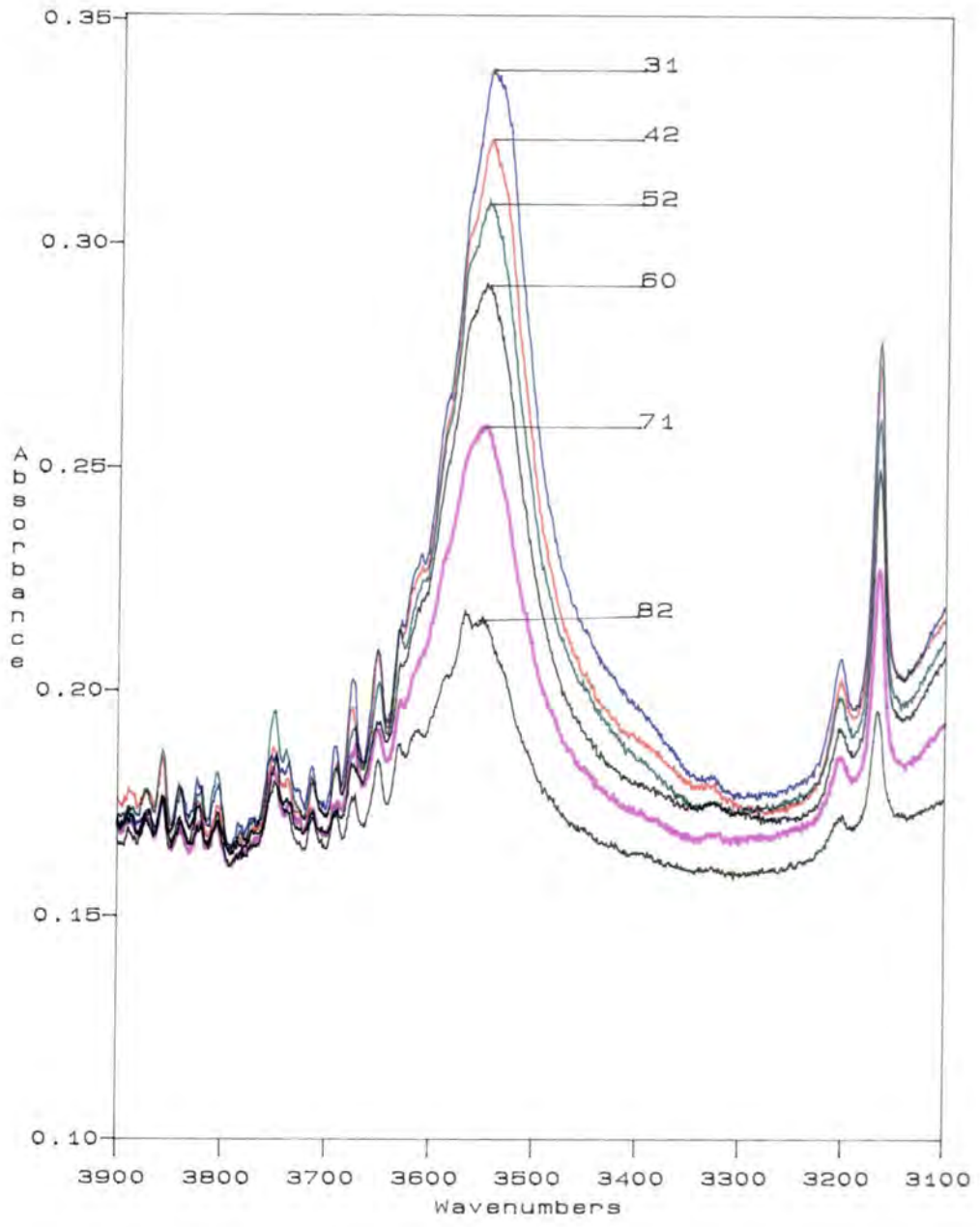

Figure 35 ν(OH) spectra of 0.04 methanol mole fraction in acetonitrile solution at different temperatures in degrees centigrade.

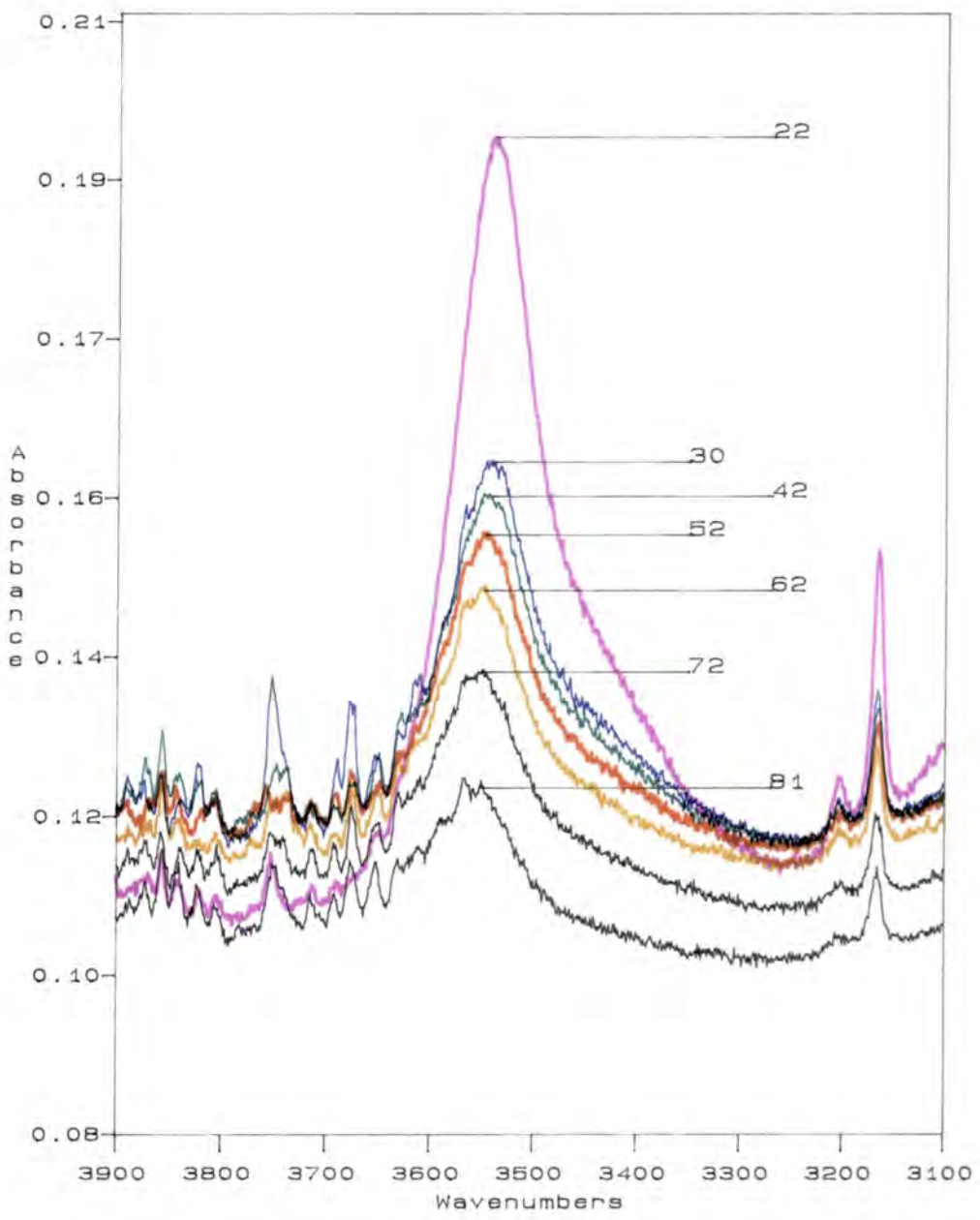

Figure 36 ν(OH) spectra of 0.06 methanol mole fraction in acetonitrile solution at different temperatures in degrees centigrade.

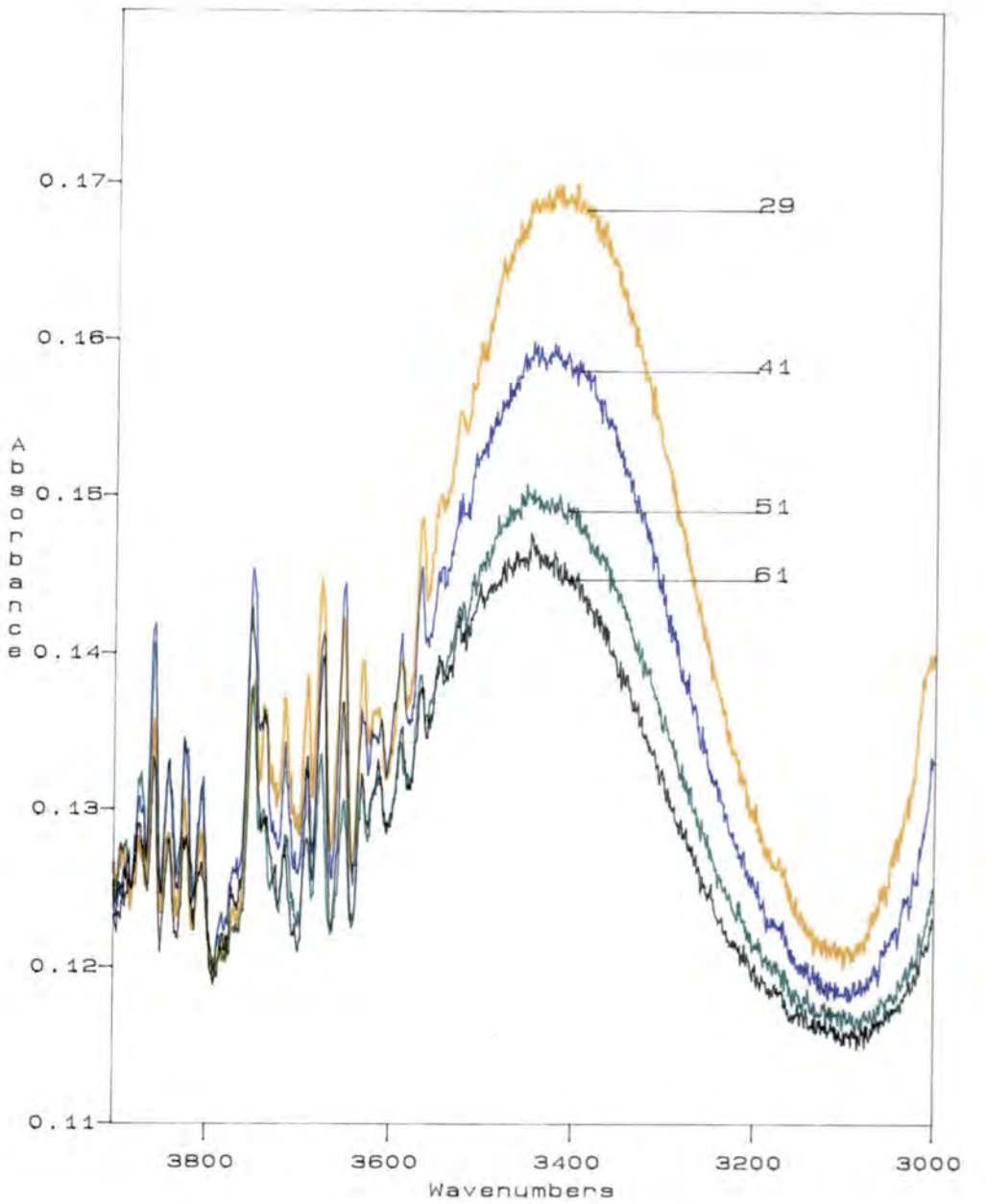

Figure 37 ν(OH) spectra of 0.55 methanol mole fraction in acetonitrile solution at different temperatures in degrees centigrade.

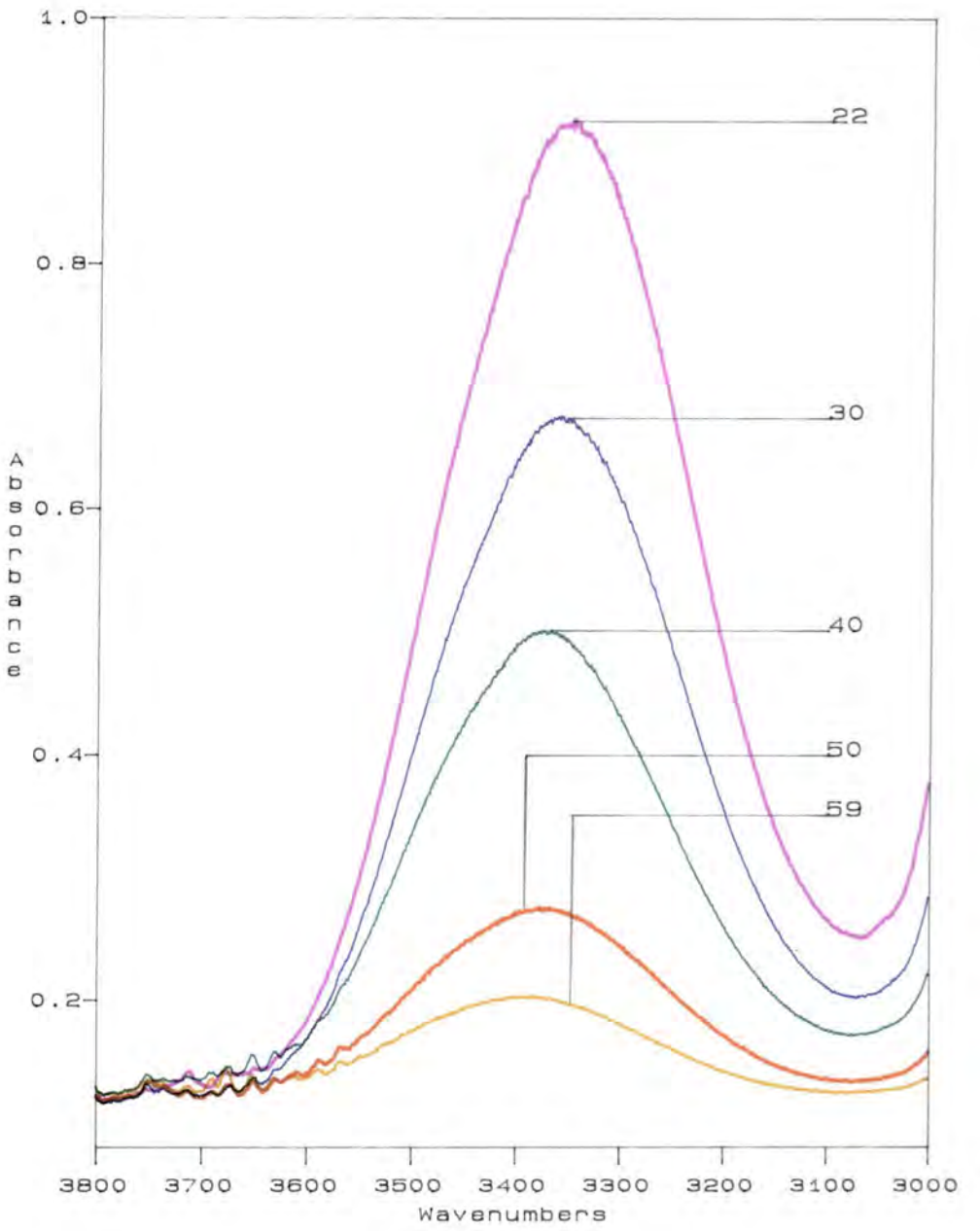

Figure 38 ν(OH) spectra of 0.9 methanol mole fraction in acetonitrile solution at different temperatures in degrees centigrade.

Table 13 **The Effect of Changing Temperature on Methanol Fundamental Bands in Binary System**

	0.04 m.f.			0.06 m.f.			0.55 m.f.			0.9 m.f.		
Temperature† (°C)	Frequency cm^{-1}	$\Delta\nu$* cm^{-1}	Absorbance	Frequency cm^{-1}	$\Delta\nu$* cm^{-1}	Absorbance	Frequency cm^{-1}	$\Delta\nu$* cm^{-1}	Absorbance	Frequency cm^{-1}	$\Delta\nu$* cm^{-1}	Absorbance
~ 30	3542	103	0.3378	3540	105	0.1644	3414	231	0.1686	3360	285	0.6742
~ 40	3545	100	0.3214	3542	103	0.16	3422	223	0.1588	3370	275	0.5018
~ 50	3546	99	0.3075	3546	99	0.1552	3432	213	0.149	3375	270	0.2746
~ 60	3549	96	0.2892	3549	96	0.1485	3442	203	0.146	3388	257	0.2034
~ 70	3550	95	0.2577	3552	93	0.138	—	–	—	—	–	—
~ 80	3560	85	0.2152	3556	89	0.1243	—	–	—	—	–	—

* $\Delta\nu = 3645 - \nu_i$

† Temperature values are within ± 2°C error

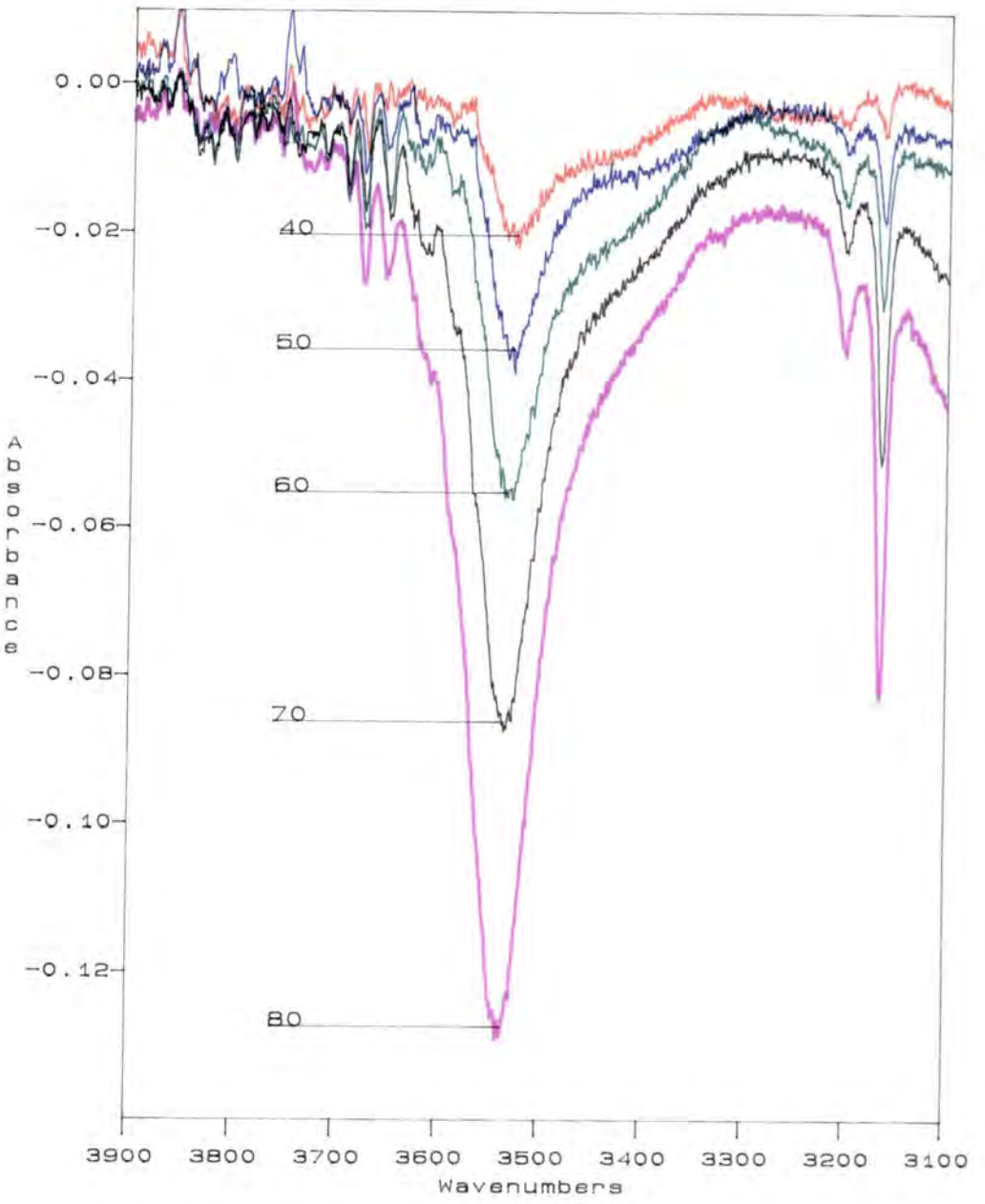

Figure 39–a ν(OH) subtracted spectra (from ν(OH) spectrum at 30°C) of 0.04 methanol mole fraction at different temperatures in degrees centigrade.

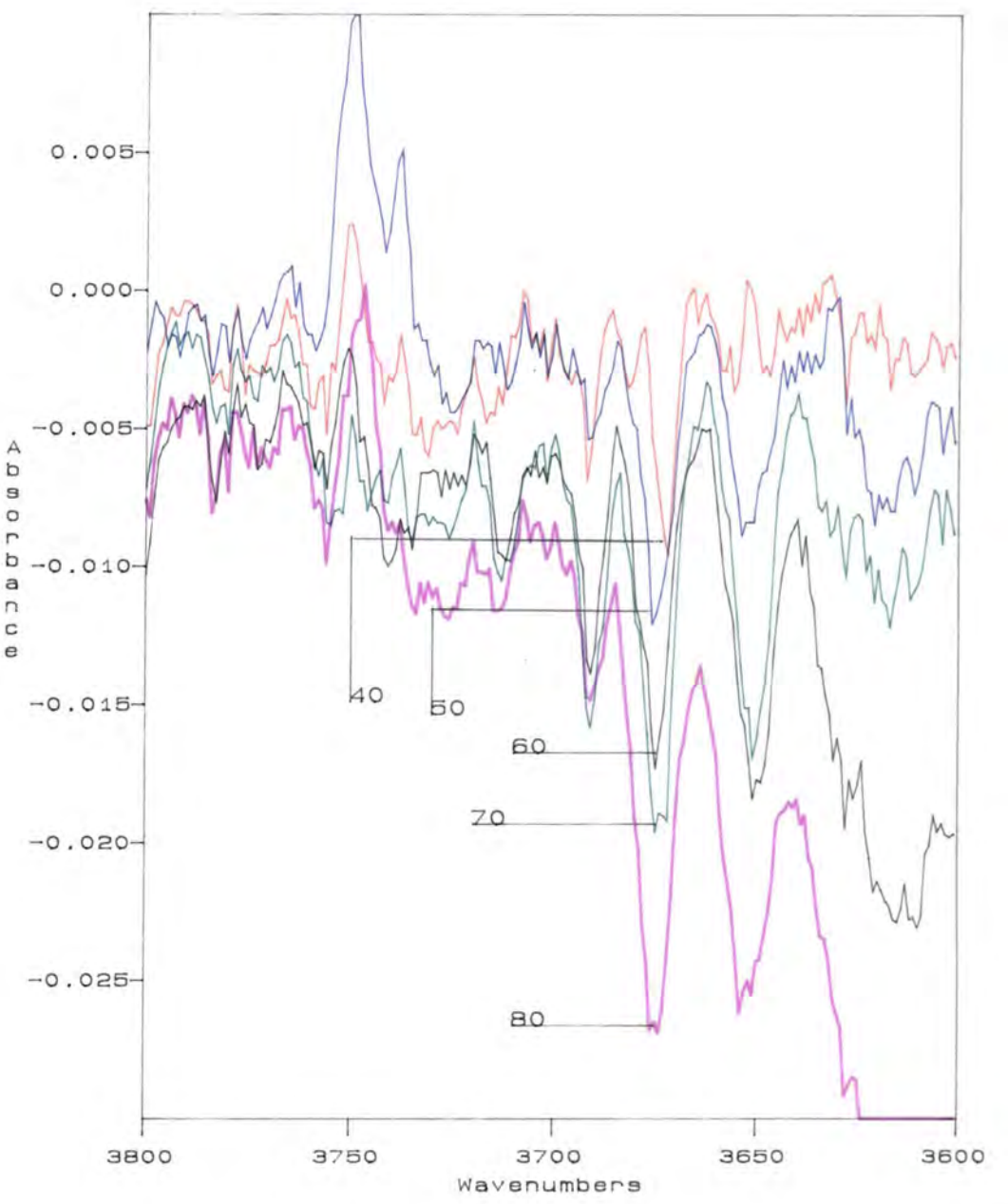

Figure 39–b ν(OH) expanded spectra of Figure 39–a

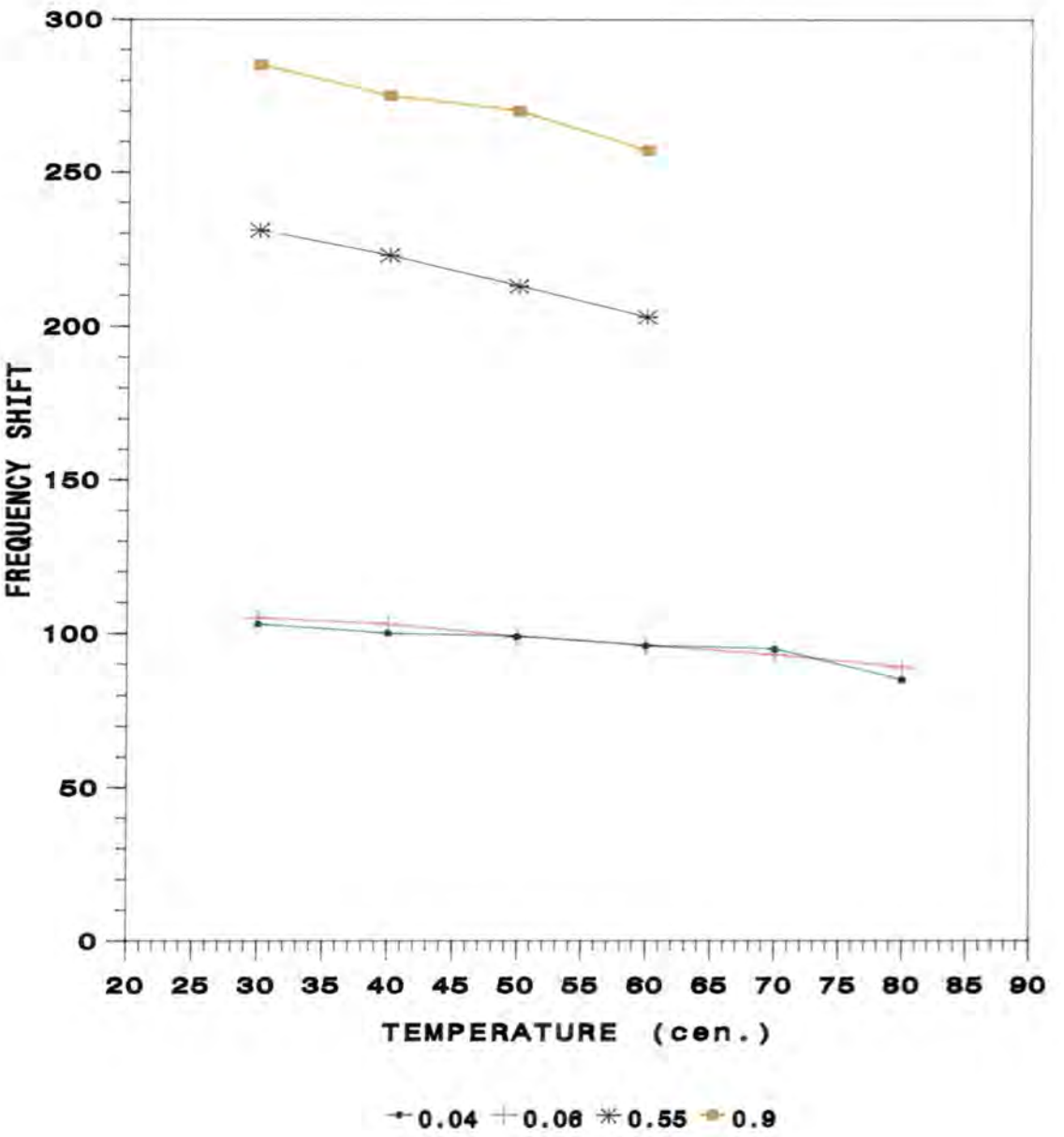

Figure 40 ν(OH) frequency shift of methanol in binary systems at different methanol mole fraction concentrations as presented in Table 13.

Looking again at the spectra shown in figures 35 to 38, it seems evident that the major band has more than one overlapping band. In addition to the two bands mentioned above, another band at 3566cm^{-1} might exist across the whole temperature range and this might be the cyclic dimer of methanol. The other band, at 3585cm^{-1}, which appears at 82°C could be due to the shift of the cyclic dimer band or to an unassigned band. Also, a very broad subsidiary peak at 3450cm^{-1}, which might be the cyclic trimer or the 2:1 methanol:acetonitrile complex could be present. This decreased in intensity with increasing temperature due to the breaking of hydrogen bonds between methanol aggregates (or the (O$\cdots$N) bond in the 2:1 methanol in acetonitrile complex).

The above analysis, was applied to all other concentrations of mixtures studied across the temperature range. At 0.06 methanol mole fraction (Figure 36), the major band is at 3536cm^{-1} (shifted from 3545cm^{-1} in 0.04 mole fraction due to the different strength of hydrogen bond). Unfortunately, due to the water vapour in the spectra (Figure 36), it was not possible to identify the two bands at higher frequency. However, subtracting all other spectra from the lowest temperature spectrum resulted in Figure 41–a and the expanded spectra in Figure 41–b. Clearly, two bands at 3750 and 3675cm^{-1} can be seen. At the same time, a band at 3400cm^{-1} might exist. Otherwise, the major band is shifted to higher frequency and reduced in intensity, as expected and explained before. Finally, the spectra of 0.55 and 0.9 mole fraction (Figures 37 and 38) have the same trend as 0.04 and 0.06 mole fraction spectra, except that the methanol aggregate can not be detected by eye and a band fitting program is needed for analyzing the band components. Unfortunately this was not done due to the time limitation.

0.04 methanol mole fraction was tested at very low temperature (–22 to 0.1 $^{\circ}$C) where the liquid (it might be glass) is well associated compared with higher temperature. Six bands were observed in the spectra (Figure 42) at: 3728cm^{-1} and 3705cm^{-1}, which were not assigned in literature before, and increased in intensity with increasing temperature; 3624cm^{-1} and 3600cm^{-1}, which had the

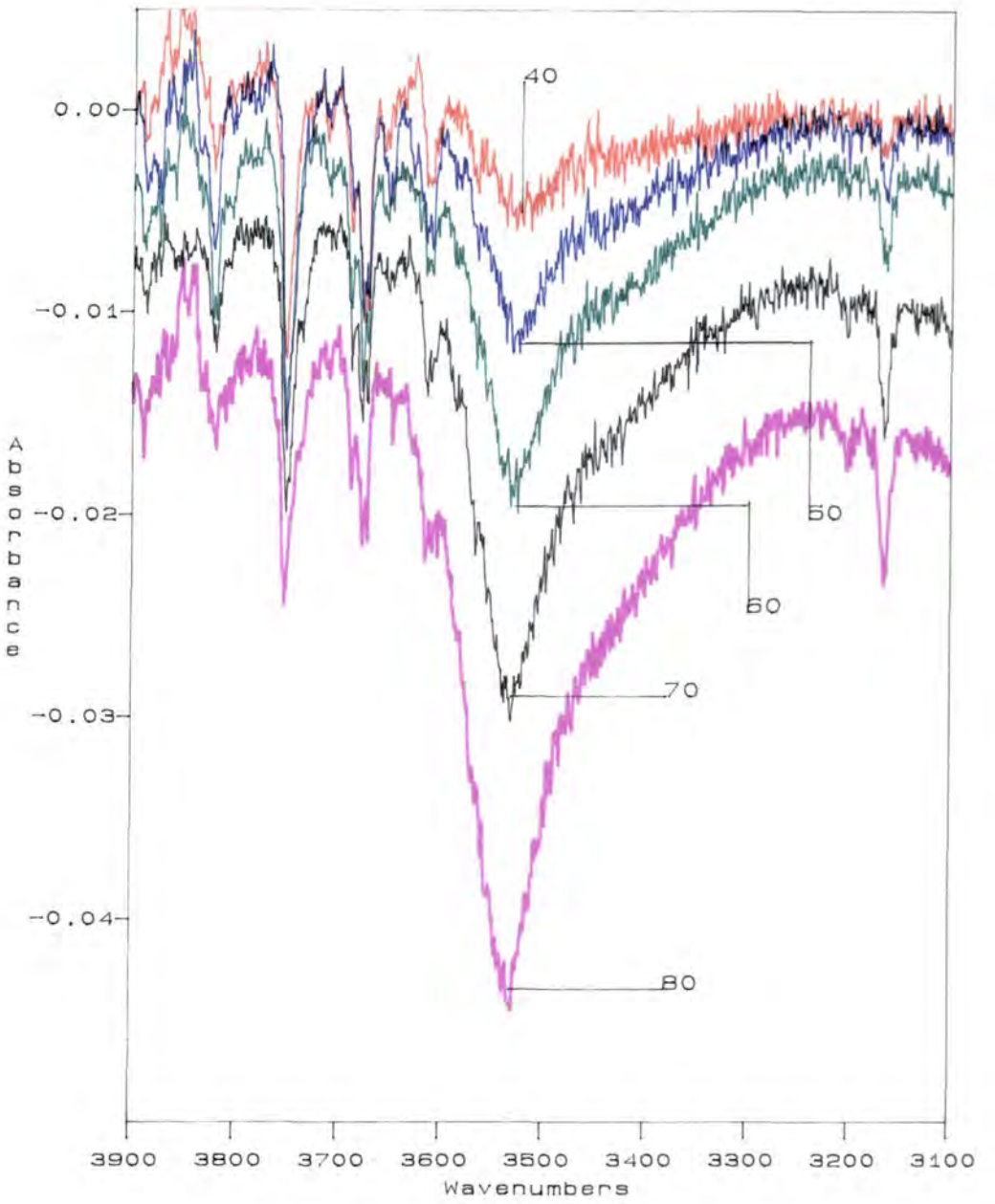

Figure 41–a ν(OH) subtracted spectra (from ν(OH) spectrum at 30°C) of 0.06 methanol mole fraction at different temperatures in degrees centigrade.

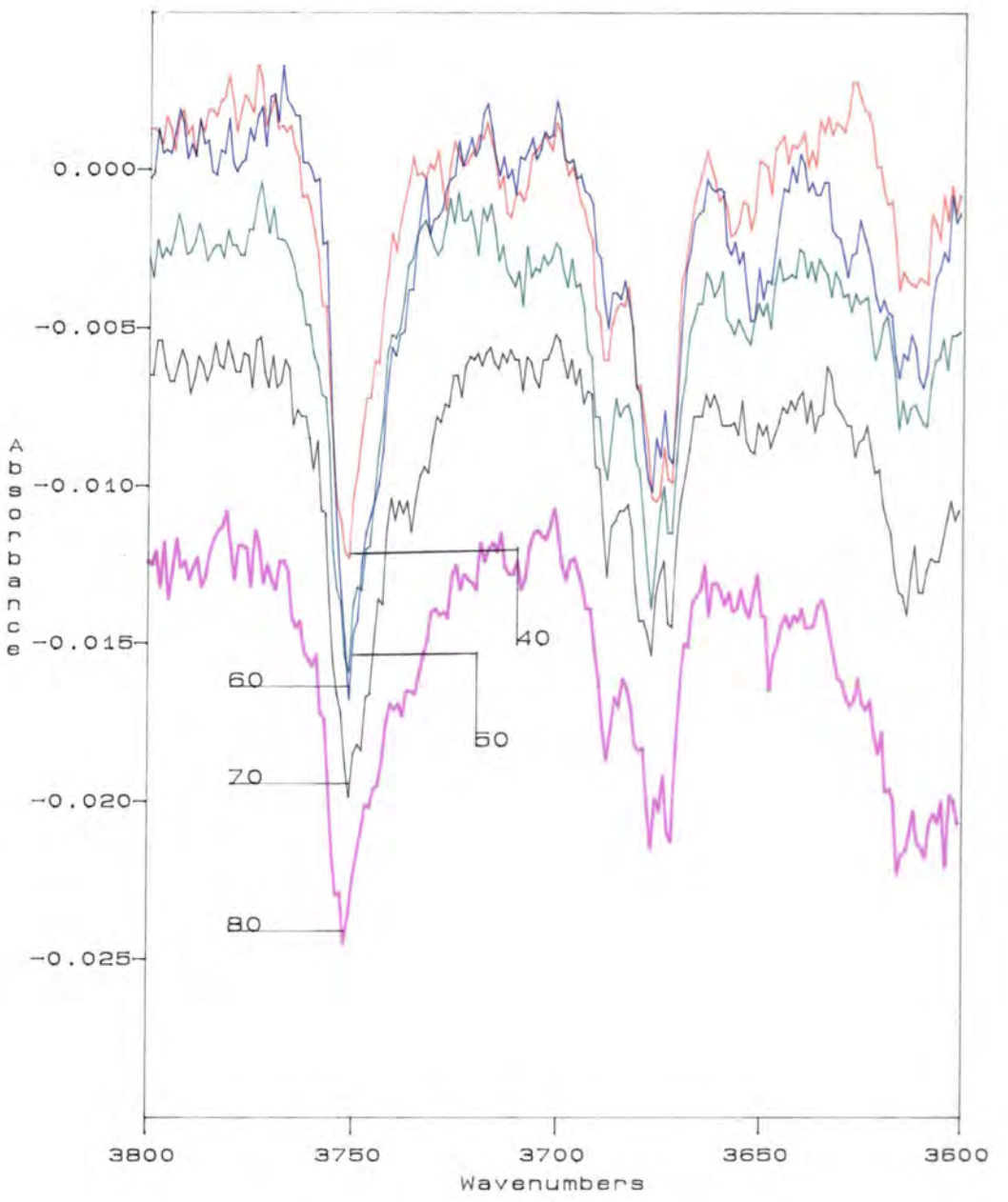

Figure 41–b ν(OH) expanded spectra of Figure 41–a

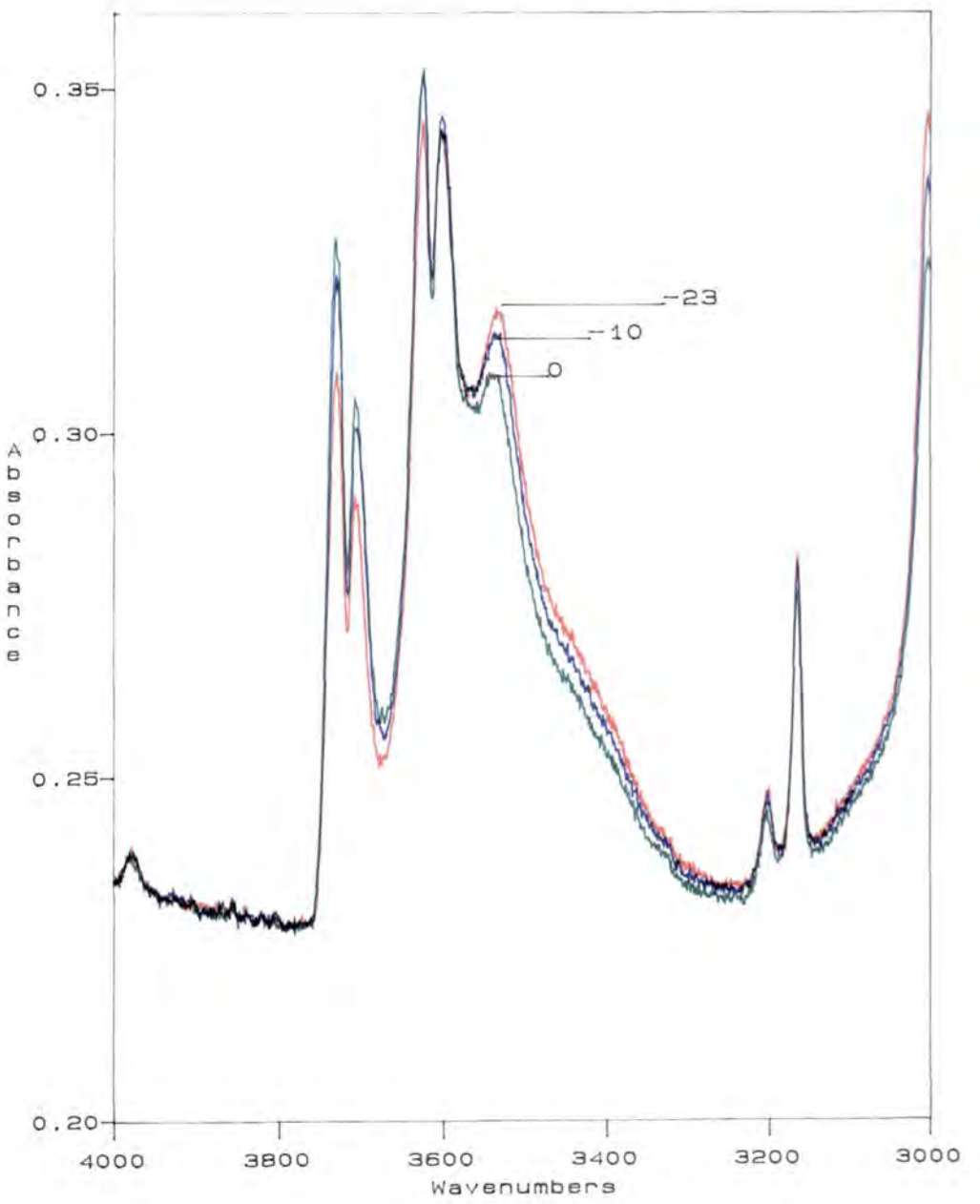

Figure 42 ν(OH) spectra of 0.04 methanol mole fraction very low temperatures in degrees centigrade.

same trend; 3532cm^{-1} and 3420cm^{-1}, which decreased in intensity with increasing temperature.

3.4.2 Band Fitting Analysis

The subtracted spectra of 0.01 – 0.9 methanol mole fraction solutions in the binary system were transferred and the data were reformatted in the way mentioned in the experimental chapter. An example is shown in Figures 43–a and 43–b. Two band fitting programs were used to fit the observed spectrum. One of them was Pitha and Jones' NRC[64] programs. It depends on methods of fitting analytical functions to I.R. absorption bands of condensed phase systems. The first part of the program (Called "BBshape") includes a correction for the spectral slit distortion. It operates on all indices (this will be described in detail below) simultaneously and handles the sum functions of Lorentzian and Gaussian components. The slit parameter was introduced and the curve generation from the calculated indices was convoluted with the spectral slit function before optimization with the experimental data. By this a band envelope was generated that conforms with the contour of the true spectrum adjusted for the finite spectral slit distortion. The indices input data were in the following order:

Lines

1 & 2 = Head 1 and Head 2 (Titles)

Line 3 = NDATA, IDECK, NP, M, KURVE, NSEC, NI, MLIST, LIMIT, NONNEG and MODE

= 1(terminal run), 2(printed data), 561–701(depends on number of data points), 2–4(depends on methanol concentration), 1(pure lorentzian) or 2(sum function), 200(computer time), 20(no. of iterations), 1(printing data), 2(no $\nu_{\frac{1}{2}}$ restrictions), 1(restrict to zero or positive values), 1(input slit width)

Line 4 = WB, WI, CAY

= 3800(starting frequency), 1(wavenumber interval), 0.8(ratio of X_4/X_3, will be defined later)

Line 5 = Up, Down, Change

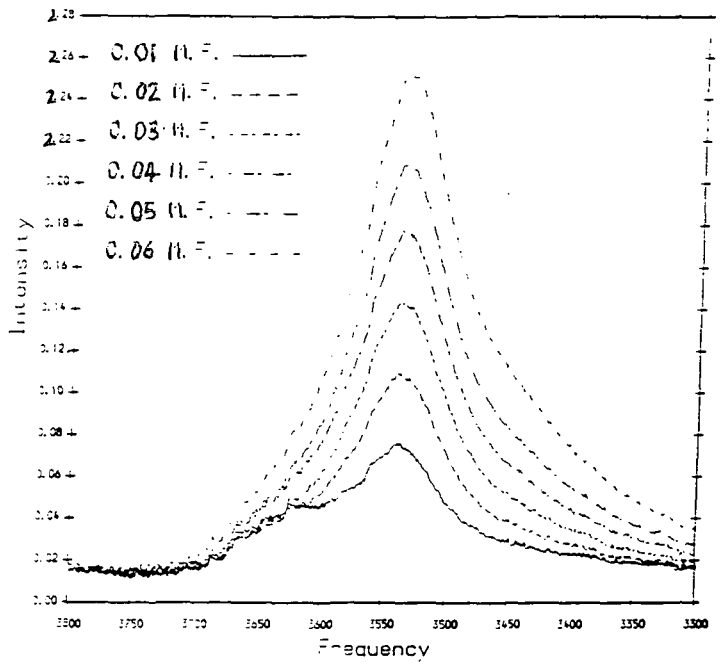

Figure 43–a ν(OH) stretching mode of methanol in binary systems at different methanol mole fraction

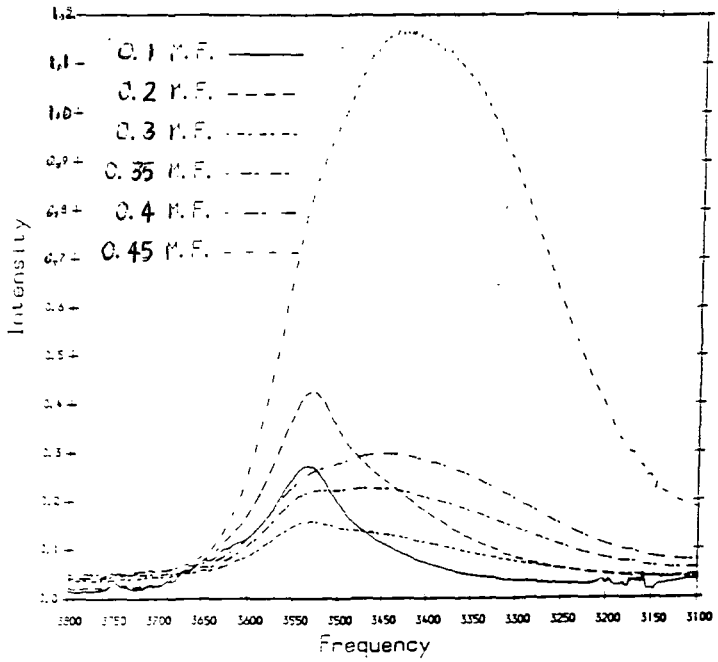

Figure 43–b ν(OH) stretching mode of methanol in binary systems at different methanol mole fraction and different path lengths as presented in Chapter 2

= 0.01, 1000, 0.5(parameters used to control the damping factors)

Line 6 = SSW = 2.5 (spectral slit width)

Line 7 = X_1, X_2, X_3 and X_5

= Lorentzian absorbance, frequency, $1/\frac{1}{2}\Delta\nu_{\frac{1}{2}}$, Gaussian absorbance

Line 8 = Base line (variable depending on the data file)

The most difficult part was to guess the number of existing bound components for each concentration data file (observed spectrum). These guesses were initially input based on three factors:

a. Literature information

b. Experience in the difference of the band shape for each spectra

and c. The outlook of the calculated spectra compared to the observed one along with keeping the sum of the square calculated value to be as low as possible.

The indices in Line 7 were altered several times until the calculated spectrum was close enough to the observed one, as mentioned in point c. The outlook of the results are shown in Figures 44-59. Note that some of the files had to be truncated at 3250cm^{-1} to avoid interference from the acetonitrile combination bands which appear at about 3200cm^{-1}. At a higher concentration (> 0.2 methanol mole fraction) this could not be done since it would affect the shape of the band of interest. Hence the part between 3200 - 3100cm^{-1} was smoothed for better computation.

The computed indices from the first program were used in the second part of the band fitting program (called "BBGEN" in our work) for recalculating the ordinates of the composite band envelope. This program calculated and listed the individual computed abscissa values of the calculated band envelope from the band indices. The abscissa units are in wavenumber in cm^{-1}, recorded at constant wavenumber intervals in diminishing sequence, while the input and

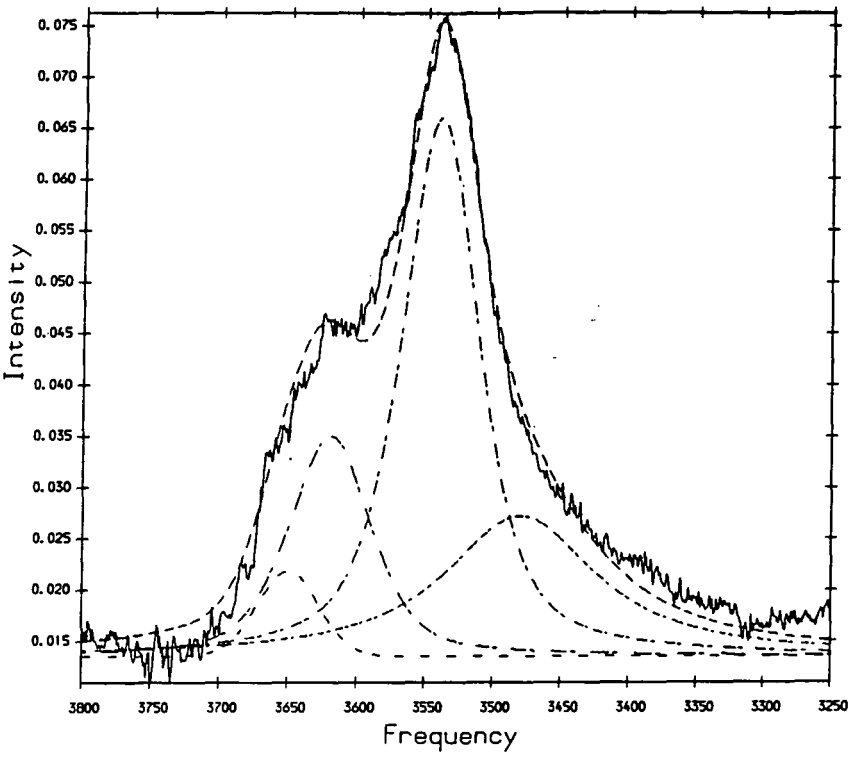

Figure 44 ν(OH) stretching mode of 0.01 methanol in 0.99 acetonitrile mole fraction: ____ experimental, – – – overall calculated, –.–.–. band component.

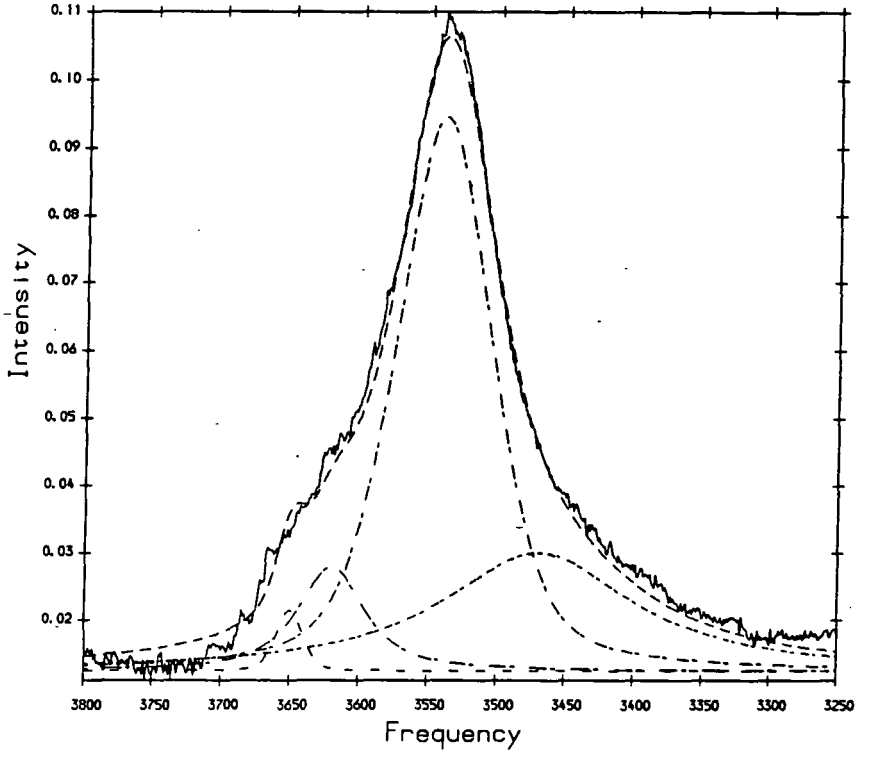

Figure 45 ν(OH) stretching mode of 0.02 methanol in 0.98 acetonitrile mole fraction: ____ experimental, – – – overall calculated, –.–.–. band component.

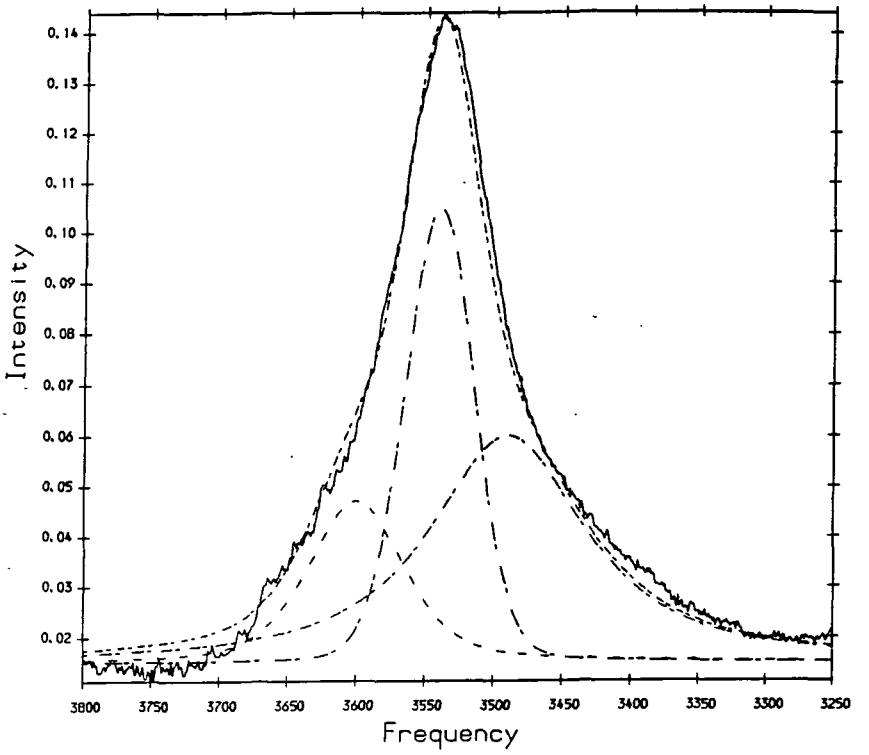

Figure 46 ν(OH) stretching mode of 0.03 methanol in 0.97 acetonitrile mole fraction: ____ experimental, – – – overall calculated, –.–.–. band component.

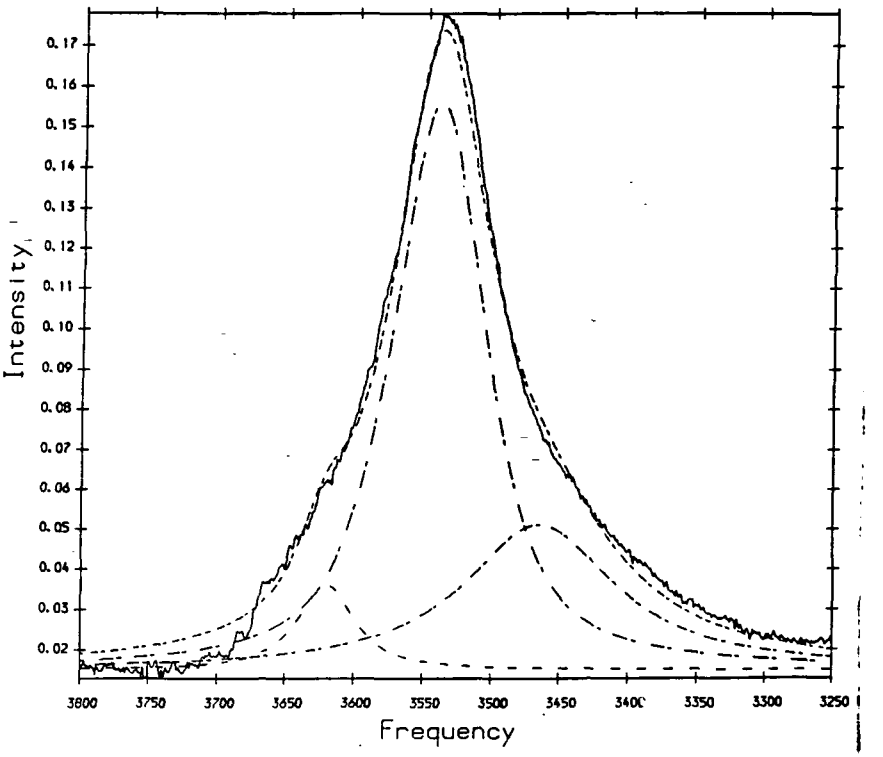

Figure 47 ν(OH) stretching mode of 0.04 methanol in 0.96 acetonitrile mole fraction: ____ experimental, – – – overall calculated, –.–.–. band component.

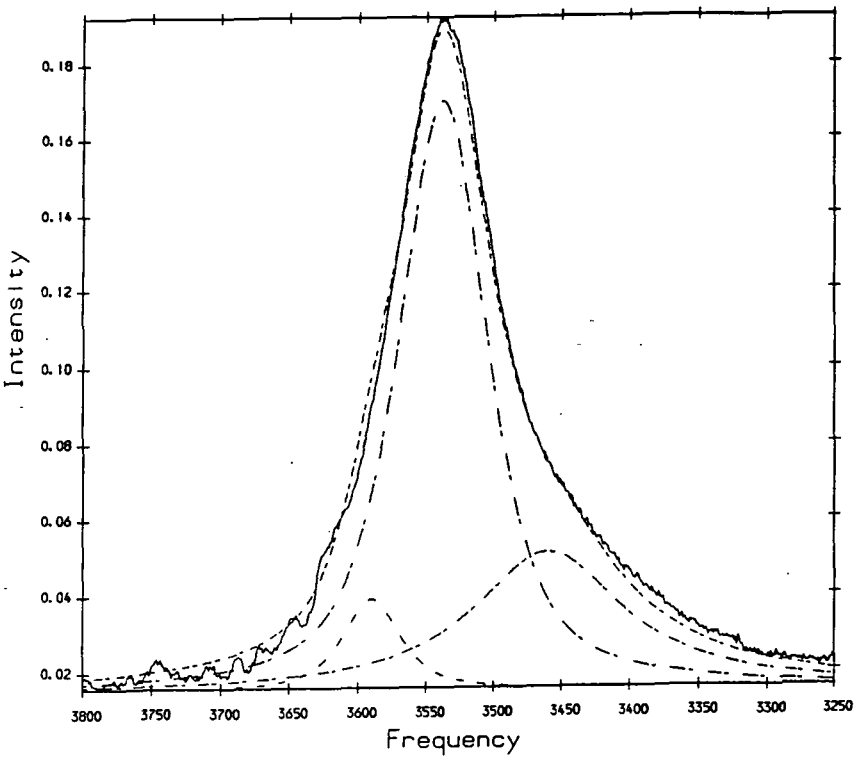

Figure 48 ν(OH) stretching mode of 0.045 methanol in 0.955 acetonitrile mole fraction: ____ experimental, – – – overall calculated, –.–.–. band component.

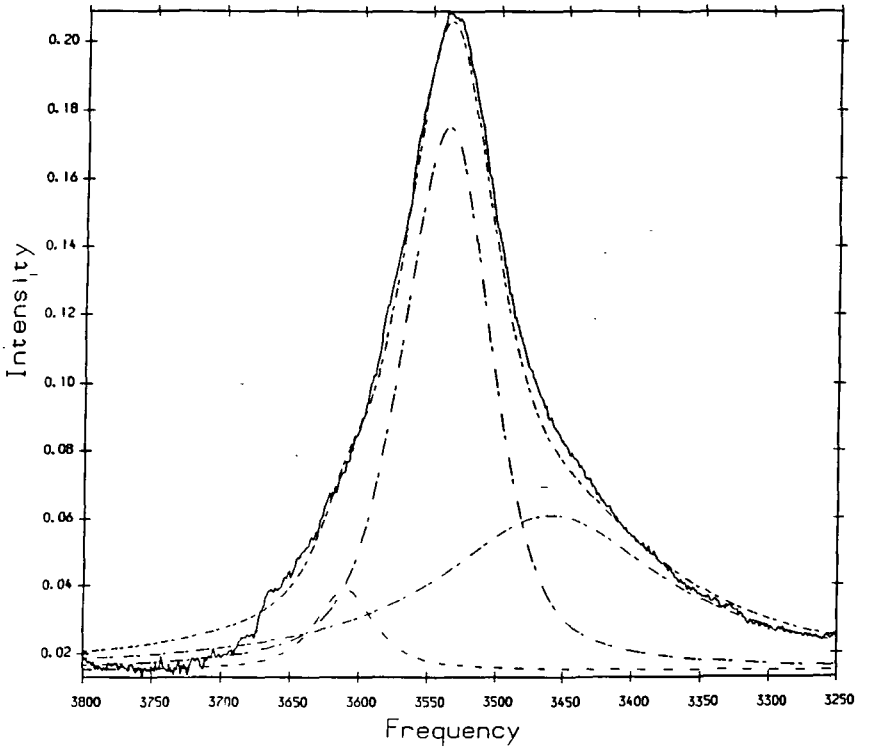

Figure 49 ν(OH) stretching mode of 0.05 methanol in 0.95 acetonitrile mole fraction: ____ experimental, – – – overall calculated, –.–.–. band component.

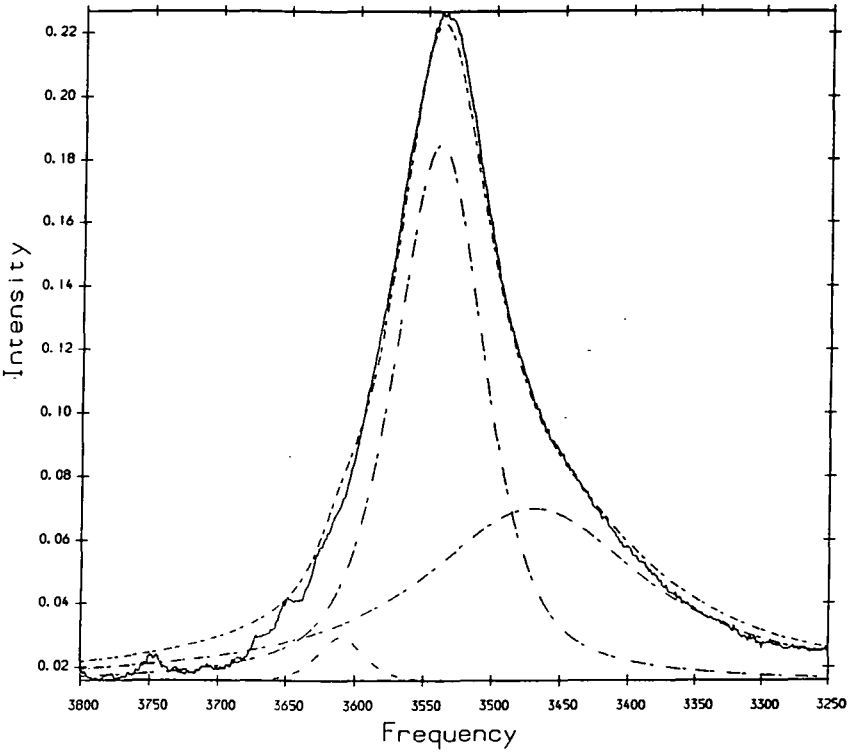

Figure 50 ν(OH) stretching mode of 0.055 methanol in 0.945 acetonitrile mole fraction: ____ experimental, – – – overall calculated, –.–.–. band component.

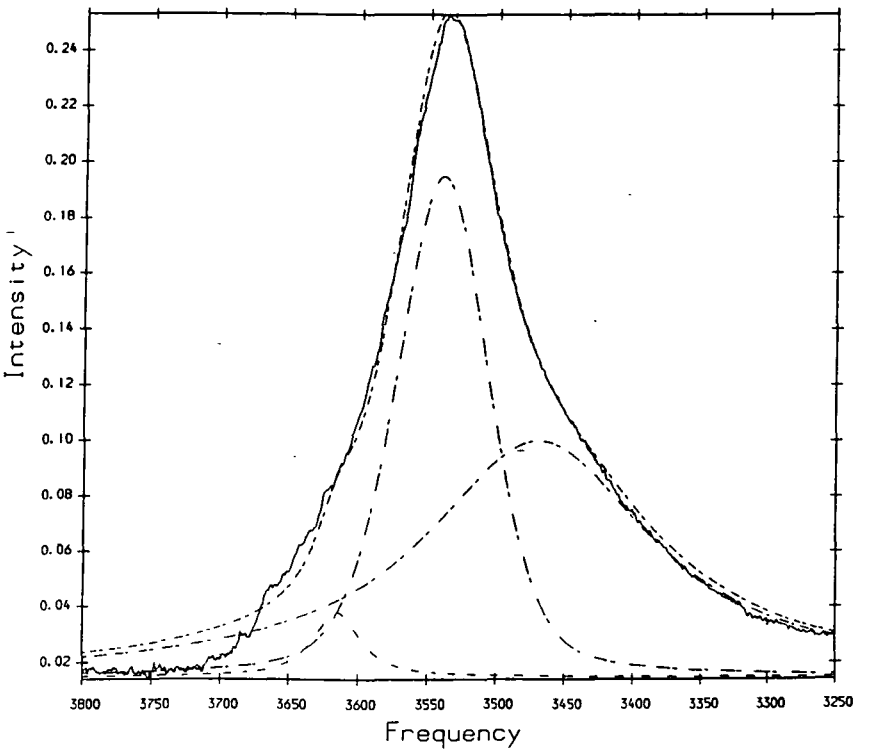

Figure 51 ν(OH) stretching mode of 0.06 methanol in 0.94 acetonitrile mole fraction: ____ experimental, – – – overall calculated, –.–.–. band component.

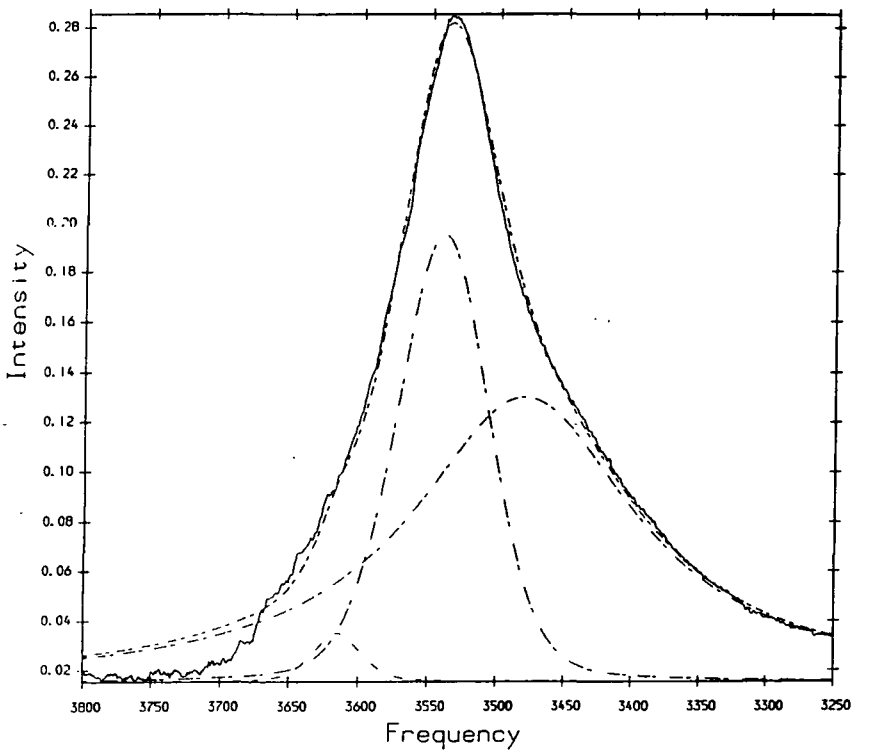

Figure 52 ν(OH) stretching mode of 0.07 methanol in 0.93 acetonitrile mole fraction: ____ experimental, – – – overall calculated, –.–.–. band component.

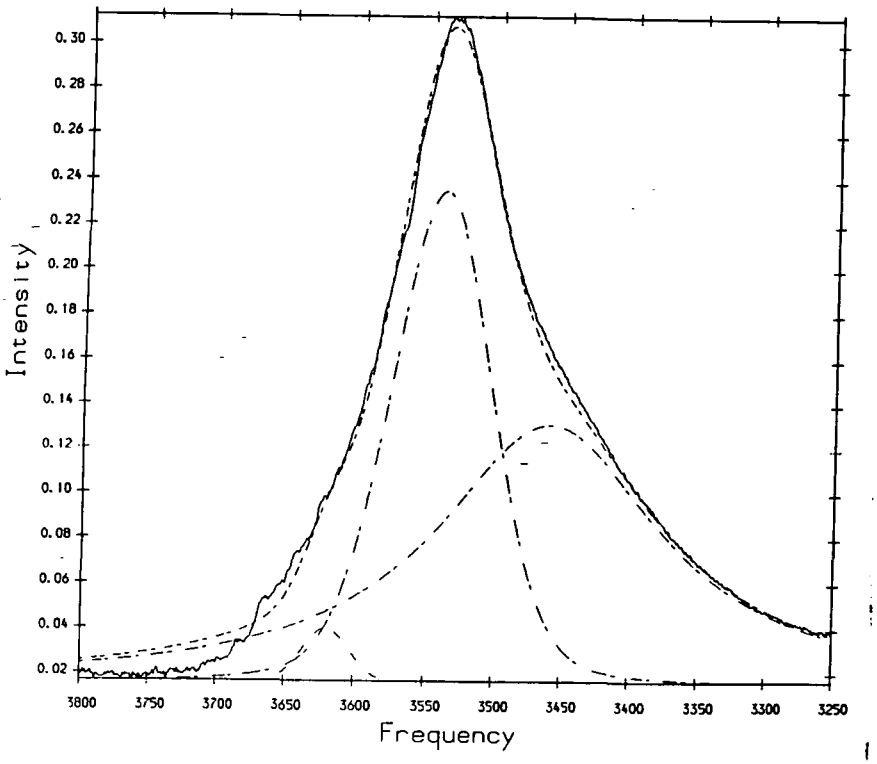

Figure 53 ν(OH) stretching mode of 0.08 methanol in 0.92 acetonitrile mole fraction: ____ experimental, – – – overall calculated, –.–.–. band component.

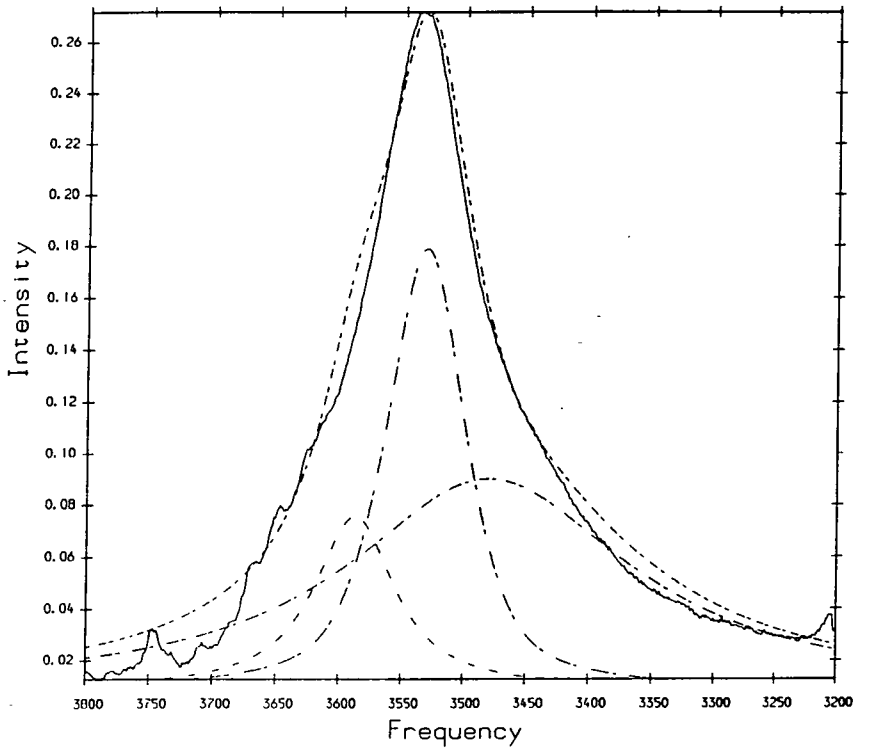

Figure 54 ν(OH) stretching mode of 0.1 methanol in 0.9 acetonitrile mole fraction: ____ experimental, – – – overall calculated, –.–.–. band component.

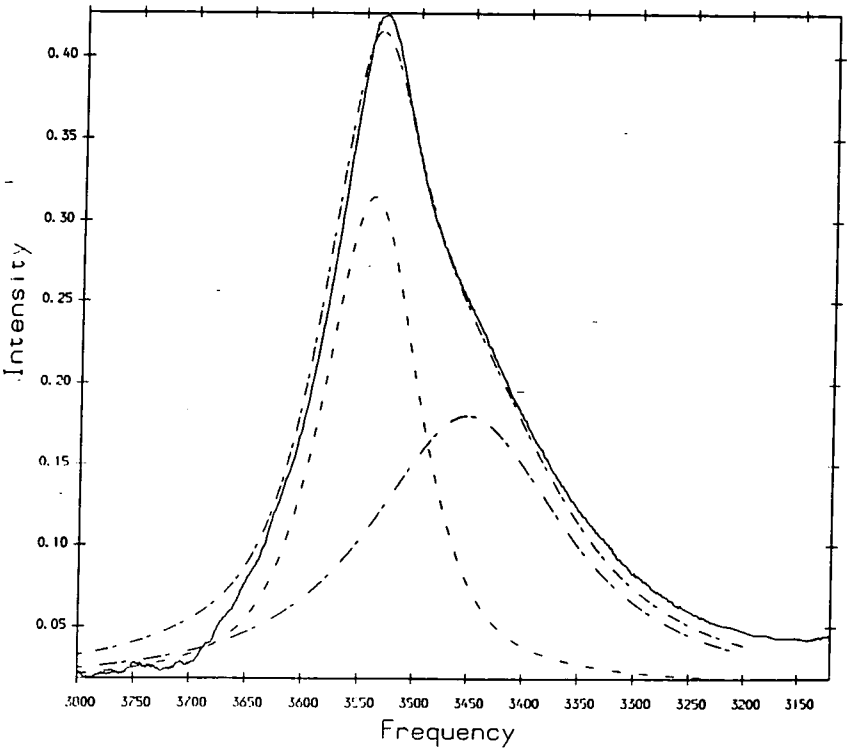

Figure 55 ν(OH) stretching mode of 0.2 methanol in 0.8 acetonitrile mole fraction: ____ experimental, – – – overall calculated, –.–.–. band component.

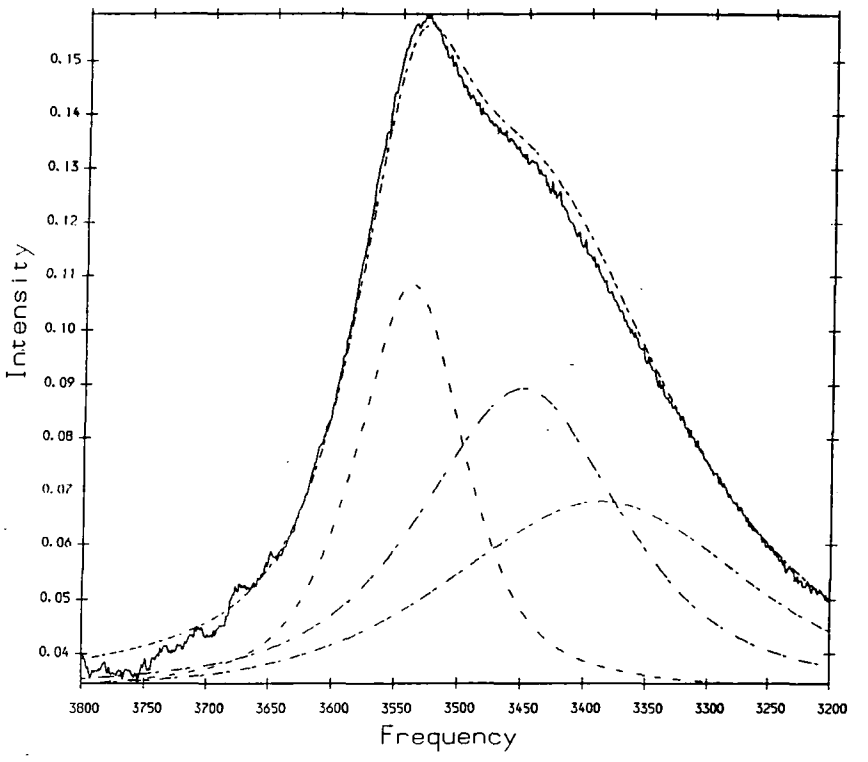

Figure 56 ν(OH) stretching mode of 0.3 methanol in 0.7 acetonitrile mole fraction: ____ experimental, – – – overall calculated, –.–.–. band component.

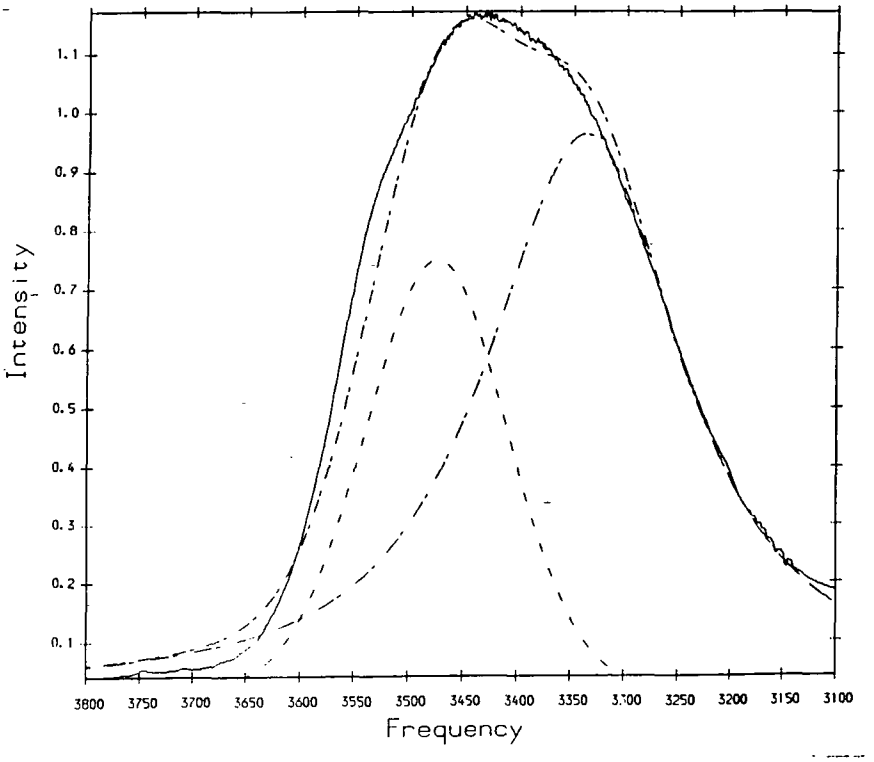

Figure 57 ν(OH) stretching mode of 0.45 methanol in 0.55 acetonitrile mole fraction: ____ experimental, – – – overall calculated, –.–.–. band component.

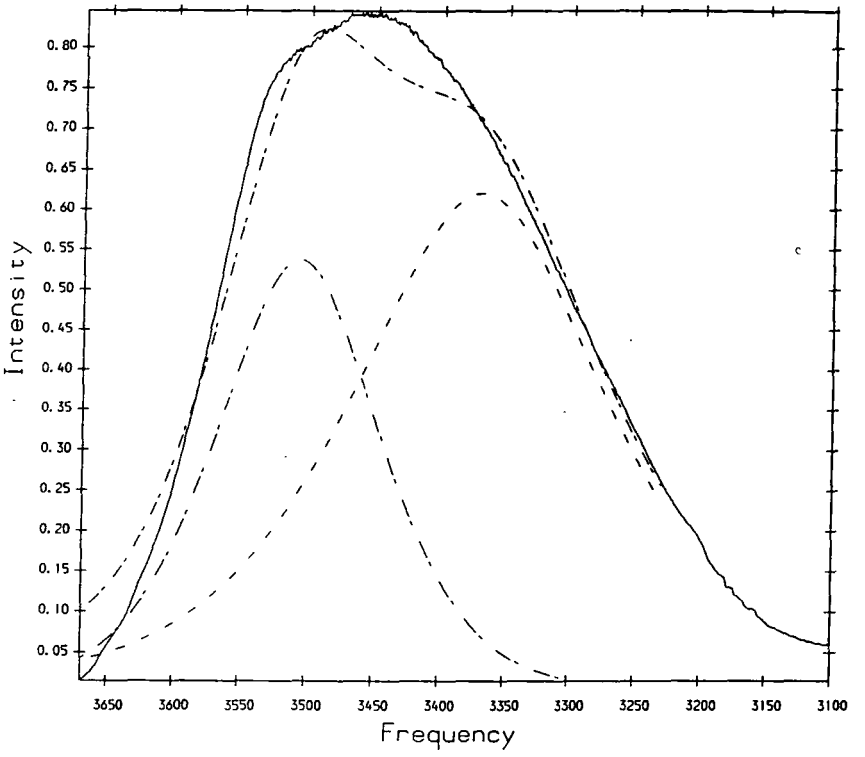

Figure 58 ν(OH) stretching mode of 0.5 methanol in 0.5 acetonitrile mole fraction: ____ experimental, – – – overall calculated, –.–.–. band component.

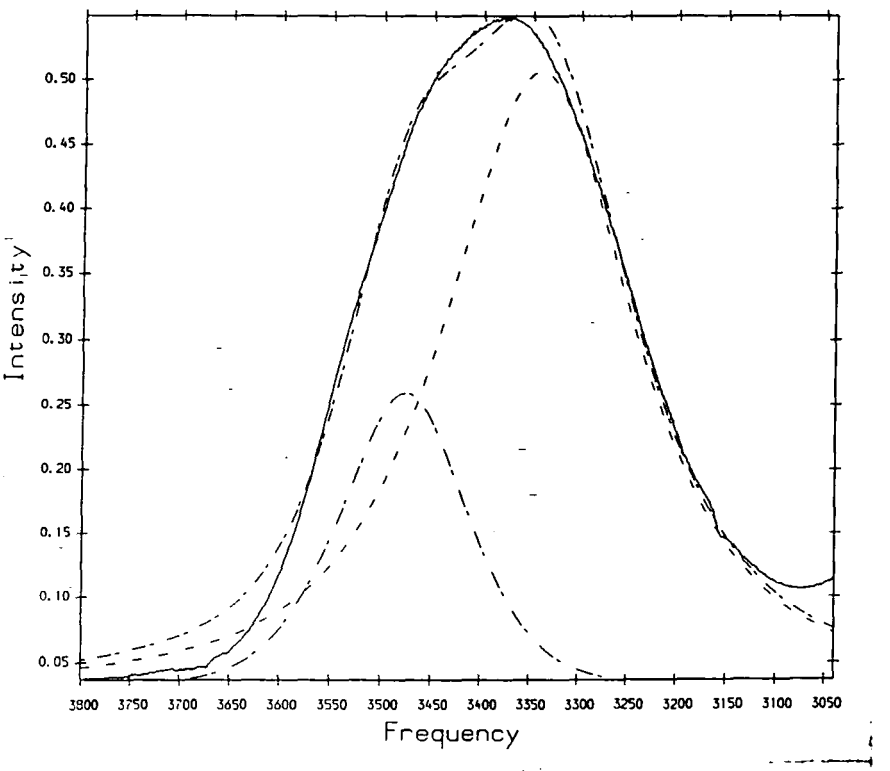

Figure 59 ν(OH) stretching mode of 0.6 methanol in 0.4 acetonitrile mole fraction: ____ experimental, – – – overall calculated, –.–.–. band component.

output indices for peak height X_1 and band centre X_2 are in units of absorbance and cm^{-1} respectively. A subroutine was used also to check the sequence of the experimental data with making a limited number of corrections. The final calculated results are collected in Table 14.

Band fitting of the lowest methanol concentration indicated the existence of the two bands at 3650 and 3620cm^{-1} (which could be monomer and dimer or dimer and trimer respectively). The existence of such bands at a very low methanol concentration (0.197 mol/dm^3) relative to acetonitrile concentration (21.94 mol/dm^3) shows that methanol aggregation is still likely to occur, *i.e.* the hydrogen bonding of (O-H···O) is sometimes more likely to happen than (O-H···N). The 3650cm^{-1} band disappears at a concentration of 0.59 mol/dm^3 of methanol (20 mol/dm^3 acetonitrile concentration) while the other band, 3620cm^{-1}, increases in intensity (till about 0.997 mol/dm^3 of methanol) then decreases in intensity when the concentration is increased until it disappears at 1.65 mol/dm^3 of methanol as shown in the plot of Figure 60. This shows that for concentration ratios of methanol in acetonitrile between 1:103 and 1:51 molecules the smallest species of methanol aggregate still exist and can be detected by I.R. spectroscopy. The existence of such aggregates in a high concentration of the second component was observed by Besnard and his co-workers[50] when they studied the acetonitrile band by Raman spectroscopy. They found that, even at a very low concentration of acetonitrile (high concentration of methanol), some "free" acetonitrile could still be detected. It was noticed that the half-width of the 3620cm^{-1} band decreases when increasing the methanol concentration. This is clearly seen in the plot of the half-width of that band versus the concentration of methanol in Figure 61. This could indicate a decrease in the number of species represented by this band when using higher methanol concentration, as well as a weakening of the strength of the hydrogen bond.

Table 14 Obtained and Calculated Band Component Parameters

CH_3OH (m.f.)	Number of Bands	X_1	X_2	X_3	X_5	Sum of squares	X_1+X_5	$\Delta\nu_{\frac{1}{2}}$	Integrated Intensity	Normalised Integrated Intensity
0.01	4	0.001	3650	0.0395	0.0082	0.0046	0.0083	12.65	0.3298	0.0581
		0.011	3620	0.029	0.0105		0.0215	17.24	1.1639	0.2051
		0.0332	3540	0.03	0.0193		0.0525	16.66	2.747	0.4840
		0.0133	3480	0.015	0.0004		0.0137	33.33	1.4339	0.2526
0.02	4	0.0025	3650	0.09	0.0065	0.0046	0.009	5.55	0.1569	0.0189
		0.013	3620	0.035	0.0025		0.0155	14.28	0.6952	0.0838
		0.035	3540	0.025	0.047		0.082	20	5.1496	0.6210
		0.017	3470	0.012	0.0005		0.0175	41.66	2.2895	0.2761
0.03	3	0.015	3600	0.025	0.017	0.0069	0.032	20	2.0096	0.1868
		0.01	3540	0.035	0.08		0.09	14.28	4.0371	0.3753
		0.04	3490	0.015	0.005		0.045	33.33	4.7099	0.4378
0.04	3	0.019	3620	0.04	0.002	0.008	0.021	12.5	0.8242	0.0596
		0.1	3540	0.024	0.041		0.141	20.83	9.2237	0.6676
		0.035	3465	0.015	0.001		0.036	33.3	3.7679	0.2727
0.045	3	0.019	3590	0.04	0.005	0.0065	0.024	12.5	0.942	0.0669
		0.1	3538	0.026	0.055		0.155	19.23	9.359	0.6652
		0.035	3460	0.015	0.001		0.036	33.3	3.767	0.2677

Table 14 Obtained and Calculated Band Component Parameters (continued)

CH_3OH (m.f.)	Number of Bands	X_1	X_2	X_3	X_5	Sum of squares	X_1+X_5	$\Delta\nu_{\frac{1}{2}}$	Integrated Intensity	Normalised Integrated Intensity
0.05	3	0.019	3610	0.04	0.005	0.0096	0.024	12.5	0.942	0.0531
		0.08	3538	0.0263	0.08		0.16	19.011	9.5513	0.5391
		0.045	3460	0.01	0.001		0.046	50	7.222	0.4076
0.055	3	0.01	3610	0.05	0.0045	0.0099	0.0145	10	0.145	0.0075
		0.1	3540	0.0259	0.07		0.17	19.30	10.305	0.5399
		0.054	3470	0.01	0.001		0.055	50	8.635	0.4524
0.06	3	0.021	3615	0.05	0.002	0.0119	0.023	10	0.7222	0.0289
		0.06	3540	0.026	0.12		0.18	19.23	10.869	0.4358
		0.084	3470	0.01	0.001		0.085	50	13.345	0.5351
0.07	3	0.01	3615	0.05	0.01	0.0136	0.02	10	0.628	0.0212
		0.04	3540	0.026	0.14		0.18	19.23	10.869	0.3677
		0.114	3480	0.01	0.001		0.115	50	18.055	0.6109
0.08	3	0.01	3615	0.05	0.01	0.0136	0.02	10	0.628	0.0212
		0.04	3540	0.026	0.14		0.18	19.23	10.86	0.3675
		0.114	3480	0.01	0.001		0.115	50	18.055	0.6111

Table 14 Obtained and Calculated Band Component Parameters (continued)

CH_3OH (m.f.)	Number of Bands	X_1	X_2	X_3	X_5	Sum of squares	X_1+X_5	$\Delta\nu_{\frac{1}{2}}$	Integrated Intensity	Normalised Integrated Intensity
0.1	3	0.0669	3587	0.0255	0.00	0.0184	0.0669	19.60	4.1189	0.1303
		0.1072	3531	0.0268	0.0629		0.1701	18.656	9.9648	0.3154
		0.0814	3480	0.0073	0.00		0.0814	68.49	17.506	0.5541
0.2	2	0.2084	3540	0.0196	0.0924	0.0237	0.3008	25.510	24.094	0.4698
		0.1379	3452	0.0096	0.0283		0.1662	52.083	27.1806	0.5300
0.3	3	0.0499	3539	0.0199	0.0257	0.0061				
		0.0403	3450	0.0108	0.0161					
		0.0174	3387	–0.007	0.0177					
0.35	3	0.0862	3534	0.0198	0.0311	0.0101				
		0.1306	3433	–0.0115	0.003					
		0.0436	3331	0.007	0.0255					
0.4	2	0.1927	3393	0.0073	0.0187	0.0210	0.2114	68.49	45.465	0.7718
		0.0639	3499	0.0155	0.0688		0.1327	32.25	13.441	0.2281
0.45	2	0.0248	3474	–0.0135	0.7062	0.066				
		0.7995	3338	–0.0092	0.1451					
0.5	2	0.4234	3369	0.0086	0.2137	0.044	0.6371	58.13		
		0.2995	3506	0.0137	0.2550		0.5545	36.49		

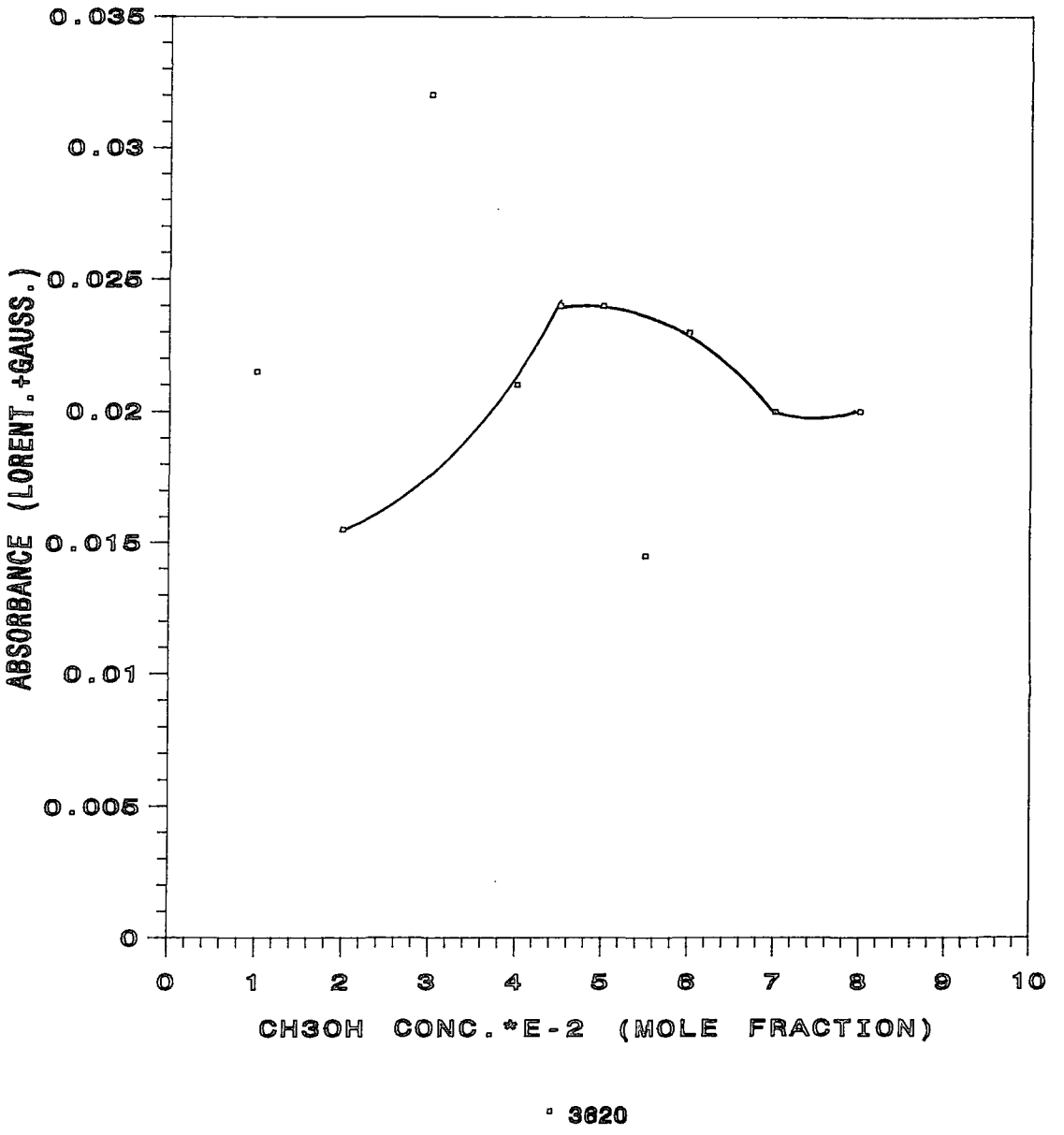

Figure 60 ν(OH) absorbance of methanol in binary systems at 3620cm^{-1}

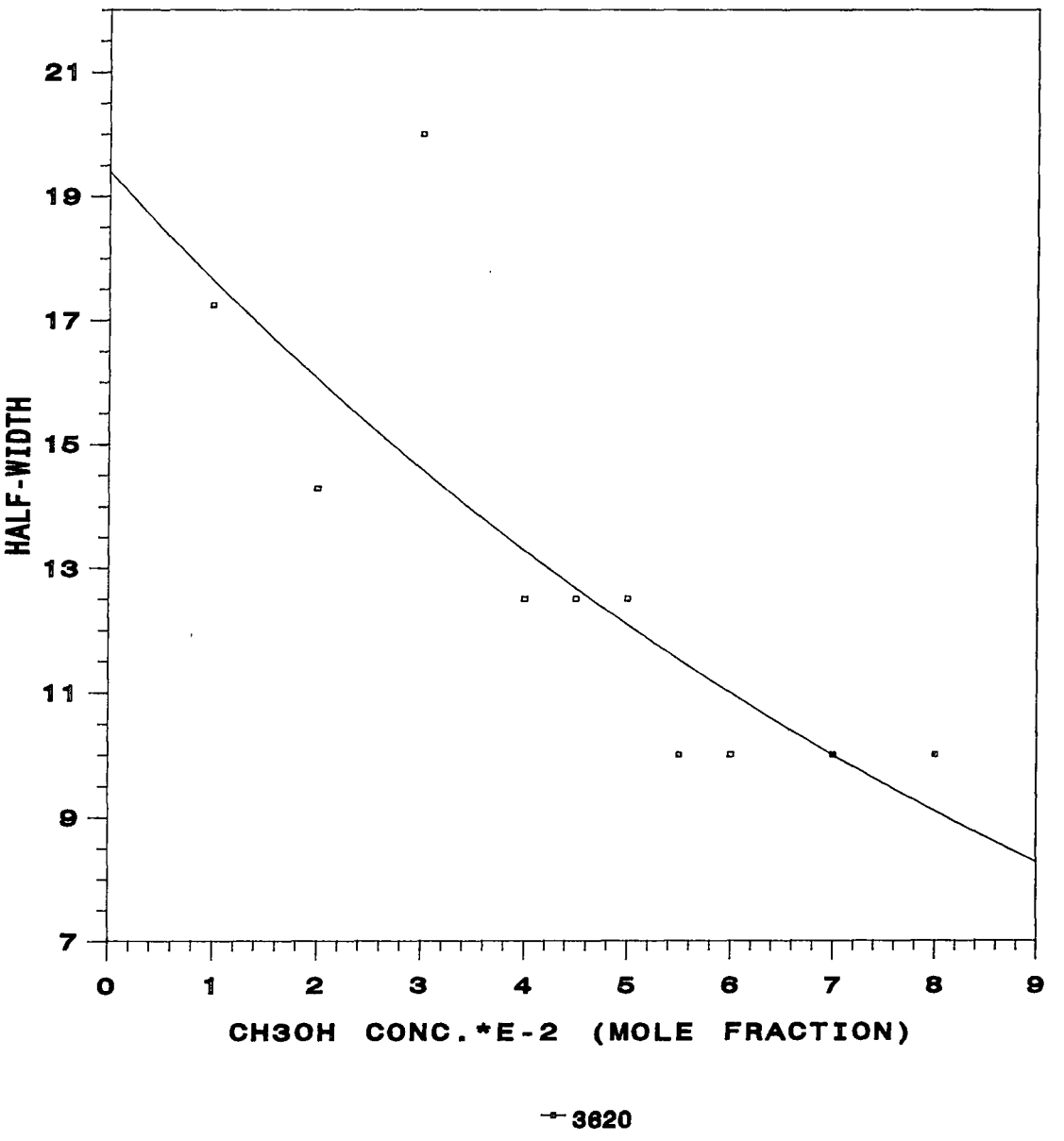

Figure 61 ν(OH) half-width of methanol in binary systems at 3620cm^{-1}

The band at 3480cm^{-1} also exists from the lowest studied methanol concentration (0.01 mole fraction). This band could be either the cyclic trimer (as assigned by Martinez[55]) and/or the 1:2 acetonitrile in methanol complex band. The idea of the possibility of detecting such a complex came from the work of Frank and Wen.[61] They explained that the hydrogen bond between an alcoholic OH-group and an aprotic hydrogen bond acceptor B (*i.e.* O-H$\cdots$B) would be strengthened by the formation of a second hydrogen bond between another alcohol ROH and the OH-group already involved in ROH$\cdots$B (*i.e.* OH$\cdots$OH$\cdots$B). On the other hand, the strength of the hydrogen bond between the two alcohol molecules in

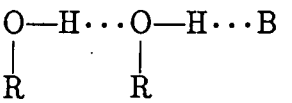

also depends on the hydrogen bond acceptor strength of B. Unfortunately, to my knowledge, this postulate (1:2 complex) was not assigned in the I.R. literature. Also this band (3480cm^{-1}) was not observed either at different temperatures or in the spectra of the ternary system studies. Figure 62 shows an increase in the absorbance of this band which is due to the increase in the hydrogen bond formation of either the 1:2 acetonitrile in methanol complex or the methanol aggregates.

The most intense band observed in the spectra is at 3540cm^{-1} which is well defined in the literature[32,64] as the ν(OH) band of the 1:1 complex. It could be overlapped with the cyclic dimer band. The absorbance of this band increases on increasing the methanol concentration, indicating an increase in the concentration of such a complex. This is shown in Figure 63. The half-width decreases as shown in Figure 64 which could be due to losing one of the existing species, as previously mentioned. It is worth saying, to remind the reader, that in the NRC program, a large Gaussian components had to be used to obtain a better fit, although such components may not be justified, physically.

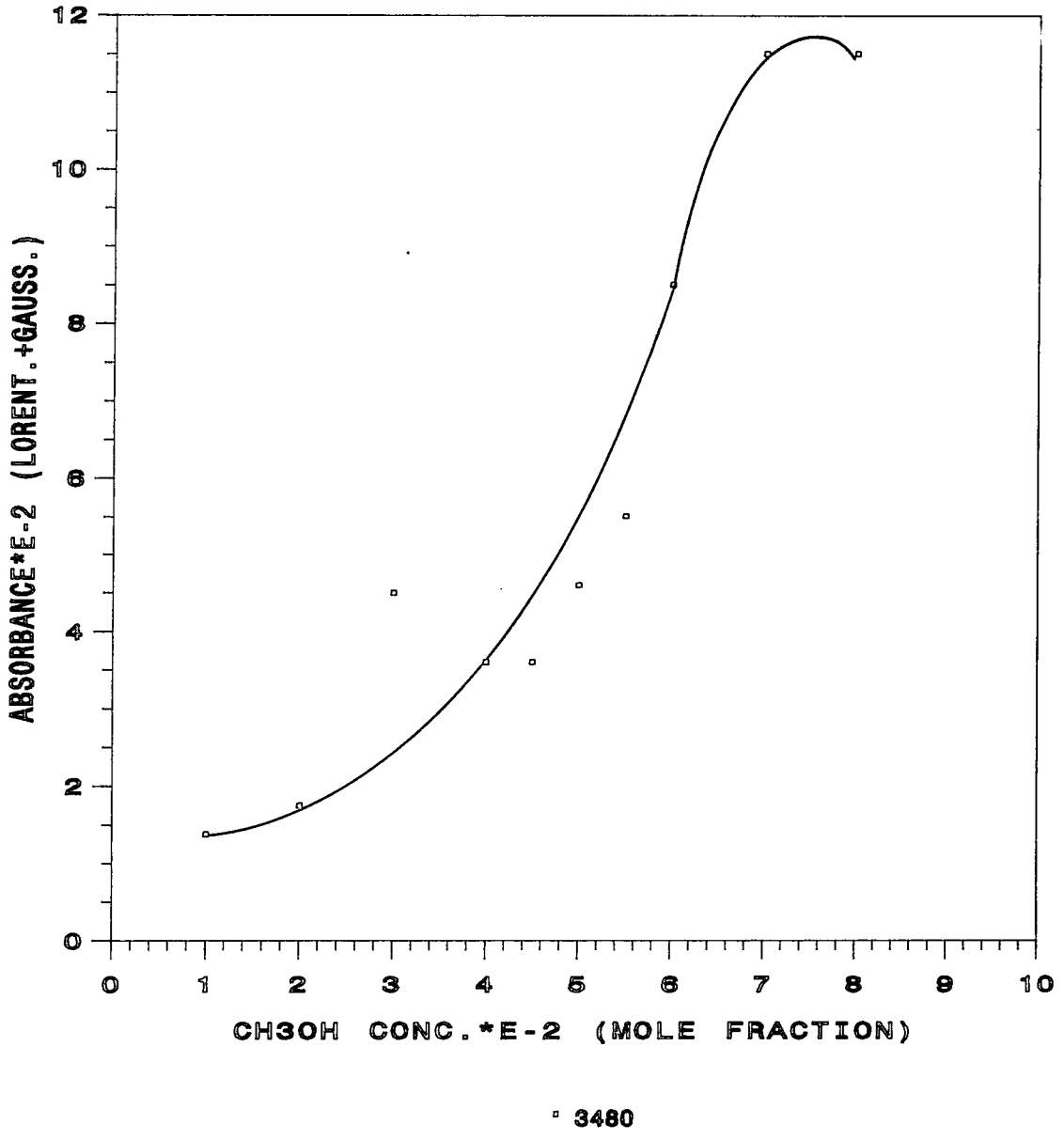

Figure 62 ν(OH) absorbance of methanol in binary systems at 3480cm^{-1}

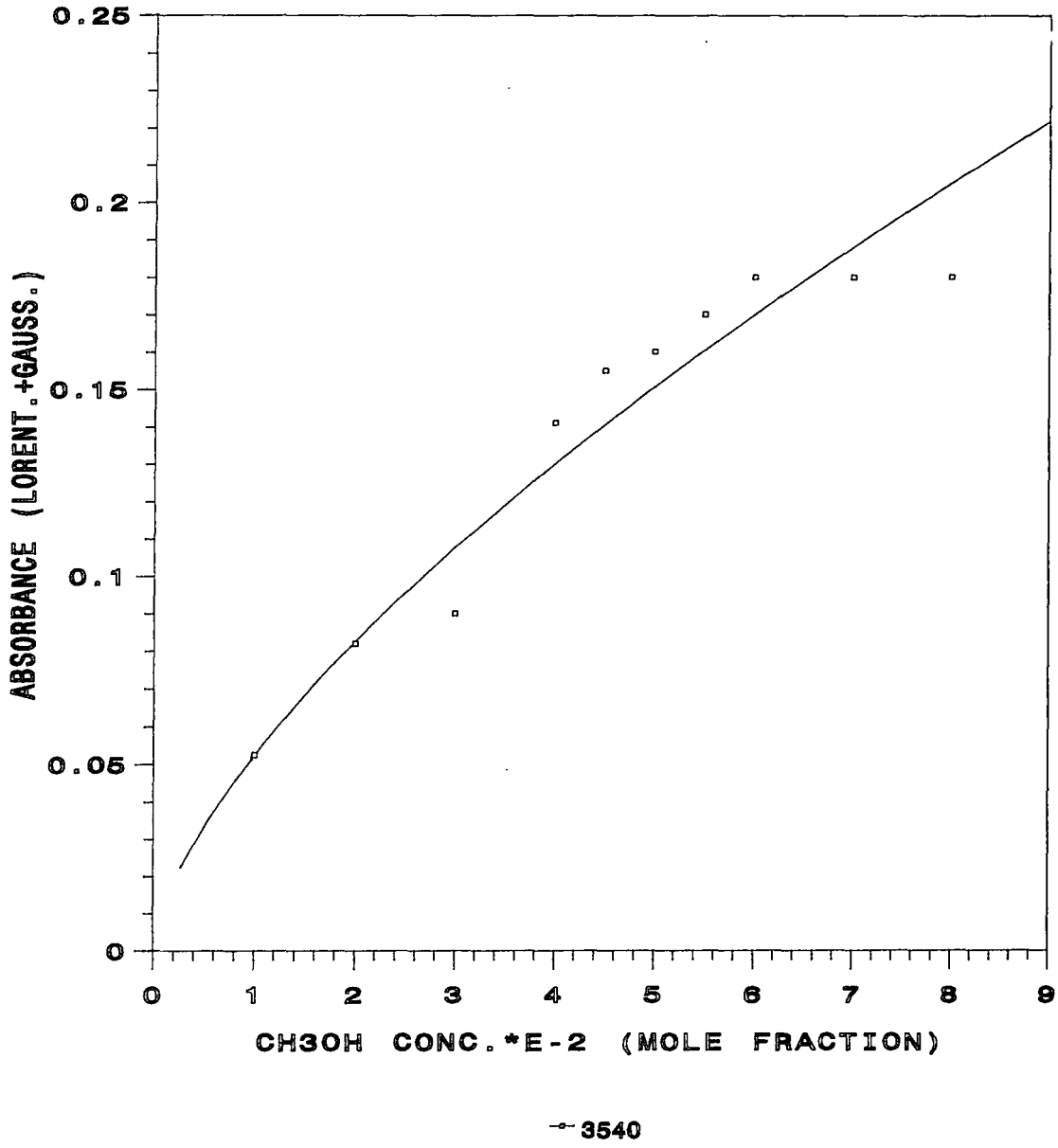

Figure 63 ν(OH) absorbance of methanol in binary systems at 3540cm^{-1}

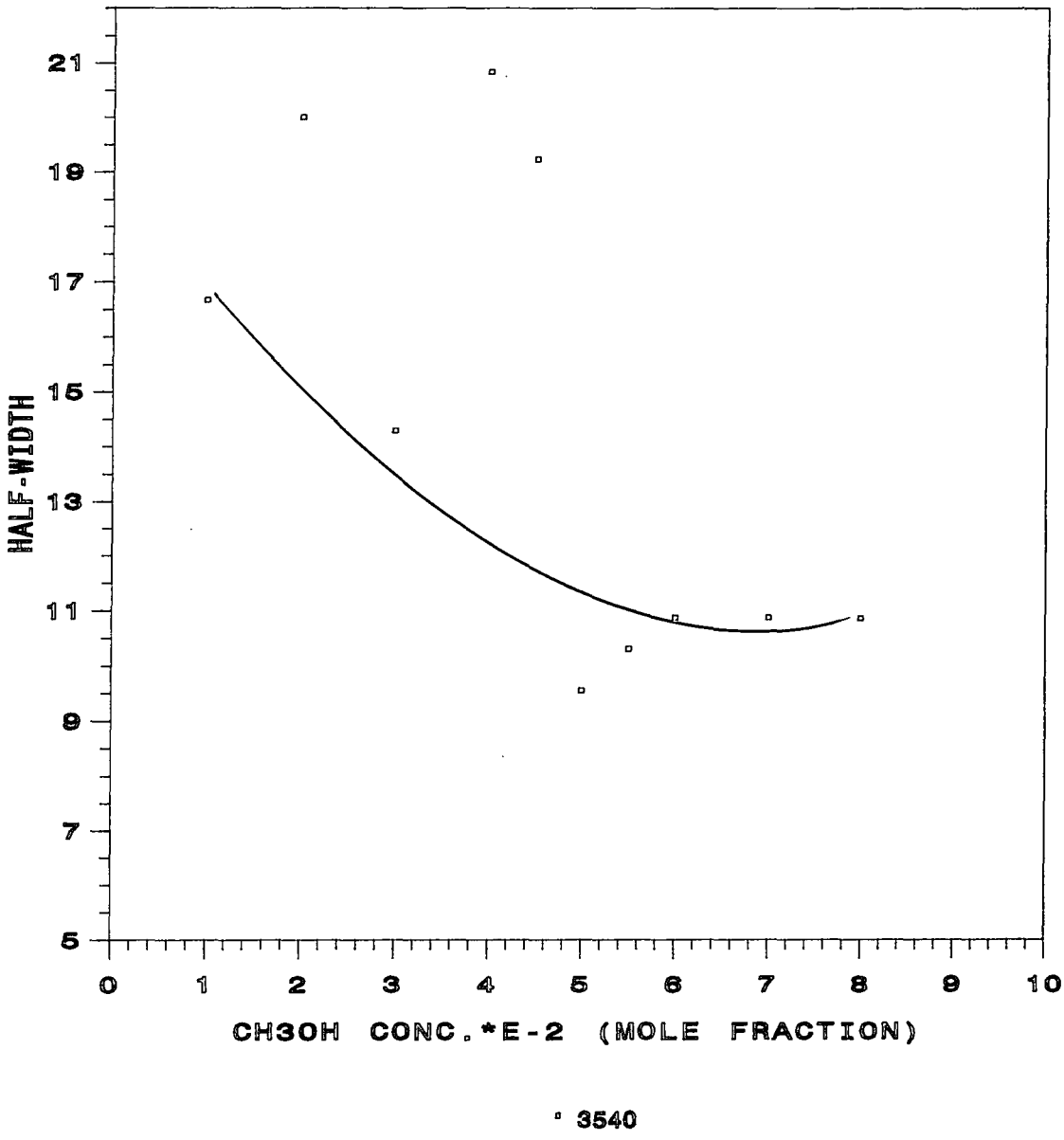

Figure 64 ν(OH) half-width of methanol in binary systems at 3540cm^{-1}

At higher methanol concentration (0.2 mole fraction), a negative sign appears in the calculated results due to the complication in resolving the overlapped bands, and the sum of the residuals (Σ) between fitted and observed data was increased (Figure 65). Because of these two reasons, and to confirm the previous results, a second band fitting program was used. This program is based on the Harwell Scientific Subroutine (VAO5A), but uses the same principles as the NRC program. The main difference was that the version used employs 100% Lorentzian band components. So the same data files were used for the analysis to obtain the calculated frequency, integrated intensity and the half-width of each band component. It was found necessary to fix the frequency and control the half-width of some bands to get an acceptable fit. Figures 66-83 represent the outlook of the experimental and calculated bands while Table 15 summarizes the results obtained.

Although care was taken when altering the indices in the (VAO5A) program to get the best fit, the sum of squares of residuals (Σ) kept increasing with concentration as shown Figure 84, in the concentration range of 0.01 - 0.1 methanol-mole fraction. This indicates how difficult the fitting procedure was, especially at higher methanol concentrations (*i.e.* when forming higher aggregates).

By using the (VAO5A) program the integrated intensity of the 3620 cm^{-1} band decreases whilst the half-width increases when the methanol concentration increases. This means that less of such a species was formed with weakening in hydrogen bonding, due to prefferable forming higher aggregates, as seen in Figures 85 and 86 respectively.

The integrated intensity of the ν(OH) band of the complex C_1 and/or the cyclic dimer band behaves differently. At 3538 cm^{-1}, the intensity increases as well as in the half-width, up to about 0.2 - 0.3 methanol mole fraction when it starts to decrease (Figures 87 and 88 respectively). This was expected since it is reasonable that, with increasing methanol concentration, the C_1 complex is gradually replaced by higher methanol aggregates.

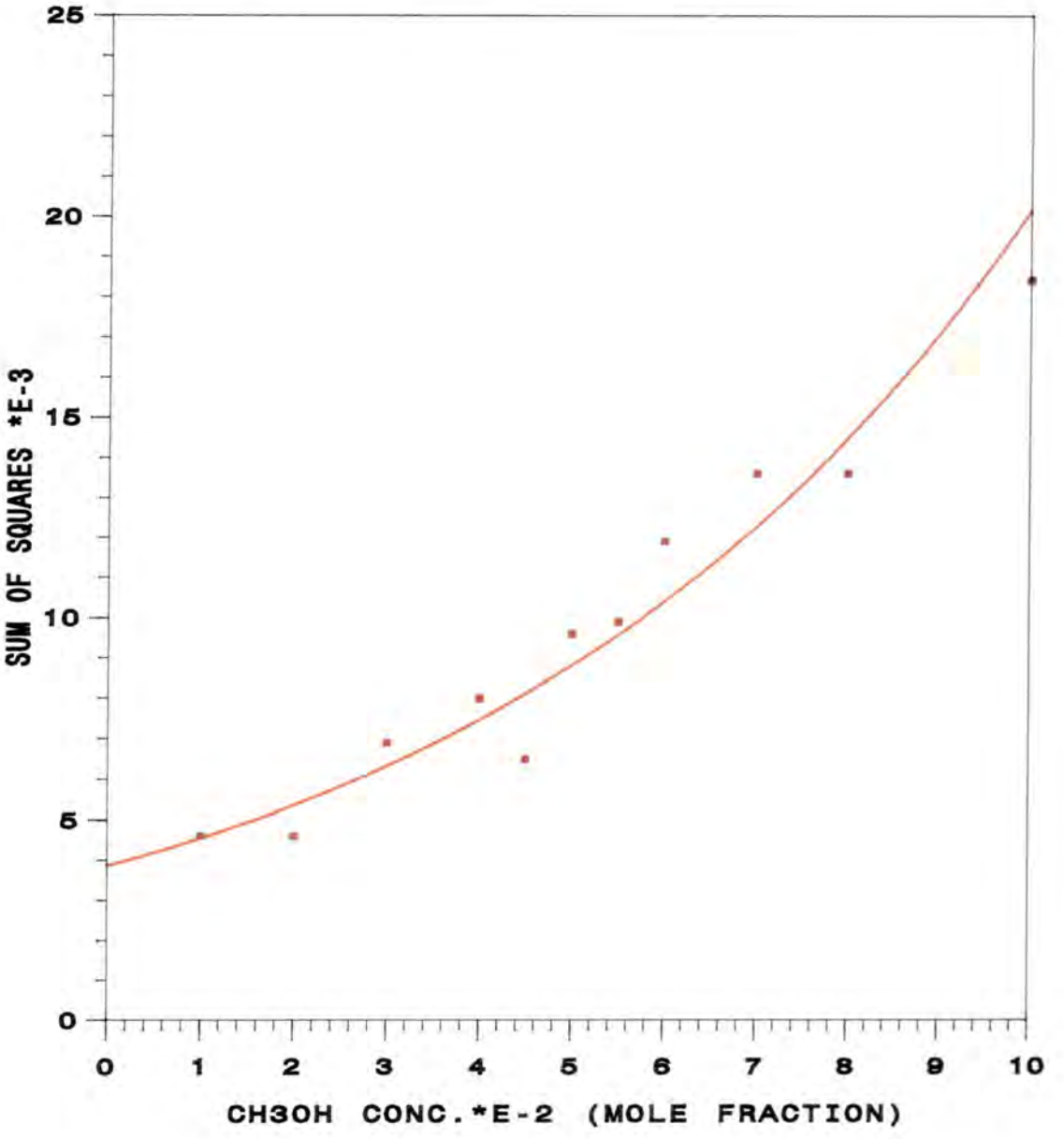

Figure 65 The NRC calculated sum of residuals in binary systems

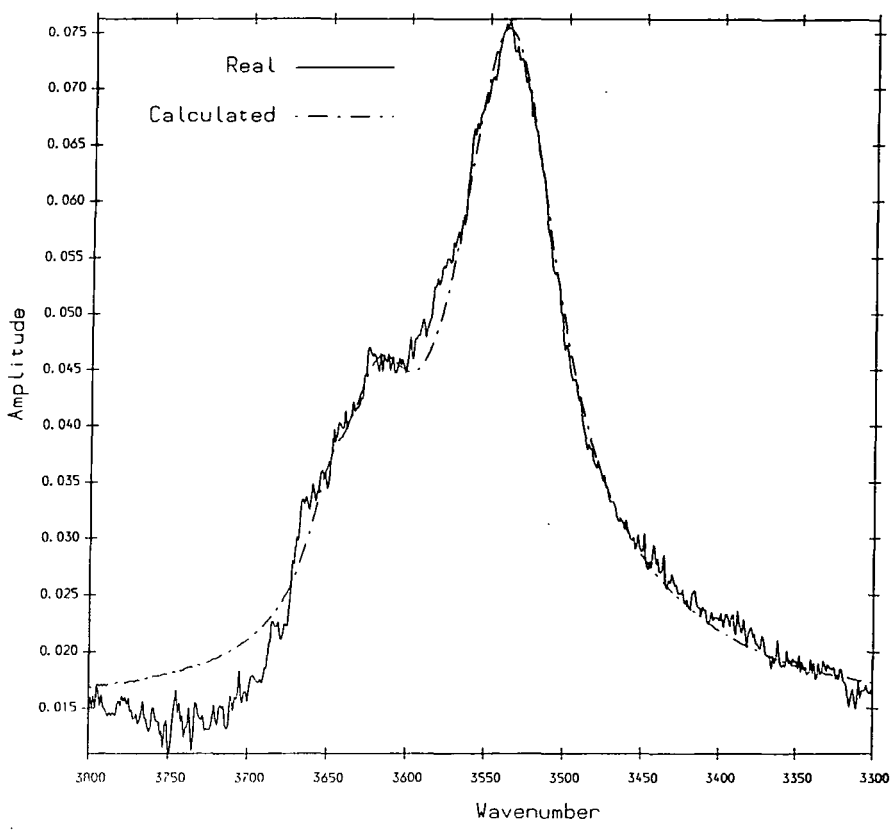

Figure 66 ν(OH) stretching mode of methanol in binary systems at 0.01 mole fraction

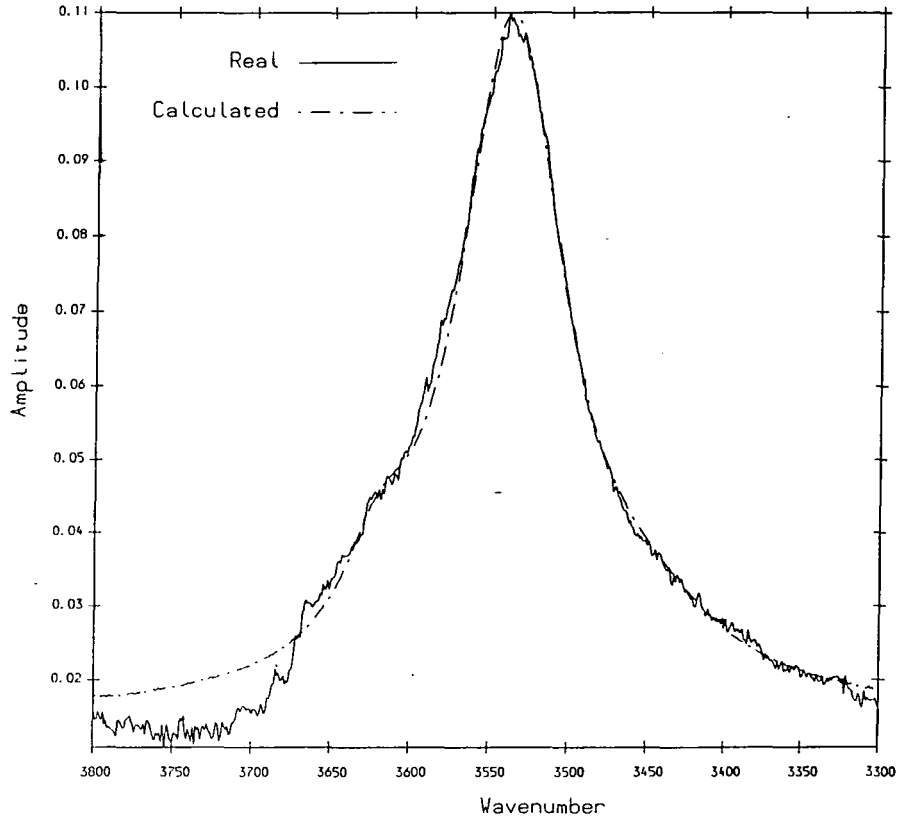

Figure 67 ν(OH) stretching mode of methanol in binary systems at 0.02 mole fraction

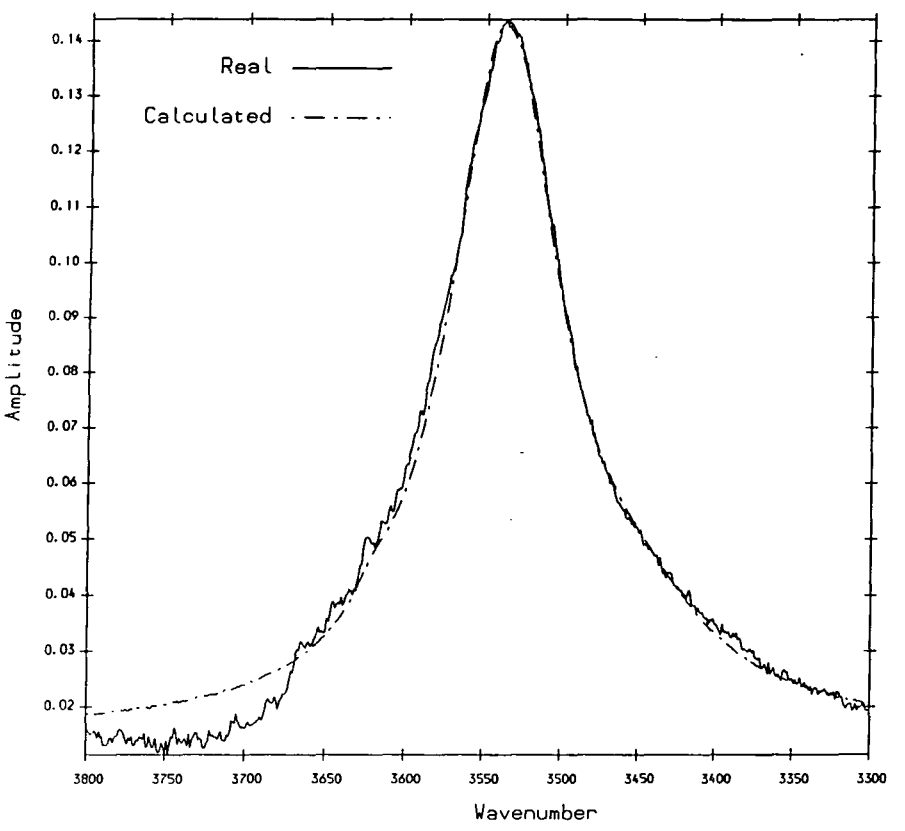

Figure 68 ν(OH) stretching mode of methanol in binary systems at 0.03 mole fraction

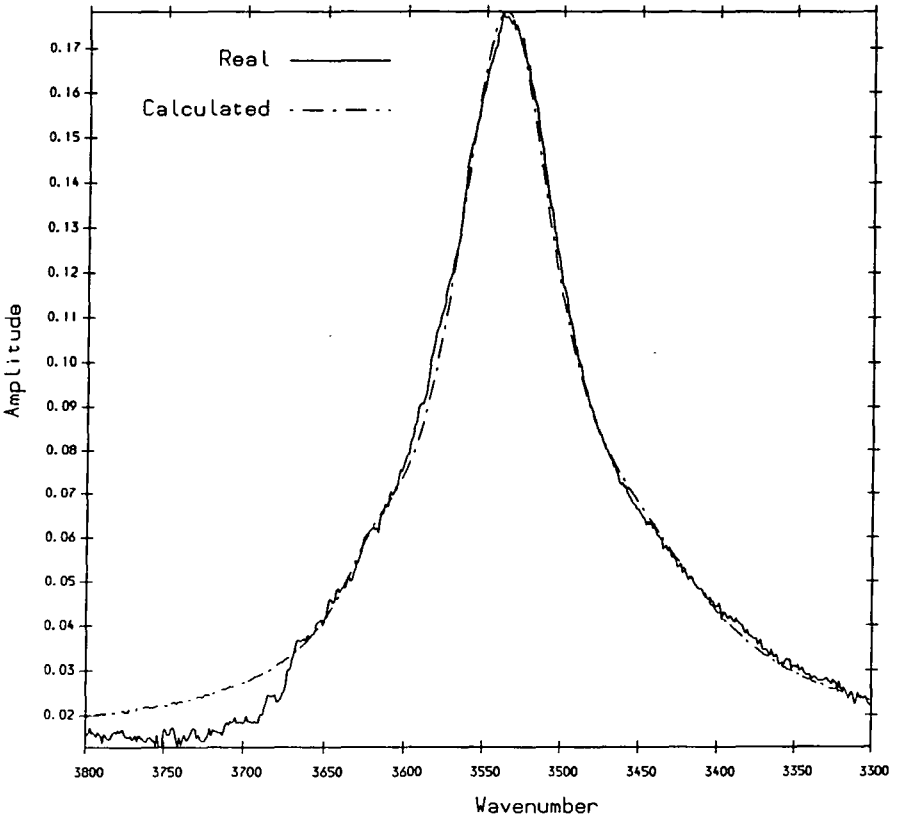

Figure 69 ν(OH) stretching mode of methanol in binary systems at 0.04 mole fraction

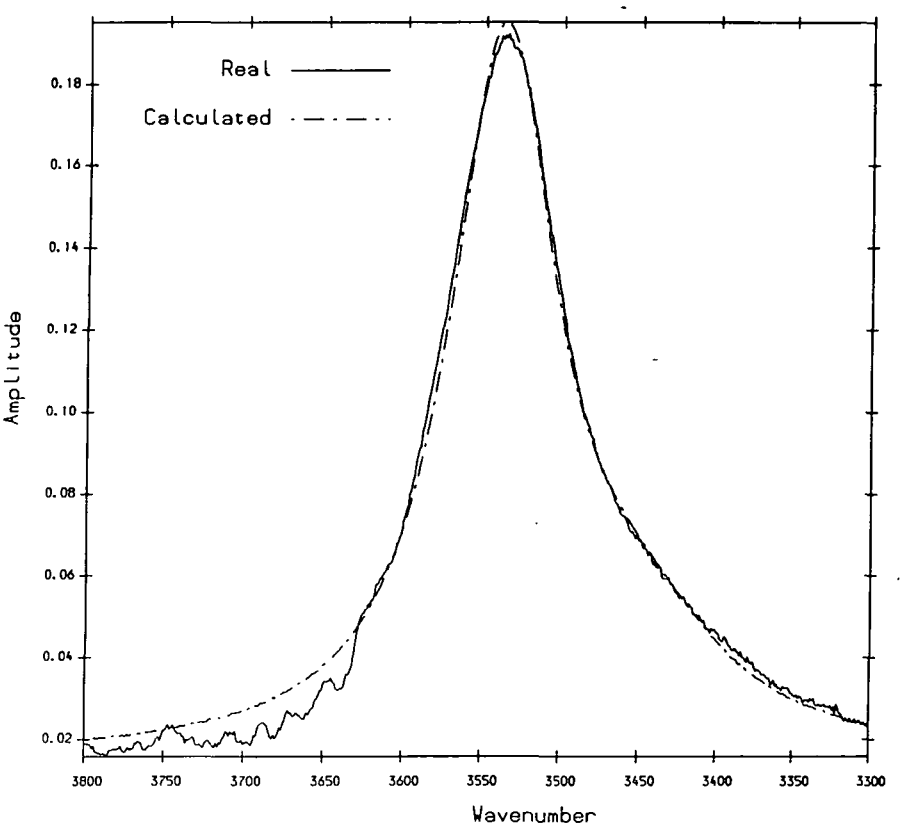

Figure 70 ν(OH) stretching mode of methanol in binary systems at 0.045 mole fraction

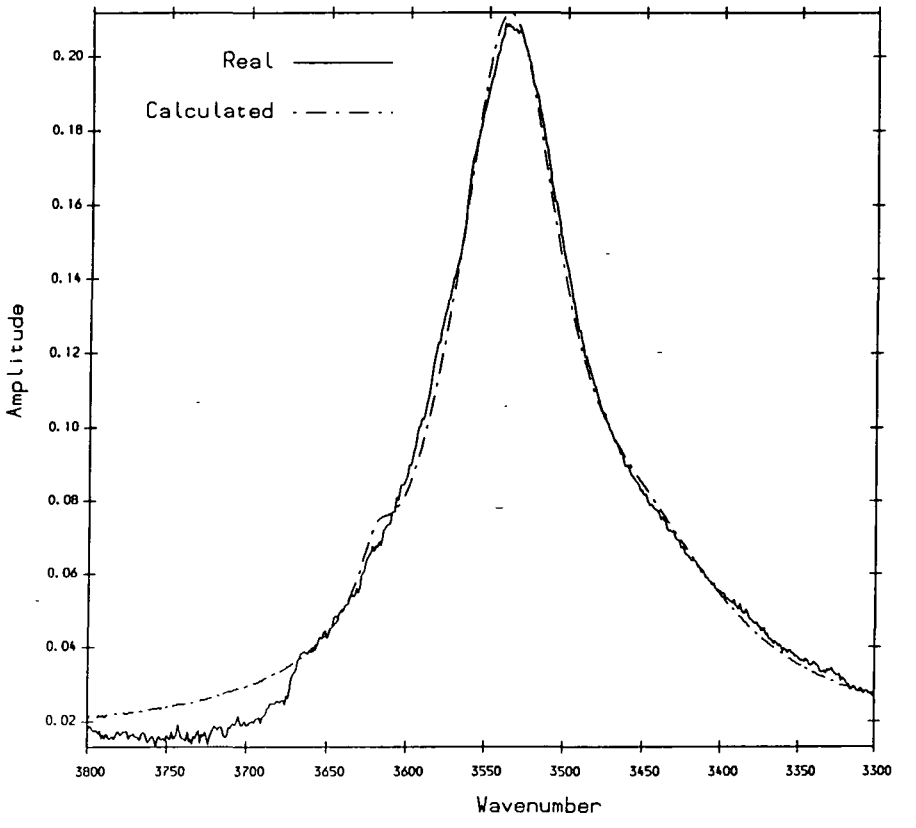

Figure 71 ν(OH) stretching mode of methanol in binary systems at 0.05 mole fraction

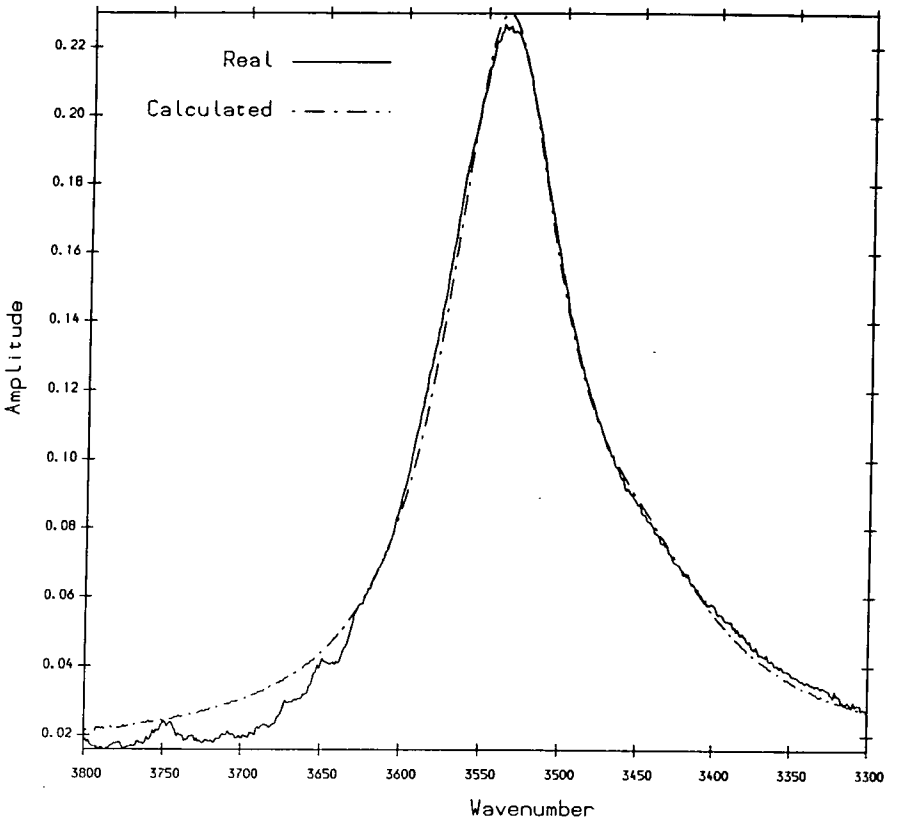

Figure 72 ν(OH) stretching mode of methanol in binary systems at 0.055 mole fraction

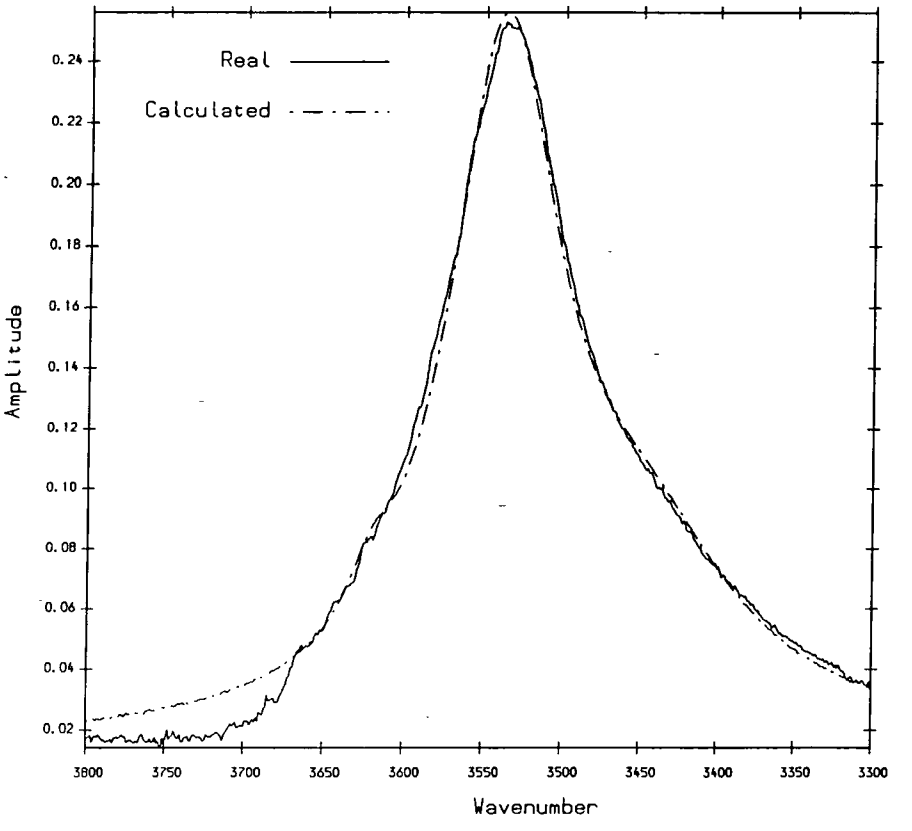

Figure 73 ν(OH) stretching mode of methanol in binary systems at 0.06 mole fraction

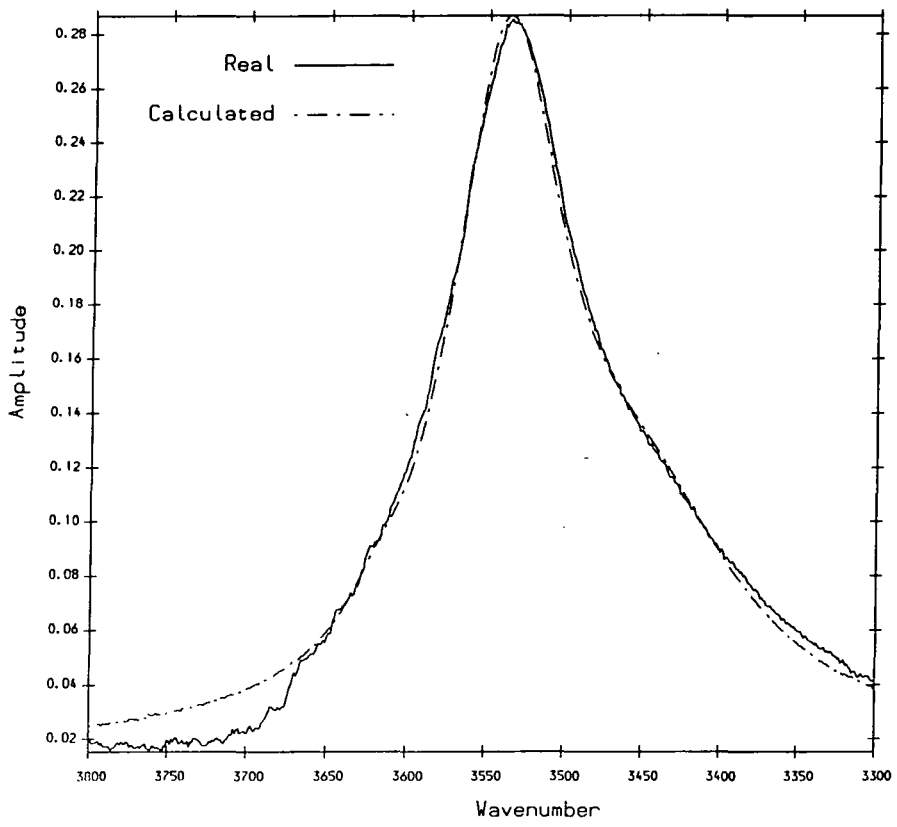

Figure 74 ν(OH) stretching mode of methanol in binary systems at 0.07 mole fraction

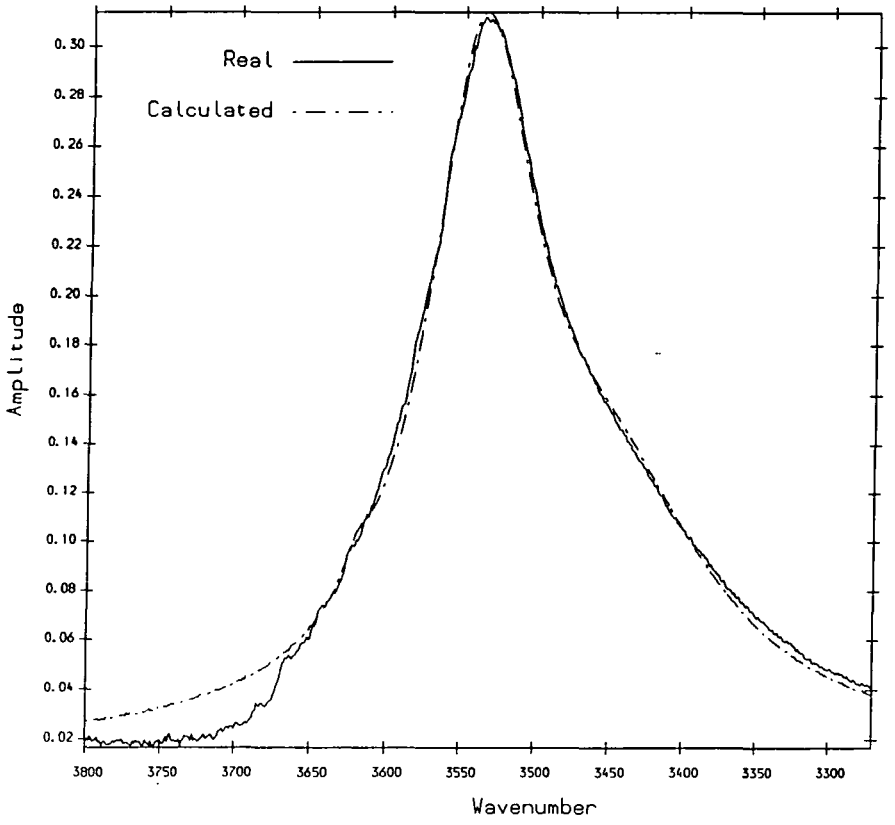

Figure 75 ν(OH) stretching mode of methanol in binary systems at 0.08 mole fraction

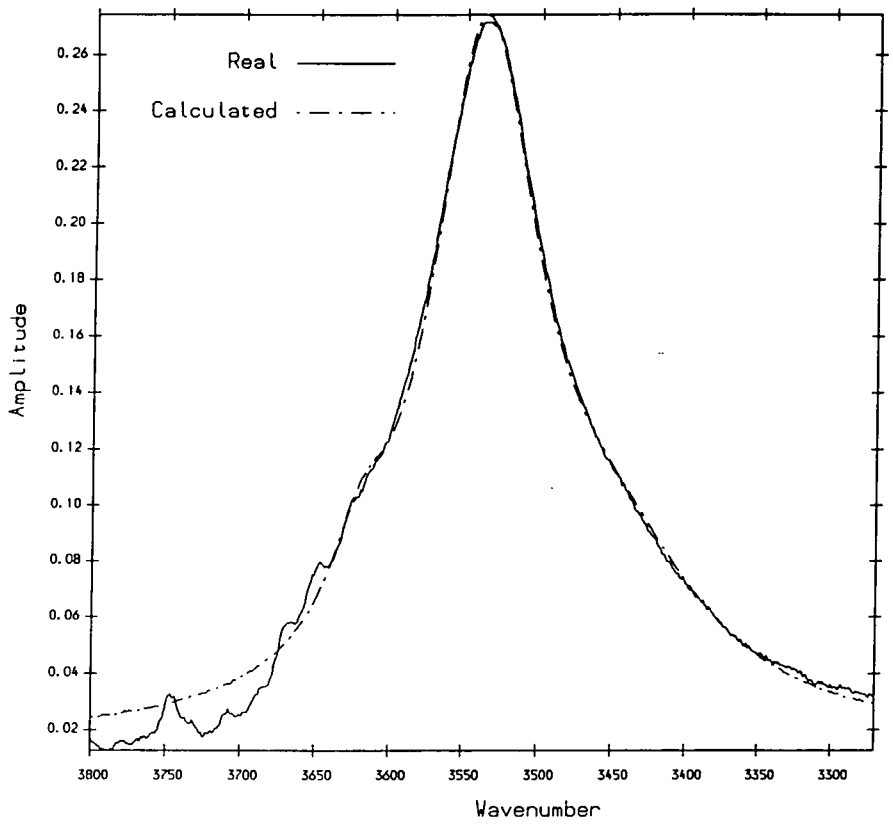

Figure 76 ν(OH) stretching mode of methanol in binary systems at 0.1 mole fraction

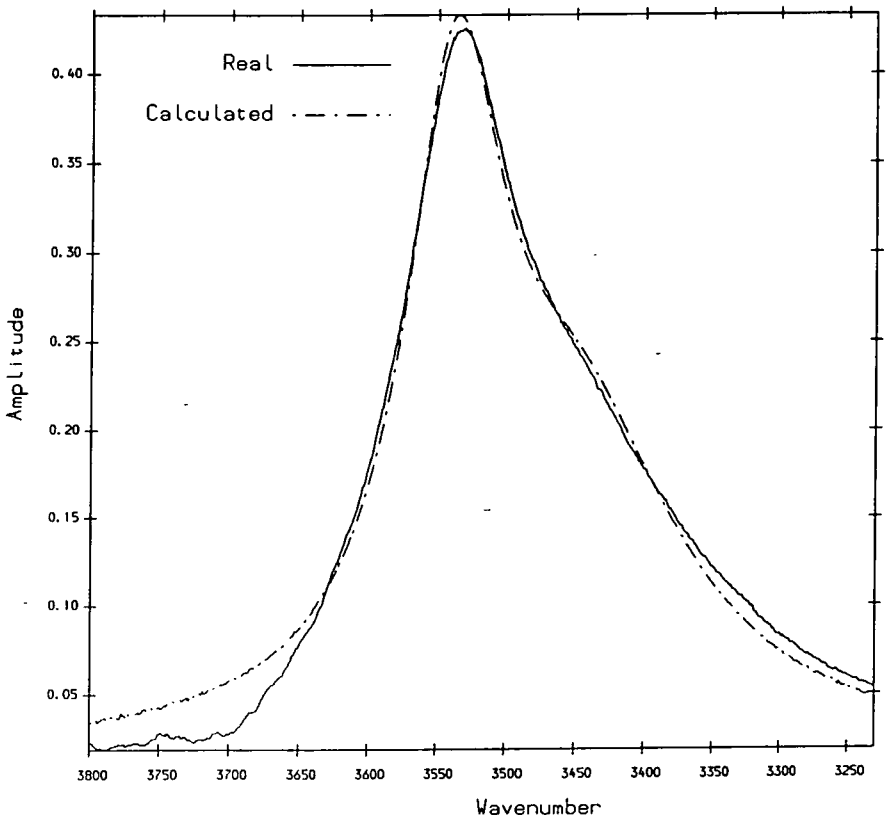

Figure 77 ν(OH) stretching mode of methanol in binary systems at 0.2 mole fraction

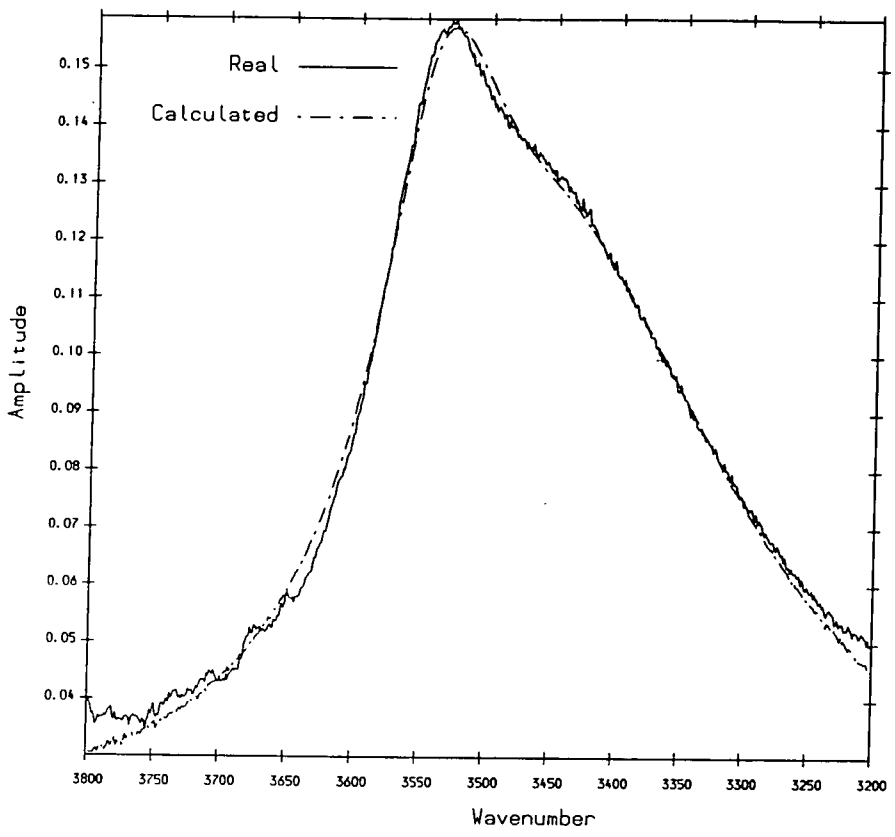

Figure 78 ν(OH) stretching mode of methanol in binary systems at 0.3 mole fraction

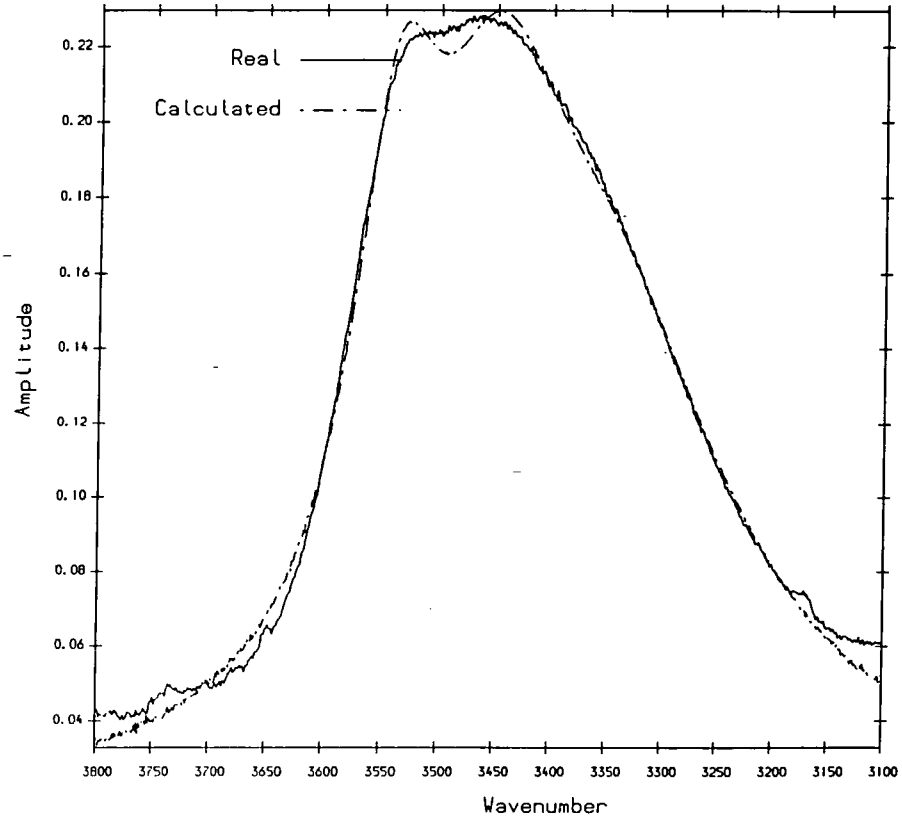

Figure 79 ν(OH) stretching mode of methanol in binary systems at 0.35 mole fraction

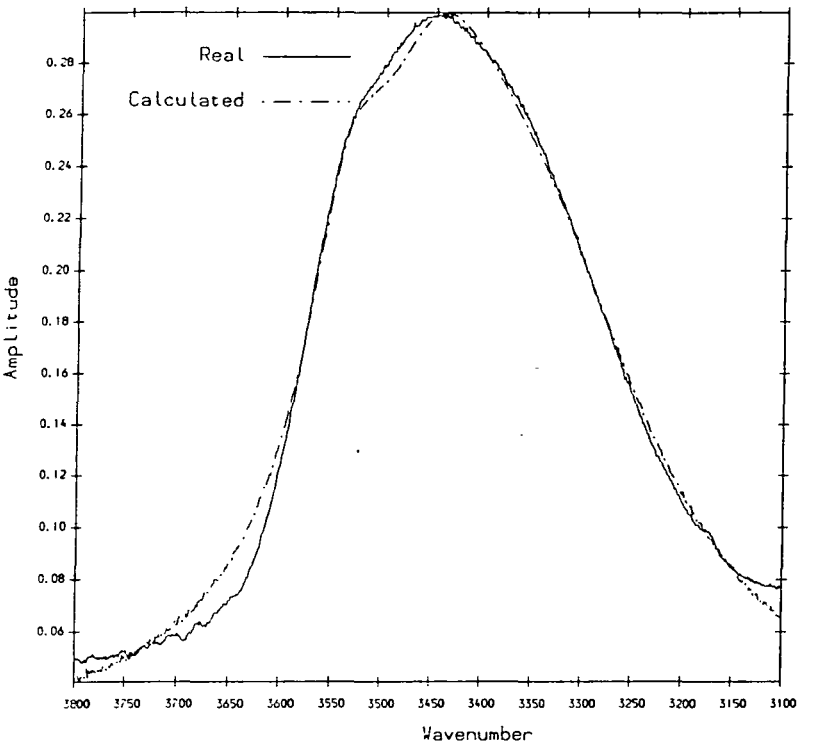

Figure 80 ν(OH) stretching mode of methanol in binary systems at 0.4 mole fraction

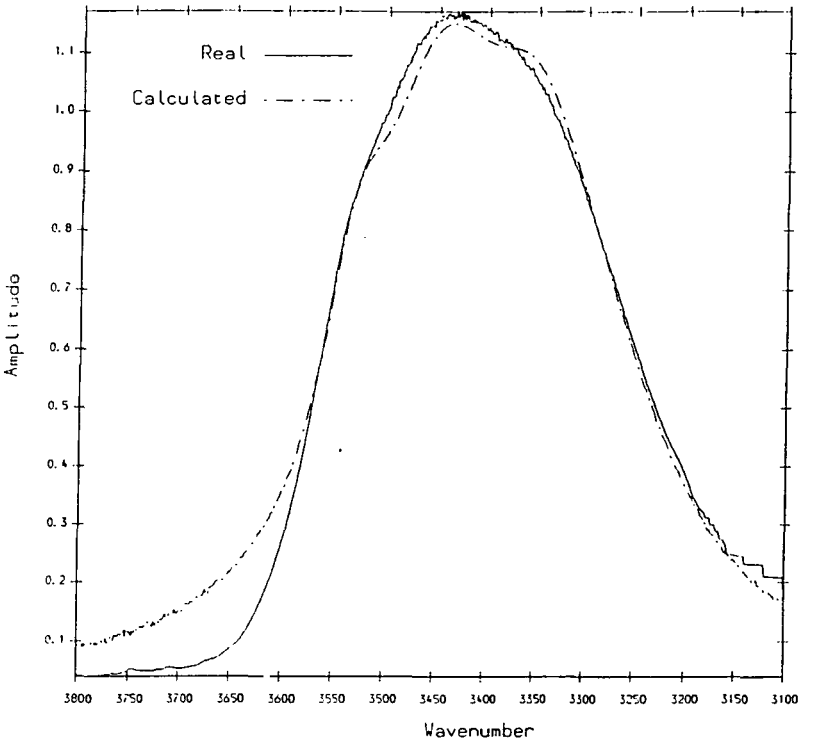

Figure 81 ν(OH) stretching mode of methanol in binary systems at 0.45 mole fraction

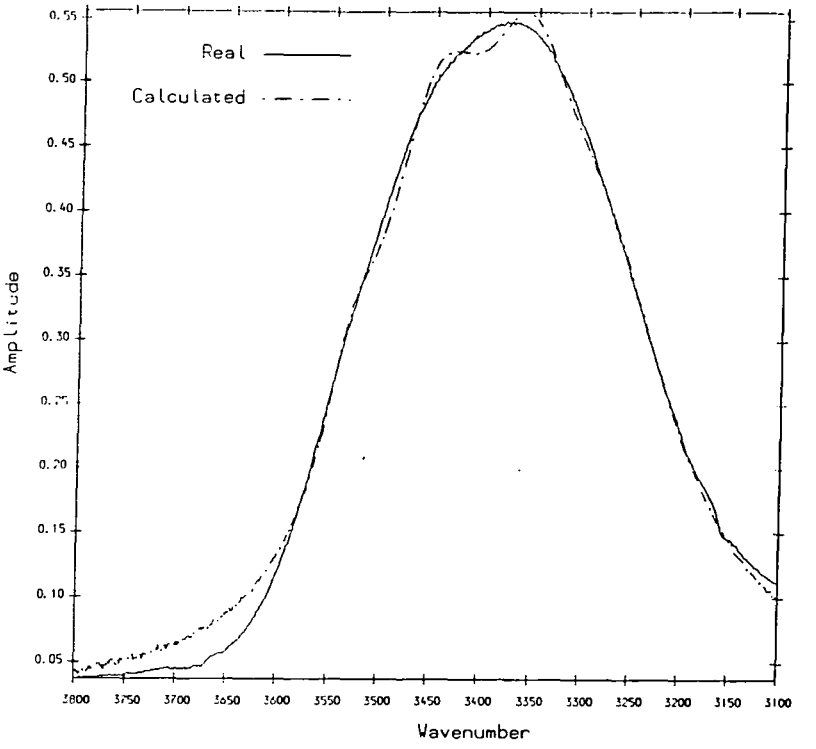

Figure 82 ν(OH) stretching mode of methanol in binary systems at 0.6 mole fraction

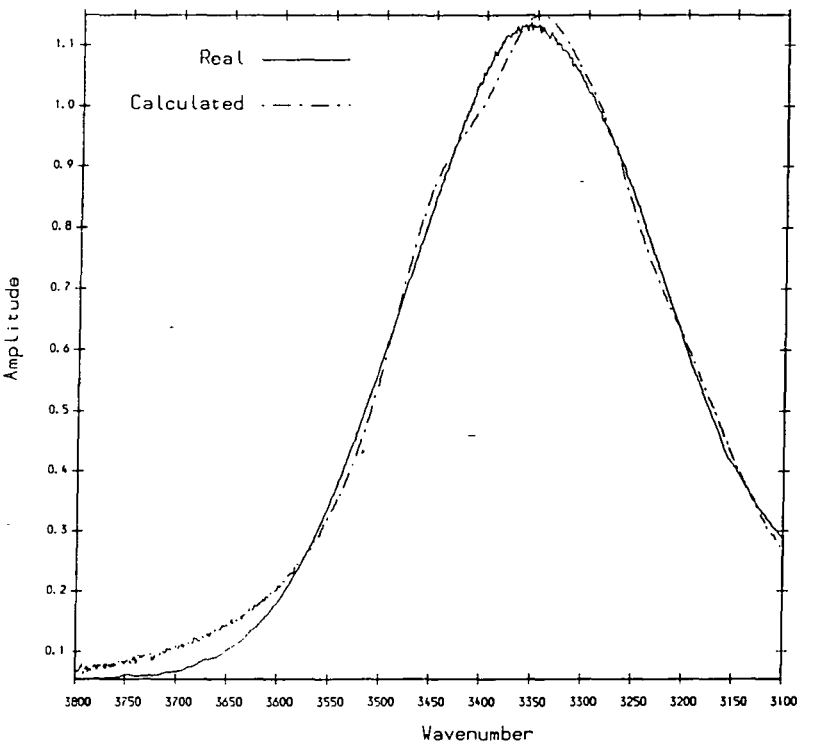

Figure 83 ν(OH) stretching mode of methanol in binary systems at 0.7 mole fraction

Table 15 Band Component Parameters Obtained and Calculated From VA05A Program

CH_3OH (m.f.)	Number of Bands	Frequency	Integrated Intensity	$\Delta\nu_{\frac{1}{2}}$	Sum of Residuals
0.01	4	3650	0.3469	12	0.00314
		3620	1.1492	22.1	
		3538	8.3157	47.1	
		3450	0.1482	58	
0.02	4	3650	0.0014	80.1	0.00506
		3620	0.999	20.1	
		3538	11.489	40	
		3450	1.4486	60.1	
0.03	3	3620	0.6325	20	0.0069
		3538	15.794	40	
		3450	3.2045	70	
0.04	3	3620	0.7477	20	0.0086
		3538	21.081	43	
		3450	4.324	64	
0.045	3	3620	0.01866	70	0.0077
		3538	22.317	41.2	
		3450	5.0793	71	
0.05	3	3620	0.5076	20.3	0.01182
		3538	24.62	43.1	
		3450	7.507	70	
0.055	3	3620	0.13214	81.1	0.0134
		3538	26.609	41.1	
		3450	7.499	70	
0.06	3	3620	0.7454	22.1	0.0184
		3538	29.594	44	
		3450	13.546	80.1	
0.07	3	3620	0.0257	80	0.03225
		3538	36.672	50	
		3450	15.896	80.1	
0.08	3	3620	0.5191	13.1	0.03156
		3538	35.722	44.1	
		3450	23.25	82.1	
0.1	3	3620	2.2583	23	0.01755
		3538	33.552	45	
		3450	11.79	77.1	

Table 15 Band Component Parameters Obtained and Calculated From VA05A Program (continued)

CH_3OH (m.f.)	Number of Bands	Frequency	Integrated Intensity	$\Delta\nu_{\frac{1}{2}}$	Sum of Residuals
0.2	3	3620	0.0014	50	0.0882
		3538	44.536	44.1	
		3450	49.721	91	
0.3	3	3538	19.76	60.8	0.0084
		3450	12.106	74.7	
		3350	21.808	136.5	
0.35	3	3538	18.470	52.6	0.0128
		3450	27.99	80.9	
		3350	49.34	138.5	
0.4	4	3538	15.322	50.6	0.0277
		3450	52.737	96.8	
		3350	48.022	129.4	
		3280	13.731	141.1	
0.45	4	3530	41.20	41.5	2.253
		3450	210	85.1	
		3350	138.8	78.7	
		3280	72.55	90.1	
0.5	4	3530	58.216	43.5	0.6556
		3450	138.108	70.9	
		3350	81.729	70	
		3280	21.172	56	
0.6	4	3530	10.477	34.4	0.1056
		3450	76.211	70.9	
		3360	47.94	60	
		3280	77.80	97.2	
0.7	4	3450	113.08	79.9	0.457
		3350	198.23	81	
		3280	47.15	57.2	
		3200	84.32	90.1	

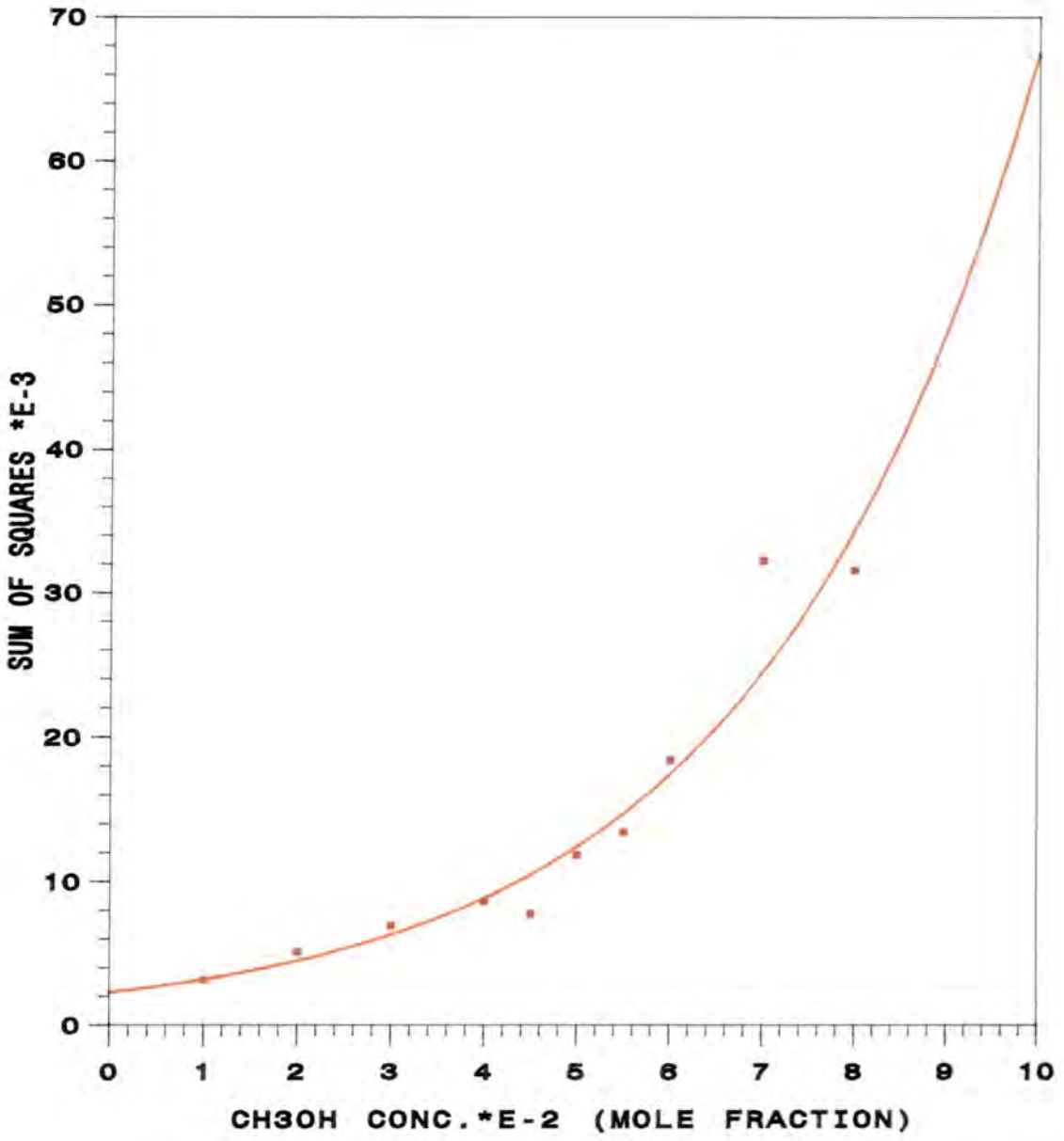

Figure 84 The VA05A calculated sum of residuals of methanol in binary systems

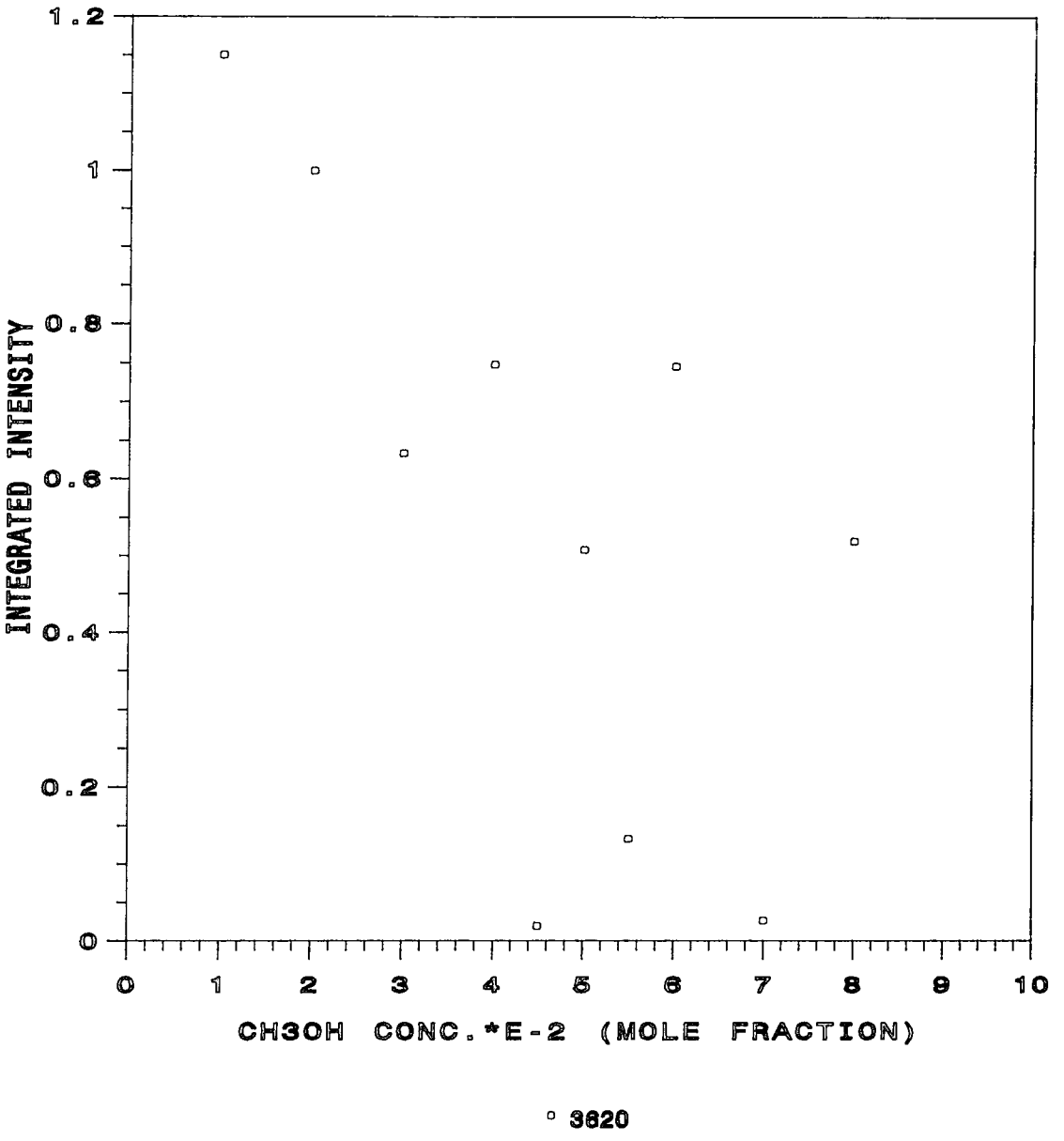

Figure 85 ν(OH) integrated intensity of methanol in binary systems at 3620cm^{-1}

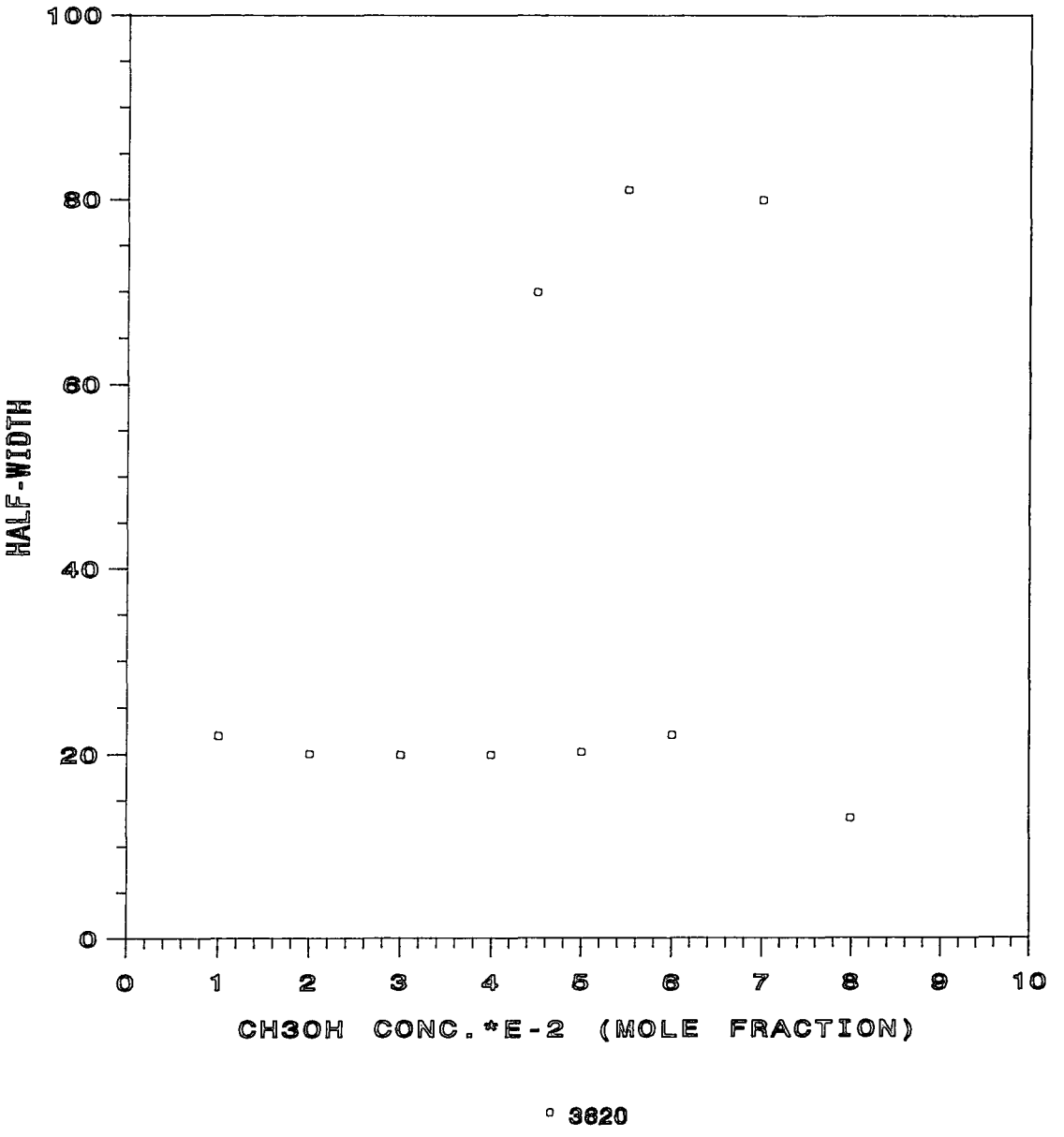

Figure 86 ν(OH) half-width of methanol in binary systems at 3620cm^{-1}

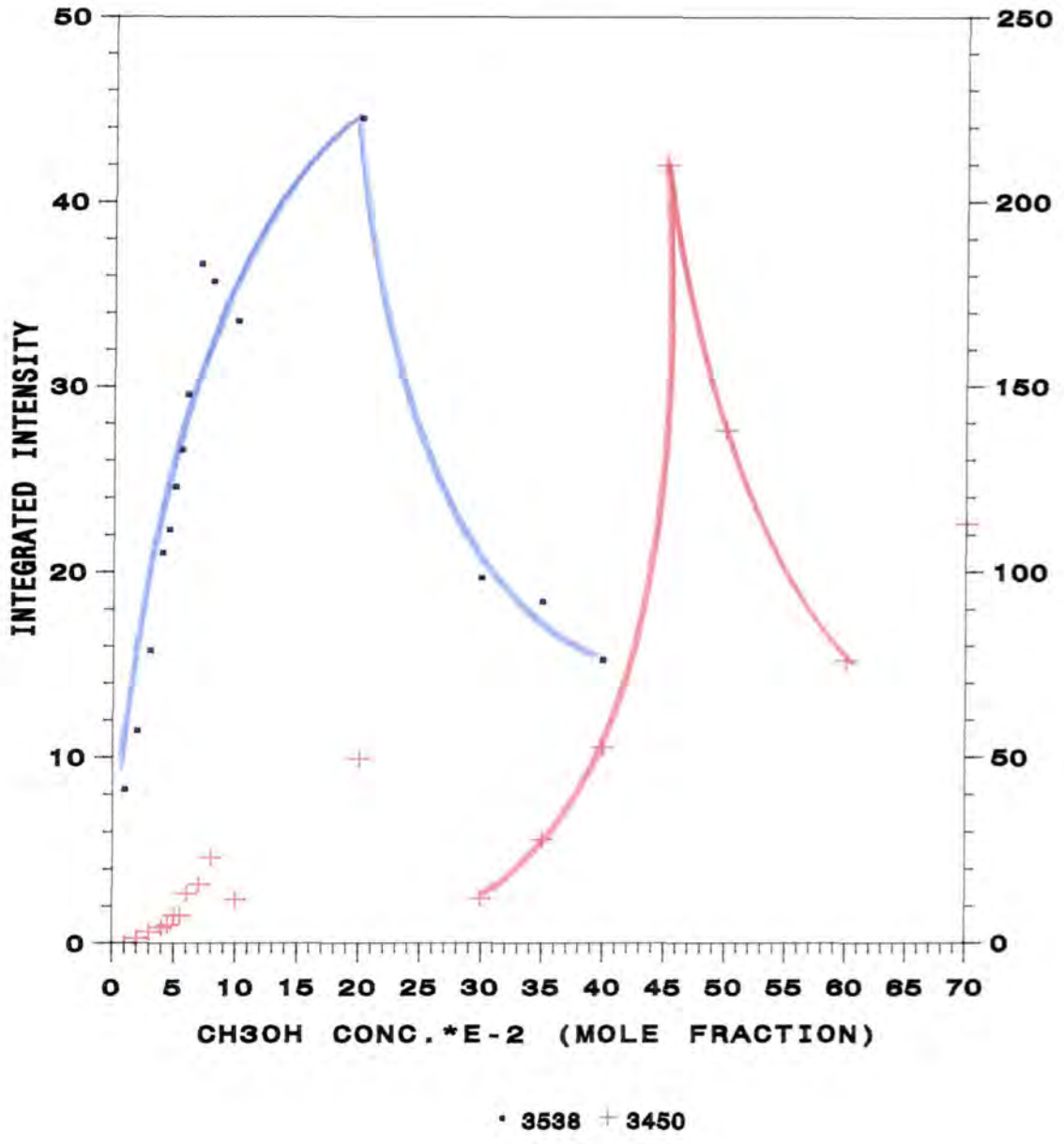

Figure 87 ν(OH) integrated intensity of methanol in binary systems at 3538cm^{-1} and 3450cm^{-1}

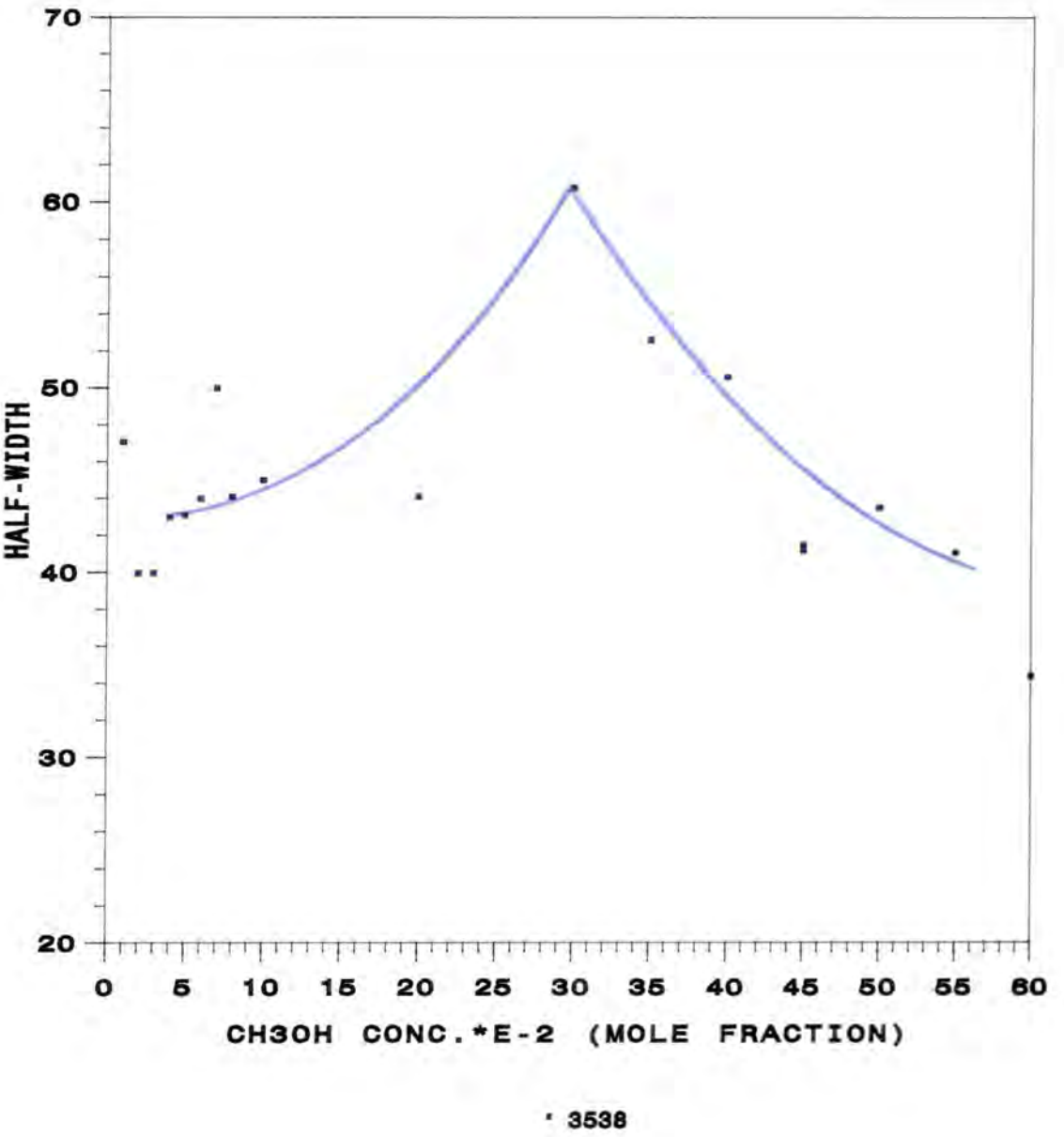

Figure 88 ν(OH) half-width of methanol in binary systems at 3538cm^{-1}

The integrated intensity and the half-width of the 3450cm^{-1} band behaves the same as shown in Figures 87, 89 and 90. This could be due to forming 1:2 acetonitrile in methanol complex or another kind of methanol aggregate. Then, by increasing the methanol concentration (to 0.4 mole fraction), one or more of the existing species were reduced or vanished.

At about 0.3 methanol mole fraction another aggregate seems to arise as indicated by the band at 3350cm^{-1}. This could be the tetramer species. This band increased in its integrated intensity when methanol concentration increases (Figure 91), while the half-width decreases due to losing another kind of species which might exist (Figure 92).

Finally, another band appears at 3280cm^{-1} at 0.4 methanol mole fraction, but having as previous trend and the same explanation (Figures 93 and 94). The only difference is that the integrated intensity of this band is less than the former one which shows that the hydrogen bonding in tetramer species are stronger (more stable) than in pentamer (less stable), as most authors[12,69,70] consider the former species in their models but not the latter.

Since the output of this program does not show the plot of each individual band component (Figures 66 - 83), the results obtained from this program were re-entered again in the composite band envelope program (NRC-BBGEN) to see each calculated band component. Some examples of the output spectrum are shown in Figures 95 - 108.

It is clear from the previous data analysis just how difficult it is to explain the spectra of a binary system. A comparison of band positions in each tested system (non-polar, ternary and binary) are summarized in Table 16 together with the band assignments for each solvent. The close frequency value of each species in each solvent suggests that the acetonitrile molecules, in binary systems, exist as complexes surrounded by self-hydrogen bonded methanol aggregates (as analyzed before).

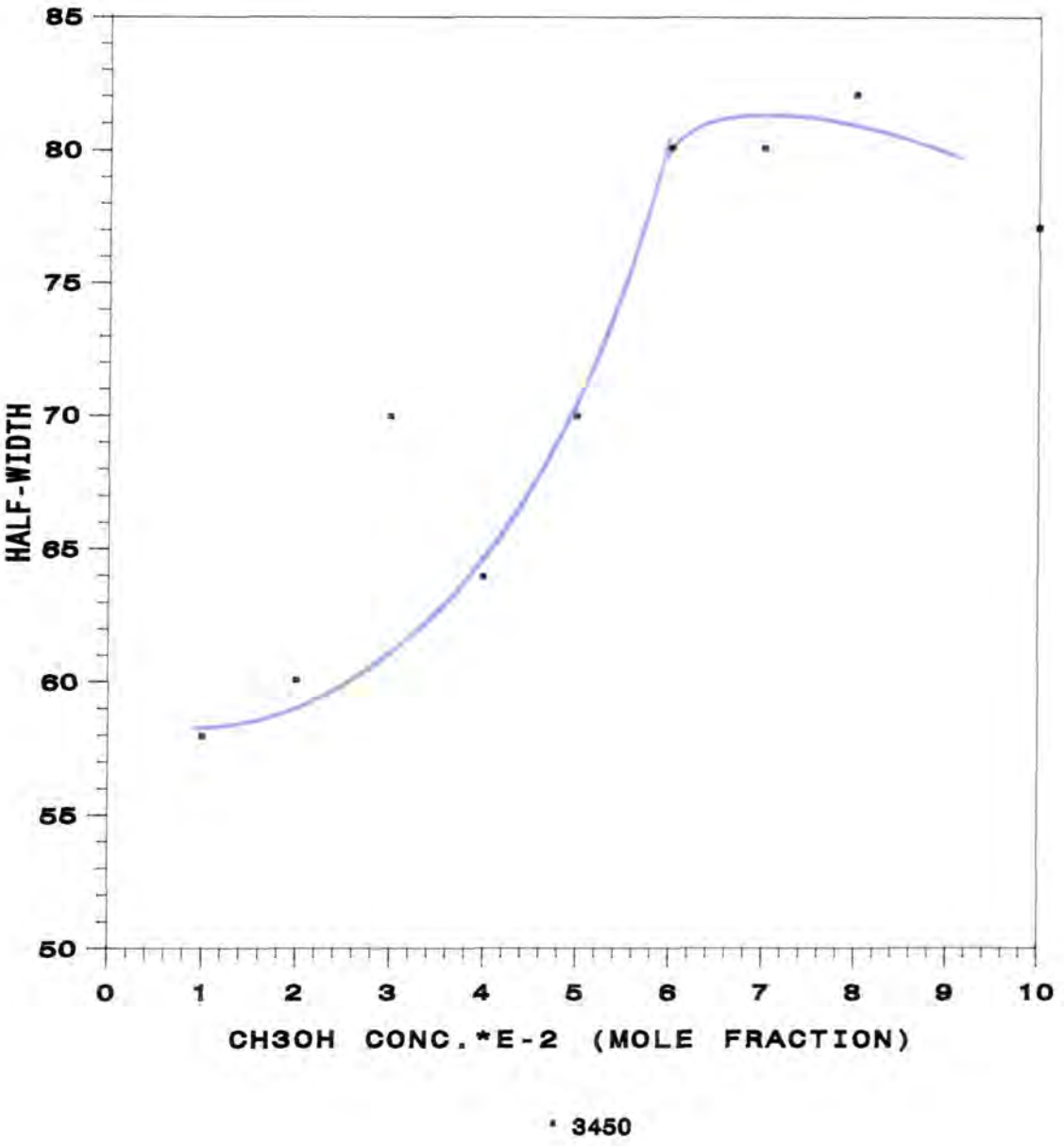

Figure 89 ν(OH) half-width of methanol in binary systems at 3450cm^{-1}

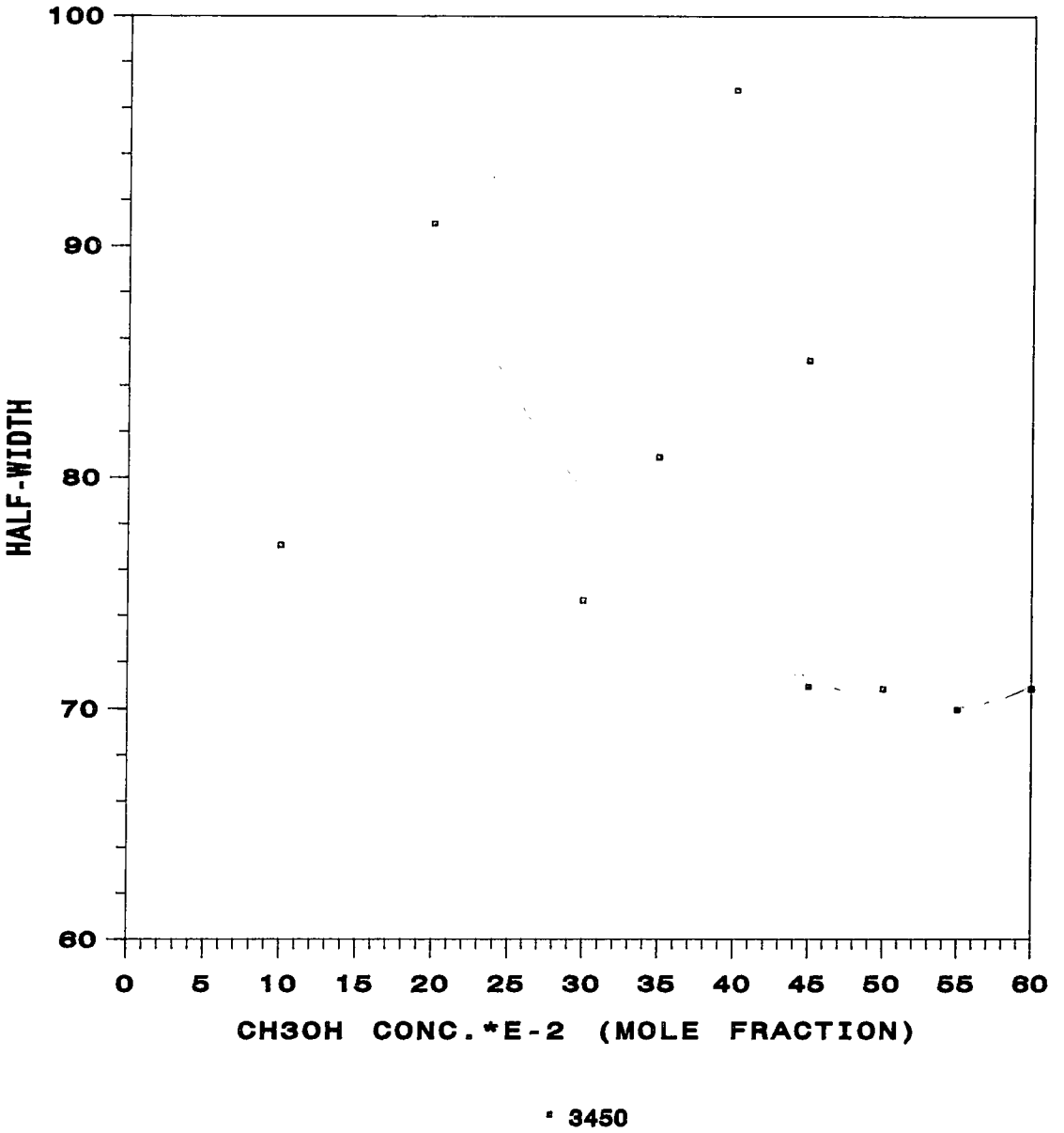

Figure 90 ν(OH) half-width of methanol in binary systems at 3450cm^{-1}

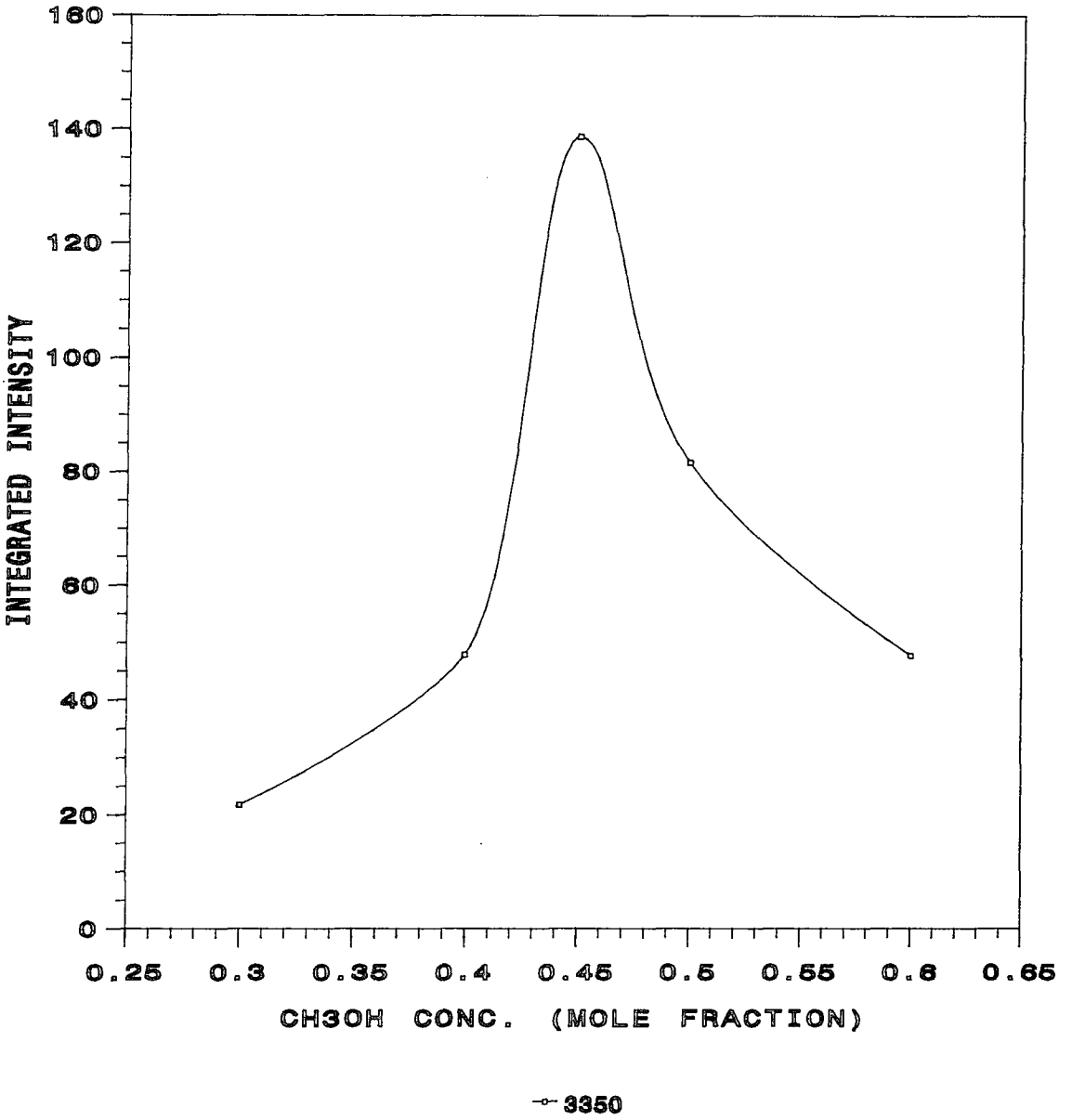

Figure 91 ν(OH) half-width of methanol in binary systems at 3350cm^{-1}

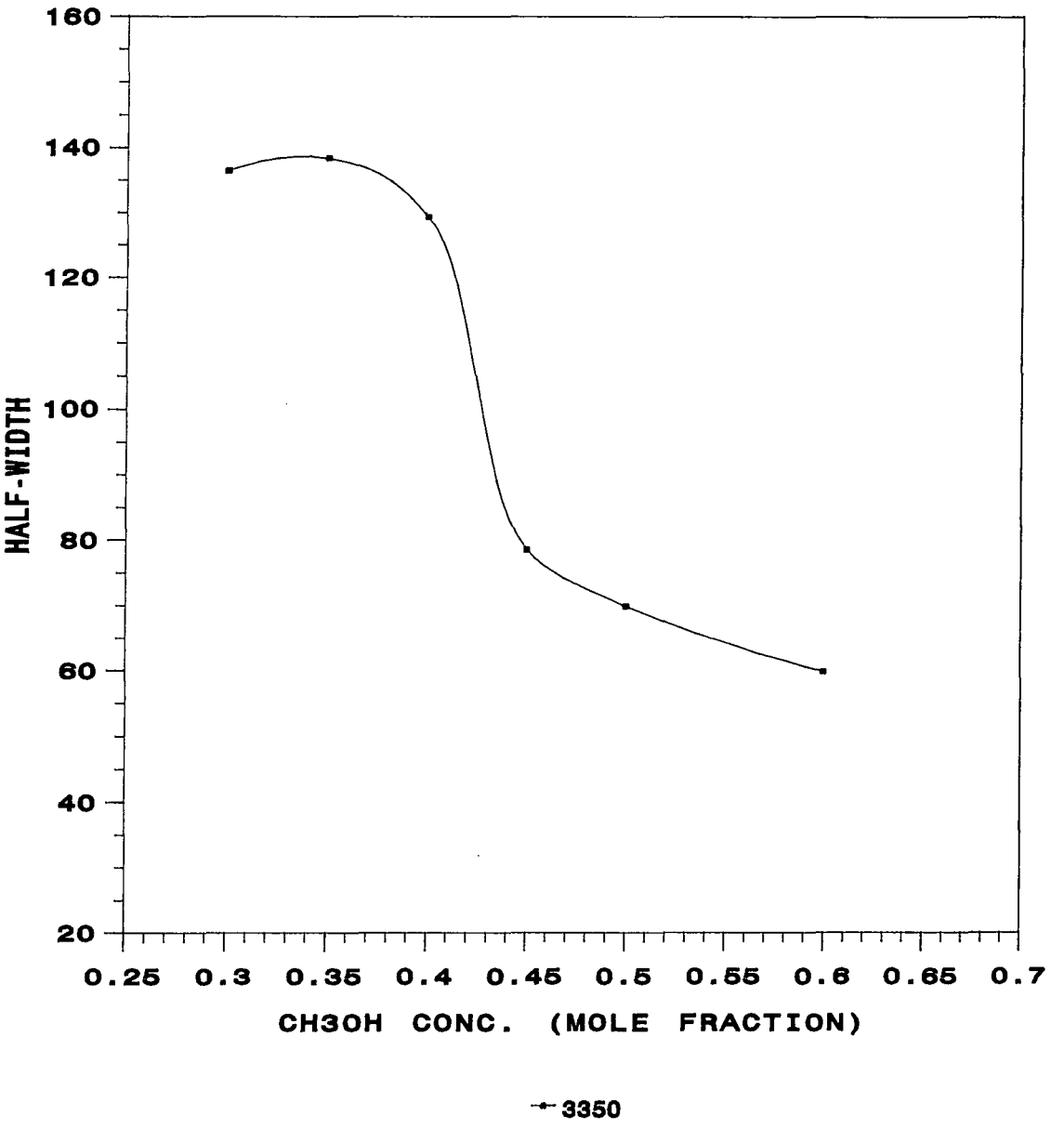

Figure 92 ν(OH) half-width of methanol in binary systems at 3350cm^{-1}

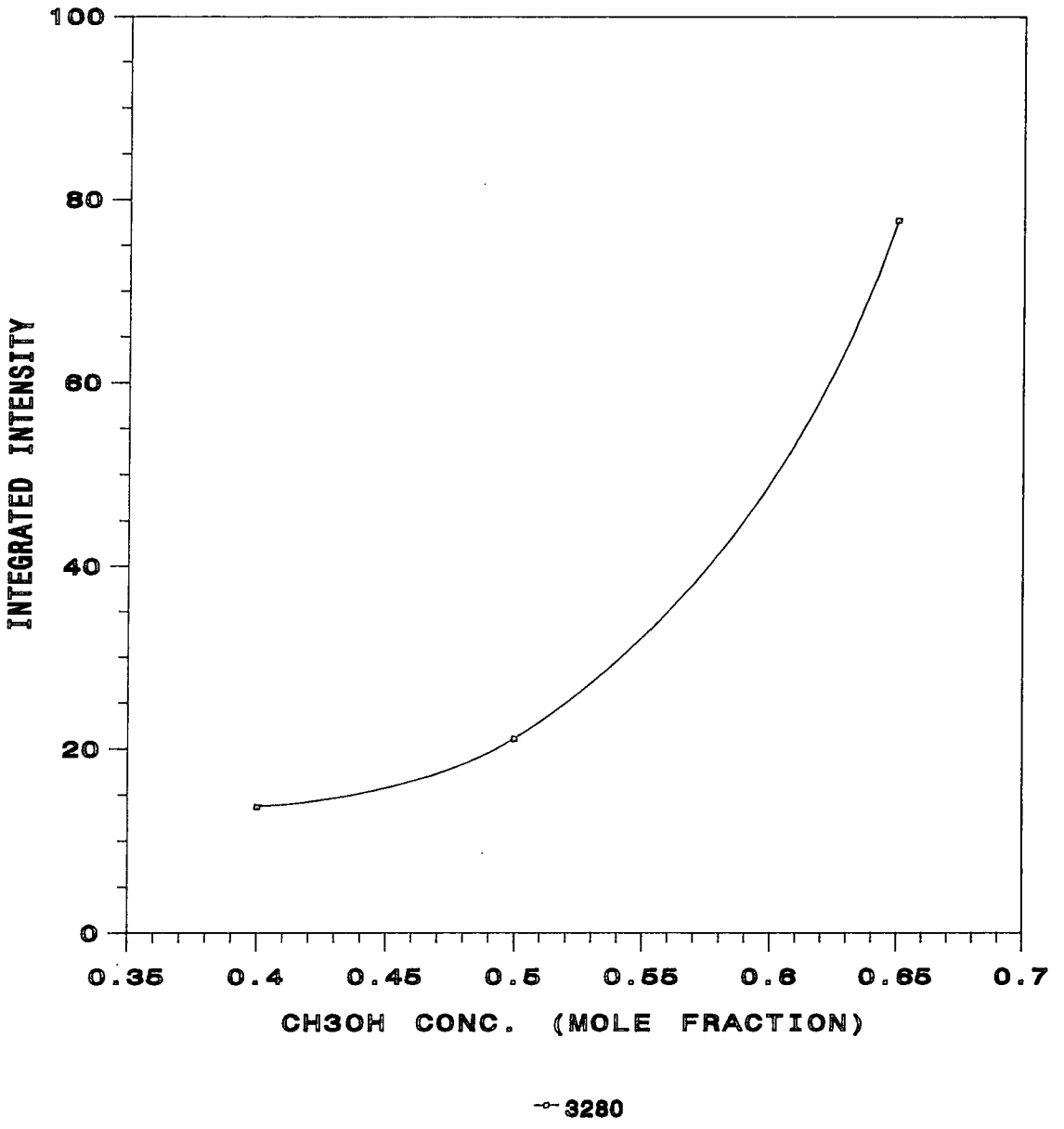

Figure 93 ν(OH) integrated intensity of methanol in binary systems at 3280cm^{-1}

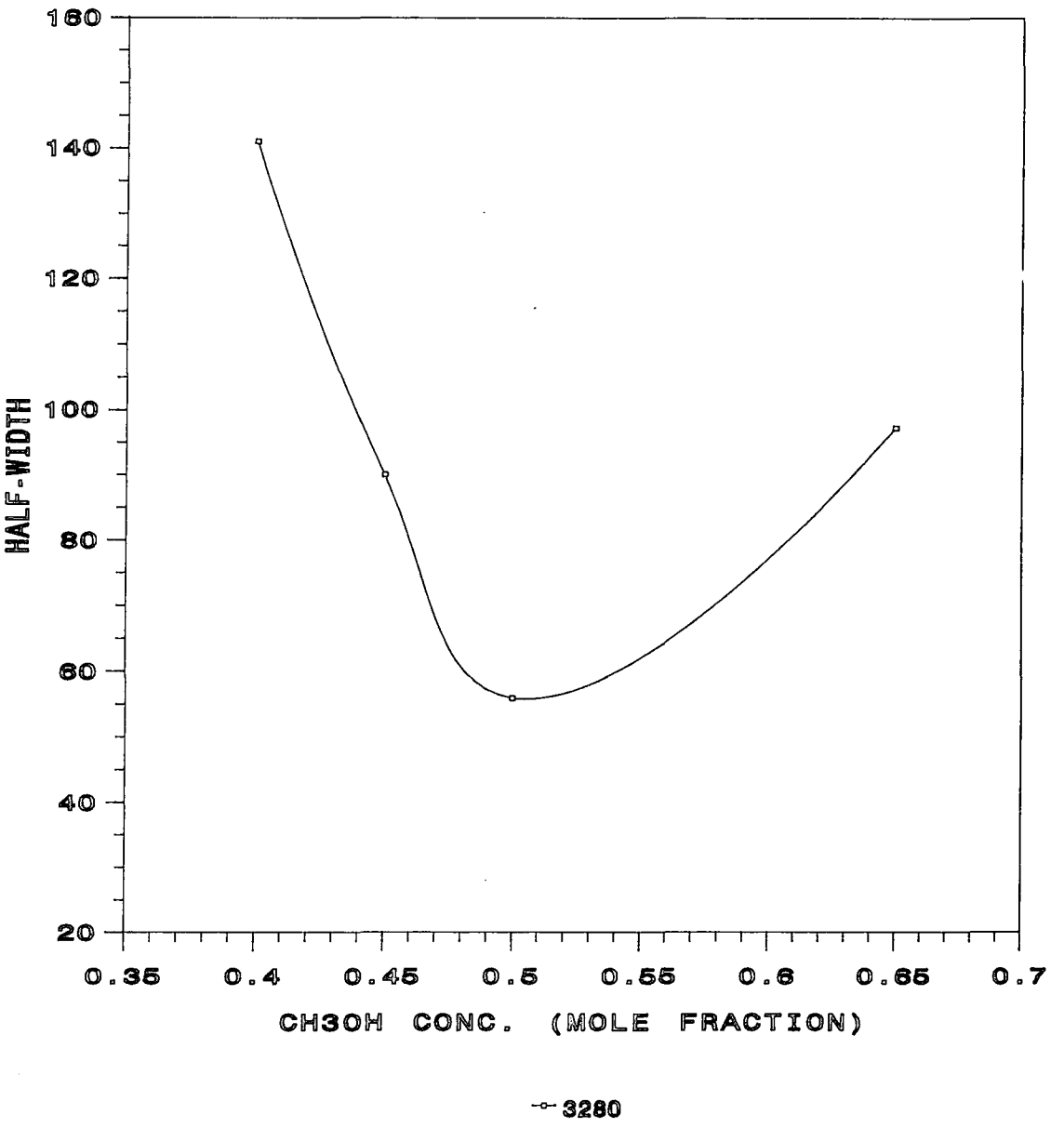

Figure 94 ν(OH) half-width of methanol in binary systems at 3280cm^{-1}

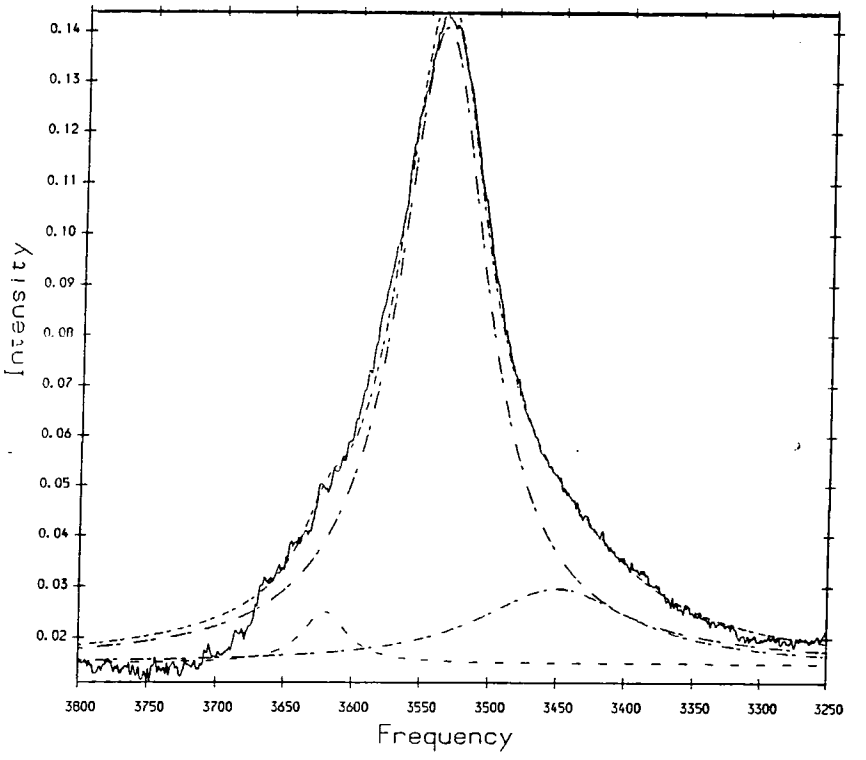

Figure 95 ν(OH) stretching mode of 0.03 methanol mole fraction in acetonitrile: _____ experimental, – – – overall calculated, –.–.–. band component.

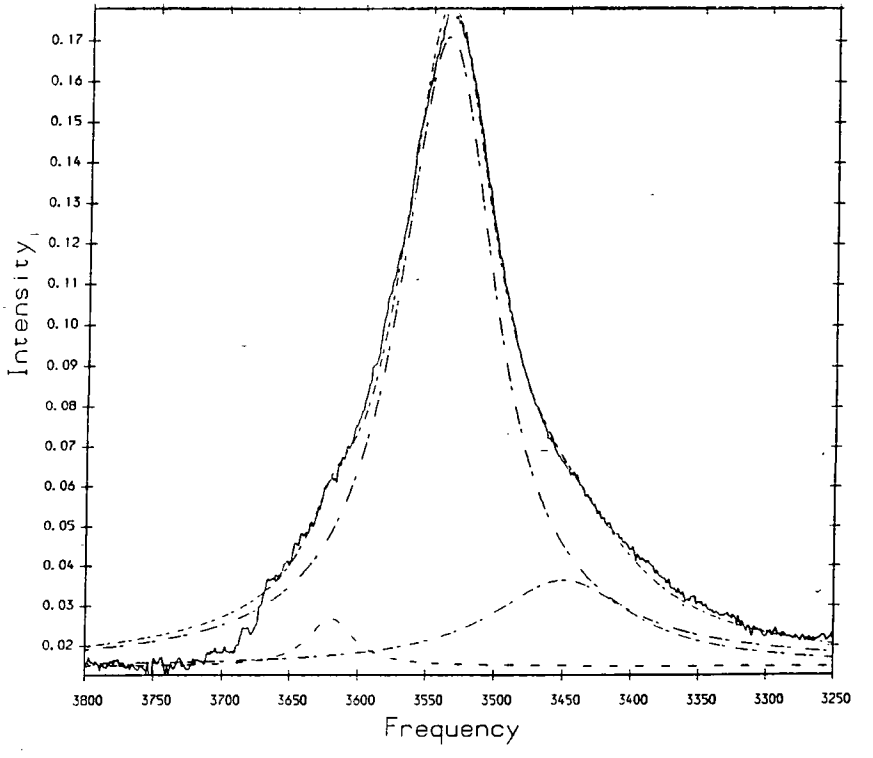

Figure 96 ν(OH) stretching mode of 0.04 methanol mole fraction in acetonitrile: _____ experimental, – – – overall calculated, –.–.–. band component.

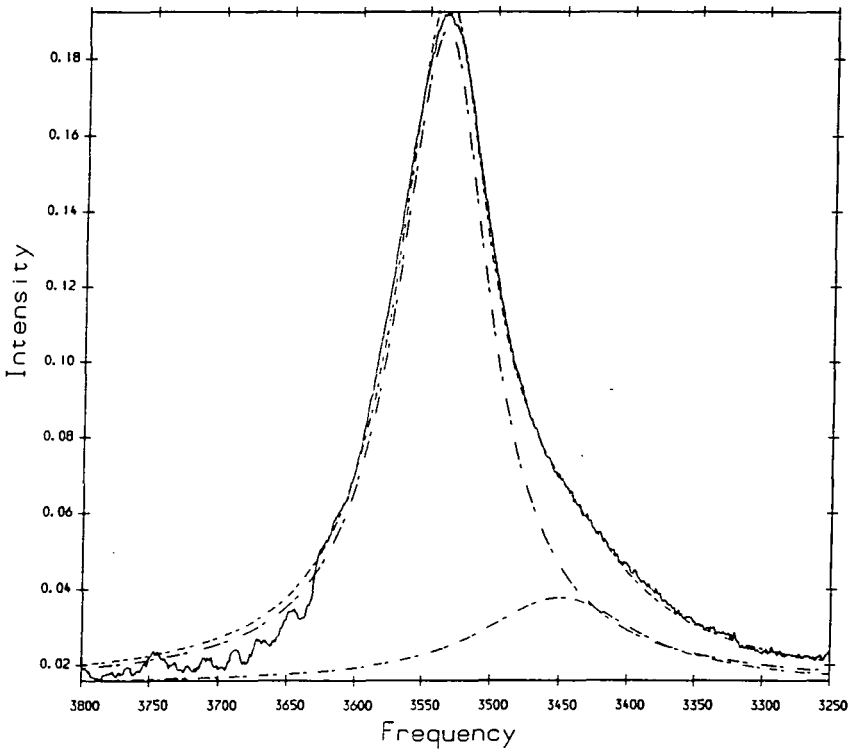

Figure 97 ν(OH) stretching mode of 0.045 methanol mole fraction in acetonitrile: ____ experimental, – – – overall calculated, –.–.–. band component.

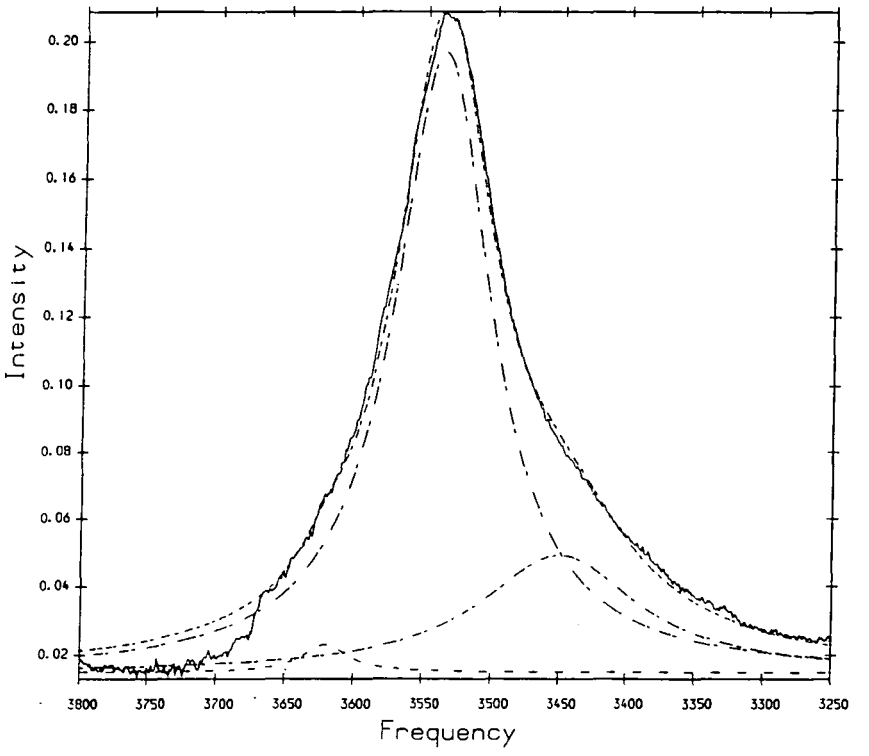

Figure 98 ν(OH) stretching mode of 0.05 methanol mole fraction in acetonitrile: ____ experimental, – – – overall calculated, –.–.–. band component.

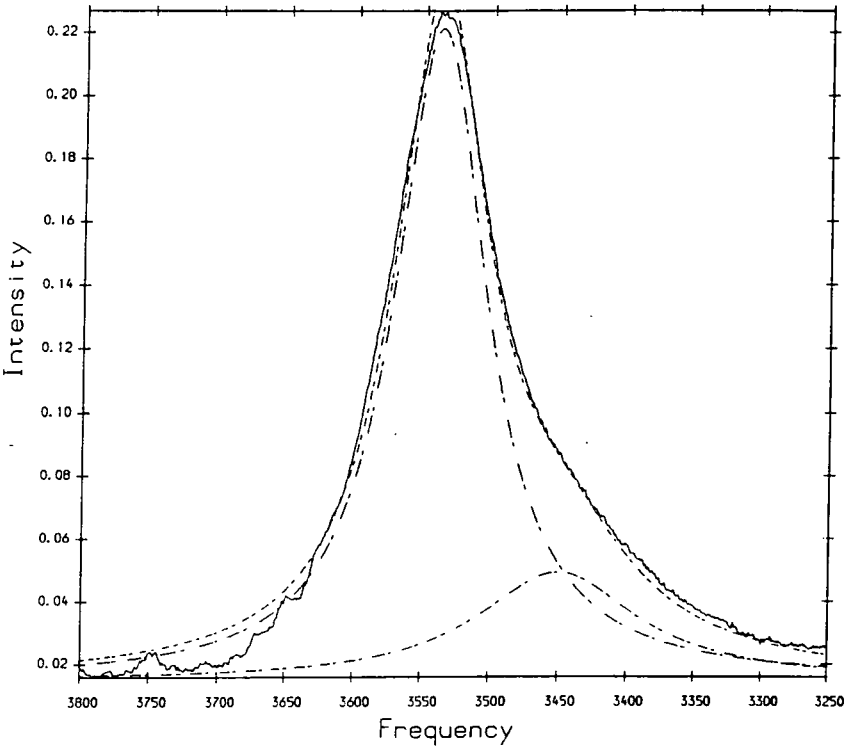

Figure 99 ν(OH) stretching mode of 0.055 methanol mole fraction in acetonitrile: ____ experimental, – – – overall calculated, –.–.–. band component.

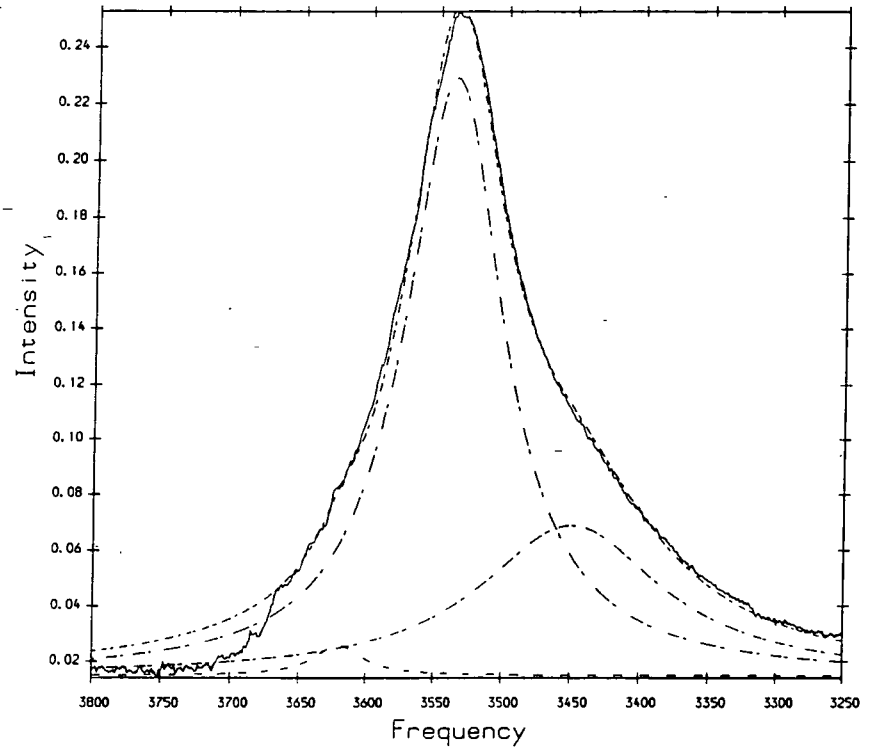

Figure 100 ν(OH) stretching mode of 0.06 methanol mole fraction in acetonitrile: ____ experimental, – – – overall calculated, –.–.–. band component.

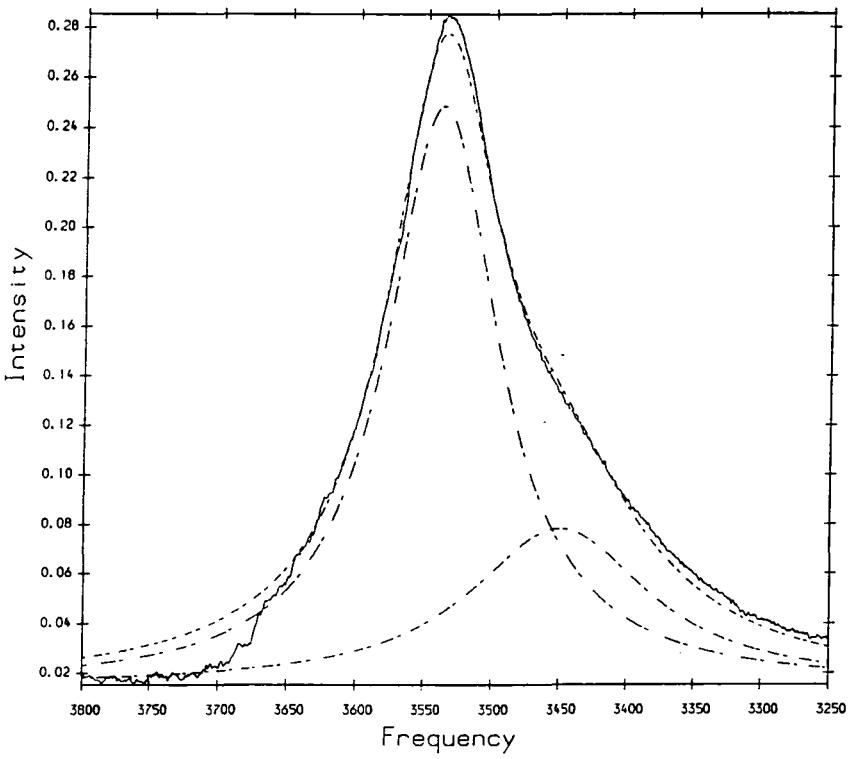

Figure 101 ν(OH) stretching mode of 0.07 methanol mole fraction in acetonitrlie: ____ experimental, – – – overall calculated, –.–.–. band component.

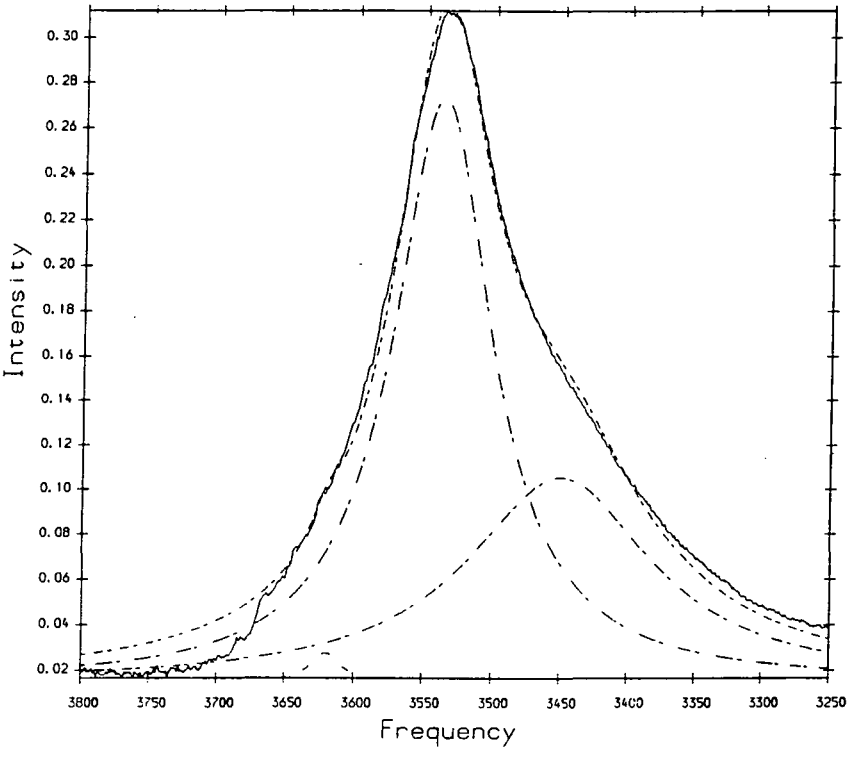

Figure 102 ν(OH) stretching mode of 0.08 methanol mole fraction in acetonitrile: ____ experimental, – – – overall calculated, –.–.–. band component.

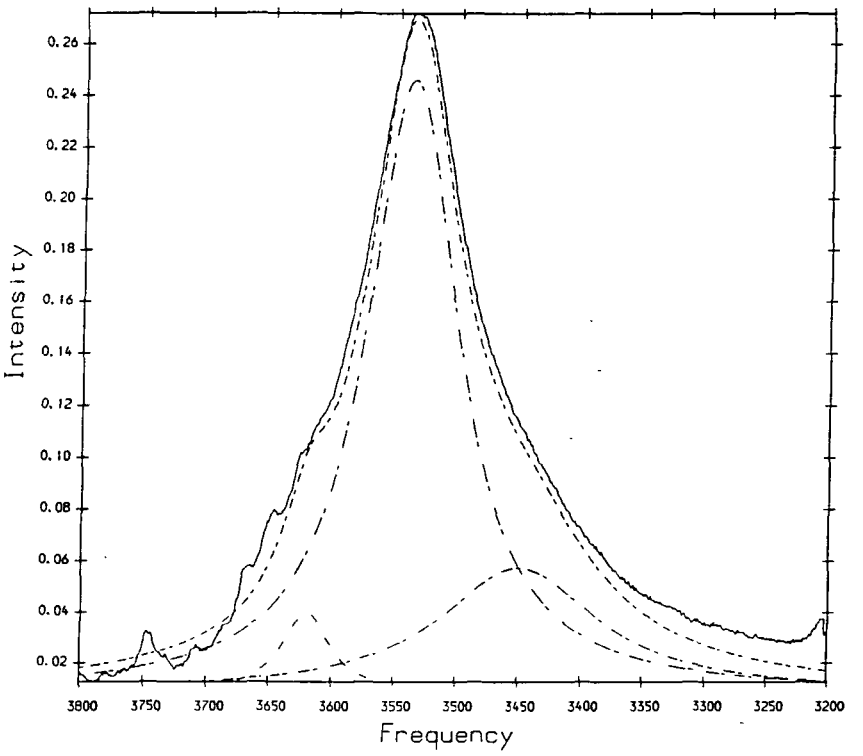

Figure 103 ν(OH) stretching mode of 0.1 methanol mole fraction in acetonitrile: ____ experimental, – – – overall calculated, –.–.–. band component.

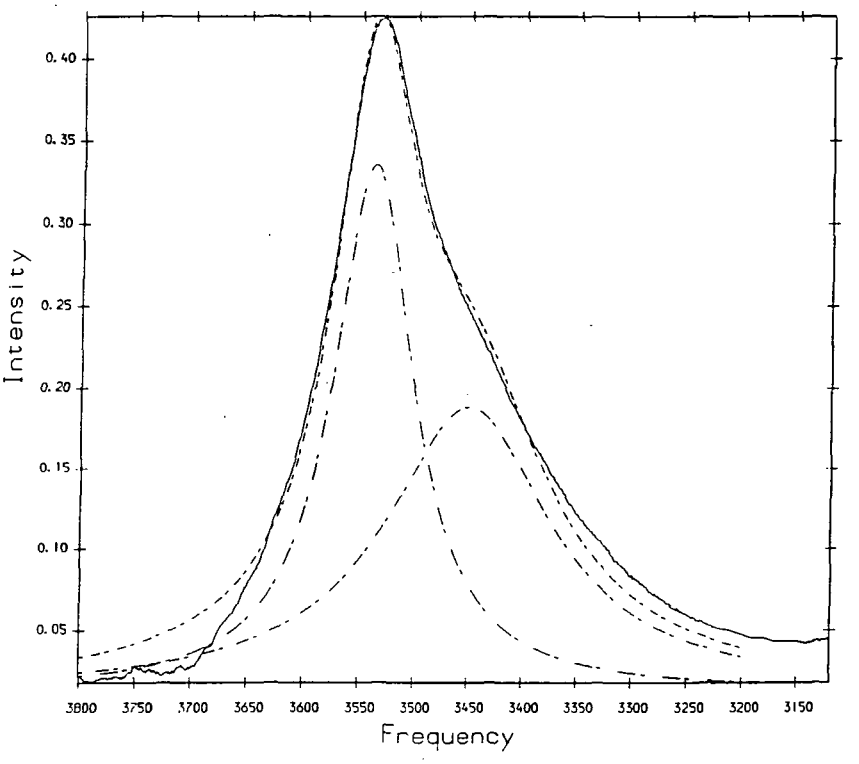

Figure 104 ν(OH) stretching mode of 0.2 methanol mole fraction in acetonitrile: ____ experimental, – – – overall calculated, –.–.–. band component.

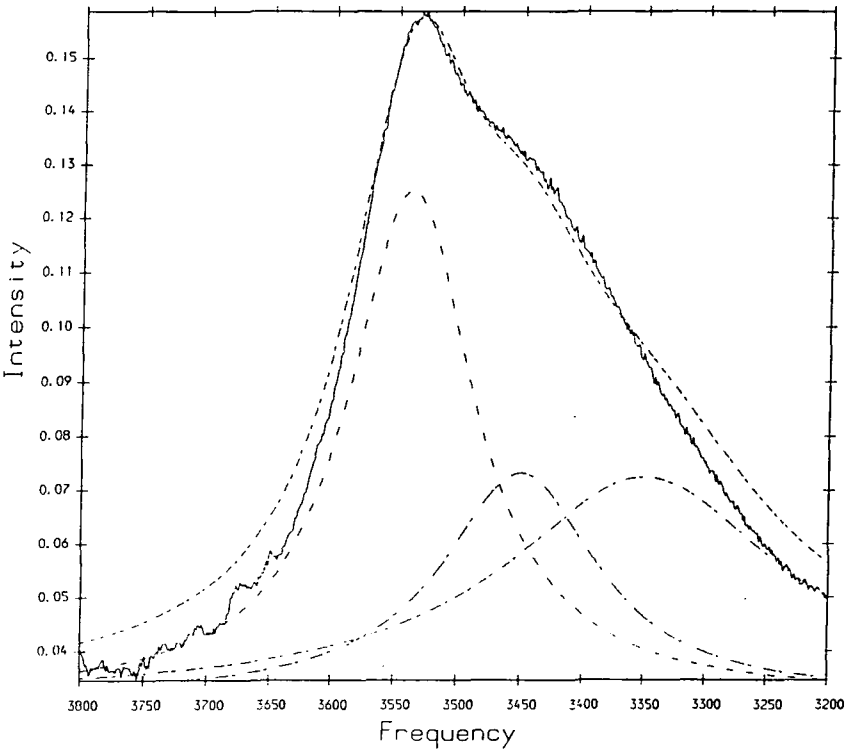

Figure 105 ν(OH) stretching mode of 0.3 methanol mole fraction in acetonitrile: ____ experimental, – – – overall calculated, –.–.–. band component.

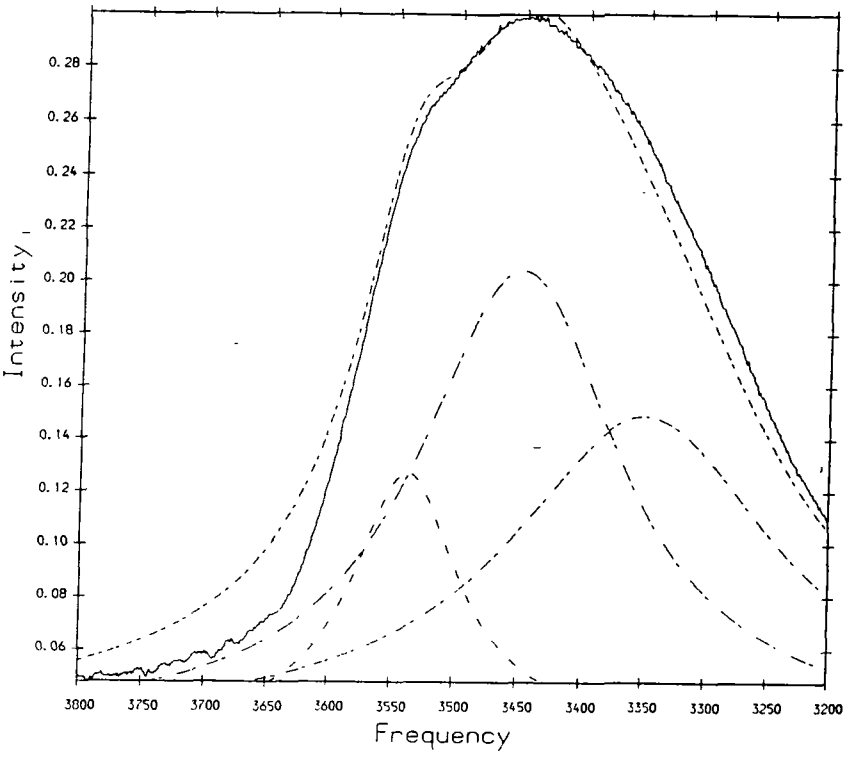

Figure 106 ν(OH) stretching mode of 0.4 methanol mole fraction in acetonitrile: ____ experimental, – – – overall calculated, –.–.–. band component.

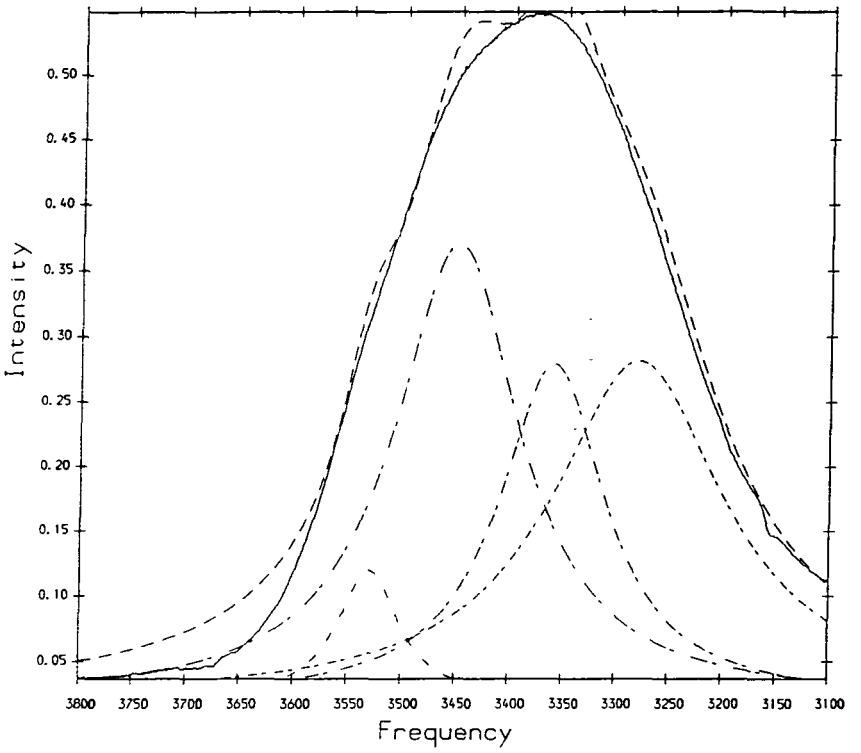

Figure 107 ν(OH) stretching mode of 0.6 methanol mole fraction in acetonitrile: _____ experimental, – – – overall calculated, –.–.–. band component.

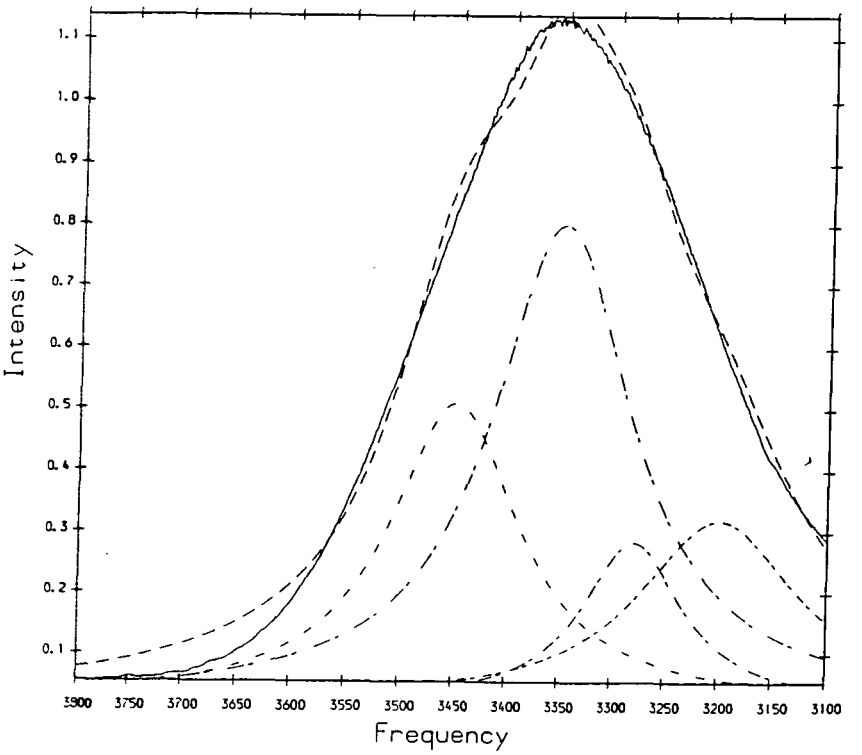

Figure 108 ν(OH) stretching mode of 0.7 methanol mole fraction in acetonitrile: _____ experimental, – – – overall calculated, –.–.–. band component.

Table 16 ν_s(OH) Band Frequencies in Different Solvents

Solvent	Monomer	Linear dimer	1:1 Complex and/or cyclic dimer	1:2 Complex and/or cyclic trimer	Tetramer
CCl_4	3645	3620	3527	3464	—
Ternary System	3642	3619	3565	—	—
Binary System	3650	3620	3538	3450	3350

— means not detected and/or does not exist

For example the cyclic dimer at 3527cm^{-1} (in non-polar solvent) would overlape with the band at 3538cm^{-1}, assigned to the C_1 complex band (in the binary system), making resolution difficult. The higher frequency shift of that band in ternary system than in the binary, suggests that the ν(O-H···B) is sensitive to the acceptor strength of B, so $\Delta\nu$ is assigned to represent the intermolecular interaction. Analysis of the band at 3450cm^{-1}, which might be overlapped between 1:2 complex with methanol aggregate but not being detected in ternary system, does not mean they don't exist. Such a 1:2 complex was investigated by Kleeberg and his co-workers[71] who studied the infra-red spectra of methanol in aprotic solvents B (to demonstrate the presence of a cooperative effect) and assigned two new bands which appear when the methanol concentration was in the range of 0.02 - 0.04 mole fraction. They assigned these two bands ν_{ox} and ν_B in

$$\begin{array}{l} \nu_{ox} \quad \nu_B \\ OH\cdots OH\cdots B \\ \quad | \quad\quad | \\ \quad CH_3 \quad CH_3 \end{array}$$

complexes.

Chapter 4

Discussion and Conclusion

Previous reports have dealt with different approaches to the study of detailed equilibria between the various associated species. For instance, some workers considered the determination of independent equilibrium constants for the association/dissociation process for each type of cluster, to be determined by a best fit of their measurements in a given concentration range. Other workers preferred, but with a poorer agreement of their fit with the data, to make use of a single equilibrium constant, supposedly approximately valid for all concentrations, thus introducing fewer parameters. Obviously, if generalized, the first approach would lead to a large number of free parameters.

A model fitting program written by Cabaco[50] *et al* was used,to identify the existing complexes in the binary mixture. The set of equilibria used were described in the Introduction (Chapter 1) and will be repeated here for convenience. Interpretation of the measured Raman spectra[50] of the ν(CN) band of acetonitrile was impossible without including methanol aggregation in the equilibrium model.

Indeed, in a similar way, it was found necessary,in the analysis of the binary system studied here to include more than one type of alcohol aggregate in order to model the equilibria in the methanol:acetonitrile mixture to calculate the free alcohol (and base) concentration at equilibrium. The following equilibria were used to explore how best to achieve this aim:

$$\underset{[A]-x_1}{CH_3CN} + \underset{[B]-x_1-x_2-2x_3-3x_4-4x_5}{CH_3OH} \rightleftharpoons \underset{x_1}{C_1}, \text{ 1:1 complex;} \quad K_1 = 2.6 \text{ dm}^3/\text{mol}$$

$$\underset{x_1-x_2}{C_1} + \underset{[B]-x_1-x_2-2x_3-3x_4-4x_5}{CH_3OH} \rightleftharpoons \underset{x_2}{C_2}, \text{ 1:2 complex;} \quad K_2 = 2.6 \text{ dm}^3/\text{mol}$$

$$\underset{[B]-x_1-x_2-2x_3}{2CH_3OH} \rightleftharpoons \underset{\text{Dimer},x_3}{(CH_3OH)_2}; \quad K_3 = 0.6 \text{ dm}^3/\text{mol}$$

$$\underset{[B]-x_1-x_2-2x_3-3x_4}{3CH_3OH} \rightleftharpoons \underset{\text{Trimer},x_4}{(CH_3OH)_3}; \quad K_4 = 3.83 \text{ (dm}^3/\text{mol)}^2$$

$$\underset{[B]-x_1-x_2-2x_3-3x_4-4x_5}{4CH_3OH} \rightleftharpoons \underset{\text{Tetramer},x_5}{(CH_3OH)_4}; \quad K_5 = 28.4 \text{ (dm}^3/\text{mol)}^3$$

The equilibrium constants were taken from literature as mentioned before. For a given model and a given set of equilibrium constants. Any particular equilibrium may be omitted by setting the corresponding equilibrium constants to zero. The concentrations of interest which may be compared with the experimental intensity (*i.e.* concentration) data are:

$$[C_1]_{eq,N} = \frac{x_1 - x}{[B]} \tag{64}$$

$$[C_2]_{eq,N} = \frac{x_2}{[B]} \tag{65}$$

$$[CH_3OH]_{eq,N} = \frac{[B] - x_1 - x_2 - 2x_3 - 3x_4 - 4x_5}{[B]} \tag{66}$$

$$[(CH_3OH)_2]_{eq,N} = \frac{x_3}{[B]} \tag{67}$$

$$[(CH_3OH)_3]_{eq,N} = \frac{x_4}{[B]} \tag{68}$$

$$[(CH_3OH)_4]_{eq,N} = \frac{x_5}{[B]} \tag{69}$$

$$[CH_3CN]_{eq,N} = \frac{[A] - x_1}{[A]} \tag{70}$$

where all the concentrations are in dm^3/mol and where (eq,N) refers to normalized equilibrium concentration. [A] and [B] are the initial experimental molar concentration of acetonitrile and methanol respectively.

From results obtained from this program, three models were tested against the experimental data:

Model 1: $K_1 = K_2 = 2.6$, $K_3 = 0.6$, $K_4 = 3.83$, $K_5 = 28.4$

Model 2: $K_1 = 2.6$, $K_2 = K_3 = K_4 = K_5 = 0.0$

and

Model 3: $K_1 = 2.6$, $K_2 = 0.0$, $K_3 = 0.6$, $K_4 = 3.83$, $K_5 = 28.4$

The initial values of x_1 to x_5 were chosen arbitrarily as 0.1, 0.09, 0.001, 0.001 and 0.001 respectively. The output obtained from each model are presented in Tables 17, 18 and 19. The normalized concentrations calculated in each model were compared with the normalized integrated intensities of each band. The integrated intensity of each component band at different methanol concentrations are presented in Table 20. The comparison between calculated models and observed data are shown in Figures 109 to 112. Accepting the assignment for the band at $3620cm^{-1}$ as the methanol cyclic dimer and comparing its normalised integrated intensity with tested models (Figure 109) we can see the experimental curve is closer to Model 1. This is also true in Figure 110, when comparing the normalized integrated intensity of the C_1 complex band at $3540cm^{-1}$ with calculated 1:1 complex concentration. Furthermore, the same general outlook from Figure 111 is also seen, when comparing the calculated 1:2 complex concentration with the normalized integrated intensity of the band at $3450cm^{-1}$. All this strengthened the belief that the mixture contains a variety of aggregates of different types (as mentioned before) in the binary mixture. The band at $3350cm^{-1}$ in Figure 112 however, behaves differently. This could be due to the complication in resolving the methanol aggregate species, so the $3350cm^{-1}$ band could contain one or more different species. The concentration of each species at different methanol concentrations are shown in Table 21 and presented in Figures 113 and 114. These indicate that the species of linear dimer, C_1, C_2 (+ trimer) all increase and then decrease in concentration with increasing methanol concentration. The methanol tetramer and pentamer bands appear at a high methanol concentration and keep on increasing with increasing concentration (Figure 115).

This work, therefore, shows that methanol aggregation can be detected by I.R. spectroscopy although it is not easy to assign the band components without further study. It also indicates that however strong the complexation of methanol with acetonitrile, methanol aggregates are still formed.

Table 17 Calculated Normalized Concentrations From Model 1

CH_3OH (m.f.)	CH_3OH mol/dm^3	CH_3CN mol/dm^3	[CN]	C_1	C_2	Dimer $x10^{-3}$	Trimer	Tetramer	[OH]
0.01	0.197	20.39	0.9906	0.9634	$9.04x10^{-3}$	4.10	$9.31x10^{-5}$	0	0.0183
0.02	0.396	20.22	0.9811	0.9457	0.0178	4.07	$1.88x10^{-4}$	0	0.0183
0.03	0.596	20.06	0.9716	0.9286	0.0263	4.03	$2.79x10^{-4}$	0	0.0183
0.04	0.796	19.89	0.9621	0.9120	0.0346	4.00	$3.72x10^{-4}$	$2.49x10^{-5}$	0.0183
0.05	0.997	19.72	0.9525	0.8959	0.0426	3.98	$4.64x10^{-4}$	$5.93x10^{-5}$	0.0183
0.06	1.24	19.52	0.9409	0.8771	0.0519	3.94	$5.73x10^{-4}$	$9.44x10^{-5}$	0.0183
0.07	1.44	19.53	0.9314	0.8620	0.0593	3.92	$6.63x10^{-4}$	$1.20x10^{-4}$	0.0183
0.08	1.65	19.18	0.9213	0.8469	0.0669	3.90	$1.18x10^{-4}$	$1.16x10^{-4}$	0.0184
0.1	2.08	18.82	0.9007	0.8165	0.0818	3.87	$9.52x10^{-4}$	$2.71x10^{-4}$	0.0185
0.2	4.2	17.06	0.7955	0.6853	0.1453	3.86	$2.01x10^{-3}$	$1.21x10^{-3}$	0.0194
0.3	6.46	15.17	0.6746	0.5635	0.2005	4.08	$3.56x10^{-3}$	$3.61x10^{-3}$	0.0211
0.4	8.77	13.38	0.5463	0.4496	0.2425	4.49	$5.95x10^{-3}$	$9.15x10^{-3}$	0.0236
0.5	10.97	11.42	0.4248	0.3389	0.2598	4.94	$9.31x10^{-3}$	0.0203	0.0268
0.6	13.71	9.13	0.3186	0.2218	0.2318	4.71	0.0120	0.0360	0.0293
0.7	16.27	7	0.2611	0.1409	0.1769	3.69	0.0113	0.0407	0.0296
0.8	18.9	4.78	0.2246	0.0808	0.1151	2.40	$8.41x10^{-3}$	0.0341	0.0289
0.9	21.94	2.28	0.1974	0.0323	0.0510	1.04	$4.04x10^{-3}$	0.0182	0.0276

Table 18 Calculated Normalized Concentrations From Model 2

CH_3OH (m.f.)	CH_3OH mol/dm^3	CH_3CN mol/dm^3	[CN]	C_1	C_2	Dimer	Trimer	Tetramer	[OH]
0.01	0.197	20.39	0.9905	0.9813	0	0	0	0	0.0186
0.02	0.396	20.22	0.9807	0.9809					0.0190
0.03	0.596	20.06	0.9708	0.9806					0.0193
0.04	0.796	19.89	0.9607	0.9802					0.0197
0.05	0.997	19.72	0.9504	0.9798					0.0201
0.06	1.24	19.52	0.9377	0.9794					0.0205
0.07	1.44	19.35	0.9271	0.9790					0.0209
0.08	0.65	19.18	0.9158	0.9785					0.0214
0.1	2.08	18.82	0.8919	0.9776					0.0223
0.2	4.2	17.06	0.7608	0.9712					0.0287
0.3	6.46	15.17	0.5916	0.9589					0.0410
0.4	8.77	13.38	0.3895	0.9312					0.0687
0.5	10.97	11.42	0.1864	0.8469					0.1530
0.6	13.71	9.13	0.0687	0.6201					0.3798
0.7	16.27	7	0.0387	0.4135					0.5864
0.8	18.9	4.78	0.0262	0.2462					0.7537
0.9	21.94	2.28	0.0191	0.1019					0.8980

Table 19 Calculated Normalized Concentrations From Model 3

CH_3OH (m.f.)	CH_3OH mol/dm^3	CH_3CN mol/dm^3	[CN]	C_1	C_2	Dimer	Trimer	Tetramer	[OH]
0.01	0.197	20.39	0.9905	0.9812	0	$4.26x10^{-3}$	$9.31x10^{-5}$	0	0.0186
0.02	0.396	20.22	0.9807	0.9807		$4.38x10^{-3}$	$2.09x10^{-4}$	0	0.0190
0.03	0.596	20.06	0.9708	0.9803		$4.51x10^{-3}$	$3.29x10^{-4}$	0	0.0193
0.04	0.796	19.89	0.9607	0.9798		$4.64x10^{-3}$	$4.64x10^{-4}$	$4.99x10^{-5}$	0.0197
0.05	0.997	19.72	0.9504	0.9793		$4.77x10^{-3}$	$6.09x10^{-4}$	$7.91x10^{-5}$	0.0200
0.06	1.24	19.52	0.9278	0.9786		$4.95x10^{-3}$	$8.04x10^{-4}$	$1.41x10^{-4}$	0.0205
0.07	1.44	19.35	0.9272	0.9779		$5.10x10^{-3}$	$9.82x10^{-4}$	$2.15x10^{-4}$	0.0209
0.08	0.65	19.18	0.9159	0.9772		$5.26x10^{-3}$	$1.18x10^{-3}$	$3.02x10^{-4}$	0.0213
0.1	2.08	18.82	0.8921	0.9755		$5.63x10^{-3}$	$1.67x10^{-3}$	$5.7\ x10^{-4}$	0.0223
0.2	4.2	17.06	0.7642	0.9577		$8.17x10^{-3}$	$6.19x10^{-3}$	$5.44x10^{-3}$	0.0282
0.3	6.46	15.17	0.6244	0.8819		0.0116	0.0172	0.0295	0.0358
0.4	8.77	13.38	0.5298	0.7173		0.0121	0.0264	0.0670	0.0389
0.5	10.97	11.42	0.4781	0.5432		0.0100	0.0268	0.0837	0.0382
0.6	13.71	9.13	0.4403	0.3726		$6.96x10^{-3}$	0.0217	0.0787	0.0356
0.7	16.27	7	0.4168	0.2508		$4.59x10^{-3}$	0.0157	0.0628	0.0330
0.8	18.9	4.78	0.3989	0.1520		$2.69x10^{-3}$	$9.97x10^{-3}$	0.0428	0.0306
0.9	21.94	2.28	0.3830	0.0641		$1.09x10^{-3}$	$4.31x10^{-3}$	0.0198	0.0282

Table 20 Normalized Band Integrated Intensities

CH_3OH (m.f.)	3650	3620	3538	3450	3350	3280
0.01	0.0348	0.1153	0.8349	0.0148	0	0
0.02	0.0001	0.0716	0.8242	0.1039		
0.03	0	0.0322	0.8045	0.1632		
0.04	0	0.0285	0.8060	0.1653		
0.045	0	0.0006	0.8140	0.1852		
0.05	0	0.0155	0.7544	0.23		
0.055		0.0038	0.7771	0.2190		
0.06		0.0169	0.6743	0.3096		
0.07		0.0004	0.6972	0.3022		
0.08		0.0087	0.6804	0.3908		
0.1		0.0474	0.7047	0.2477	0	0
0.2		0	0.4724	0.5274	0	0
0.3		0	0.3681	0.2255	0.4062	0
0.35		0	0.1927	0.2921	0.5150	0
0.4		0	0.1180	0.4062	0.3699	0.1057
0.45			0.0890	0.4539	0.3001	0.1568
0.5			0.1945	0.4615	0.2731	0.0707
0.6			0.0493	0.3587	0.2257	0.3662
0.7			0	0.2553	0.446	0.1064

Table 21 Concentrations of each species

CH_3OH M.F.	CH_3OH mol/dm^3	3650 mol/dm^3	3620 mol/dm^3	3540 mol/dm^3	3480 mol/dm^3	3350 mol/dm^3	3280 mol/dm^3
0.01	0.197	0.0068	0.0227	0.1644	0.0029	0	0
0.02	0.369	0	0.0283	0.3263	0.0411	0	0
0.03	0.596	0	0.0191	0.4794	0.0972	0	0
0.04	0.796	0	0.0226	0.6415	0.1315	0	0
0.045	0.897	0	0.0005	0.7301	0.1661	0	0
0.05	0.997	0	0.0154	0.7521	0.2293	0	0
0.055	1.099	0	0.0041	0.8540	0.2406	0	0
0.06	1.24	0	0.0209	0.8361	0.3826	0	0
0.07	1.44	0	0.0005	1.0039	0.4351	0	0
0.08	1.65	0	0.0143	0.9906	0.6448	0	0
0.1	2.08	0	0.0985	1.4657	0.5152	0	0
0.2	4.2	0	0	1.9840	2.2150	0	0
0.3	6.45	0	0	2.3742	1.4544	2.6199	0
0.35	7.59	0	0	1.4625	2.2170	3.9088	0
0.4	8.77	0	0	1.0348	3.5623	3.2440	0.9269
0.45	9.98	0	0	0.8882	4.5299	2.9949	1.5648
0.5	10.97	0	0	2.1336	5.0626	2.9959	0.7755
0.6	13.71	0	0	0.6759	4.9177	3.0943	5.0206
0.7	16.27	0	0	0	4.1537	7.2824	1.7311

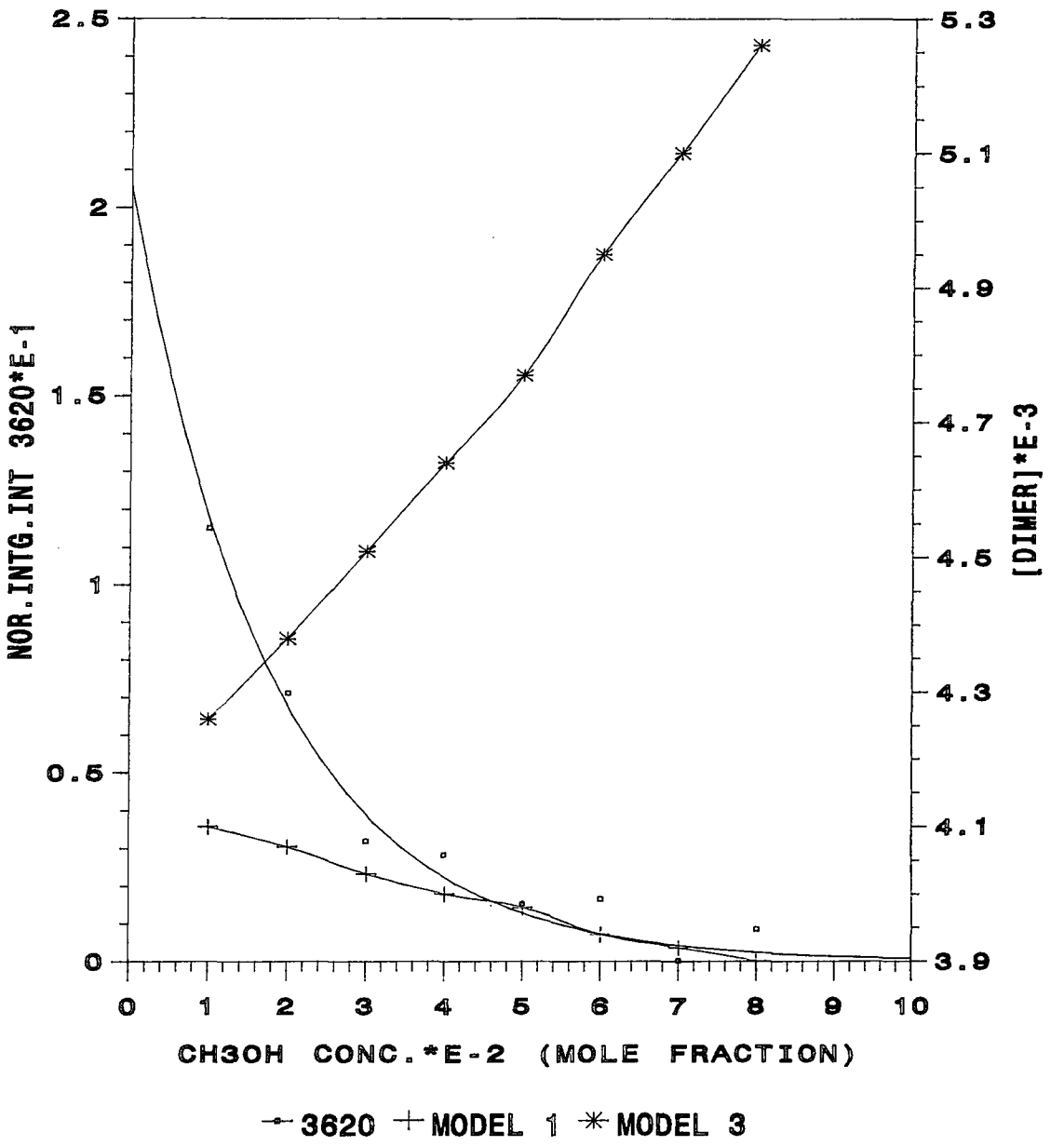

Figure 109 ν(OH) normalised integrated intensity at 3620cm^{-1} and normalised dimer concentration (right hand Y-axis) of methanol in binary systems

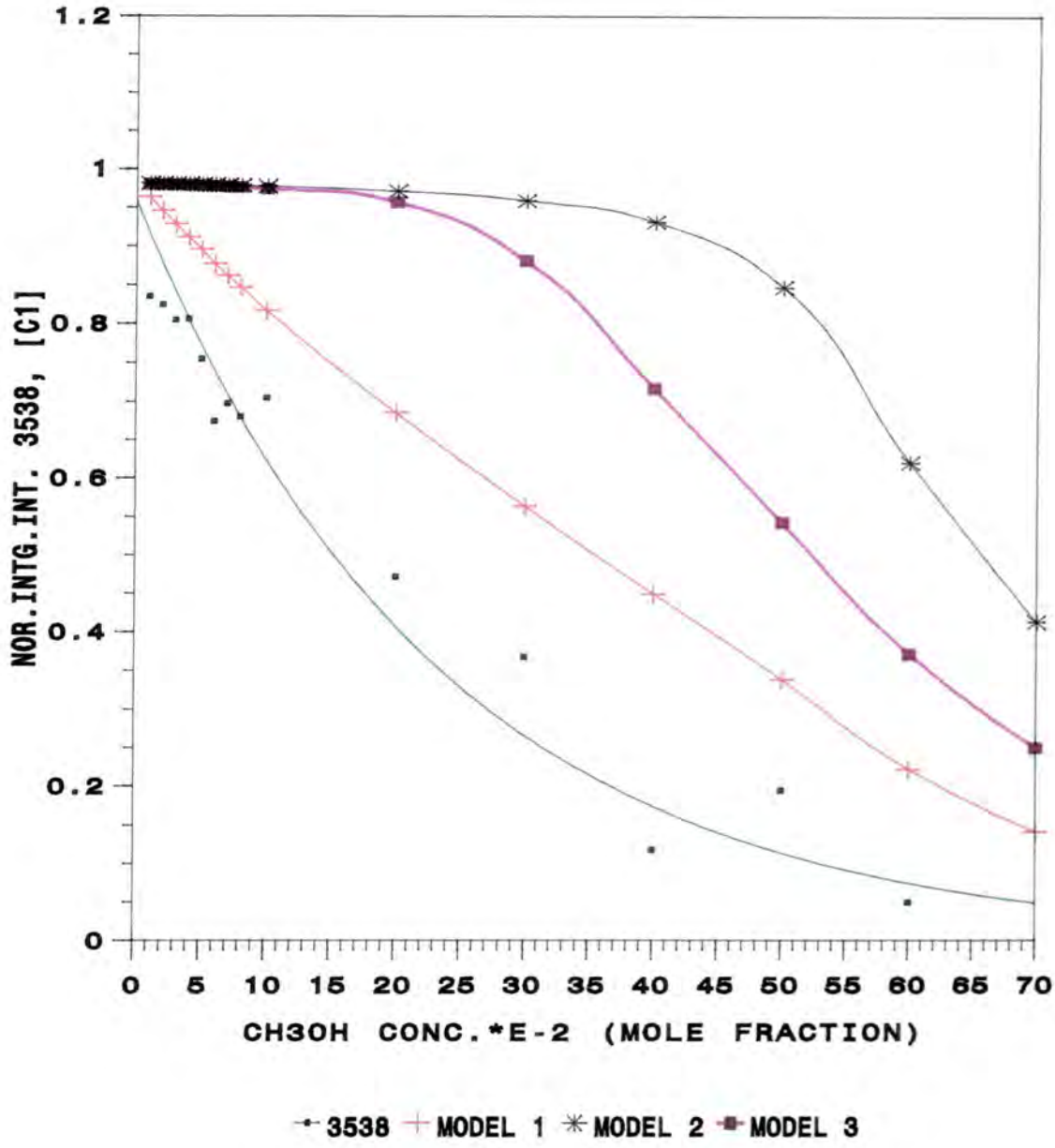

Figure 110 ν(OH) normalised integrated intensity at 3538cm^{-1} and normalised C_1 concentration of methanol in binary systems

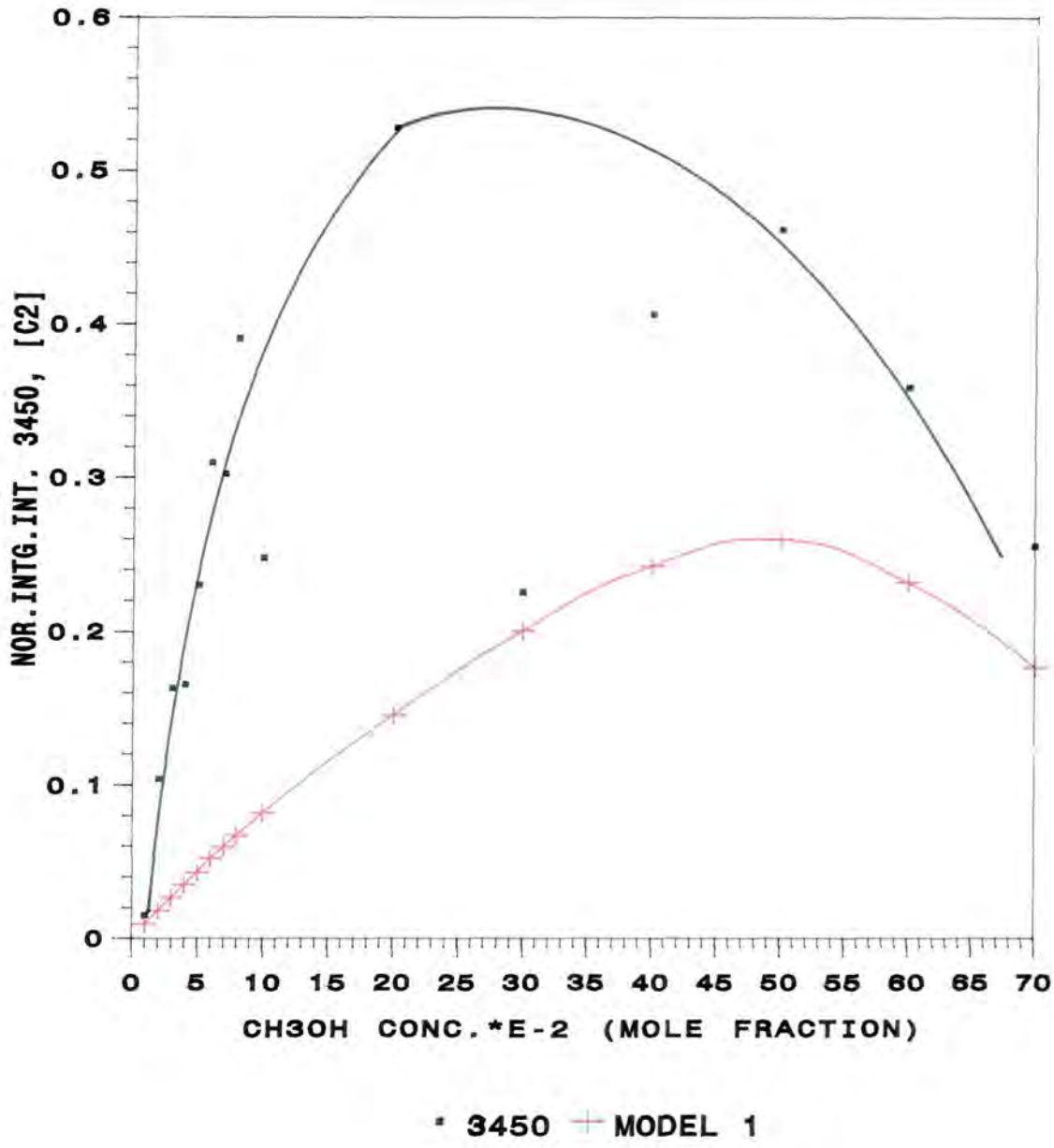

Figure 111 ν(OH) normalised integrated intensity at 3450cm^{-1} and normalised C_2 concentration of methanol in binary systems

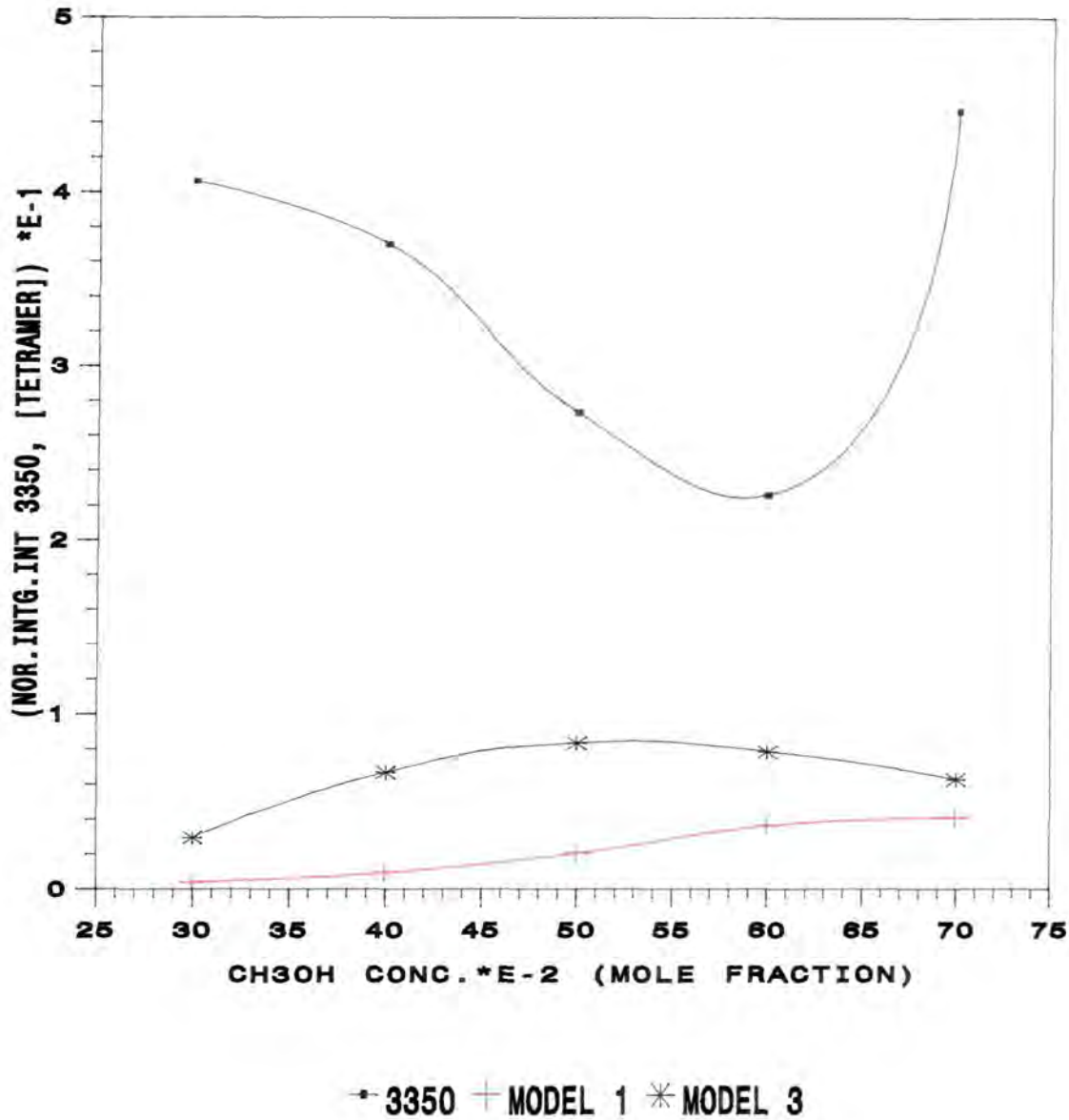

Figure 112 ν(OH) normalised integrated intensity at 3350cm^{-1} and normalised tetramer concentration of methanol in binary systems

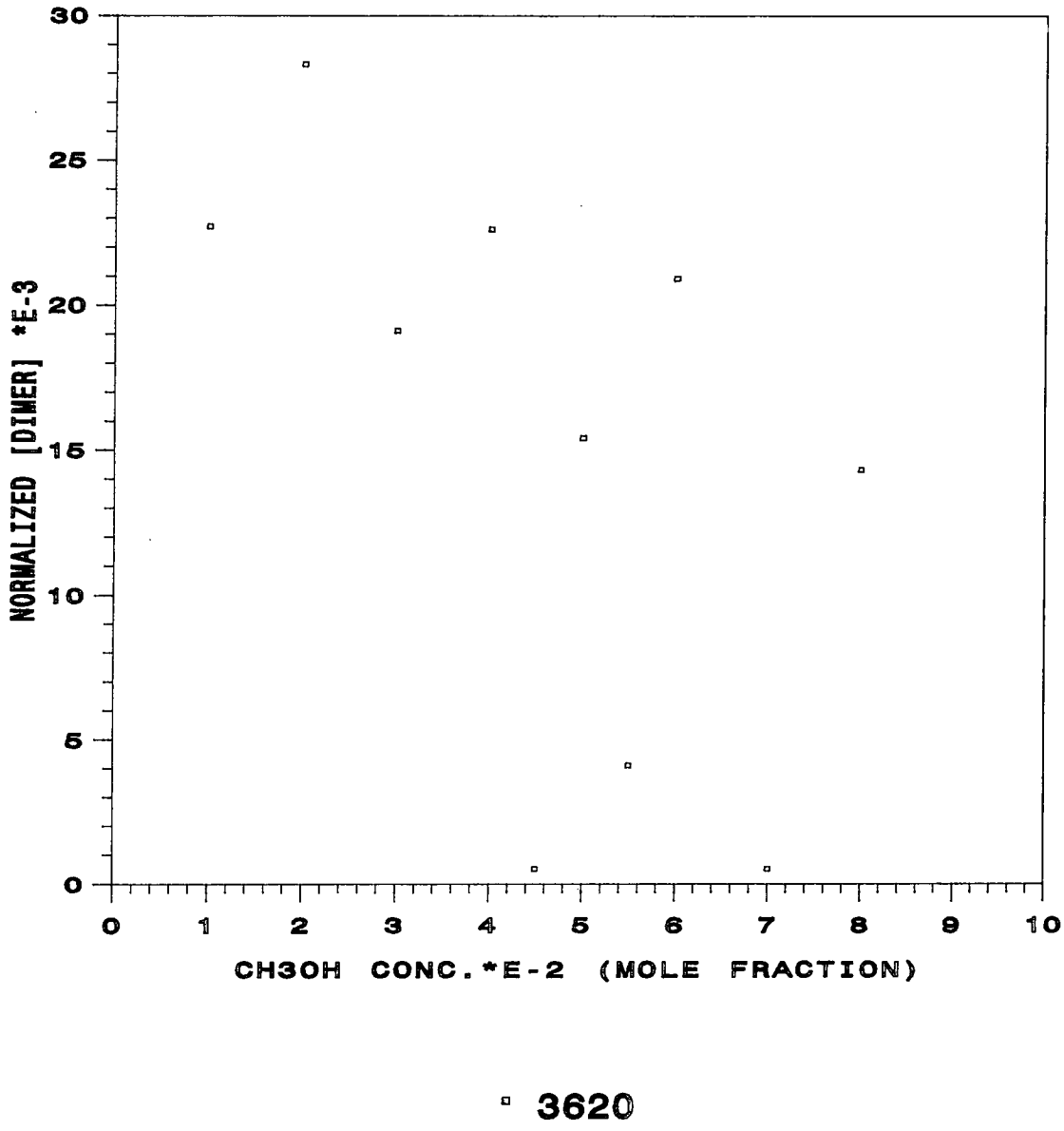

Figure 113 ν(OH) normalised dimer concentration at 3620cm^{-1} of methanol in binary systems

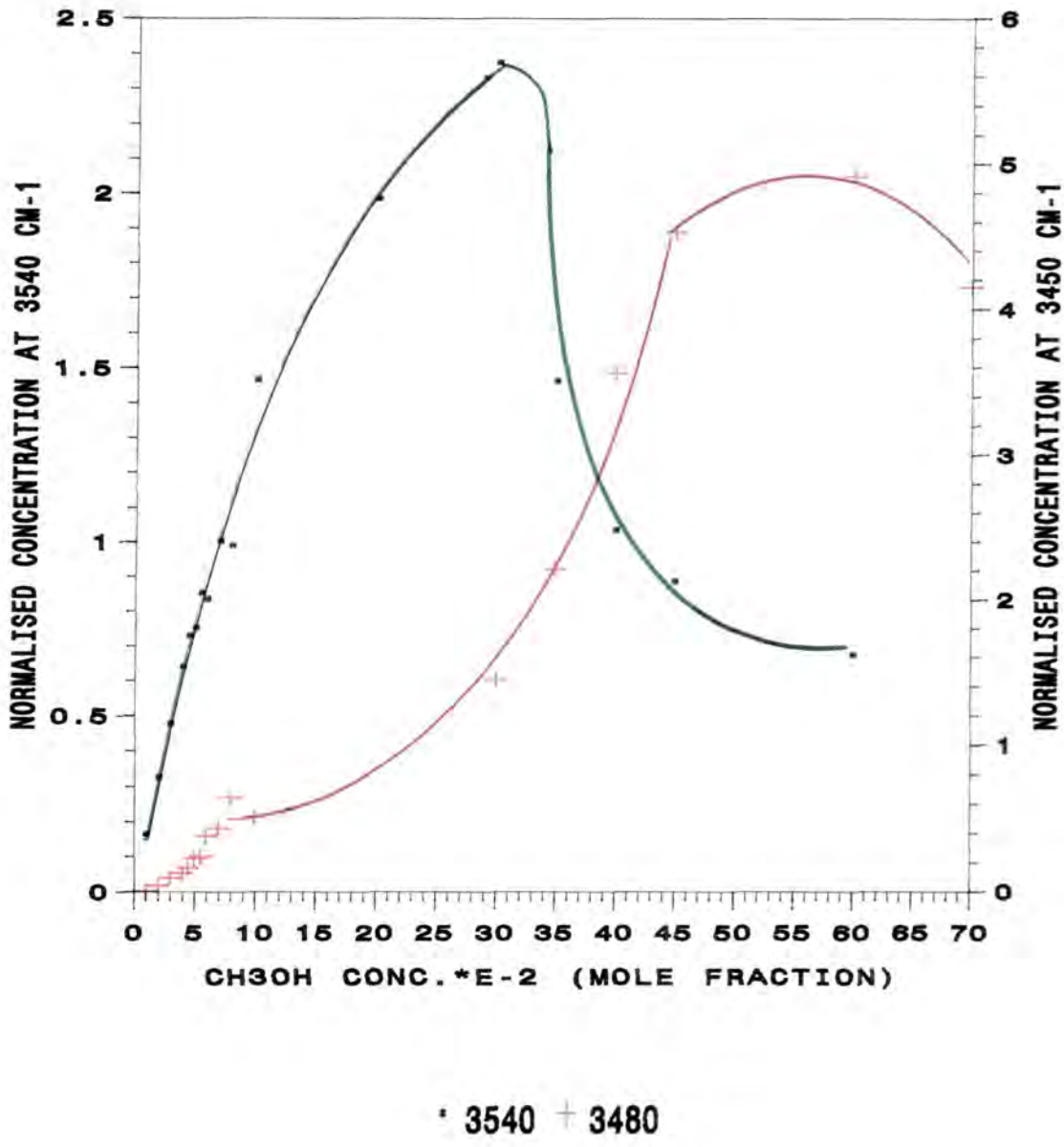

Figure 114 ν(OH) normalised concentrations at 3540cm^{-1} and 3450cm^{-1} (right hand Y-axis) of methanol in binary systems

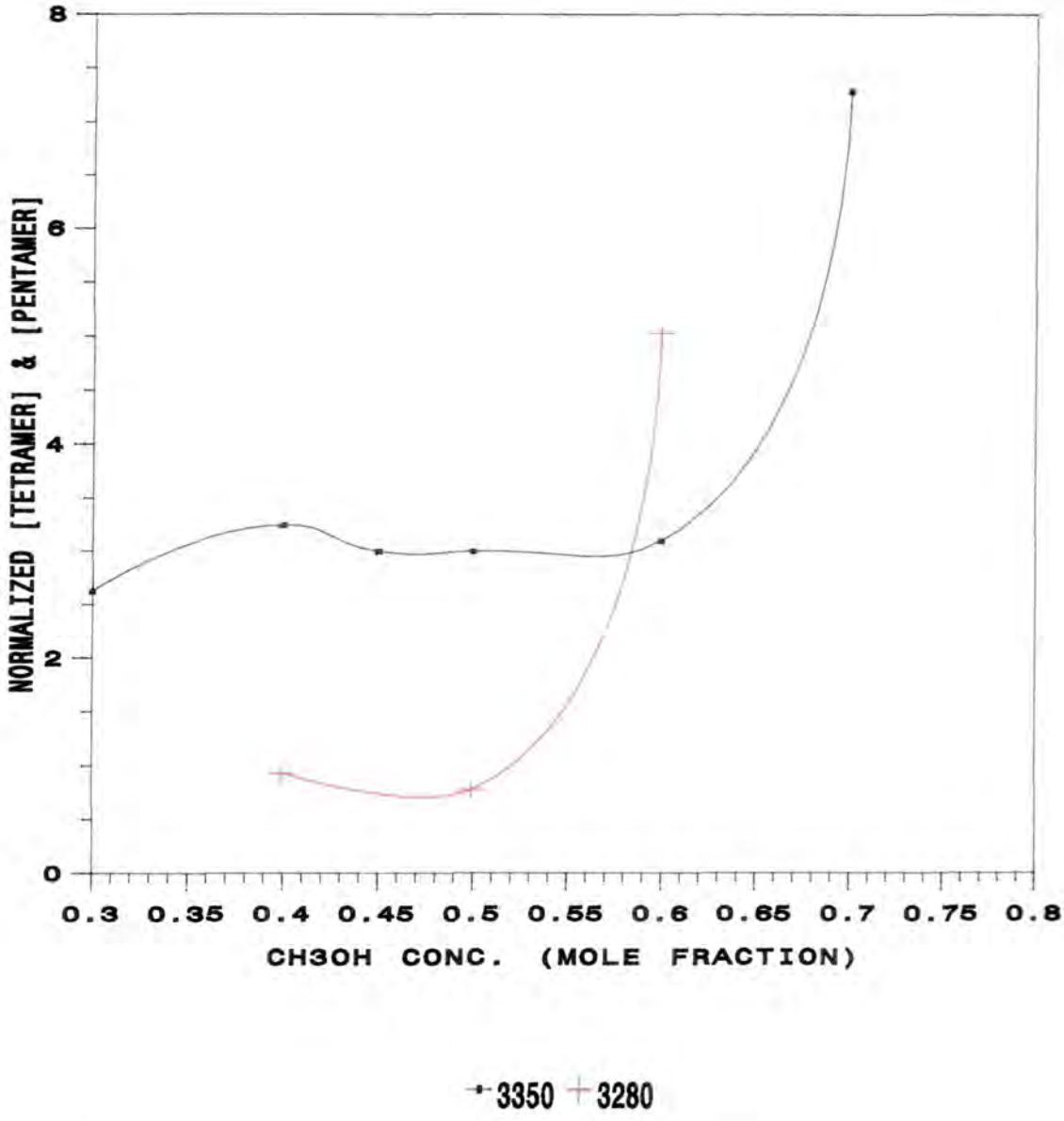

Figure 115 ν(OH) normalised tetramer and pentamer concentrations at 3350cm^{-1} and 3280cm^{-1} of methanol in binary systems

The Raman data obtained by studying acetonitrile in methanol solution led to the conclusion that no 1:2 complex was necessary. This might be accepted if we understand that the Raman spectra of acetonitrile are less sensitive (than infra–red spectra) to hydrogen bonding (the ν(OH) Raman stretching band is very much weaker than in the infrared and has not been studied in detail). Thus the Raman and infrared spectral data collected from different vibrational modes might be expected to lead to somewhat different conclusions. Thus the infrared ν(OH) is apparently much more sensitive to the formation of 1:2 complexes of CH_3CN:CH_3OH. This is not unexpected since the ν(CN) Raman band is relatively little affected by the addition of another methanol molecule. The Raman ν(CN) band is, however, sensitive to methanol aggregation[55]. Thus the examination of different modes in the same system gives different perspectives on the microscopic phenomena occurring in this binary mixture.

This study has shown that the infra–red data for methanol in a number of solvents (polar and non-polar) can be elucidated. In the binary system of methanol in acetonitrile the best fitted model contained: monomer, dimer, C_1 and C_2 complexes, trimer, tetramer and pentamer species. Furthermore, we have shown that reaching such a conclusion was not easy and more work is needed to confirm the results. But the trends obtained from infrared data compared to the calculated models provided good support for our conclusion.

References

1. Y. Marcus, in *Introduction to Liquid State Chemistry*, Wiley, 1977

2. G. Pimentel and A. McClellan, in *The Hydrogen Bond*, Freeman, 1960

3. V. Cheam, S.B. Farnham and S.D. Christian, *J. Phys. Chem.*, Vol. 74, No.23, 4157, 1970

4. L.A. Curtiss, *J. Chem. Phys.*, Vol. 67, No.3, 1144, 1977

5. W. Weltner and K. Pitzer, *J. Am. Chem. Soc.*, 73, 2606, 1951

6. C.N. Kietschner and R. Wiebe R., *J. Am. Chem. Soc.*, 76, 2579, 1954

7. W. Lathan and L. Curtiss, *Progress in Phys. Org. Chem.*, Vol. 11, p. 175, Wiley, 1974

8. J. Del Bene, *J. Chem. Phys.*, 55, 4633, 1971

9. J. Del Bene and J. Pople, *J. Chem. Phys.*, 52, 4858, 1970

10. M. Joesten and L. Schaad, *Hydrogen Bonding*, Marcel Dekkar, 1974

11. L. Curtiss and J. Pople, *J. Mol. Spec.*, 55, 1, 1975

12. G. Brink and L. Glasser, *J. Comp. Chem.*, Vol. 2, No.1, 14, 1981

13. P. Venkateswarlu and W. Gordy, *J. Chem. Phys.*, 23, 1200, 1955

14. E. Lippincott and R. Schroeder, *J. Chem. Phys.*, 23, 1099, 1955

15. T. Renner, G. Kucer and M. Blander, *J. Chem. Phys.*, 66, 177, 1977

16. E. Tucker, S. Farnham and S. Christian, *J. Phys. Chem.*, Vol. 73, No. 11, 3820, 1969

17. E.R. Lippincott, *J. Chem. Phys.*, 23, 603, 1955

18. R. Schroeder and E.R. Lippincott, *J. Phys. Chem.*, 61, 921, 1957

19. W. Moore, *Physical Chemistry*, Longman, 1972

20. A.S.N. Murthy and C.N.R. Rao, *Appl. Spec. Revs.* 2, 69,1968

21. C.A. Coulson, *Research (London)* 10, 149, 1957

22. C.A. Coulson, "*Valence*", Oxford University Press, 1961

23. J. Yarwood in *Spectroscopy and Structure of Molecular Complexes*, Plenum 1973

24. F. Franks, *Water: A Comprehensive Treatise, Vol. 1*, Plenum 1972

25. R. Freymann, *Compt. Rend.*, 195, 39, 1932

26. White and Thompson, *Proc. Roy. Soc.*, A, Vol. 291, 461, 1965

27. R. Badger and S. Bauer, *J. Chem. Phys.*, 5, 839, 1937

28. R. Mecke, *Discussion Faraday Soc.*, 9, 161, 1950

29. N. Fuson and M.L. Josien, *J. Opt. Soc. Amer.* 43, 1102, 1953

30. M. Davies and G.B.B.M. Sutherland, *J. Chem. Phys.*, 6, 755, 1938

31. U. Liddel and E. Becker, *J. Chem. Phys.*, 25, 173, 1956

32. L. England–Kretzer, M. Fritzsche and W.A.P. Luck., *J. Mol. Struc.* 175, 277, 1988

33. W.A.P. Luck and H.Y. Zheng, *J. Chem. Soc., Faraday Trans. 2*, 80, 1253, 1984

34. E. Fishman, *J. Phys. Chem.*, 65, 2204, 1961

35. L.J. Bellamy, K.J. Morgan and R.J. Pace, *Spectrochim. Acta*, 221, 535, 1966

36. A. Allerhand and P. von R. Schleyer, *J. Am. Chem. Soc.*, 85, 371, 1963

37. J.G. Kirkwood and R.T. Edwards, *J. Chem. Phys.*, 5, 14, 1937

38. A.D.E. Pullin, *Spectrochim. Acta*, 16, 12, 1960

39. A.D. Buckingham, *Proc. Roy. Soc.*, A248, 169, 1958

40. K.F. Purcell and R.S. Drago, *J. Am. Chem. Soc.*, , 89, 2874, 1967

41. H. Kempter and R. Mecke, *Z. Physik. Chem.*, 48, 229,1941

42. N. Coggeshall and E. Saier, *J. Am. Chem. Soc.*, 73, 5414, 1951

43. F. Franks, *Water: A Comprehensive Treatise* Vol. 2, Plenum, 1973

44. U. Liddel and E. Becker, *Spectrochim. Acta*, Vol. 10, p.70, 1957

45. H. Kempter and R. Mecke, *Z. Phys. Chem. Abt.*, B 46, 229,1940

46. E.G. Hoffman, *Z. Phys. Chem.*, 53, 179, 143

47. E.D. Becker, V. Liddel and J.N. Schoolery, *J. Mol. Spectr.*, 2, 1, 1959

48. L.J. Bellamy and R.C. Pace, *Spectrochim. Acta.*, 22, 525, 1966

49. L.J. Bellamy and R.C. Pace, *Spectrochim. Acta.*, 25, 319, 1969

50. M. Besnard, M. Cabaco, F. Strehle and J. Yarwood, *Chem. Phys.*, (in press)

51. M. Saunders and J. Hyne, *J. Chem. Phys.* Vol. 29, No.6, 1319, 1958

52. G. Eaton, A. Pena–Nunez and M. Symons, *J. Chem. Soc. Faraday Trans. 1*, 84, 2181, 1988

53. D. Montague and J. Dore, *Mol. Phys.*, 57, No.5, 1035, 1986

54. G. Palinkas, Y. Tamura, E. Spohr and K. Heimzinger, *Z. Naturforsch*, 43a, 43, 1988

55. S. Martinez, *Spectrochim. Acta.*, Vol. 42 A, No. 4, p.531, 1986

56. S. Chen, R. Wilhoit and B. Zwolinski, *J. Phys. Chem.*, Ref. Data, 6, 105, 1977

57. L. Wilson, R. Alencastro and C. Sandorfy, *Can. J. Chem.*, Vol. 63, 40, 1985

58. M. St. C. Flett, *J. Soc. Dyers Colourists*, 68, 59, 1952

59. S. Mitra, *J. Chem. Phys.*, Vol. 36, No. 12, 3286, 1962

60. A. Burneau, J.P. Perchard and G. Zuppiroli, *Mol. Phys.*, Vol. 41, No. 6, 1373, 1980

61. H.S. Frank, W.Y. Wen, *Discuss. Faraday Soc.*, 24, 133, 1957

62. F.A. Smith and E.C. Creitz, *J. Res. Natl. Bur.*, 46, 154, 1951

63. R.N. Jones and J. Pitha, *Optimisation Methods for Fitting Curves to I.R. band envelopes, Computer programs, NRC Bulletin 12*, 1968

64. C. Laurence, M. Berthelot, M. Helbert and K. Sraidi, *J. Phys. Chem.*, 93, 3799, 1989

65. T. Iskanderov, Ya. Kimel'fel'd and E. Smiknova, *J. Chem. Phys.*, 112, 379, 1987

66. R. Inskeep, J. Kelliher, P. McMahan and B. Somers, *J. Chem. Phys.*, 28, 1033, 1958

67. C. Brot, *Z. Phys. D–Atoms, Molecules and Clusters*, 11, 249, 1989

68. J. Errera, R. Gaspart and H. Sack, *J. Chem. Phys.*, Vol. 8, 63, 1940

69. E. Schulman, D. Dwyer and D. Doetschman, *J. Phys. Chem.*, 94, 7308, 1990

70. G. Brink and L. Glasser, *J. Phys. Chem.*, Vol. 82, No. 9, 1000, 1978

71. H. Kleeberg, D. Klein and W. Luck, *J. Phys. Chem.*, 1987, 91, 3200

Appendix

The Board of Studies in Department of Chemistry at Durham University requires all postgraduate students to attend at least eight departmental seminars arranged in each academic year and appendix them. Because of the two operations I had during February 1991, I had to stay away for almost two months. Because of that I attended only four seminars, which are listed below:–

7 November 1990	Dr D. Gerrard (B.P. Research) ***Raman Spectroscopy for Industrial Analysis***
14 November 1990	Prof. J. Bell (SUNY, Stonybrook) ***Functional Molecular Architecture and Molecular Recognition***
28 November 1990	Dr B.J. Whitaker (Leeds University) ***Two Dimensional Velocity Imaging of State Selected Reaction Products***
23 January 1991	Prof. J.S. Higgins (Imperial College) ***Rheology and Molecular Structure of Ionomer Solutions***